

MODELING THE TRANSMISSION DYNAMICS OF BRUCELLOSIS

By

PARIDE ORESTO LOLIKA PARIDE

A Dissertations Presented to the

DEPARTMENT OF MATHEMATICS FACULTY OF SCIENCES UNIVERSITY OF ZIMBABWE

In Partial Fulfillment of the Requirements for the Degree

of

DOCTOR OF PHILOSOPHY IN MATHEMATICS

Supervisor: Professor Steady Mushayabasa

December 2018

Abstract

Brucellosis, a neglected zoonotic disease remains a major public health problem world over. It affects domesticated animals, wildlife and humans. With large pastoral communities, and demand for meat and livestock production to double by 2050, brucellosis poses a major threat to the public health and economic growth of several developing nations whose economies rely heavily on agricultural exports. Since human-to-human transmission of the disease is rare the ultimate management of human brucellosis can be achieved through effective control of brucellosis in animal population. Hence there is need to gain a better and more comprehensive understanding of effective ways to control the disease in animal populations. Mathematical modeling, analysis and simulation offer a useful means to understand the transmission and spread of brucellosis so that effective disease control measures could be designed. In this dissertation, five epidemiological models that seek to evaluate the role of intervention strategies on the transmission dynamics of brucellosis in animal population have been studied. Firstly, a non-autonomous model that focuses on evaluating the impact of animal vaccination and environmental decontamination in a periodic environment, is introduced. Secondly, a modeling framework that seeks to improve our quantitative understanding of the influence of chronic brucellosis and culling control on brucellosis dynamics in periodic and non-periodic environments, is considered. Thirdly, a deterministic brucellosis model that incorporates heterogeneity and seasonality is studied. Fourthly, we evaluated the effects of short-term animal movements on the transmission dynamics of brucellosis through a two-patch model. Finally a model that incorporates two discrete delays and culling of infected animals displaying signs of brucellosis infection is proposed and analysed. All the proposed models incorporate relevant biological and ecological factors as well as possible disease intervention strategies. Epidemic and endemic analysis of the models have been performed, with a focus on the threshold dynamics characterized by the basic reproduction numbers. In addition, numerical simulation results are presented to demonstrate the analytical findings. A brief summary of the main results of the thesis and an outline of some possible future research directions rounds up the thesis.

Preface and Declaration

The study described in this thesis was carried out in the Faculty of Science, Department of Mathematics, University of Zimbabwe, during the period 1 August 2015 to 20 October 2018. This thesis was completed under the supervision of Professor S. Mushayabasa. This study represents original work by the author and has not been submitted in any form to another University. Where use was made of the work of others it has been duly acknowledged in the text.

Copyright © 2018 Paride Oresto Lolika

Acknowledgements

I would like to give thanks and appreciation to my supervisor, Professor Steady Mushayabasa, for being a tremendous mentor for me. I thank him for guiding me, for teaching me Mathematical Biology, for encouraging my work and for allowing me to grow as a research scientist. I would like also to thank my late supervisor, Professor Claver P. Bhunu, for introducing me to Biomathematics, and for being kind and supportive. I also thank the Post Graduate Center and the Department of Mathematics at the University of Zimbabwe, for supporting me. Finally, I would like to thank my Colleagues, Family and Friends. Your prayers and support are what sustained me thus far.

Dedication:

I dedicate this dissertation to my wife, Christine Matti, and my children, Emmanuella, Gracia, Patricia, Cericia and Kevin who missed me so much and sacrificed a lot for me during my long and repeated absence when I was a PhD student. I would like also to dedicate this work to my brother Jervasio O. Okot, for his support during my PhD studies

Contents

1	Intr	oduction	1
	1.1	Background	1
	1.2	Brucellosis in animal population	2
	1.3	Brucellosis in human	2
	1.4	Seasonality in brucellosis transmission	3
	1.5	Review of mathematical models for brucellosis	3
	1.6	Motivation	5
	1.7	Objectives of the research project	5
	1.8	Thesis outline	6
2	Mat	hematical preliminaries	7
	2.1	Introduction	7
	2.2	Stability	7
		2.2.1 Stability: Basic definition	7
		2.2.2 Dynamical properties	9
	2.3	Monotone systems	10
		2.3.1 Monotone dynamical system	11
		2.3.2 Triangular system	11
	2.4	Lyapunov methods	12
		2.4.1 LaSalle invariance principle	12
	2.5	Matrices	13
		2.5.1 Lozinskii measures	14
		2.5.2 The second additive compound matrix	14
	2.6	Calculation of basic reproduction number	14

ð	MO	aenng	and analyzing the effects of seasonality on brucehosis	
	infe	ction		18
	3.1	Introd	uction	18
	3.2	Model	with seasonal variation	21
		3.2.1	Model framework	21
		3.2.2	Feasible region	23
		3.2.3	Disease-free equilibrium	24
		3.2.4	The reproduction number	25
		3.2.5	Disease extinction	28
		3.2.6	Disease persistence	30
	3.3	Optim	al control	34
		3.3.1	Existence of the optimal control set	35
		3.3.2	Characterization of the optimal control problem	36
		3.3.3	Uniqueness of the optimality system	40
	3.4	Numer	rical results	44
	3.5	Conclu	usion and discussion	51
4	On	the dr	vnamics of brucellosis infection in bison population with	
4		ŭ	ansmission and culling	53
	4.1		uction	
	4.1		llosis model without seasonal variations	
	4.2	4.2.1	Model construction	
		4.2.1	The reproduction number	
		4.2.3	Equilibria	
	4.3	_	llosis model with seasonal variations	66
	4.0	4.3.1	Model construction	66
		4.3.1		66
		4.3.3	The reproduction number	
	4 4		•	67
	4.4	4.4.1	al control	71
				71
	4 5	4.4.2	Numerical results	
	4.5	Conclu	uding remarks	8

5	Mo	deling the spatiotemporal variations in brucellosis transmission	83
	5.1	Introduction	83
	5.2	A two-patch autonomous model	85
		5.2.1 Feasible region	86
		5.2.2 Disease-free equilibrium	87
		5.2.3 The reproduction number	88
		5.2.4 Global stability of the disease-free equilibrium	89
		5.2.5 Nontrivial equilibria	90
		5.2.6 Local and global dynamics	92
	5.3	A two-patch periodic model	99
		5.3.1 The reproduction number	100
		5.3.2 Threshold dynamics	l01
	5.4	Numerical results	105
	5.5	Conclusion and discussion	109
6	On	the role of short-term animal movements on the persistence of	
	bru	cellosis 1	11
	6.1	Introduction	l11
	6.2	Modeling framework	l13
	6.3	Disease dynamics for a single patch	l15
	6.4	The reproduction number	l15
	6.5	Disease invasion and persistence	l18
	6.6	Uniform persistence	l 19
	6.7	Optimal culling	122
	6.8	Discussion	128
7	Dyı	namics and stability analysis of a brucellosis model with two	
	disc	crete delays 1	35
	7.1	Introduction	135
	7.2	Mathematical model	137
	7.3	Analytical results	138
		7.3.1 Initial conditions	138
		7.3.2 The basic reproduction Number	138

		7.3.3	Stability of the disease-free equilibrium	138
		7.3.4	Disease persistence	141
		7.3.5	Existence of the endemic equilibrium	144
		7.3.6	Stability of the endemic equilibrium	145
		7.3.7	Hopf bifurcation analysis	156
	7.4	Nume	rical results	161
	7.5	Concl	usion	169
8	Con	clusio	n and future work	171
A	Appe	ndix:	Publications arising from this thesis	174
Ε	Biblic	ograph	.y	174

List of Figures

3.1	Flowchart illustrating the dynamics of brucellosis	22
3.2	Numerical results of the average basic reproduction number $[\mathcal{R}_0]$ and the	
	basic reproduction number \mathcal{R}_0 versus a_j , $(j = 1, 2)$: (a) $[\mathcal{R}_0]$ and \mathcal{R}_0 versus	
	a_1 ; (b) $[\mathcal{R}_0]$ and \mathcal{R}_0 versus a_2	28
3.3	Control profiles for the autonomous model (3.1)	44
3.4	Control profiles for the periodic model (3.2)	45
3.5	The concentration of $brucella$ for the autonomous model (3.1)	45
3.6	The concentration of $brucella$ for the periodic model (3.2)	45
3.7	The numbers of exposed and infectious animals for the periodic model	
	(3.2): (a) exposed population; (b) infectious population	46
3.8	The numbers of exposed and infectious animals for the autonomous	
	model (3.1): (a) exposed population; (b) infectious population	47
3.9	Control profiles for the periodic model (3.2) with low costs	47
3.10	Control profiles for the periodic model (3.2) with high costs	48
3.11	The concentration of $brucella$ for the periodic model (3.2) with high	
	costs	48
3.12	The number of exposed animals for the periodic model (3.2) with high	
	costs	48

4.1	Phase portrait depicting the global stability of (a) the disease-free equilib-	
	rium \mathcal{E}^0 which exists for $\mathcal{R}_0 \leq 1$, here we set $\beta = 0.28$ to get $\mathcal{R}_0 = 0.41548$	
	(b) the endemic equilibrium point which exists whenever $\mathcal{R}_0 > 1$, note that	
	we set $\beta = 0.8$ to obtain $\mathcal{R}_0 = 1.0103$. The numerical results depicted in	
	(a) supports that analytical findings in Theorem 4.2.1 (i), that whenever	
	$\mathcal{R}_0 < 1$ then system (4.2) has a globally asymptotically stable disease-free	
	equilibrium. Similarly, plot (b) demonstrate the analytical predictions in	
	Theorem 4.2.1 (ii) that if $\mathcal{R}_0 > 1$, system (4.2) has a unique endemic	
	equilibrium \mathcal{E}^* , which is globally asymptotically stable	65
4.2	Simulation results of the autonomous model with and without the con-	
	trol (a) susceptible animals (b) clinically infected animals (c) chronically	
	infected animals (d) recovered animals. The dotted blue and solid red	
	curves in all the figures represent the total population over a 50 year pe-	
	riod with and without control, respectively. The time varying optimal	
	culling associated with these figures is shown in Figure 4.3. Note that the	
	basic reproduction number $\mathcal{R}_0 = 1.576$, $\beta = 0.35$ and $C_4 = 10$	76
4.3	Simulation results showing the control profile for the autonomous model,	
1.0	over a period of 50 years, with (a) $C_4 = 10$ and (b) $C_4 = 100$. We can	
	observe that in all cases the control profile admits a bang-bang solution	
	with one switch.	77
4.4	Simulation results of the non-autonomous model with and without the con-	' '
4.4	trol (a) susceptible animals (b) clinically infected animals (c) chronically	
	infected animals (d) recovered animals. The dotted blue and solid black	
	curves represent the total population, with and without control, respec-	
	tively. The time varying optimal culling associated with these figures is	
	shown in Figure 4.5. Note that the basic reproduction number $\mathcal{R}_0 = 1.312$	=0
	and $C_4 = 10$	79
4.5	Simulation results showing the control profile for the non-autonomous	
	model, over a period of 50 years, with (a) $C_4 = 10$ and (b) $C_4 = 100$.	
	We can observe that in both scenarios the control profile exhibits a bang-	
	bang solution with more than one switch	80

0.1	Phase portrait illustrating the global stability of \mathcal{E}_1 for system (5.1) in the
	S_2 - I_2 plane with $\mathcal{R}_1 < 1, \ \mathcal{R}_2 > 1$. Each curve in the plot corresponds to a
	different initial condition, and all these curves converge to the equilibrium
	\mathcal{E}_1 (where $S_2 \doteq 2.39 \times 10^7$, $I_2 \doteq 3.22 \times 10^7$) over time
5.2	Phase portrait illustrating the global stability of \mathcal{E}_2 for system (5.1) in
	the S_2 - I_2 plane with $\mathcal{R}_1 > 1$. Each curve in the plot corresponds to a
	different initial condition, and all these curves converge to the equilibrium
	\mathcal{E}_2 (where $S_2 \doteq 2.29 \times 10^7, \ I_2 \doteq 2.71 \times 10^7$) over time
5.3	The infection curves for the two patches associated with system (5.27)
	when $R_0 < 1$. Both curves converge to the disease-free equilibrium \mathcal{E}_0 over
	time
5.4	The infection curves for the two patches associated with system (5.27)
	when $R_0 > 1$. Each curve converges to a periodic oscillation with a period
	$\omega = 12 \text{ months.} \dots \dots$
6.1	Phase portrait illustrating the global stability of \mathcal{E}^* for system (6.1) in the
	S_1 - I_1 plane with $\mathcal{R}_0 = 2.84$ (we set $\beta_1 = \beta_2 = 1.5$). Each curve in the plot
	corresponds to a different initial condition, and all these curves converge
	to the equilibrium \mathcal{E}^* (where $S_1=S_2\doteq 1500,\ I_1=I_2\doteq 1000$) over time . 122
6.2	Simulation results of the proposed two patch brucellosis model for
	scenario 1 under weak symmetric coupling (a) the number of infected
	animals in patch 1 (b) the number of infected animals in patch 2 . In
	all the figures the dotted blue and solid black curves represent the
	infected population, without and with control, respectively 130
6.3	Simulation results of the proposed two patch brucellosis model for
	scenario 1 under strong symmetric coupling (a) the number of infected
	animals in patch 1 (b) the number of infected animals in patch 2 . In
	all the figures the dotted blue and solid black curves represent the
	infected population, without and with control, respectively 130

6.4	Numerical illustrations demonstrating the effects of optimal interven-
	tion strategies on controlling the long-term brucellosis dynamics for
	scenario 1 under weak asymmetric coupling (a) the number of in-
	fected animals in patch 1 (b) the number of infected animals in patch
	2. In all the figures the dotted blue and solid black curves represent
	the infected population, without and with control, respectively 131
6.5	Numerical illustrations demonstrating the effects of optimal interven-
	tion strategies on controlling the long-term brucellosis dynamics for
	scenario 1 under strong asymmetric coupling (a) the number of in-
	fected animals in patch 1 (b) the number of infected animals in patch
	2. In all the figures the dotted blue and solid black curves represent
	the infected population, without and with control, respectively 131
6.6	The control profile for scenario 1 (a) low costs (b) high cost of culling 132
6.7	Simulation results of the proposed two patch brucellosis model for
	scenario 2 under weak symmetric coupling (a) the number of infected
	animals in patch 1 (b) the number of infected animals in patch 2 . In
	all the figures the dotted blue and solid black curves represent the
	infected population, without and with control, respectively 132
6.8	Simulation results of the proposed two patch brucellosis model for
	scenario 2 under strong symmetric coupling (a) the number of infected
	animals in patch 1 (b) the number of infected animals in patch 2 . In
	all the figures the dotted blue and solid black curves represent the
	infected population, without and with control, respectively 133
6.9	Numerical illustrations demonstrating the effects of optimal interven-
	tion strategies on controlling the long-term brucellosis dynamics for
	scenario 2 under weak asymmetric coupling (a) the number of in-
	fected animals in patch 1 (b) the number of infected animals in patch
	2. In all the figures the dotted blue and solid black curves represent
	the infected population, without and with control, respectively 133

6.10	Numerical illustrations demonstrating the effects of optimal interven-	
	tion strategies on controlling the long-term brucellosis dynamics for	
	scenario 1 under strong asymmetric coupling (a) the number of in-	
	fected animals in patch 1 (b) the number of infected animals in patch	
	2. In all the figures the dotted blue and solid black curves represent	
	the infected population, without and with control, respectively	. 134
6.11	The control profile for scenario 2	. 134
7.1	Stability of the infected and free-infected equilibrium of model system	
	(7.1) showing plots of $I_1(t)$ and $I_2(t)$ with varying delay $(\tau_1 = \tau_2)$.	
	The direction of the arrow depict an increase in delay with a step size	
	of 2.0 starting from 2.0 to 10. The blue patterns in both (a) and (b)	
	highlights brucellosis dynamics when $\mathcal{R}_0 < 1$ while the red pattern	
	are for $\mathcal{R}_0 > 1$. Initial population levels were assumed as follows	
	$S(0) = 1000$ animals, $V(0) = 500$ animals, $I_1(0) = 500$ animals and	
	$I_2(0) = 0$ animals	. 163
7.2	Numerical solutions of model system (7.1) illustrating the effects of	
	different time delay on brucellosis infection level in the community.	
	Initial population levels were assumed as follows $S(0) = 1000$ animals,	
	$V(0)=500$ animals, $I_1(0)=500$ animals and $I_2(0)=0$ animals	. 164
7.3	Numerical solutions demonstrating the stability of \mathcal{E}^0 equilibrium of	
	model system (7.1) with $\mathcal{R}_0 = 0.686281$. We set $\tau_1 = 30$, $\tau_2 =$	
	5, $\beta = 6.844 \times 10^{-6} \text{ animal}^{-1} \text{ year}^{-1}$, $\gamma = 0.2$, $\alpha = 0.15 \text{ year}^{-1}$,	
	A=16434 animals year ⁻¹ and the remainder retained the baseline	
	values in Table 7.1. Further, we set the initial conditions as follows	
	$S(0) = 100$ animals, $V(0) = 0$ animals, $I_1(0) = 10$ animals and	
	$I_2(0) = 0$ animals	. 165

7.4	Dynamics of model system (7.1) for different values of (τ_1, τ_2) , which	
	illustrate the stability of infection-free equilibrium \mathcal{E}^0 at $\mathcal{R}_0 = 0.686281$.	
	We set $\beta = 6.844 \times 10^{-6} \text{ animal}^{-1} \text{ year}^{-1}$, $\gamma = 0.2$, $\alpha = 0.15 \text{ year}^{-1}$,	
	A=16434 animals year ⁻¹ and the remainder retained the baseline	
	values in Table 7.1. Further, we set the initial conditions as follows	
	$S(0) = 100$ animals, $V(0) = 0$ animals, $I_1(0) = 10$ animals and	
	$I_2(0) = 0$ animals	166
7.5	Stability of \mathcal{E}^* equilibrium of model system (7.1) with $\mathcal{R}_0 = 3.77333$.	
	The time delay τ_1 was fixed to be 60 and τ_2 was fixed to be 1. We	
	set the model parameters and variables as follows: $\beta = 6.844 \times 10^{-6}$	
	animal ⁻¹ year ⁻¹ , $\gamma = 0.2$, $\alpha = 0.015$ year ⁻¹ , $S(0) = 100$ animals,	
	$V(0)=0$ animals, $I_1(0)=10$ animals, $I_2(0)=0$ animals while the	
	other parameter values are as in Table 7.1.	167
7.6	Numerical results of model system (7.1) for different values of (τ_1, τ_2) ,	
	which demonstrate the stability of infected equilibrium \mathcal{E}^* at $\mathcal{R}_0 =$	
	3.77333. We set the model parameters and variables as follows: $\beta =$	
	$6.844 \times 10^{-6} \text{ animal}^{-1} \text{year}^{-1}$, $\gamma = 0.2, \alpha = 0.015 \text{ year}^{-1}, S(0) = 100$	
	animals, $V(0) = 0$ animals, $I_1(0) = 10$ animals, $I_2(0) = 0$ animals	
	while the other parameter values are as in Table 7.1	168
7.7	Sensitivity index for \mathcal{R}_0 with respect to model parameters that define	
	it	160

List of Tables

3.1	Parameters and values
4.1	Parameters and values
4.2	Additional model parameters and their values
4.3	The total number of newly infected animals over 50 years and the total
	$\cos J$ with respect to different control strategies for the autonomous
	model with $\mathcal{R}_0 = 1.5679$ 78
4.4	The total number of newly infected animals over 50 years and the
	total cost J with respect to different control strategies for the non-
	autonomous model with $\mathcal{R}_0 = 1.312.$
5.1	Parameters and their values
6.1	Parameters and values
6.2	Association between the basic reproduction number and the residence-
	time matrix
6.3	The total number of newly infected animals over a ten-year period and
	the total cost J with respect to the control strategy under scenario 1. 125
6.4	The total number of newly infected animals over a ten-year period and
	the total cost J with respect to the control strategy under scenario 2. 127
7.1	Model parameters and variables and their baseline values

Chapter 1

Introduction

1.1 Background

Brucellosis, a highly contagious bacterial disease, is one of the world's major zoonoses responsible for a considerable economic and health burden. Currently there are more than 500,000 new cases of brucellosis reported annually and the disease remains endemic in many countries and settings, including Spain, Latin America, the Middle East, and Africa [1, 2]. Among these, the majority of brucellosis cases are found in sub-Sahara Africa, where Ethiopia, Chad, Tanzania, Nigeria, Uganda, Kenya, Zimbabwe and Somalia have been reporting persistence of brucellosis in humans attributed to the infection of domestic cattle, camels, goats and sheep [3].

Caused by various species of the bacteria *Brucella* [4], the disease can be transmitted to animals and humans with exposure to infected animals or ingestion of contaminated water, food, and dust, etc [2]. Brucellosis survival in the environment ranges from one to four months in the contaminated soil and water, and two months in milk and meat [5]. However the *Brucella* bacteria is easily killed by direct sunlight, high temperature and effective disinfection [6].

Historically the scientist David Bruce (1887) was the first to isolate the organism from the spleen of a British solider with Malta fever and named it Microccocus melitensis and genus the *Brucella* was named after his name. Zammit (1905) identified goats as the reservoir of brucellosis. Malta fever, Mediterranean fever, Mediterranean gastric fever, remittent and goats fever were often synonymously used for undulant fever [7].

1.2 Brucellosis in animal population

Prevalence of brucellosis in both the wildlife (such as bison, buffalo, elk) and domesticated animals (such as sheep, goats, camels, pigs and cattle) is well documented. Transmission of the disease in both domesticated and wild animals occurs through direct contact transmission-when a susceptible animal comes into contact with an infectious animal or indirect contact transmission-when animals ingest contaminated forages or the excrement containing large quantities of bacteria, generally discharged by infected animals [8]. Vertical transmission of the bacteria from the mother to the offspring has also been confirmed to be another dominant mode of transmission of the disease in animal population [38].

In both domesticated and wild animals, the bacteria induces abortion, sterility, vertical transmission, and poor growth of offspring [8]. Control measures available to prevent animal infection are vaccination and culling of infected animals. Vaccination is often regarded as the first step in the control of the disease [5]. Although the disease is less fatal in adult animals it can lead to chronic infection [10].

In public farms where there is mixed feeding of domesticated species, cross infection has been reported [5]. Cross transmission of brucellosis from wildlife to domestic animals has also been observed in many parts of Africa where the disease is endemic [10]. Pastoralism and poor maintenance of game reserves have been attributed to cross transmission of the disease between the wild and domestic animal in Africa.

1.3 Brucellosis in human

The occurrence of brucellosis in humans predominantly depends on the occurrence of the disease in both wild and domestic species. Precisely, humans acquire the disease through exposure to infected animals or their products such as the consumption of raw milk [10]. Clinical signs of the disease in humans include undulant fever, tiredness, night sweats, headaches and chills may be present for as long as three months before illness becomes so severe and debilitating as to require medical attention [10].

Although mortality due to infection is rare the illness can last for several years [14]. Tetracyclines and a parenteral aminoglycoside or tetracyclines and rifampin are the common regimens that are used to treat brucellosis infection. Since human

to human transmission of the disease is negligible, it follows that human brucellosis is not sustainable. Hence effective prevention and control of the disease in humans requires consistent, concurrent and long-term programs that target eradication of the disease in animal population.

1.4 Seasonality in brucellosis transmission

Like many other infectious diseases, brucellosis is significantly influenced by seasonal changes, and prior field studies have already demonstrated a strong correlation between brucellosis outbreaks and seasonal oscillations [27, 28, 26]. For example, a recent analysis of brucellosis datasets in a few countries [26] reveals that there is a marked seasonal variation in the incidence of acute brucellosis, with most cases occurring in the spring and summer. Factors such as periodic changes in temperature, seasonal precipitation which directly affects the availability of forage, environmental fluctuations in humidity and exposure to UV light which impact the survival of Brucella, and seasonal rituals in Africa which are associated with animal migration and slaughtering, all contribute to seasonal fluctuations in the transmission and spread of brucellosis.

1.5 Review of mathematical models for brucellosis

Mathematical modeling has the potential to shed light on mechanisms of transmission and the complexity of epidemiological characteristics of infectious diseases, and can highlight new approaches to prevent and control future epidemics [33]. The first account of mathematical modeling of spread of disease was carried out in 1766 by Daniel [23]. Bernoulli created a mathematical model to defend the practice of inoculating against smallpox. His calculations showed that universal inoculation against smallpox would increase the life expectancy from 26 years 7 months to 29 years 9 months [24].

Daniel Bernoulli's research preceded our modern understanding of germ theory, and it was not until the work of Ronald Ross into the spread of malaria, that modern theoretical epidemiology began. This was soon followed by the work of A. G. McKendrick and W. O. Kermack, whose paper A Contribution to the Mathematical Theory of Epidemics was published in 1927. A simple deterministic (compartmental) model was formulated in this paper. The paper [25] was successful in predicting the behavior of outbreaks very similar to that observed in many recorded epidemics.

In recent years, several mathematical models have been proposed to study the transmission dynamics of brucellosis [5, 30, 32, 33, 28, 34, 30, 35, 36, 37, 39, 38, 40, 41, 86]. Jorge and Raul [40] developed a dynamic model that comprise of susceptible, aborting infectious, infectious carriers and immunized animals with a view to investigate the transmission dynamics of brucellosis among animal population, and their findings concluded that the dynamics of aborting infectious at the initial time is much more rapid then the formation of infectious carriers.

Zinsstag et al. [37] studied cross transmission of brucellosis between livestock and humans. They proposed a dynamic model which subdivided the population of interest into the following epidemiological classes: susceptible, seropositive and immunized, and their findings confirmed that the occurrence of brucllosis in human predominantly depends on the occurrence of brucellosis in animal population. Alnseba et al. [41] proposed an susceptible, infected and the contaminated environment dynamical model for brucellosis epidemic in ovine with direct and indirect transmission, and their work indicated that environmental contamination plays an important role in the persistence of brucellosis. Hou and co-workers [30] employed a system of ordinary differential equations (ODEs) to model the transmission of brucellosis and the effects of vaccination on brucellosis prevention and intervention, their results indicated that a combination of intervention methods (vaccination and environmental decontamination) is an effective strategy in controlling animal brucellosis.

Li et al. [32] proposed a model to investigate the transmission of brucellosis among sheep and from sheep to humans, and their findings indicated that a combination of intervention methods (such as prohibiting mixed feeding, vaccination, and detection and elimination) is useful in controlling human brucellosis.

Although these studies produced many useful results and improved the existing knowledge on brucellosis dynamics, several challenges remain in the mathematical modeling of brucellosis, and some of these challenges will be explored in this thesis.

1.6 Motivation

Despite having been successfully controlled or eradicated in many developed nations the disease continues to pose a formidable challenge in many low-income countries such as Ethiopia, Chad, Tanzania, Nigeria, Uganda, Kenya, Zimbabwe and Somalia. Considering that agriculture is the backbone of the economy of the aforementioned countries, it is therefore essential to gain a better and more comprehensive understanding of effective ways to control brucellosis. Since mathematical models can be useful tools to provide a comprehensive guide to epidemiologist and policy-makers on effective ways to control brucellosis, the topic become worth studying.

1.7 Objectives of the research project

The aim of this study is to formulate mathematical epidemiological models that can be useful and important tools for studying the transmission dynamics of brucellosis in animal population. In this study, we target animal population since human brucellosis is not sustainable. The specific objectives of this research project are

- (i) To model and analyze the effects of seasonality on brucellosis transmission.
- (ii) To investigate the effects of vertical transmission as well as disease control strategies on controlling the spread of the disease in both periodic and nonperiodic environment.
- (iii) To investigate the role of spatial and temporal heterogeneities on the dynamics of brucellosis.
- (iv) To evaluate the impact of short-term animal mobility on the transmission dynamics of brucellosis infection.
- (v) To investigate the dynamics and stability of brucellosis model with two discrete delays.

1.8 Thesis outline

The organization of this thesis is as follows: In Chapter 2, we introduce some mathematical preliminaries relevant to the thesis. In Chapter 3, we present a mathematical model for the transmission dynamics of brucellosis that incorporates the effects of seasonality. In Chapter 4, we introduce a mathematical modeling that seeks to improve our quantitative understanding of the influence of chronic brucellosis and culling control in periodic and non-periodic environments. In Chapter 5, we propose a model to investigate the transmission dynamics of brucellosis, incorporating both the spatial and seasonal variations. In Chapter 6, we consider a dynamical model to describe the role of short-term animal movements on the persistence of brucellosis. In Chapter 7, we present a new mathematical model of brucellosis infection, with two discrete delays. Finally in Chapter 8 we conclude by presenting a general conclusion and future remarks on brucellosis dynamics.

Chapter 2

Mathematical preliminaries

2.1 Introduction

This chapter introduces some of the key mathematical theories, methodologies and classical results from dynamical systems theory relevant to the thesis.

2.2 Stability

A system without stability would be a poor model, so some kind of stability is needed in modeling. There are two types of stability and these concepts are of great importance in applications of differential equations; That is stability with respect to perturbation of initial values for fixed equations and stability with respect to perturbation of the equations itself. In the first case we say the system is persistent and second case robust. The equilibrium point is locally stable if all solutions which start near \bar{x} (implying that the initial conditions are in the neighborhood of \bar{x}) remain near \bar{x} for all future time.

2.2.1 Stability: Basic definition

Consider the following definitions

Definition 1 (Autonomous system [46]). Let Ω be a subset of \mathbb{R}^n . Consider the autonomous differential equation defined by:

$$\dot{x}(t) = f(x), \ x \in \Omega, \tag{2.1}$$

where the dot represents the differentiation with respect to time $(\frac{d}{dt})$. Suppose that $f: \Omega \subset \mathbb{R}^n \to \mathbb{R}^n$ is continuous and satisfies the conditions as a solution of (2.1), is unique and continuously depend on the initial conditions. The stationary or equilibrium points of the system (2.1) are the points $x_0 \in \Omega$ satisfying $f(x_0) = 0$. For each $x \in \Omega$, we denote by $f_t(x)$ the solution of the system (2.1) satisfying $f_0(x) = x$. We suppose that f satisfies the conditions that $f_t(x)$ is continuous in (t, x).

Definition 2 (Equilibrium point). A point $\bar{x} \in \mathbb{R}^n$ is an equilibrium point of the system (2.1) if $f(\bar{x},t) = 0$.

Definition 3 (Lyapunov stability [47]). Let $\bar{x} \in \omega$ be an equilibrium point. System (2.1) is stable or Lyapunov stable at \bar{x} or \bar{x} is a stable equilibrium position for (2.1), if for each $\epsilon > 0$ there exists a positive real number δ such that for each x with $|x - \bar{x}| < \delta$, the solution f(t(x)) is defined for all $t \geq 0$ and satisfies $|f(t(x)) - \bar{x}| < \epsilon$ for all t > 0, when (2.1) is not Lyapunov stable at \bar{x} , we say that it is unstable at \bar{x} .

Definition 4 (Attractivity). The steady state \bar{x} is said to be attractive or system (2.1) is attractive at \bar{x} if there exists neighborhood $U \subset \Omega$ of \bar{x} such that for any initial condition x belonging to U, the corresponding solution f(t(x)) of (2.1) is defined for all $t \geq 0$ and tends to \bar{x} as t tends to infinity, that is $\lim_{t \to +\infty} f(t(x)) = \bar{x}$.

Definition 5 (Asymptotic stability). We say that \bar{x} is stable if solutions starting close to it at a given time, remain close to it for all future times. It is said to be asymptotically stable if nearby solutions actually converge to \bar{x} as $t \to +\infty$, that means it is Lyapunov stable and attractive.

Definition 6 (Exponential stability). The system (2.1) is exponentially stable, (globally stable respectively) at \bar{x} , if there exits two positive constants K and λ such that $|f(x) - \bar{x}| < \epsilon < K|x - \bar{x}|e^{\lambda t}$ for all x in a neighbourhood of \bar{x} (respectively for all $x \in \Omega$) and all positive time t.

Definition 7 (Attractor). This refers to a compact, nonempty set K which attracts some neighborhood N of itself. It is assumed that K is invariant, that is, it contains the orbits of all its equilibrium points. The neighbourhood N can always be chosen to be invariant also by simply replacing it with the union of all its points. The largest

of such N, ie. the set of all points attracted to K is called the basin of K. An attractor enjoys some kind of stability. Any trajectory starting near it may wonder away, but eventually returns to approach it asymptotically

Definition 8 (Global stability). An equilibrium point \bar{x} is globally asymptotically stable if it is stable for all initial conditions $x_0 \in \mathbb{R}^n$.

2.2.2 Dynamical properties

Definition 9 (Invariant set). Given the dynamical system $\dot{x} = h(x)$ and a trajectory $x(t, x_0)$ where x_0 is the initial point. Let $\mathcal{D} \triangleq \{x \in \mathbb{R}^n | \phi = 0\}$ where ϕ is a real valued function. Then the set \mathcal{D} is said to be positively invariant if $x_0 \in \mathcal{D}$ implies that $x(t, x_0) \in \mathcal{D}$ for all $t \geq 0$. This means that once a trajectory of the system enters \mathcal{D} , it will not leave it again.

Definition 10 (Orbit). The orbit $\mathcal{O}^+(x_0)$ is called a positive orbit if for all x_0 in the set $\{x(t,x_0)|t\geq 0\}$, the orbit is defined by:

$$\mathcal{O}^+(x_0) = \{ x(t, x_0) | t \in \mathbb{R} \}.$$

The set is positively invariant if $\mathcal{O}^+(M) \subset M$, and invariant if it contains the orbits of each of its points.

Definition 11 (ω -limit point). A point l is called an ω -limit point of $f_t(x)$ if there exists a sequence $t_n \in \mathbb{R}$ such that $\lim_{n \to +\infty} t_n = +\infty$ and $\lim_{n \to +\infty} f_{t_n}(x) = l$. The set of all ω -limit points is the ω -limit set of x and is denoted by $\omega(x)$. This means that the sequence t_n tends to $+\infty$ as n tends to infinity and the flow through x tends to l as n tends to $+\infty$.

Theorem 2.2.1 If the positive orbit $\mathcal{O}^+(x_0)$ is bounded then the set $\omega(\mathcal{O}^+)$ of ω -limit points is non- empty, connected, compact and invariant.

Theorem 2.2.2 (Poincaré-Bendixon). Consider the equation $\dot{x} = h(x)$ in \mathbb{R}^2 . Suppose that \mathcal{O}^+ is a bounded positive orbit and $\omega(\mathcal{O}^+)$ does not contain equilibrium points. Then $\omega(\mathcal{O}^+)$ is a periodic orbit. If $\omega(\mathcal{O}^+) \neq \mathcal{O}^+$ this periodic orbit is called a limit cycle.

Definition 12 For the C^1 autonomous system $\dot{x} = h(x)$ and an equilibrium point x_0 , the linearised system in x_0 is defined by

 $\dot{x} = Dh(x_0)x$, where $Dh(x_0)$ is the derivative of h at x_0 .

Theorem 2.2.3 (Poincaré-Lyapunov [47]). Consider that a C^1 system $\dot{x} = h(x)$ and an equilibrium point x_0 .

- 1. If $Dh(x_0)$ has the real parts of all its eigenvalues negative, then x_0 is asymptotically stable.
- 2. If $Dh(x_0)$ has at least one of its eigenvalues with real positive parts, then x_0 is unstable.
- 3. If $Dh(x_0)$ has one eigenvalue equal to zero and all other negative, then x_0 is a critical point where the system changes its behavior from stable to unstable.

2.3 Monotone systems

Consider the system (2.1) where f is \mathcal{C}^1 and Ω is an open set in \mathbb{R}^n .

- 1. f is said to be of type K in Ω if for each i; $f_i(a) \leq f_i(b)$ for any two points a and b in Ω satisfying $a_k \leq b_k$ and $a_i = b_i$, $(i \neq j \text{ and } i, k = 1, 2, ..., n)$;
- 2. We say that Ω is l-convex if $tx+(1-t)y\in\Omega$, for all $t\in[0,1]$ where $x,y\in\Omega$ and $x\leq y$;
- 3. The system (2.1) is said to be cooperative system if Ω is l-convex and

$$\frac{\partial f_i(x)}{\partial x_i} \ge 0, \ i \ne j, \ x \in \Omega$$

4. We say that system (2.1) is competitive system if Ω is l-convex and

$$\frac{\partial f_i(x)}{\partial x_i} \le 0, \ i \ne j, \ x \in \Omega$$

2.3.1 Monotone dynamical system

Consider a dynamical system with a flow $\psi_t: x \to \psi_t(x)$. This dynamical system is said to be monotone if it is defined on an ordered metric space with the following property;

$$t \ge 0, \ x \le y \Longrightarrow \psi_t(x) \le \psi_t(y)$$

It is said to be strongly monotone if

$$t \ge 0, \ x < y \Longrightarrow \psi_t(x) \ll \psi_t(y)$$

We say the system is anti-monotone if

$$t \ge 0, \ x \le y \Longrightarrow Df(x) > Df(y) \ and$$

It is strictly anti-monotone if

$$t \ge 0, \ x < y \Longrightarrow Df(x) > Df(y).$$

2.3.2 Triangular system

A triangular system is precisely an $\mathbb{R}^n \times \mathbb{R}^m$ system of the form

$$\begin{cases} \dot{x}_1 = h_1(x_1), \\ \dot{x}_2 = h_2(x_1, x_2), \end{cases}$$
 (2.2)

where h_1 is a map from \mathbb{R}^n to \mathbb{R}^n and h_2 from \mathbb{R}^n to \mathbb{R}^m . Suppose that the conditions for existence and uniqueness of solutions are satisfied, for example h_1 and h_2 are \mathcal{C}^1 . The trajectories of the system have the system projection on $\mathbb{R}^n \times \{0\}$ and hence the name triangular. Notice that the Jacobian of this system is a lower triangular block, and it is also said to be hierarchical.

Theorem 2.3.1 (Vidyasagar). Consider the following C^1 system

$$\begin{cases} \dot{x}_1 = h_1(x_1), \\ \dot{x}_2 = h_2(x_1, x_2), \end{cases}$$
 (2.3)

If the origin of \mathbb{R}^n is globally asymptotically stable for the system $\dot{x}_1 = h_1(x_1)$ in \mathbb{R}^n and the origin of \mathbb{R}^m is globally asymptotically stable for $\dot{x}_2 = h_x(0, x_2)$ on \mathbb{R}^n , then the origin of $\mathbb{R}^n \times \mathbb{R}^m$ is asymptotically stable. Further if all trajectories are bounded, then the origin is globally asymptotically stable for (2.3) on $\mathbb{R}^n \times \mathbb{R}^m$.

2.4 Lyapunov methods

The Lyapunov function has a major role in the study of dynamical systems stability. Let $\mathcal{L}: \Omega \subset \mathbb{R}^n \to \mathbb{R}$ be a continuous function.

Definition 13

We consider the following definitions

- 1. The function $\mathcal{L}(x)$ is said to be positive definite if $\mathcal{L}(x) = 0$ and $\mathcal{L}(x) > 0$ in a neighborhood Ω_0 of x_0 for all $x \neq x_0$ in the neighborhood.
- 2. The function $\mathcal{L}(x)$ is said to be negative definite if $-\mathcal{L}(x)$ is positive definite.
- 3. The function $\mathcal{L}(x)$ is said to be semi-positive if $\mathcal{L}(x) = 0$ and $\mathcal{L}(x) \geq 0$ in a neighborhood Ω of x_0 .

Theorem 2.4.1 (Lyapunov Theorem). Let $\mathcal{L}(x)$ be a function

- If a function $\mathcal{L}(x)$ is positive definite and $\dot{\mathcal{L}}(x)$ is negative semi-definite in Ω , then the equilibrium point x_0 is stable for the system (2.1)
- If the function $\mathcal{L}(x)$ is positive definite and $\mathcal{L}(x)$ is negative definite in Ω , then the equilibrium point x_0 is asymptotically stable for the system (2.1)

In this theorem to show that an equilibrium point x_0 is stable, it is sufficient to find a Lyapunov function for the point x_0 . Moreover, to use the original Lyapunov theorem to show the asymptotic stability of a given system, we must find a function $\mathcal{L}(x)$ whose derivative is non-negative definite and the derivative $\dot{\mathcal{L}}(x)$ is negative definite. In a general case, this is not straightforward. The condition on the derivative $\dot{\mathcal{L}}(x)$ can be relaxed by using the LaSalle Invariance principle introduced in the next section.

2.4.1 LaSalle invariance principle

Theorem 2.4.2 (LaSalle Invariance Principle [45, 46]). Let $\Omega \subset \mathbb{R}^n$ be a compact set that is positively invariant with respect to the system (2.1). Let $\mathcal{L}(x) : \Omega \to \mathbb{R}$ be continuously differentiable such that $\dot{\mathcal{L}}(x) \leq 0$ in Ω . Let S be the set of all points

in Ω where $\mathcal{L}(x) = 0$. Let L be the largest invariant set in S. Then every solution starting in Ω approaches L as $t \to \infty$.

This theorem is one of the important tools for systems analysis, and is different from Lyapunov, as it does not require $\mathcal{L}(x)$ to be non-negative definite and $\dot{\mathcal{L}}(x)$ to be negative definite. However, it only provides information on the attractiveness of the considered system at the equilibrium x_0 . For example, it can be used to prove that the solutions tend toward an equilibrium point when the set L is reduced to that equilibrium point. It does not indicate whether this equilibrium is stable or unstable. To establish asymptotic stability of an equilibrium $x_0 \in \Omega$, we use the following corollary which is a consequence of the LaSalle invariance principle.

Corollary 2.4.1 (LaSalle,[46]). Let us consider the compact set $\Omega \in \mathbb{R}^n$ with $x_0 \in \Omega$. Let $\mathcal{L} : \mathbb{U} \to \mathbb{R}$ be a continously differentiable non-negative definite function such that $\mathcal{L}(x) \leq 0$ in \mathbb{U} . Let $S = \{x \in \mathbb{U} | \dot{\mathcal{L}}(x) = 0\}$. Assume that the largest positively invariant set contained in S is reduced to the point x_0 . Then x_0 is an asymptotically stable equilibrium point for the system (2.1). If these conditions are satisfied for $\mathbb{U} = \Omega$, if in addition \mathcal{L} is in Ω ie. $\lim \mathcal{L} = +\infty$ when $d(x, \frac{\partial}{\partial x}\Omega) + \|x\| \to +\infty$ then all trajectories are bounded for $t \geq 0$ and x_0 is a globally stable equilibrium point for the system (2.1).

Corollary 2.4.2 Under the assumptions of the previous theorem, if the set L is reduced to the point $x_0 \in \Omega$, then x_0 is a globally stable equilibrium point for the system (2.1) defined on Ω .

2.5 Matrices

Definition 14 (Stability Modulus, Spectral radius). Let P be a square matrix. We denote by Spec(P) the set of all eigenvalues of P. The stability modulus of P is the number defined by

$$\alpha(P) = \max\{Re(\lambda) : \lambda \in Spec(P)\}$$

The matrix P is said to be stable if $\alpha(P) < 0$. The spectral radius is the real number $\rho(P)$ defined by

$$\rho(P) = \max_{\lambda \in Spec(P)} |\lambda|.$$

We say that a matrix P is stable if its eigenvalues have strictly negative real parts. Such a matrix is also said to be Hurwitz.

2.5.1 Lozinskii measures

Let |.| denote a vector norm in \mathbb{R}^n and the corresponding matrix norm it induces. The *Lozinskii Measure* m on matrices with respect to |.| is defined by

$$m(Q) = \lim_{h \to 0+} \frac{|I_n + hA| - 1}{h}$$

for an $n \times n$ matrix A and identity matrix I_n . For properties and calculations of Lozinskii we refer the reader to [48].

2.5.2 The second additive compound matrix

Let \mathcal{A} be a linear operator on \mathbb{R}^n and also denote its matrix representation with respect to standard basis of \mathbb{R}^n . Let $\wedge^2 \mathbb{R}^n$ denote the exterior product of \mathbb{R}^n . \mathcal{A} induces canonically a linear operator $\mathcal{A}^{[2]}$ on $\wedge^2 \mathbb{R}^n$: for $u_1, u_2 \in \mathbb{R}$, define

$$\mathcal{A}^{[2]}(u_1 \wedge u_2) = \mathcal{A}(u_1) \wedge u_2 + u_1 \wedge \mathcal{A}(u_2)$$

and extend the definition over $\wedge^2\mathbb{R}$ by linearity. The matrix representation of $\mathcal{A}^{[2]}$ with respect to canonical basis in $\wedge^2\mathbb{R}^n$ is called the second additive compound matrix of \mathcal{A} . This is a $(n \times n)$ matrix and satisfies the property $(\mathcal{A} + \mathcal{B})^{[2]} = \mathcal{A}^{[2]} + \mathcal{B}^{[2]}$. In the special case when n = 2, we have $\mathcal{A}_{2 \times 2}^{[2]} = tr \mathcal{A}$. In general, each entry of $\mathcal{A}^{[2]}$ is a linear expression of those of \mathcal{A} . For example, when n = 3, the second additive compound matrix of

$$\mathcal{A} = \begin{bmatrix} a_{11} & a_{12} & a_{13} \\ a_{21} & a_{22} & a_{23} \\ a_{31} & a_{32} & a_{33} \end{bmatrix} \quad \text{is} \quad \mathcal{A}^{[2]} = \begin{bmatrix} a_{11} + a_{22} & a_{23} & -a_{13} \\ a_{32} & a_{11} + a_{33} & a_{12} \\ -a_{31} & a_{21} & a_{22} + a_{33} \end{bmatrix} \quad (2.4)$$

For detail discussion of compound matrices and their properties see [49].

2.6 Calculation of basic reproduction number

Definition 15 (Basic Reproduction Number \mathcal{R}_0). The basic reproduction number, denoted by \mathcal{R}_0 , is the expected number of secondary cases produced, in a completely

susceptible population, by a typical infected individual. If $\mathcal{R}_0 < 1$ then on average an infected individual produces less than one new infected individual over the course of its infectious period and the infection can not grow. If $\mathcal{R}_0 > 1$, then each infected individual produces, on average, more than one new infection, and the disease can invade the population.

To calculate basic reproduction number we demonstrate here the method developed by van den Driessche and Watmough [50]. Consider an epidemiological model with heterogeneous population, whose individuals can be grouped into n homogeneous compartments. Let $x = (x_1, \ldots, x_n)^t$ with each $x_i \geq 0$, be the number (or concentration) of individuals, in each compartment. The compartments are classified in such a way that the first m compartments corresponds to infected individuals, while others say $i = m + 1, \ldots, n$ are free of infection (susceptible). We define \mathbf{X}_S to be the set of all disease free states. That is

$$\mathbf{X}_S = \{x \ge 0 | x_i = 0, i = 1, \dots, m\}$$

Let $\mathcal{F}_i(x)$ be the rate of appearance of new infections in compartment i, $\mathcal{V}_i^+(x)$ be the rate of transfer of individuals into compartment i by all other means (for example, birth, immigration), and $\mathcal{V}_i^-(x)$ be the rate of transfer of individuals out of compartment i (for example, deaths, recovery and emigration). Thus the dynamics of the compartments is is governed by the following ordinary differential system:

$$\dot{x}_i = f_i(x) = \mathcal{F}_i(x) - \mathcal{V}_i(x), i = 1, \dots, n,$$

where $\mathcal{V}_i(x) = \mathcal{V}_i^-(x) - \mathcal{V}_i^+(x)$.

For biological feasible domain we have the following assumptions:

- (a) Since each function represents a directed transfer of individuals, they are all non-negative. Thus if $x \geq 0$, then $\mathcal{F}_i(x), \mathcal{V}_i^+(x), \mathcal{V}_i^-(x) \geq 0$ for $i = 1, \ldots, n$.
- (b) If a compartment is empty, then there can be no transfer of individuals, out of the compartment by death, infection nor any other means. Thus if $x_i = 0$ then $\mathcal{V}_i^-(x) = 0$. In particular, if $x \in \mathbf{X}_S$, then $\mathcal{V}_i^-(x) = 0$ for $i = 1, \ldots, m$.
- (c) $\mathcal{F}_i(x) = 0$, if i > m, that is, the incidence of infection for uninfected compartment is zero.

- (d) We assume that if the population is free of disease then the the population will remain free. That is, there is no (density independent) immigration of infectives and the condition is stated as follows: If $x \in \mathbf{X}_S$ then $\mathcal{F}_i(x) = 0$ and $\mathcal{V}_i^+(x) = 0$ for $i = 1, \ldots, m$.
- (e) Consider a population near the DFE x_0 . If the population remains near the DFE, that is if the introduction of a few infective individual does not result in an epidemic then the population will return to the DFE according to the linearized system

$$\dot{x} = Df(x_0)(x - x_0).$$

where $Df(x_0)$ is the Jacobian that is $\frac{\partial f_i}{\partial x_j}$. Thus if $\mathcal{F} = 0$, then all eigenvalues of $Df(x_0)$ have negative real parts.

The following results is the partition matrix $Df(x_0)$

Lemma 2.1 If x_0 is DFE and $f_i(x)$ satisfies (a) through (e), then the derivatives $D\mathcal{F}(x_0)$ and $D\mathcal{V}(x_0)$ are partitioned in blocks as follows

$$D\mathcal{F}(x_0) = \begin{bmatrix} F & 0 \\ 0 & 0 \end{bmatrix} \qquad and \qquad D\mathcal{V}(x_0) = \begin{bmatrix} V & 0 \\ J_3 & J_4 \end{bmatrix}$$
 (2.5)

where F and V are the $m \times m$ matrices defined by

$$F = \begin{bmatrix} \frac{\partial \mathcal{F}_i}{\partial x_j}(x_0) \end{bmatrix} \quad and \quad V = \begin{bmatrix} \frac{\partial \mathcal{V}_i}{\partial x_j}(x_0) \end{bmatrix} \quad with \quad 1 \le i, j \le m.$$
 (2.6)

F is non-negative, V is non-singular M-matrix and all eigenvalues of J_4 have positive real part

For the complete prove of this theorem see [50].

Definition 16 (Basic Reproduction Number, \mathcal{R}_0). The basic reproduction number \mathcal{R}_0 is the spectral radius of the next generation matrix FV^{-1} , that is

$$\mathcal{R}_0 = \rho(FV^{-1}).$$

The entries of FV^{-1} has a meaningful definition of \mathcal{R}_0 . Consider the infected individual introduced into compartment k of disease free population. The (j, k) entry

of V^{-1} is the average length of time this individual spends in compartment j during its life time, assuming that the population remain near DFE and barring reinfection. The (i,j) entry of F is the rate at which infected individuals in compartment j produce new infection in compartment i. Hence, the (i,k) entry of the product FV^{-1} is the expected number of new infections in compartment i produced by the infected individual originally introduced into compartment k. The matrix FV^{-1} is called the next generation matrix for the model and set $\mathcal{R}_0 = \rho(FV^{-1})$, where $\rho(A)$ is the spectral radius of matrix A.

Chapter 3

Modeling and analyzing the effects of seasonality on brucellosis infection

3.1 Introduction

Brucellosis, a highly contagious disease of humans and animals, is caused by various species of the genus *brucella* [5]. It is one of the most common bacterial zoonoses worldwide and it poses a major threat to human and animal health, and animal production [51].

Humans are usually infected through consumption of non-pasteurized dairy products and close-contact manipulation of infected animals. In humans, brucellosis is life threatening and exhibits nonspecific symptoms, including intermittent fever, weight loss, depression, hepatomegaly, and splenomegaly [32, 52]. Arthritis, spondylitis, osteomyelitis, epididymitis, and orchitis, as well as more severe complications such as neurobrucellosis, liver abscesses, and endocarditis, are also common in some patients [52]. In animals, the transmission occurs when susceptible animals are exposed to infected animals or through ingestion of contaminated water, dust, improperly treated dairy products and so on [32]. Meanwhile, brucellosis is primarily a reproductive disease and is associated with abortion, retained placenta, and impaired fertility in the principal animal hosts [52].

Although tremendous progress has been made in controlling the disease, there is still a number of countries/regions where the infection persists in domestic animals and, consequently, transmission to the human population frequently occurs. Recent reports on animal infections [32] demonstrate that the disease is endemic in the Middle East, Asia, Africa, Latin America, the Mediterranean Basin, and the Caribbean.

Recently, several mathematical models have been developed to analyze brucellosis outbreaks in an effort to better understand the intrinsic disease transmission and determine the strength and weakness of current prevention and control strategies [5, 30, 32, 33, 28, 34, 30, 35, 36, 37, 39, 38, 40, 41]. In particular, Hou and co-workers [30] proposed the following system of ordinary differential equations to model the transmission dynamics of brucellosis:

$$\begin{cases}
\dot{S}(t) = A - \beta_1 [E(t) + I(t)] S(t) - \beta_2 B(t) S(t) - (\mu + \tau) S(t) + kH(t), \\
\dot{H}(t) = \tau S(t) - \gamma \beta_1 [E(t) + I(t)] H(t) - \gamma \beta_2 H(t) B(t) - (\mu + k) H(t), \\
\dot{E}(t) = \beta_1 [S(t) + \gamma H(t)] [E(t) + I(t)] + \beta_2 [S(t) + \gamma H(t)] B(t) - (\sigma + \mu) E(t), \\
\dot{I}(t) = \sigma E(t) - (\mu + c) I(t), \\
\dot{B}(t) = \beta_3 (E + I) - (d + \delta) B,
\end{cases}$$
(3.1)

where S(t), H(t), E(t), and I(t) are the numbers of the susceptible, vaccinated, exposed (latent), and infectious animals at time t, respectively. The total animal population at time t is N(t) = S(t) + H(t) + E(t) + I(t). Further, B(t) is the concentration of brucella in the environment, the parameter A is the recruitment rate, μ is the natural mortality rate, c is the disease-related death rate, τ is the vaccination rate, k is the immunity waning rate, k is the direct disease transmission rate, k is the indirect disease transmission rate, k is the indirect disease transmission rate, k is the modification factor, k is the incubation rate, and k represents pathogen decay rate. As highlighted in prior studies [30, 39], exposed animals have no clinical manifestations and, without loss of generality, they can be assumed to have the same infectivity as that of the infectious animals.

This work and several other studies (see, for example, [5, 32]) have certainly produced many useful results and improved the existing knowledge on brucellosis dynamics. One of the limitations of these models, however, is that they assumed that

the model parameters are constant in time, implying that the disease contact rates and pathogen population growth rate, etc., all take fixed values independent of time. In fact, like many other infectious diseases, brucellosis is significantly influenced by seasonal variations, and prior studies have demonstrated a strong connection between brucellosis infection and seasonal variations [26, 27, 28]. Factors such as the seasonal availability of forage which in turn lead to nomadic animal farming, may be attributed to seasonality of brucellosis dynamics. Further, the survival of brucella in the environment depends critically on humidity, temperature and exposure to UV light. For example, its survival in ideal environments is reported to last up to 135 days, while a field study in the spring in Montana, USA found that brucella abortus survived in the environment for only 21–81 days [27, 28]. In addition, an analysis of brucellosis datasets in countries with temperate or cold climates [26] underscores that there is a marked seasonal variation in the incidence of acute brucellosis, with most cases occurring in the spring and summer. Seasonal variations also lead to periodic changes in pastures that induce animal movement and seasonal migration, resulting in disease dynamics not captured by mathematical models with constant model parameters.

From an applied perspective, understanding the mechanisms that link seasonal variations to diseases dynamics may aid in forecasting the long-term human and animal health risks, in developing an effective public health program, and in setting objectives for utilizing limited resources more effectively [53]. So far no published work has discussed the influence of seasonal variation on the transmission dynamics of brucellosis. The purpose of the present chapter is to present a general brucellosis model in a periodic environment, by extending the autonomous model proposed in [30] to include seasonal variation in both the pathogen dynamics and the disease transmission pathways. We will then conduct a careful analysis on this periodic model, with a focus on its threshold dynamics characterized by the associated basic reproduction number. In addition, we will explore optimal disease control measures based on animal vaccination and environmental decontamination to contain brucellosis outbreaks, through an optimal control study. Our results are new and, to our knowledge, very little work has appeared so far on the optimal control study of periodic epidemiological models.

The remainder of this chapter is organized as follows. In Section 3.2, we present details of our periodic brucellosis model, followed by an analysis on disease extinction and persistence that are determined by the basic reproduction number. In Section 3.3, we perform an optimal control study on the use of animal vaccination and environmental decontamination, through both mathematical analysis and numerical simulation. Finally, we conclude the chapter with some discussion in Section 3.5.

3.2 Model with seasonal variation

3.2.1 Model framework

Motivated by the model (3.1), we propose the following non-autonomous dynamical system to describe the transmission dynamics of brucellosis in a time-periodic environment:

$$\begin{cases}
\dot{S}(t) &= A - \beta_1(t)[E(t) + I(t)]S(t) - \beta_2(t)B(t)S(t) - (\mu + \tau)S(t) + kH(t), \\
\dot{H}(t) &= \tau S(t) - \gamma \beta_1(t)H(t)[E(t) + I(t)] - \gamma \beta_2(t)H(t)B(t) - (\mu + k)H(t), \\
\dot{E}(t) &= \beta_1(t)[S(t) + \gamma H(t)][E(t) + I(t)] + \beta_2(t)[S(t) + \gamma H(t)]B(t) \\
&- (\sigma + \mu)E(t), \\
\dot{I}(t) &= \sigma E(t) - (\mu + c)I(t), \\
\dot{B}(t) &= \beta_3(t)(E + I) - d(t)B(t) - \delta B(t).
\end{cases}$$
(3.2)

All the variables and model parameters are assumed to be positive and they retain the same definitions as in model (3.1). Model parameters and their baseline values in Table 3.1. The model flow diagram is depicted in Figure 3.1.

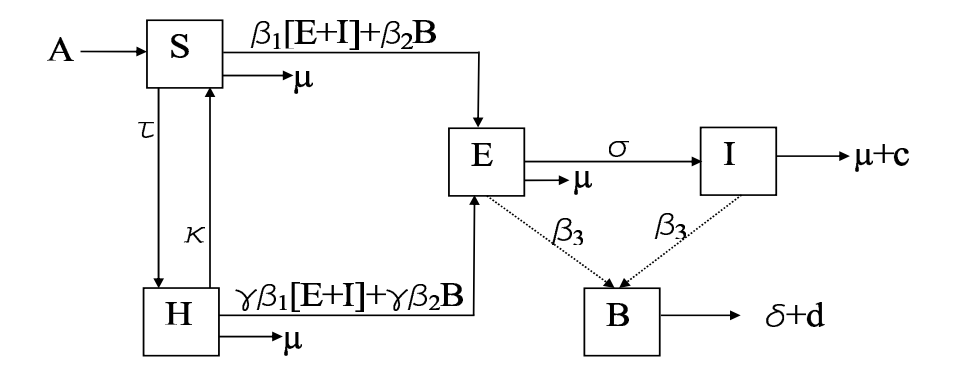


Figure 3.1: Flowchart illustrating the dynamics of brucellosis.

Further, we assume that $\beta_j(t)$, (j = 1, 2, 3) are periodic continuous functions in t with a period $\omega > 0$ (specifically, $\omega = 12$ months). Thus,

$$\beta_j(t) = a_j \left[1 + b_j \sin\left(\frac{\pi t}{6}\right) \right], \tag{3.3}$$

where a_j (j = 1, 2, 3) is the baseline value or the times average of $\beta_j(t)$, and b_j $(0 < b_j < 1)$ denotes the magnitude of seasonal fluctuations. In addition, we define

$$d(t) = d_0 \left[1 + d_1 \sin\left(\frac{\pi t}{6}\right) \right], \tag{3.4}$$

Table 3.1: Parameters and values

Symbo	ol Definition	Value	Units	Source
c	Elimination rate caused by brucellosis	s 0.15	$year^{-1}$	[30]
δ	Environmental decontamination rate	25	$year^{-1}$	[30]
a_1	Averaged direct transmission rate	1.48×10^{-8}	$animal^{-1}year^{-1}$	[30]
a_2	Averaged indirect transmission rate	1.7×10^{-10}	$pathogen^{-1}year^{-1}$	[30]
a_3	Averaged $brucella$ shedding rate	15	$pathogen\ animal^{-1}year^{-1}$	[30]
d_0	Averaged pathogen decay rate	3.6	$year^{-1}$	[30]
b_1	Amplitude of oscillation in $\beta_1(t)$	0.8	-	Assumed
b_2	Amplitude of oscillation in $\beta_2(t)$	0.8	-	Assumed
b_3	Amplitude of oscillation in $\beta_3(t)$	0.8	-	Assumed
d_1	Amplitude of oscillation in $d(t)$	0.8	-	Assumed
μ	Natural elimination rate	0.22	$year^{-1}$	[30]
k	Vaccination waning rate	0.4	$year^{-1}$	[30]
γ	Modification factor	0.18	-	[30]
A	Recruitment rate	11629200	$animals\ year^{-1}$	[30]
au	Vaccination rate	0.316	$year^{-1}$	[30]
σ	Incubation rate	1	$year^{-1}$	[30]
U_1	Upper bound of $u_1(t)$	20	-	Assumed
U_2	Upper bound of $u_2(t)$	3	-	Assumed
S(0)	Initial number of susceptible	4.341×10^7	animals	[30]
H(0)	Initial vaccinated animals	8.44×10^{6}	animals	[30]
E(0)	Initial exposed animals	0	animals	[30]
I(0)	Initial infected animals	1.33×10^6	animals	[30]
B(0)	Initial number of brucella	6×10^6	pathogens	[30]
W_1	Cost parameter of vaccination	Varied	$animals\ dollars\ year^{-1}$	-
W_2	Cost parameter of decontamination	Varied	$animals\ dollars\ year^{-1}$	-

where d_0 denotes the basic pathogen decay rate without seasonal forcing and d_1 (0 < d_1 < 1) denotes the magnitude of seasonal fluctuations.

3.2.2 Feasible region

For the model (3.2), it is obvious that all solutions with non-negative initial conditions remain non-negative. Let N(t) = S(t) + H(t) + E(t) + I(t). Adding the first

four equations of (3.2) we have

$$\dot{N}(t) = A - \mu S - \mu H - \mu E - \mu I - cI = A - \mu N - cI \le A - \mu N$$

It implies that $\limsup_{t\to\infty} N(t) \leq \frac{A}{\mu}$. Since $\dot{N}(t)$ is bounded by $A-\mu N$, a standard comparison principle theorem [54] can be use to show that $N(t) \leq N(0)e^{-\mu t} + \frac{A}{\mu}(1-e^{-\mu t})$. In particular, $N(0) \leq \frac{A}{\mu} \Rightarrow N(t) \leq \frac{A}{\mu}$. Also we can show that every solution of the system (3.2) with initial conditions in Γ remains there for t>0. The ω -limit sets of the system (3.2) are contained in Γ . As a consequence, the last equation of system (3.2) gives

$$\dot{B}(t) = \beta_3(t)(E+I) - (\delta + d(t))
\leq \beta_3(t) \left[\frac{A}{\mu} + \frac{A}{\mu} \right] - (\delta + d(t))
\leq 2a_3(1+b_3)\frac{A}{\mu} - (d_0 + d_0d_1 + \delta)B.$$

Thus, $\limsup_{t\to\infty} B(t) \leq \frac{2a_3(1+b_3)A}{\mu(d_0+d_0d_1+\delta)}$. Hence the feasible domain,

$$\Gamma = \left\{ (S, H, E, I, B) \in \mathbb{R}^5_+ : S + H + E + I \le \frac{A}{\mu}, \ B \le \frac{2a_3(1 + b_3)A}{\mu(d_0 + d_0d_1 + \delta)} \right\}$$
(3.5)

is invariant for system (3.2). Thus we will study the dynamics of our model in the closed set Γ . In addition, we note that there is a constant influx (at rate A) into the susceptible class. Hence, without loss of generality, we assume that the susceptible population is positive at the initial time; that is,

$$S(0) > 0. (3.6)$$

3.2.3 Disease-free equilibrium

A constant solution to a system of equations is referred to as an equilibrium solution. A disease-free equilibrium refers to the equilibrium that exists in the absence of the disease (i.e $S = S_0 > 0$, $H = H_0 > 0$, E = I = B = 0). The disease-free equilibrium is determined by equations:

$$\begin{cases}
A - \beta_1(t)[E(t) + I(t)]S(t) - \beta_2(t)B(t)S(t) - (\mu + \tau)S(t) + kH(t) &= 0, \\
\tau S(t) - \gamma \beta_1(t)H(t)[E(t) + I(t)] - \gamma \beta_2(t)H(t)B(t) - (\mu + k)H(t) &= 0, \\
\beta_1(t)[S(t) + \gamma H(t)][E(t) + I(t)] + \beta_2(t)[S(t) + \gamma H(t)]B(t) - (\sigma + \mu)E(t) &= 0, \\
\sigma E(t) - (\mu + c)I(t) &= 0, \\
\beta_3(t)(E + I) - d(t)B(t) - \delta B(t) &= 0.
\end{cases}$$
(3.7)

Substituting $S = S_0$, $H = H_0$ and E = I = B = 0 into equation (3.7) yields

$$\begin{cases} A - (\mu + \tau)S_0(t) + kH_0(t) = 0, \\ \tau S_0(t) - (\mu + k)H_0(t) = 0. \end{cases}$$
(3.8)

solving equation (3.8) for S_0 and H_0 implies that system (3.2) has an evident diseasefree equilibrium given by $P_0 = (S_0, H_0, 0, 0, 0)$, with

$$S_0 = \frac{A(\mu + k)}{\mu(\mu + \tau + k)}, \quad H_0 = \frac{A\tau}{\mu(\mu + \tau + k)}, \quad \text{and} \quad S_0 + \gamma H_0 = \frac{A(\mu + k + \gamma \tau)}{\mu(\mu + \tau + k)}.$$

3.2.4 The reproduction number

Utilizing the next-generation method [50], and adopting the matrix notations therein, the matrices for new infection terms (denoted by F(t)) and the transfer terms (denoted by V(t)) at the disease–free equilibrium are given by

$$F(t) = \begin{pmatrix} \frac{\beta_1(t)A(\mu + k + \gamma\tau)}{\mu(\mu + k + \tau)} & \frac{\beta_1(t)A(\mu + k + \gamma\tau)}{\mu(\mu + k + \tau)} & \frac{\beta_2(t)A(\mu + k + \gamma\tau)}{\mu(\mu + k + \tau)} \\ 0 & 0 & 0 \\ \beta_3(t) & \beta_3(t) & 0 \end{pmatrix}$$
(3.9)

and

$$V(t) = \begin{pmatrix} (\sigma + \mu) & 0 & 0 \\ -\sigma & (\mu + c) & 0 \\ 0 & 0 & d(t) + \delta \end{pmatrix}$$
(3.10)

It follows that the basic reproduction number of the time-averaged autonomous system is

$$[\mathcal{R}_{0}] = \frac{1}{2} \left[\frac{a_{1}(c+\mu+\sigma)(S_{0}+\gamma H_{0})}{(c+\mu)(\mu+\sigma)} \right] + \frac{1}{2} \left[\sqrt{\frac{(c+\mu+\sigma)(S_{0}+\gamma H_{0})}{(c+\mu)(\mu+\sigma)}} \left(\frac{a_{1}^{2}(c+\mu+\sigma)}{(c+\mu)(\mu+\sigma)} + \frac{4a_{2}a_{3}}{(d_{0}+\delta)} \right) \right] (3.11)$$

In order to establish the basic reproduction number in periodic environments, Wang and Zhao [55] extended the classical framework (for autonomous systems) of van den Driessche and Watmough [50] by introducing the next infection operator

$$(L\phi)(t) = \int_0^\infty Y(t, t-s)F(t-s)\phi(t-s)ds, \qquad (3.12)$$

where Y(t,s), $t \geq s$, is the evolution operator of the linear ω -periodic system $\frac{dy}{dt} = -V(t)y$ and $\phi(t)$, the initial distribution of infectious animals, is ω -periodic and always positive. The effective reproduction number for a periodic model is then determined by calculating the spectral radius of the next infection operator,

$$\mathcal{R}_0 = \rho(L). \tag{3.13}$$

Through direct calculation, the evolution operator Y(t,s) for system (3.2) is found as

$$Y(t,s) = \begin{pmatrix} e^{-(\sigma+\mu)(t-s)} & 0 & 0\\ \frac{\sigma}{(c-\sigma)} [e^{-(\sigma+\mu)(t-s)} - e^{-(\mu+c)(t-s)}] & e^{-(\mu+c)(t-s)} & 0\\ 0 & 0 & \tilde{Y}(t,s) \end{pmatrix}, \quad (3.14)$$

with

$$\tilde{Y}(t,s) = \exp\left\{-(d_0 + \delta)(t-s) - \frac{6d_0d_1}{\pi} \left(\cos\left[\frac{\pi s}{6}\right] - \cos\left[\frac{\pi t}{6}\right]\right)\right\}.$$

In addition, the next infection operator can be numerically evaluated (see, e.g., [56]) by

$$(L\phi)(t) = \int_0^\infty Y(t, t-s)F(t-s)\phi(t-s)ds = \int_0^\omega G(t, s)\phi(t-s)ds$$
 (3.15)

where

$$G(t,s) \approx \sum_{k=0}^{M} Y(t,t-s-k\omega)F(t-s)$$

$$\approx \sum_{k=0}^{M} \begin{pmatrix} m_{11} & m_{12} & m_{13} \\ m_{21} & m_{22} & m_{23} \\ m_{31} & m_{32} & 0 \end{pmatrix}$$

for some positive integer M large enough, and

$$m_{11} = m_{12} = \frac{A(\mu + k + \gamma \tau)}{\mu(\mu + k + \tau)} \beta_1(t - s)e^{-(\mu + \sigma)(s + k\omega)},$$

$$m_{13} = \frac{A(\mu + k + \gamma \tau)}{\mu(\mu + k + \tau)} \beta_2(t - s)e^{-(\mu + \sigma)(s + k\omega)},$$

$$m_{21} = m_{22} = \frac{\sigma \beta_1(t - s)}{(c - \sigma)} \left(\frac{A(\mu + k + \gamma \tau)}{\mu(\mu + k + \tau)}\right) \left(e^{-(\mu + \sigma)(s + k\omega)} - e^{-(\mu + c)(s + k\omega)}\right),$$

$$m_{23} = \frac{\sigma \beta_2(t - s)}{(c - \sigma)} \left(\frac{A(\mu + k + \gamma \tau)}{\mu(\mu + k + \tau)}\right) \left(e^{-(\mu + \sigma)(s + k\omega)} - e^{-(\mu + c)(s + k\omega)}\right),$$

$$m_{31} = m_{32} = \beta_3(t - s) \exp\left\{-(d_0 + \delta)(t - s) - \frac{6d_0d_1}{\pi} \left(\cos\left[\frac{\pi s}{6}\right] - \cos\left[\frac{\pi t}{6}\right]\right)\right\}.$$

Using parameter values in Table 3.1 and numerical computations, we obtained the curves of the time averaged reproduction number $[\mathcal{R}_0]$ (3.11) and basic reproduction number \mathcal{R}_0 (3.13), with respect to a_j (j=1,2), in Fig 3.2. We note that the average basic reproduction number $[\mathcal{R}_0]$ is always greater than the basic reproduction number \mathcal{R}_0 in all cases. The results demonstrate that the risk of infection will be overestimated whenever the average basic reproduction number is used. The

results established here are in agreement with findings from [53].

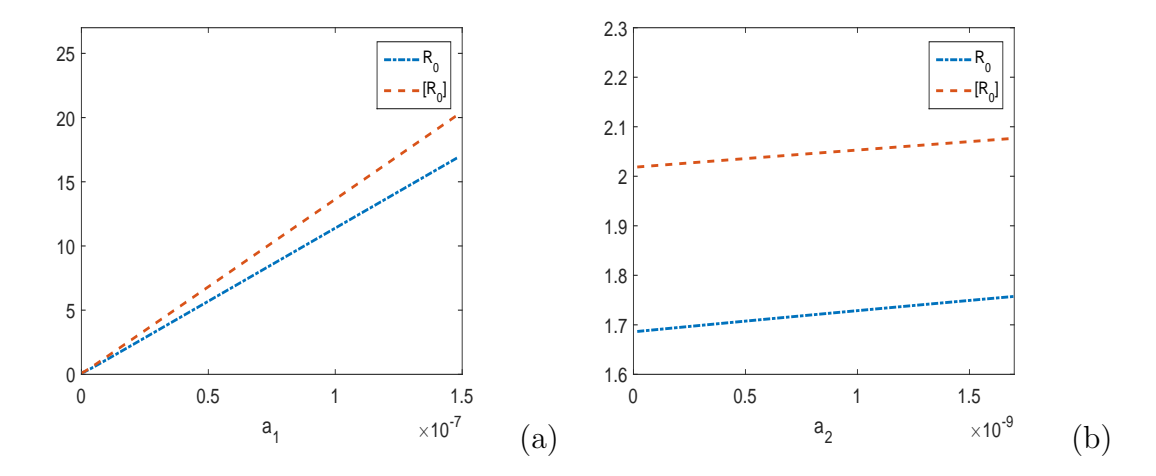


Figure 3.2: Numerical results of the average basic reproduction number $[\mathcal{R}_0]$ and the basic reproduction number \mathcal{R}_0 versus a_j , (j = 1, 2): (a) $[\mathcal{R}_0]$ and \mathcal{R}_0 versus a_1 ; (b) $[\mathcal{R}_0]$ and \mathcal{R}_0 versus a_2 .

3.2.5 Disease extinction

We aim to establish the condition $\mathcal{R}_0 = 1$, where the basic reproduction number \mathcal{R}_0 is defined in (3.13), as a sharp threshold for the disease dynamics of our periodic brucellosis model. The following theorem analyzes the global stability of the disease–free equilibrium of system (3.2) and provides a criterion for the extinction of the disease.

Theorem 3.2.1 If $\mathcal{R}_0 < 1$, then the disease-free equilibrium of system (3.2) is globally asymptotically stable in Γ .

To prove this result, let us consider the matrix function F(t) - V(t) given by

$$\begin{pmatrix}
\frac{A\beta_{1}(t)(\mu+k+\gamma\tau)}{\mu(\mu+k+\tau)} - (\sigma+\mu) & \frac{A\beta_{1}(t)(\mu+k+\gamma\tau)}{\mu(\mu+k+\tau)} & \frac{A\beta_{2}(t)(\mu+k+\gamma\tau)}{\mu(\mu+k+\tau)} \\
\sigma & -(\mu+c) & 0 \\
\beta_{3}(t) & \beta_{3}(t) & -d(t)-\delta
\end{pmatrix}$$
(3.16)

We can easily verify that (3.16) is continuous, cooperative, irreducible and ω periodic. Further, let $\Phi_{(F-V)(\cdot)}(t)$ be the fundamental solution matrix of the linear

ordinary differential system:

$$\dot{x} = [F(t) - V(t)]x,\tag{3.17}$$

and $\rho(\Phi_{(F-V)(\cdot)}(\omega))$ be the spectral radius of $\Phi_{(F-V)(\cdot)}(\omega)$. From Theorem 2.2 in [55], we have $\mathcal{R}_0 > (=, <)$ 1 if and only if $\rho(\Phi_{(F-V)}(\omega)) > (=, <)$ 1. Meanwhile, based on Lemma 2.1 in [57], we immediately have the following result which will be used to establish Theorem 3.2.1.

Lemma 3.1 Let $\nu = (1/\omega) \ln \rho(\Phi_{(F-V)(\cdot)}(\omega))$. Then there exists a positive ω -periodic function v(t) such that $e^{\nu t}v(t)$ is a solution to (3.17).

Now we present the proof of Theorem 3.2.1.

Proof 1 From the first two equations of the system (3.2), we can easily obtain

$$S(t) \le \frac{A(\mu+k)}{\mu(\mu+\tau+k)} \triangleq S_0, \quad and \quad V(t) \le \frac{A\tau}{\mu(\mu+\tau+k)} \triangleq V_0.$$

Then from the last three equations of the system (3.2), we have

$$\frac{d}{dt} \begin{bmatrix} E \\ I \\ B \end{bmatrix} \le (F - V) \begin{bmatrix} E \\ I \\ B \end{bmatrix}. \tag{3.18}$$

Based on Lemma 3.1, there exists v(t) such that

$$x(t) = (\tilde{E}(t), \tilde{I}(t), \tilde{B}(t)) = e^{\nu t} v(t)$$

is a solution to equation (3.17), with $\nu = (1/\omega) \ln \rho(\Phi_{(F-V)(\cdot)}(\omega))$. Since $\mathcal{R}_0 < 1$, we have $\rho(\Phi_{(F-V)(\cdot)}(\omega)) < 1$, and thus $\nu < 0$. Hence,

$$(E(t), I(t), B(t)) \le (\tilde{E}(t), \tilde{I}(t), \tilde{B}(t))$$

when t is large, which would imply that

$$\lim_{t \to \infty} E(t) = 0, \qquad \lim_{t \to \infty} I(t) = 0, \qquad \text{and} \qquad \lim_{t \to \infty} B(t) = 0. \tag{3.19}$$

Meanwhile, from the first two equations of the system (3.2), we have

$$\frac{d}{dt}(S+H) \to A - \mu(S+H)$$
, as $t \to \infty$,

which implies that

$$S(t) + H(t) \to \frac{A}{\mu}, \quad t \to \infty.$$

Therefore,

$$\frac{dH}{dt} \to \tau \left(\frac{A}{\mu} - H(t)\right) - (\mu + k)H(t) = \tau \frac{A}{\mu} - (\mu + \tau + k)H(t),$$

or

$$H(t) \to \frac{A\tau}{\mu(\mu + \tau + k)} = H_0,$$

and clearly it leads to

$$S(t) \to \frac{A}{\mu} - H_0 = \frac{A(\mu + k)}{\mu(\mu + \tau + k)} = S_0.$$

Therefore,

$$\lim_{t \to \infty} x(t) = (S_0, H_0, 0, 0, 0)$$

for every solution x(t) of system (3.2).

3.2.6 Disease persistence

Now we proceed to investigate the dynamics of the system (3.2) when $\mathcal{R}_0 > 1$. We will show that when $\mathcal{R}_0 > 1$, the brucellosis infection persists and there exists a positive periodic solution. Following the framework in [58, 59], we define

$$X = \mathbb{R}^5_+; \qquad X_0 = \mathbb{R}^2_+ \times \operatorname{Int}(\mathbb{R}_+)^3; \qquad \partial X_0 = X \setminus X_0.$$

Let $P: X \longrightarrow X$ be the Poincaré map associated with our model (3.2) such that $P(x_0) = u(\omega, x_0) \ \forall x_0 \in X$, where $u(t, x_0)$ denotes the unique solution of the system with $u(0, x_0) = x_0$.

Definition 17 The solutions of system (3.2) are said to be uniformly persistent if there exists some $\eta > 0$ such that

$$\begin{aligned} & \liminf_{t \to \infty} S(t) \ge \eta, & & \liminf_{t \to \infty} H(t) \ge \eta, & & \liminf_{t \to \infty} E(t) \ge \eta, \\ & \liminf_{t \to \infty} I(t) \ge \eta, & & \liminf_{t \to \infty} B(t) \ge \eta, \end{aligned}$$

whenever S(0) > 0, H(0) > 0, E(0) > 0, I(0) > 0, B(0) > 0.

Theorem 3.2.2 If $\mathcal{R}_0 > 1$, then the solutions of the system (3.2) are uniformly persistent, and the system admits at least one positive ω -periodic solution.

Proof 2 Let us define

$$M_{\partial} = \{ (S(0), H(0), E(0), I(0), B(0)) \in \partial X_0 \}$$

such that

$$P^{m}(S(0), H(0), E(0), I(0), B(0)) \in \partial X_{0}, \forall m \geq 0$$

and

$$\widetilde{M}_{\partial} = \{(S, H, 0, 0, 0) : S \ge 0, H \ge 0\}.$$

We first show that

$$M_{\partial} = \widetilde{M}_{\partial}. \tag{3.20}$$

It is evident that $M_{\partial} \supseteq \widetilde{M}_{\partial}$. Consider any initial values $(S(0), H(0), E(0), I(0), B(0)) \in \partial X_0 \backslash \widetilde{M}_{\partial}$. If E(0) = I(0) = 0 and B(0) > 0, then based on the assumption (3.6) we have E'(0) > 0. Similarly, if E(0) = B(0) = 0 and I(0) > 0, then E'(0) > 0, and B'(0) > 0. If I(0) = B(0) = 0 and E(0) > 0, then I'(0) > 0, and B'(0) > 0. It follows that $(S(t), H(t), E(t), I(t), B(t)) \notin \partial X_0$ for $0 < t \ll 1$. The positive invariance of X_0 implies that $M_{\partial} = \widetilde{M}_{\partial}$, and hence, equation (3.20) holds.

Now, let us consider the fixed point $M_0 = \left(\frac{A(\mu+k)}{\mu(\mu+\tau+k)}, \frac{A\tau}{\mu(\mu+\tau+k)}, 0, 0, 0\right)$ and define $W^S(M_0) = \{x_0 : P^m(x_0) \to M_0, m \to \infty\}$. From the system (3.2) it is easy to deduce that when E = I = B = 0, we have $S(t) \to S_0 = \frac{A(\mu+k)}{\mu(\mu+\tau+k)}$, $H(t) \to H_0 = \frac{A\tau}{\mu(\mu+\tau+k)}$ as $t \to \infty$. We prove that

$$W^S(M_0) \cap X_0 = \emptyset. (3.21)$$

Let $\|\cdot\|$ denote a norm on \mathbb{R}^5_+ . Based on the continuity of solutions with respect to the initial conditions, for any $\epsilon > 0$, there exists $\delta > 0$ small enough such that for all

 $(S(0), H(0), E(0), I(0), B(0)) \in X_0 \text{ with } ||(S(0), H(0), E(0), I(0), B(0)) - M_0|| \le \delta,$ we have

$$||u(t, (S(0), H(0), E(0), I(0), B(0))) - u(t, M_0)|| < \epsilon, \quad \forall t \in [0, \omega].$$
 (3.22)

We claim that

$$\limsup_{m \to \infty} \|P^m(S(0), H(0), E(0), I(0), B(0)) - M_0\| \ge \delta,$$

$$\forall (S(0), H(0), E(0), I(0), B(0)) \in X_0. \tag{3.23}$$

We prove this claim by contradiction. Suppose

$$\lim_{m \to \infty} \|P^m(S(0), H(0), E(0), I(0), B(0)) - M_0\| < \delta$$
(3.24)

for some $(S(0), H(0), E(0), I(0), B(0)) \in X_0$. Without loss of generality, we assume that

$$||P^m(S(0), H(0), E(0), I(0), B(0)) - M_0|| < \delta, \quad \forall m \ge 0.$$

Thus,

$$||u(t, P^{m}(S(0), H(0), E(0), I(0), B(0))) - u(t, M_{0})|| < \epsilon,$$

$$\forall t \in [0, \omega], \ m > 0.$$
(3.25)

Furthermore, for any $t \ge 0$, we can write $t = t' + n\omega$ with $t' \in [0, \omega]$ and n being the greatest integer less than or equal to t/ω . Then we get

$$\begin{split} \|u(t,(S(0),H(0),E(0),I(0),B(0)))-u(t,M_0)\| &= \\ \|u(t',P^m(S(0),H(0),E(0),I(0),B(0)))-u(t',M_0)\| &< \epsilon, \end{split}$$

for any $t \ge 0$. Let (S(t), H(t), E(t), I(t), B(t)) = u(t, (S(0), H(0), E(0), I(0), B(0))). It follows that

$$\frac{A(\mu+k)}{(\mu+\tau+k)} - \epsilon < S(t) < \frac{A(\mu+k)}{(\mu+\tau+k)} + \epsilon,$$

$$\frac{A\tau}{(\mu+\tau+k)} - \epsilon < H(t) < \frac{A\tau}{(\mu+\tau+k)} + \epsilon,$$

$$0 < E(t) < \epsilon,$$

$$0 < I(t) < \epsilon,$$

$$0 < B(t) < \epsilon$$
.

Then we have

$$\frac{dE(t)}{dt} = \beta_1(t)[S(t) + \gamma H(t)][E(t) + I(t)] + \beta_2(t)[S(t) + \gamma H(t)]B(t)
-(\sigma + \mu)E(t)$$

$$\geq [\beta_1(t)(E(t) + I(t))] \left[\frac{A(\mu + k)}{\mu(\mu + \tau + k)} - \epsilon + \gamma \left(\frac{A\tau}{\mu(\mu + \tau + k)} - \epsilon \right) \right]
+ [\beta_2(t)B(t)] \left[\frac{A(\mu + k)}{\mu(\mu + \tau + k)} - \epsilon + \gamma \left(\frac{A\tau}{\mu(\mu + \tau + k)} - \epsilon \right) \right]
-(\sigma + \mu)E(t)$$

$$= -(\sigma + \mu)E(t) + [\beta_1(t)(E(t) + I(t)) + \beta_2(t)B(t)] \left[\frac{A(\mu + k + \gamma \tau)}{\mu(\mu + \tau + k)} \right]
-[\beta_1(t)(E(t) + I(t)) + \beta_2(t)B(t)]\epsilon(1 + \gamma).$$

Hence we obtain

$$\frac{d}{dt} \begin{bmatrix} E \\ I \\ B \end{bmatrix} \ge [F - V - \epsilon K] \begin{bmatrix} E \\ I \\ B \end{bmatrix}, \tag{3.26}$$

where F - V is given by (3.16) and

$$\epsilon \cdot K = \epsilon \cdot \begin{pmatrix} (1+\gamma)\beta_1(t) & (1+\gamma)\beta_1(t) & (1+\gamma)\beta_2(t) \\ 0 & 0 & 0 \\ \beta_3(t) & \beta_3(t) & 0 \end{pmatrix}$$
(3.27)

Note that $R_0 > 1$ if and only if $\rho(\Phi_{F-V}(\omega)) > 1$. Thus, for $\epsilon > 0$ small enough we have $\rho(\Phi_{F-V-\epsilon \cdot K}(\omega)) > 1$. Using Lemma 3.1 and the comparison principle, we immediately obtain

$$\lim_{t \to \infty} E(t) = \infty \quad , \lim_{t \to \infty} I(t) = \infty \quad \text{and} \quad \lim_{t \to \infty} B(t) = \infty, \tag{3.28}$$

which is a contradiction.

Hence, M_0 is acyclic in M_∂ , and P is uniformly persistent with respect to $(X_0, \partial X_0)$, which implies the uniform persistence of the solutions to the original system [58]. Consequently, the Poincaré map P has a fixed point $(\tilde{S}(0), \tilde{H}(0), \tilde{E}(0), \tilde{I}(0), \tilde{B}(0)) \in X_0$ with $\tilde{S}(0), \tilde{H}(0) \neq 0$. Thus, $(\tilde{S}(0), \tilde{H}(0), \tilde{E}(0), \tilde{I}(0), \tilde{B}(0)) \in Int(\mathbb{R}_+)^5$ and

$$(\tilde{S}(t), \tilde{H}(t), \tilde{E}(t), \tilde{I}(t), \tilde{B}(t)) = u(t, (\tilde{S}(0), \tilde{H}(0), \tilde{E}(0), \tilde{I}(0), \tilde{B}(0)))$$

is a positive ω -periodic solution of the system.

3.3 Optimal control

Having analyzed the threshold dynamics, we now turn to an optimal control study of our brucellosis model, with an aim of exploring effective prevention and intervention strategies that could best balance the outcomes and costs of the control. To that end, we will perform the optimal control study to both the autonomous model (3.1) and the periodic model (3.2). We will then compare the results and highlight the impact of seasonality on brucellosis control. Optimal control theory is used to identify ways of producing maximum performance at a minimal cost under some assumptions. Here we introduce two types of controls, which are represented as functions of time and assigned reasonable upper and lower bounds. The goal of the first control $u_1(t)$ is to strengthen the impact of vaccination, and the second control $u_2(t)$ attempts to strengthen the effort on environmental decontamination. Using the same variable and parameter names as in (3.1) and (3.2), the system of differential equations describing our model with controls is

$$\begin{cases}
\dot{S}(t) &= A - \beta_1[E(t) + I(t)]S(t) - \beta_2 B(t)S(t) - (\mu + u_1(t)\tau)S(t) + kH(t), \\
\dot{H}(t) &= u_1(t)\tau S(t) - \gamma \beta_1[E(t) + I(t)]H(t) - \gamma \beta_2 H(t)B(t) - (\mu + k)H(t), \\
\dot{E}(t) &= \beta_1[S(t) + \gamma H(t)][E(t) + I(t)] + \beta_2[S(t) + \gamma H(t)]B(t) - (\sigma + \mu)E(t), \\
\dot{I}(t) &= \sigma E(t) - (\mu + c)I(t), \\
\dot{B}(t) &= \beta_3(E + I) - (d + u_2(t)\delta)B,
\end{cases}$$
(3.29)

The control set is defined as

$$\Omega = \{ (u_1(t), u_2(t)) \mid 1 \le u_1(t) \le U_1, 1 \le u_2(t) \le U_2 \}, \tag{3.30}$$

where U_1 and U_2 denote the upper bounds for the efforts of vaccination and decontamination, respectively. The bounds reflect practical limitation on the maximum rate of control that can be implemented in a given time period. If, however, $u_1(t) = u_2(t) = 1$ for all t, then the model (3.29) is reduced to the original model (3.1) or (3.2), with regular (i.e., minimum) controls.

Below we introduce an objective functional J to formulate the optimization problem of interest, namely, that of identifying the most effective strategies over the admissible set Ω of controls $(u_1(t), u_2(t))$. The overall objective is to minimize the numbers of exposed and infectious animals over a finite time interval [0, T] at minimal costs. The objective functional J is thus defined as

$$J(u_1(t), u_2(t)) = \int_0^T \left[C_1 E(t) + C_2 I(t) + \frac{W_1}{2} u_1^2(t) + \frac{W_2}{2} u_2^2(t) \right] dt.$$
 (3.31)

The control efforts are assumed to be nonlinear, in order to prevent the bangbang solutions in the control. Moreover, a quadratic structure in the control has mathematical advantages. We choose (as it is customary) to model the control effects using a linear combination of quadratic terms, $u_1^2(t)$, and $u_2^2(t)$, where the coefficients C_1 , C_2 , W_1 , W_2 are weight constants. The weights, constant over the prescribed time frame, are a measure of the relative costs of the interventions over a finite time horizon. The optimal control problem hence becomes that we seek optimal functions, $(u_1^*(t), u_2^*(t))$, such that

$$J(u_1^*(t), u_2^*(t)) = \min_{\Omega} J(u_1(t), u_2(t))$$
(3.32)

subject to the state equations in system (3.29) with initial conditions.

3.3.1 Existence of the optimal control set

Theorem 3.3.1 Consider the control problem with system equations (3.29). There exists an optimal control set $(u_1^*(t), u_2^*(t) \in \Omega)$ such that:

$$J(u_1^*(t), u_2^*(t)) = \min_{\Omega} J(u_1(t), u_2(t))$$

To prove this theorem, the following conditions must be satisfied:

Proof 3 1. The class of all initial conditions must with an optimal control set $u_1(t)$ and $u_2(t)$ in the admissible control set a long with each state equation being satisfied is not empty.

- 2. The admissible control Ω set is closed and convex.
- 3. The right-hand side of the state system is continuous, is bonded by a linear function in the state and control variables.
- 4. The integrand of the objective functional is convex on Ω .
- 5. The integrand of the objective functional is bounded below by $A_1(|u_1|^2+|u_2|^2)^{\frac{\beta}{2}}-A_2$, where A_1 , A_2 are positive constants and $\beta > 1$.

In order to verify these conditions, we use a result by Lukes[60] to give the existence of solutions of ODE's (3.29) with bounded coefficients which gives condition 1. We note that our solutions are bounded. The control set is convex and closed by definition, thus it satisfies condition 2. Since our state system is bilinear in u_1 , u_2 , the right-hand side of (3.29) satisfies condition 3, using the boundedness of the solutions. The integrand in the objective functional (3.31) $C_1E(t) + C_2I(t) + \frac{W_1}{2}u_1^2(t) + \frac{W_2}{2}u_2^2(t)$ is clearly convex on Ω . Moreover, there are $A_1, A_2 > 0$ and $\beta > 1$ satisfying

$$C_1E(t) + C_2I(t) + \frac{W_1}{2}u_1^2(t) + \frac{W_2}{2}u_2^2(t) \ge A_1(|u_1|^2 + |u_2|^2)^{\frac{\beta}{2}} - A_2$$
 (3.33)

because the state variable are bounded. We conclude that there exists an optimal control pair.

3.3.2 Characterization of the optimal control problem

The existence of optimal control follows from standard results in optimal control theory [61, 62]. The necessary conditions that optimal controls must satisfy are derived using Pontryagin's Maximum Principle [63]. Thus, system (3.29) is converted into an equivalent problem, namely the problem of minimizing the Hamiltonian $\mathcal{H}(t)$

given by:

$$\mathcal{H}(t) = C_{1}E(t) + C_{2}I(t) + \frac{W_{1}}{2}u_{1}^{2}(t) + \frac{W_{2}}{2}u_{2}^{2}(t) + \lambda_{S} \Big[A - \beta_{1}[E(t) + I(t)]S(t) - \beta_{2}B(t)S(t) - (\mu + u_{1}(t)\tau)S(t) + \kappa H(t) \Big] + \lambda_{H} \Big[u_{1}(t)\tau S(t) - \gamma\beta_{1}[E(t) + I(t)]H(t) - \gamma\beta_{2}H(t)B(t) - (\mu + \kappa)H(t) \Big] + \lambda_{E} \Big[\beta_{1}[S(t) + \gamma H(t)][E(t) + I(t)] + \beta_{2}[S(t) + \gamma H(t)]B(t) - (\sigma + \mu)E(t) \Big] + \lambda_{I} \Big[\sigma E(t) - (\mu + c)I(t) \Big] + \lambda_{B} \Big[\beta_{3}(E(t) + I(t)) - (d + u_{2}(t)\delta)B(t) \Big],$$

Theorem 3.3.2 Given an optimal control pair (u_1^*, u_2^*) and solutions (S, H, E, I, B), of the corresponding states system (3.29) there exist adjoint functions $\lambda_S(t)$, $\lambda_H(t)$, $\lambda_E(t)$, $\lambda_I(t)$ and $\lambda_B(t)$ [61] satisfying

$$\frac{d\lambda_{S}(t)}{dt} = \lambda_{S}(t) \Big(\beta_{1}(E(t) + I(t)) + \beta_{2}B(t) + \mu + u_{1}(t)\tau \Big) - \lambda_{H}(t)u_{1}(t)\tau \\
-\lambda_{E}(t) \Big(\beta_{1}(E(t) + I(t)) + \beta_{2}B(t) \Big), \qquad (3.34)$$

$$\frac{d\lambda_{H}(t)}{dt} = -\lambda_{S}(t)\kappa + \lambda_{H}(t) \Big(\gamma\beta_{1}(E(t) + I(t)) + \gamma\beta_{2}B(t) + \mu + \kappa \Big) \\
-\lambda_{E}(t) \Big(\beta_{1}\gamma(E(t) + I(t)) + \beta_{2}\gamma B(t) \Big), \qquad (3.35)$$

$$\frac{d\lambda_{E}(t)}{dt} = -C_{1} + \lambda_{S}(t)\beta_{1}S(t) + \lambda_{H}(t)\gamma\beta_{1}H(t) \\
-\lambda_{E}(t) \Big(\beta_{1}(S(t) + \gamma H(t)) - (\sigma + \mu) \Big) - \lambda_{I}(t)\sigma - \lambda_{B}(t)\beta_{3}, \qquad (3.36)$$

$$\frac{d\lambda_{I}(t)}{dt} = -C_{2} + \lambda_{S}(t)\beta_{1}S(t) + \lambda_{H}(t)\gamma\beta_{1}H(t) - \lambda_{E}(t) \Big(\beta_{1}(S(t) + \gamma H(t)) \Big) \\
+\lambda_{I}(t)(\mu + c) - \lambda_{B}(t)\beta_{3}, \qquad (3.37)$$

$$\frac{d\lambda_{B}(t)}{dt} = \lambda_{S}(t)\beta_{2}S(t) + \lambda_{H}(t)\gamma\beta_{2}H(t) - \lambda_{E}(t)(\beta_{2}(S(t) + \gamma H(t))) \\
+\lambda_{B}(t)(d + u_{2}(t)\delta), \qquad (3.38)$$

with transversality conditions $\lambda_P(T) = 0$ for P = S, H, E, I, B. Furthermore, the optimal controls are characterized by the optimality conditions:

$$u_1^*(t) = \max[1, \min(\bar{u}_1(t), U_1)], \qquad u_2^*(t) = \max[1, \min(\bar{u}_2(t), U_2)],$$
 (3.39)

where

$$\bar{u}_1(t) = \frac{(\lambda_S(t) - \lambda_H(t))\tau S(t)}{W_1}, \qquad \bar{u}_2(t) = \frac{\lambda_B(t)\delta B(t)}{W_2}.$$
 (3.40)

Proof 4 The form of the adjoint equations and transversality conditions are standard results from Pontryagin's maximum principle [63]. The adjoint principle can be obtained as follows:

$$\frac{d\lambda_{S}(t)}{dt} = -\frac{\partial \mathcal{H}}{\partial S} = \lambda_{S}(t) \Big(\beta_{1}(E(t) + I(t)) + \beta_{2}B(t) + \mu + u_{1}(t)\tau \Big) - \lambda_{H}(t)u_{1}(t)\tau \\
-\lambda_{E}(t) \Big(\beta_{1}(E(t) + I(t)) + \beta_{2}B(t) \Big), \qquad (3.41)$$

$$\frac{d\lambda_{H}(t)}{dt} = -\frac{\partial \mathcal{H}}{\partial H} = -\lambda_{S}(t)\kappa + \lambda_{H}(t) \Big(\gamma\beta_{1}(E(t) + I(t)) + \gamma\beta_{2}B(t) + \mu + \kappa \Big) \\
-\lambda_{E}(t) \Big(\beta_{1}\gamma(E(t) + I(t)) + \beta_{2}\gamma B(t) \Big), \qquad (3.42)$$

$$\frac{d\lambda_{E}(t)}{dt} = -\frac{\partial \mathcal{H}}{\partial E} = -C_{1} + \lambda_{S}(t)\beta_{1}S(t) + \lambda_{H}(t)\gamma\beta_{1}H(t) \\
-\lambda_{E}(t) \Big(\beta_{1}(S(t) + \gamma H(t)) - (\sigma + \mu) \Big) - \lambda_{I}(t)\sigma - \lambda_{B}(t)\beta_{3}, \qquad (3.43)$$

$$\frac{d\lambda_{I}(t)}{dt} = -\frac{\partial \mathcal{H}}{\partial I} = -C_{2} + \lambda_{S}(t)\beta_{1}S(t) + \lambda_{H}(t)\gamma\beta_{1}H(t) - \lambda_{E}(t) \Big(\beta_{1}(S(t) + \gamma H(t)) \Big) \\
+\lambda_{I}(t)(\mu + c) - \lambda_{B}(t)\beta_{3}, \qquad (3.44)$$

$$\frac{d\lambda_B(t)}{dt} = -\frac{\partial \mathcal{H}}{\partial B} = \lambda_S(t)\beta_2 S(t) + \lambda_H(t)\gamma\beta_2 H(t) - \lambda_E(t)(\beta_2(S(t) + \gamma H(t))) + \lambda_B(t)(d + u_2(t)\delta).$$
(3.45)

The optimality equations were given by:

$$\frac{\partial \mathcal{H}}{\partial u_1} = W_1 u_1^*(t) - \lambda_S \tau S(t) + \lambda_H \tau H(t) = 0 \quad at \quad u_1^*
\frac{\partial \mathcal{H}}{\partial u_2} = W_2 u_2^*(t) - \lambda_B \delta B(t) = 0 \quad at \quad u_2^*.$$
(3.46)

Hence,

$$u_1^* = \frac{(\lambda_S - \lambda_H)\tau S}{W_1}$$
 , $u_1^* = \frac{\lambda_B \delta B(t)}{W_2}$. (3.47)

By using the bounds for the control u_1 , we get

$$u_{1}^{*} = \begin{cases} \frac{(\lambda_{S}(t) - \lambda_{H}(t))\tau S(t)}{W_{1}} & \text{if } 1 \leq \frac{(\lambda_{S}(t) - \lambda_{V}(t))\tau S(t)}{W_{1}} \leq U_{1}, \\ 1 & \text{if } \frac{(\lambda_{S}(t) - \lambda_{H}(t))\tau S(t)}{W_{1}} \leq 1, \\ U_{1} & \text{if } \frac{(\lambda_{S}(t) - \lambda_{H}(t))\tau S(t)}{W_{1}} \geq U_{1}. \end{cases}$$
(3.48)

In compact notation,

$$u_1^*(t) = \max[1, \min(\bar{u}_1(t), U_1)] \tag{3.49}$$

where

$$\bar{u}_1(t) = \frac{(\lambda_S(t) - \lambda_H(t))\tau S(t)}{W_1}.$$
(3.50)

By using the bounds for the control u_2 , we

$$u_{1}^{*} = \begin{cases} \frac{\lambda_{B}(t)\delta B(t)}{W_{2}} & if \quad 1 \leq \frac{\lambda_{B}(t)\delta B(t)}{W_{2}} \leq U_{2} \\ 1 & if \quad \frac{\lambda_{B}(t)\delta B(t)}{W_{2}} \leq 1 \\ U_{2} & if \quad \frac{\lambda_{B}(t)\delta B(t)}{W_{2}} \geq U_{2} \end{cases}$$
(3.51)

In compact notation,

$$u_2^*(t) = \max[1, \min(\bar{u}_2(t), U_2)],$$
 (3.52)

where

$$\bar{u}_2(t) = \frac{\lambda_B(t)\delta B(t)}{W_2}. (3.53)$$

Using (3.49) and (3.52), we have the following optimality system:

$$\begin{aligned} & \text{Using } (3.49) \text{ and } (3.52), \text{ we have the following optimality system:} \\ & \begin{cases} \dot{S}(t) & = A - \beta_1[E(t) + I(t)]S(t) - \beta_2B(t)S(t) \\ & - (\mu + \max[1, \min(\bar{u}_1(t), U_1)]\tau)S(t) + kH(t), \end{cases} \\ & \dot{H}(t) & = \max[1, \min(\bar{u}_1(t), U_1)]\tau S(t) - \gamma\beta_1[E(t) + I(t)]H(t) - \gamma\beta_2H(t)B(t) \\ & - (\mu + k)H(t), \end{cases} \\ & \dot{E}(t) & = \beta_1[S(t) + \gamma H(t)][E(t) + I(t)] + \beta_2[S(t) + \gamma H(t)]B(t) - (\sigma + \mu)E(t), \end{cases} \\ & \dot{I}(t) & = \sigma E(t) - (\mu + c)I(t), \\ & \dot{B}(t) & = \beta_3(E + I) - (d + \max[1, \min(\bar{u}_2(t), U_2)]\delta)B, \\ & \lambda_S(t)(t) & = \lambda_S(t) \left(\beta_1(E(t) + I(t)) + \beta_2B(t) + \mu + \max[1, \min(\bar{u}_1(t), U_1)]\tau\right) \\ & - \lambda_H(t) \max[1, \min(\bar{u}_1(t), U_1)]\tau - \lambda_E(t) \left(\beta_1(E(t) + I(t)) + \beta_2B(t)\right), \end{cases} \\ & \lambda_H(t)(t) & = -\lambda_S(t)\kappa + \lambda_H(t) \left(\gamma\beta_1(E(t) + I(t)) + \gamma\beta_2B(t) + \mu + \kappa\right) \\ & - \lambda_E(t) \left(\beta_1\gamma(E(t) + I(t)) + \beta_2\gamma B(t)\right), \end{cases} \\ & \lambda_E(t)(t) & = -C_1 + \lambda_S(t)\beta_1S(t) + \lambda_H(t)\gamma\beta_1H(t) \\ & - \lambda_E(t) \left(\beta_1(S(t) + \gamma H(t)) - (\sigma + \mu)\right) - \lambda_I(t)\sigma - \lambda_B(t)\beta_3, \end{cases} \\ & \lambda_I(t)(t) & = -C_2 + \lambda_S(t)\beta_1S(t) + \lambda_H(t)\gamma\beta_1H(t) - \lambda_E(t) \left(\beta_1(S(t) + \gamma H(t))\right) \\ & + \lambda_I(t)(\mu + c) - \lambda_B(t)\beta_3, \end{cases} \\ & \lambda_B(t)(t) & = \lambda_S(t)\beta_2S(t) + \lambda_H(t)\gamma\beta_2H(t) - \lambda_E(t)(\beta_2(S(t) + \gamma H(t))), \\ & + \lambda_B(t)(d + \max[1, \min(\bar{u}_2(t), U_2)]\delta), \end{cases} \end{aligned} \tag{3.54}$$

 $S(0) = S_0, H(0) = H_0, E(0) = E_0, I(0) = I_0, B(0) = B_0 \text{ and } \lambda_P(T) = 0 \text{ for } P = S, H, E, I, B.$

3.3.3 Uniqueness of the optimality system

In this section, we prove the uniqueness of the solution of the optimality system (3.54)

Lemma 3.2 The function $u^*(s) = \max[\min(s, a), b]$ is Lipschitz continuous in s, where

a < b are some fixed positive constants.

Theorem 3.3.3 For T sufficiently small, bounded solutions to the optimality system are unique.

Proof 5 Suppose $(S, H, E, I, B, \lambda_S, \lambda_H, \lambda_E, \lambda_I, \lambda_B)$ and

 $(\bar{S}, \bar{H}, \bar{E}, \bar{I}, \bar{B}, \bar{\lambda_S}, \bar{\lambda_H}, \bar{\lambda_E}, \bar{\lambda_I}, \bar{\lambda_B})$ are two different solutions of an optimality system (3.54). Let $S = e^{\lambda t} p_1$, $H = e^{\lambda t} p_2$, $E = e^{\lambda t} p_3$, $I = e^{\lambda t} p_4$, $B = e^{\lambda t} p_5$, $\lambda_S = e^{-\lambda t} q_1$, $\lambda_H = e^{-\lambda t} q_2$, $\lambda_E = e^{-\lambda t} q_3$, $\lambda_I = e^{-\lambda t} q_4$, $\lambda_B = e^{-\lambda t} q_5$ similarly $\bar{S} = e^{\lambda t} \bar{p}_1$, $\bar{H} = e^{\lambda t} \bar{p}_2$, $\bar{E} = e^{\lambda t} \bar{p}_3$, $\bar{I} = e^{\lambda t} \bar{p}_4$, $\bar{B} = e^{\lambda t} \bar{p}_5$, $\bar{\lambda_S} = e^{-\lambda t} \bar{q}_1$, $\bar{\lambda_H} = e^{-\lambda t} \bar{q}_2$, $\bar{\lambda_E} = e^{-\lambda t} \bar{q}_3$, $\bar{\lambda_I} = e^{-\lambda t} \bar{q}_4$, and $\bar{\lambda_B} = e^{-\lambda t} \bar{q}_5$, where $\lambda > 0$ is to be chosen. Further we let

$$u_1^*(t) = \max[1, \min(\frac{(p_1q_1 - p_1q_2)\tau}{W_1}, U_1)], \quad u_2^*(t) = \max[1, \min(\frac{p_5q_5\delta}{W_2}, U_2)]$$

and

$$\bar{u}_1^*(t) = \max[1, \min(\frac{(\bar{p}_1\bar{q}_1 - \bar{p}_1\bar{q}_2)}{W_1}, U_1)], \quad \bar{u}_2^*(t) = \max[1, \min(\frac{\bar{p}_5\bar{q}_5\delta}{W_2}, U_2)]$$

$$|u_1^* - \bar{u}_1^*| \le \frac{\tau}{W_1} |(p_1 q_1 - p_1 q_2) - (\bar{p}_1 \bar{q}_1 - \bar{p}_1 \bar{q}_2)| \tag{3.55}$$

$$|u_2^* - \bar{u}_2^*| \le \frac{\delta}{W_2} |p_5 q_5 - \bar{p}_5 \bar{q}_5| \tag{3.56}$$

Substitute $S = e^{\lambda t}p_1$ into the first ODE of (3.54), the state equation becomes

$$\dot{p}_1 + \lambda p_1 = Ae^{-\lambda t} - \beta_1 e^{\lambda t} (p_1 p_3 + p_1 p_4) - \beta_2 e^{\lambda t} p_1 p_5 - \mu p_1 - u_1^* \tau p_1 + \kappa p_2$$
 (3.57)

Also substituting $\lambda_S = e^{-\lambda t}q_1$ in the equation $\frac{d\lambda_S}{dt}$, the adjoint equation becomes

$$\dot{q}_1 + \lambda q_1 = \beta_1 e^{\lambda t} (p_3 q_1 + p_4 q_1) + \beta_2 e^{\lambda t} p_5 q_1 + \mu q_1 + u_1^* \tau q_1 - u_1^* \tau q_2 -\beta_1 e^{\lambda t} (p_3 q_3 + p_4 q_3) - \beta_2 e^{\lambda t} p_5 q_3$$
(3.58)

Now we subtract the equations for S and \bar{S} , λ_S and $\bar{\lambda_S}$. Then multiplying each equation by appropriate difference of functions $(p_1 - \bar{p}_1)$ and $(q_1 - \bar{q}_1)$ respectively and integrating from 0 to T we obtain

$$\frac{1}{2}(p_{1} - \bar{p}_{1})^{2} + \lambda \int_{0}^{T} (p_{1} - \bar{p}_{1})^{2} dt = -\beta_{1} \int_{0}^{T} e^{\lambda t} [(p_{1}p_{3} + p_{1}p_{4})](p_{1} - \bar{p}_{1}) dt
+ \beta_{1} \int_{0}^{T} e^{\lambda t} [(\bar{p}_{1}\bar{p}_{3} + \bar{p}_{1}\bar{p}_{4})](p_{1} - \bar{p}_{1}) dt
- \beta_{2} \int_{0}^{T} (p_{1}p_{5} - \bar{p}_{1}\bar{p}_{5})(p_{1} - \bar{p}_{1}) dt
- \mu \int_{0}^{T} (p_{1} - \bar{p}_{1})^{2} dt
- \tau \int_{0}^{T} (u_{1}^{*}p_{1} - \bar{u}_{1}^{*}\bar{p}_{1})(p_{1} - \bar{p}_{1}) dt +
\kappa \int_{0}^{T} (p_{2} - \bar{p}_{2})(p_{1} - \bar{p}_{1}) dt.$$
(3.59)

Following the same procedure for the remaining state variables and adjoint variables, the following equations are obtained:

$$\frac{1}{2}(p_2 - \bar{p}_2)^2 + \lambda \int_0^T (p_2 - \bar{p}_2)^2 dt = -\gamma \beta_1 \int_0^T e^{\lambda t} [(p_2 p_3 + p_2 p_4)](p_2 - \bar{p}_2) dt
+ \gamma \beta_1 \int_0^T e^{\lambda t} [(\bar{p}_2 \bar{p}_3 + \bar{p}_2 \bar{p}_4)](p_2 - \bar{p}_2) dt
- \gamma \beta_2 \int_0^T (p_2 p_5 - \bar{p}_2 \bar{p}_5)(p_2 - \bar{p}_2) dt
- (\mu + \kappa) \int_0^T (p_2 - \bar{p}_2)^2 dt
+ \tau \int_0^T (u_1^* p_1 - \bar{u}_1^* \bar{p}_1)(p_2 - \bar{p}_2) dt \qquad (3.60)$$

$$\frac{1}{2}(p_3 - \bar{p}_3)^2 + \lambda \int_0^T (p_3 - \bar{p}_3)^2 dt = \beta_1 \int_0^T e^{\lambda t} [(p_1 + \gamma p_2)(p_3 + p_4)](p_3 - \bar{p}_3) dt$$

$$-\beta_{1} \int_{0}^{T} e^{\lambda t} [(\bar{p}_{1} + \gamma \bar{p}_{2})(\bar{p}_{3} + \bar{p}_{4})](p_{3} - \bar{p}_{3}) dt$$

$$+\beta_{2} \int_{0}^{T} e^{\lambda t} [(p_{1}p_{5} + \gamma p_{2}p_{5})](p_{3} - \bar{p}_{3}) dt$$

$$-\beta_{2} \int_{0}^{T} e^{\lambda t} [(\bar{p}_{1}\bar{p}_{5} + \gamma \bar{p}_{2}\bar{p}_{5})](p_{3} - \bar{p}_{3}) dt$$

$$-(\sigma + \mu) \int_{0}^{T} (p_{3} - \bar{p}_{3}) dt \qquad (3.61)$$

$$\frac{1}{2}(p_4 - \bar{p}_4)^2 + \lambda \int_0^T (p_4 - \bar{p}_4)^2 dt = \sigma \int_0^T (p_3 - \bar{p}_3)(p_4 - \bar{p}_4) dt - (\mu + c) \int_0^T (p_4 - \bar{p}_4)^2 dt \qquad (3.62)$$

$$\frac{1}{2}(p_5 - \bar{p}_5)^2 + \lambda \int_0^T (p_5 - \bar{p}_5)^2 dt = \beta_3 \int_0^T [(p_3 + p_4) - (\bar{p}_3 + \bar{p}_4)](p_5 - \bar{p}_5) dt$$

$$-d \int_0^T (p_5 - \bar{p}_5)^2 dt$$

$$-\delta \int_0^T (u_2^* p_5 - \bar{u}_2^* \bar{p}_5)(p_5 - \bar{p}_5) dt \qquad (3.63)$$

We illustrate one case of the estimate by using $|u_1^* - \bar{u}_1^*|$ estimate. They involve separating terms that involve squares and several multiplied terms.

$$\frac{1}{2}(p_{1} - \bar{p}_{1})^{2} + \lambda \int_{0}^{T} (p_{1} - \bar{p}_{1})^{2} dt \leq \beta_{1} \int_{0}^{T} |e^{\lambda t}[(p_{1}p_{3} + p_{1}p_{4})]||(p_{1} - \bar{p}_{1})|dt
-\beta_{1} \int_{0}^{T} |e^{\lambda t}[(\bar{p}_{1}\bar{p}_{3} + \bar{p}_{1}\bar{p}_{4})]||(p_{1} - \bar{p}_{1})|dt
+\beta_{2} \int_{0}^{T} |(p_{1}p_{5} - \bar{p}_{1}\bar{p}_{5})||(p_{1} - \bar{p}_{1})|dt
+\mu \int_{0}^{T} |(p_{1} - \bar{p}_{1})^{2}|dt
+\tau \int_{0}^{T} |(u_{1}^{*}p_{1} - \bar{u}_{1}^{*}\bar{p}_{1})||(p_{1} - \bar{p}_{1})|dt$$

$$+\kappa \int_{0}^{T} |(p_{2} - \bar{p}_{2})| |(p_{1} - \bar{p}_{1})| dt$$

$$\leq C_{1} \int_{0}^{T} [|p_{1} - \bar{p}_{1}|^{2} + |p_{2} - \bar{p}_{2}|^{2} + |p_{5} - \bar{p}_{5}|^{2}$$

$$+ |q_{1} - \bar{q}_{1}|^{2} + |q_{2} - \bar{q}_{2}|^{2}] dt$$

$$+ C_{2} e^{\lambda t} \int_{0}^{T} [|p_{1} - \bar{p}_{1}|^{2} + |p_{3} - \bar{p}_{3}|^{2}$$

$$+ |p_{4} - \bar{p}_{4}|^{2}] dt, \qquad (3.64)$$

where the constants C_1 and C_2 depend on the coefficients and the bounds on state and adjoint variables. This shows that the uniqueness and the integral equations are combined, this combination produces

$$\frac{1}{2}(p_{1} - \bar{p}_{1})^{2}(T) + \frac{1}{2}(p_{2} - \bar{p}_{2})^{2}(T) + \frac{1}{2}(p_{3} - \bar{p}_{3})^{2}(T) + \frac{1}{2}(p_{4} - \bar{p}_{4})^{2}(T) + \frac{1}{2}(p_{5} - \bar{p}_{5})^{2}(T) + \frac{1}{2}(q_{1} - \bar{q}_{1})^{2}(0) + \frac{1}{2}(q_{2} - \bar{q}_{2})^{2}(0) + \frac{1}{2}(q_{3} - \bar{q}_{3})^{2}(0) + \frac{1}{2}(q_{4} - \bar{q}_{4})^{2}(0) + \frac{1}{2}(q_{5} - \bar{q}_{5})^{2}(0) + \lambda \int_{0}^{T} [(p_{1} - \bar{p}_{1})^{2} + (p_{2} - \bar{p}_{2})^{2} + (p_{3} - \bar{p}_{3})^{2} + (p_{4} - \bar{p}_{4})^{2} + (p_{5} - \bar{p}_{5})^{2} + (q_{1} - \bar{q}_{1})^{2} + (q_{2} - \bar{q}_{2})^{2} + (q_{3} - \bar{q}_{3})^{2} + (q_{4} - \bar{q}_{4})^{2} + (q_{5} - \bar{q}_{5})^{2}]dt$$

$$\leq (\lambda - \tilde{C}_{1} - \tilde{C}_{2}e^{3\lambda T}) \int_{0}^{T} [(p_{1} - \bar{p}_{1})^{2} + (p_{2} - \bar{p}_{2})^{2} + (p_{3} - \bar{p}_{3})^{2} + (p_{4} - \bar{p}_{4})^{2} + (p_{5} - \bar{p}_{5})^{2}]dt$$

$$+ \int_{0}^{T} [(q_{1} - \bar{q}_{1})^{2} + (q_{2} - \bar{q}_{2})^{2} + (q_{3} - \bar{q}_{3})^{2} + (q_{4} - \bar{q}_{4})^{2} + (q_{5} - \bar{q}_{5})^{2}]dt \qquad (3.65)$$

Thus from the above equation, using non-negativity of the variable expressions we conclude that

$$\leq (\lambda - \tilde{C}_1 - \tilde{C}_2 e^{3\lambda T}) \int_0^T [(p_1 - \bar{p}_1)^2 + (p_2 - \bar{p}_2)^2 + (p_3 - \bar{p}_3)^2 + (p_4 - \bar{p}_4)^2 + (p_5 - \bar{p}_5)^2$$

$$(q_1 - \bar{q}_1)^2 + (q_2 - \bar{q}_2)^2 + (q_3 - \bar{q}_3)^2 + (q_4 - \bar{q}_4)^2 + (q_5 - \bar{q}_5)^2 dt \le 0$$
 (3.66)

where \tilde{C}_1 , \tilde{C}_2 depend on the coefficients and the bounds on p_1 , p_2 , p_3 , p_4 , p_5 , q_1 , q_2 , q_3 , q_4 , q_5 . If we choose λ such that $\lambda > \tilde{C}_1 + \tilde{C}_2$ and $T < (\frac{1}{3\lambda}) \ln[\frac{(\lambda - \tilde{C}_1)}{\tilde{C}_2}]$, then $p_1 = \bar{p}_1$, $p_2 = \bar{p}_2$, $p_3 = \bar{p}_3$, $p_4 = \bar{p}_4$, $p_5 = \bar{p}_5$, $q_1 = \bar{q}_1$, $q_2 = \bar{q}_2$, $q_3 = \bar{q}_3$, $q_4 = \bar{q}_4$, $q_5 = \bar{q}_5$. Hence the solution is unique for small time.

3.4 Numerical results

In the formulation above, the parameters β_1 , β_2 and β_3 can be either constants, for the autonomous model (3.1), or periodic functions in the form of equation (3.3), for the periodic model (3.2). For each case, the state equations, adjoint equations and optimality conditions constitute an optimal control problem, which is then solved numerically. We use the same values of model parameters and initial conditions from [30], listed here in Table 3.1. For simplicity, in our numerical simulation we set $C_1 = C_2 = 1$ so that the minimization of the exposed animal population has the same importance/weight as that of the infectious animal population. As a result, the values of W_1 and W_2 represent the relative costs of their respective controls. We further assume that vaccination incurs higher costs than the cost of decontamination, so that $W_1 > W_2$.

For ease of comparison, we will refer to the original models (3.1) and (3.2) as with regular control, where, essentially, both u_1 and u_2 are fixed at the minimum $u_1 = u_2 = 1$ for all time. We will then compare the results from the optimal control and the regular control in our numerical simulation.

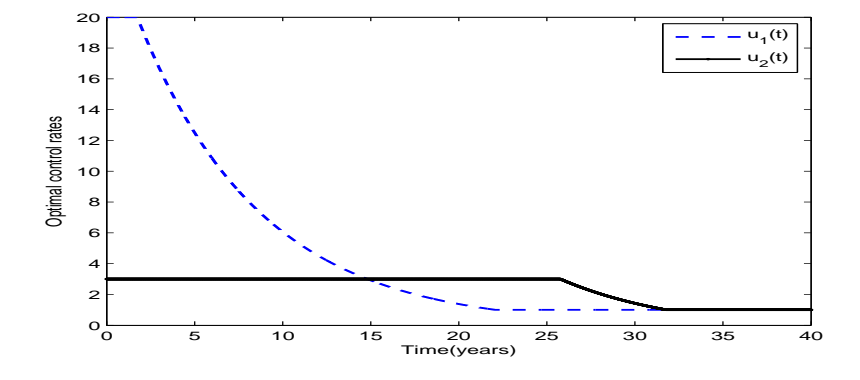


Figure 3.3: Control profiles for the autonomous model (3.1).

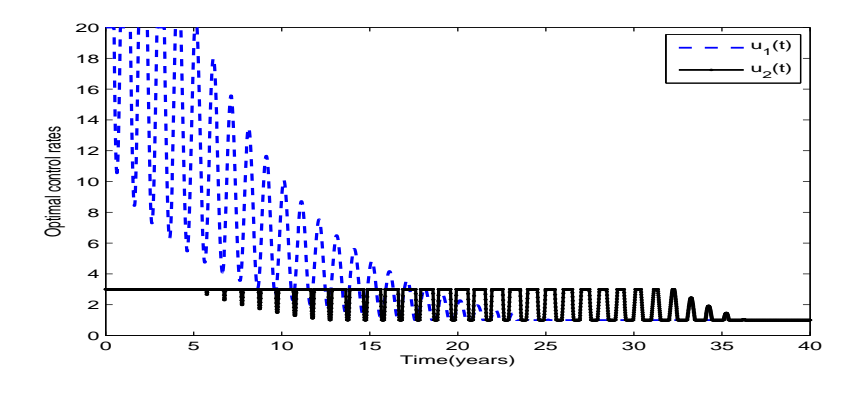


Figure 3.4: Control profiles for the periodic model (3.2).

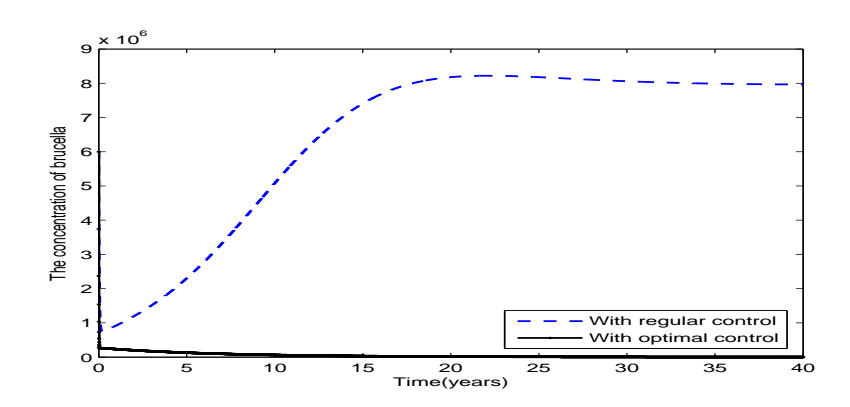


Figure 3.5: The concentration of brucella for the autonomous model (3.1).

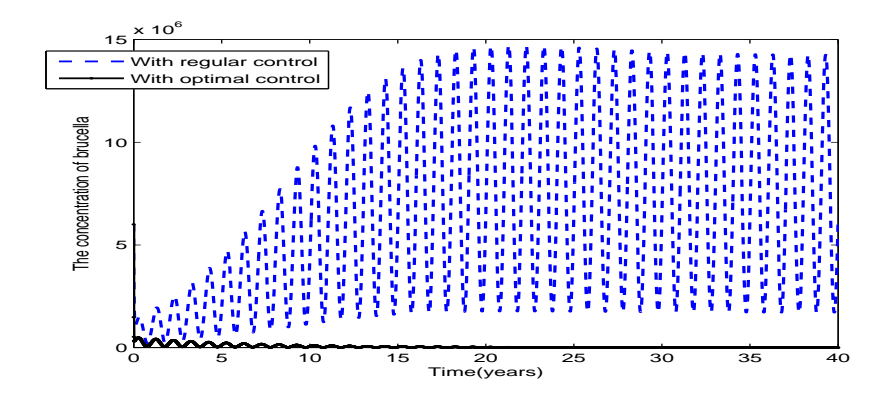


Figure 3.6: The concentration of brucella for the periodic model (3.2).

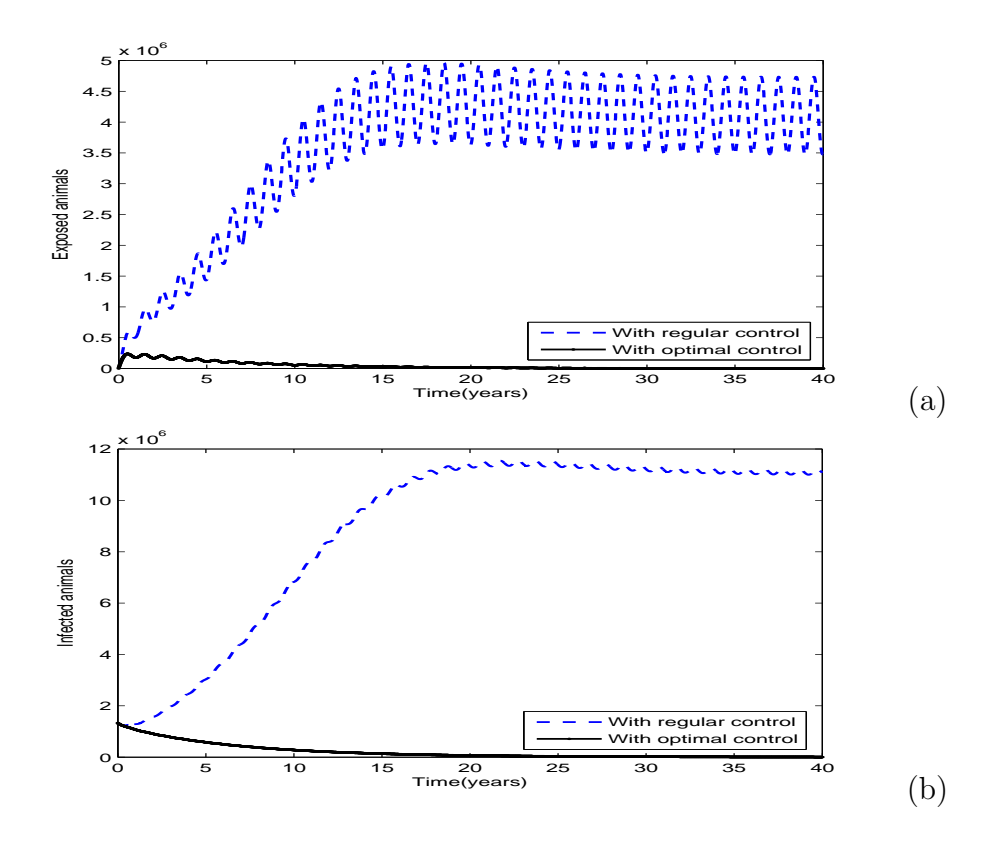


Figure 3.7: The numbers of exposed and infectious animals for the periodic model (3.2): (a) exposed population; (b) infectious population.

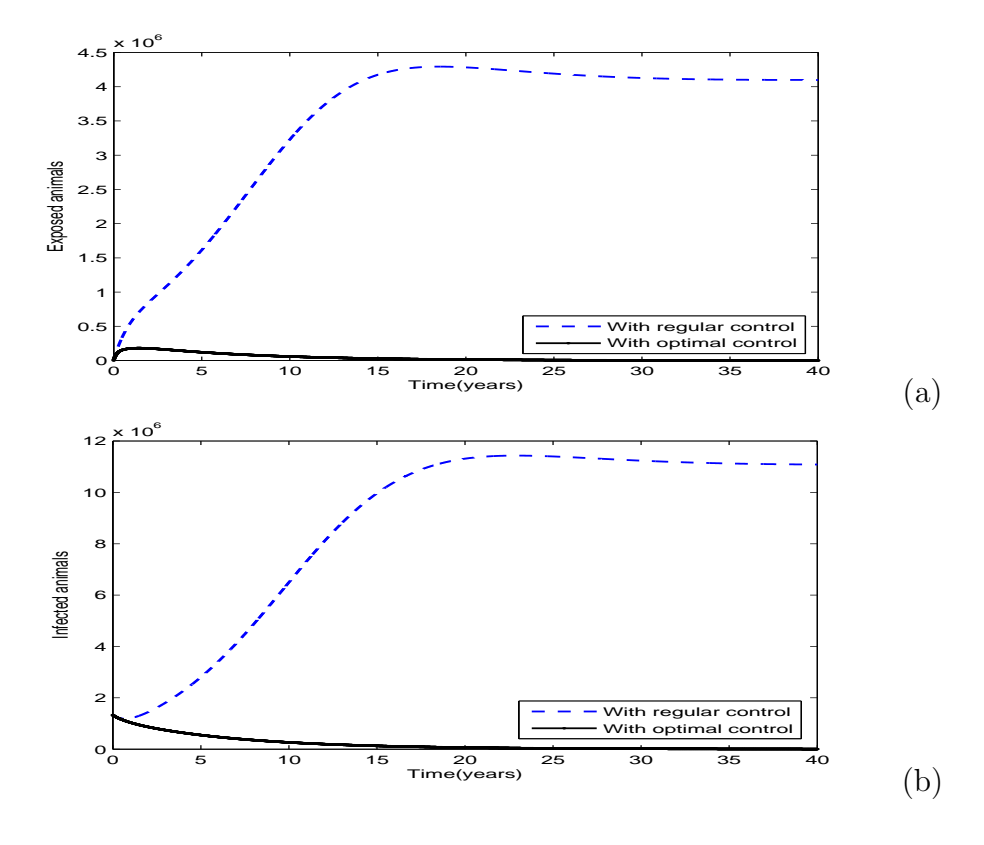


Figure 3.8: The numbers of exposed and infectious animals for the autonomous model (3.1): (a) exposed population; (b) infectious population.

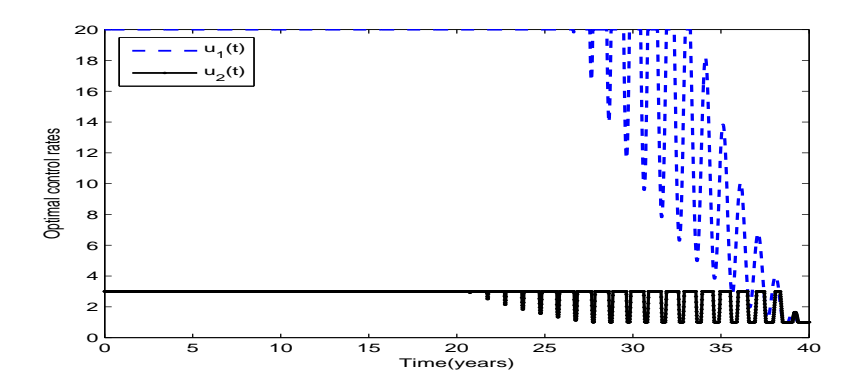


Figure 3.9: Control profiles for the periodic model (3.2) with low costs.

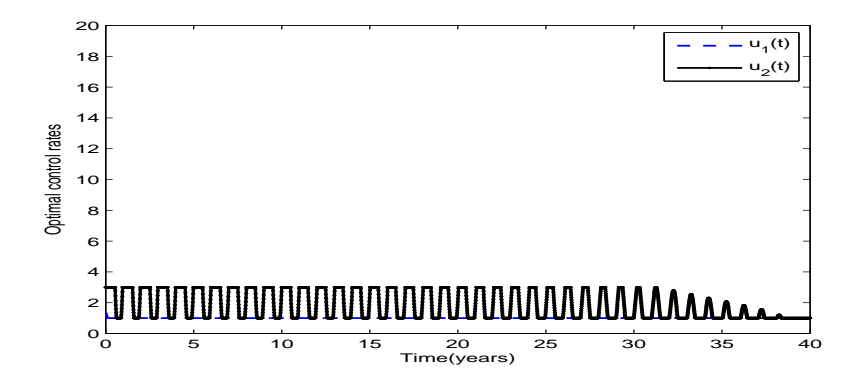


Figure 3.10: Control profiles for the periodic model (3.2) with high costs.

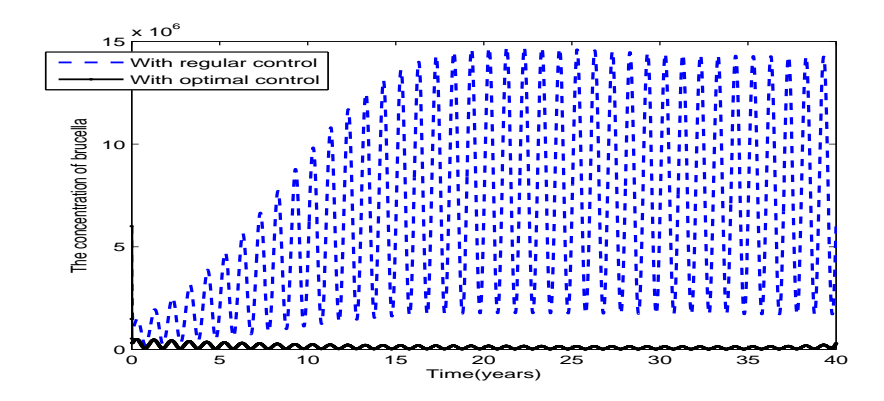


Figure 3.11: The concentration of brucella for the periodic model (3.2) with high costs.

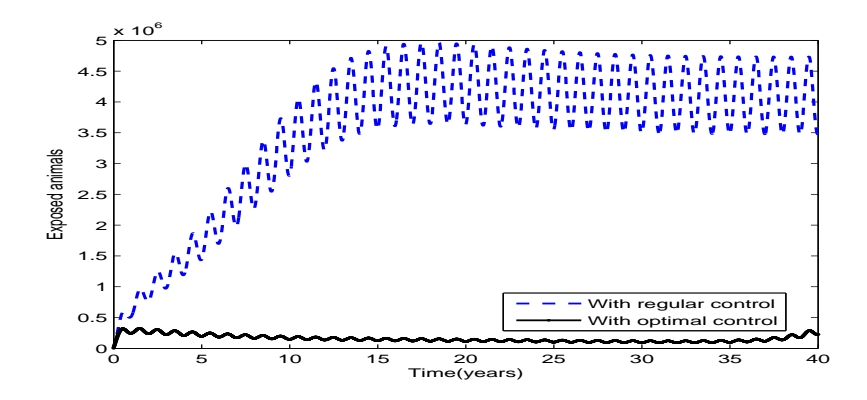


Figure 3.12: The number of exposed animals for the periodic model (3.2) with high costs.

Let us first consider a case with the cost parameters $W_1 = 1000$ and $W_2 = 10$.

Figure 3.3 shows the optimal control profiles for $u_1(t)$ and $u_2(t)$ for the autonomous model (3.1). We clearly observe that u_1 starts from the maximum ($U_1 = 20$) and stays at that level for about 2 years, before it gradually decreases to the minimum, $u_1 = 1$. The vaccination rate would remain at the minimum for all $t \geq 22$ years. The profile of u_2 shows a similar pattern, except that u_2 stays at the maximum ($U_2 = 3$) for a longer period (about 25 years), due to the lower costs related to the environmental decontamination.

Figure 3.4 shows the optimal control profiles for the time-periodic model (3.2), with the same values for the cost parameters. As we can observe, u_1 also starts from the maximum initially, but only for a very short time, followed by a decrease to some lower level, and then it goes back to the maximum again after approximately 1 year. This pattern continues for the second year, third year, and so on, corresponding to the annual periodic oscillation of the contact rates (see equation 3.3). The mean of these oscillations, however, gradually decreases, accompanied by reduced amplitudes of the oscillations. After about 24 years, the oscillations settle at the minimum $u_1 = 1$. The profile of u_2 stays at its maximum ($U_2 = 3$) for the first 5 years. Then the oscillations kick in and continue until t = 35 years, when the oscillations stabilize at the minimum $u_2 = 1$.

Figures 3.5 and 3.6 show the concentration of brucella as a function of time for the autonomous model (3.1) and the periodic model (3.2), respectively. Particularly, from Figure 3.6 we see that with regular control (i.e., the original model 3.2), the bacterial concentration oscillates from the beginning with the amplitude increasing with time, and quickly approaches a steady periodic oscillation with a maximum close to 15×10^6 . This is a demonstration of the persistence result in Theorem 3.2.2, where it is proven that there exists a positive periodic solution when $\mathcal{R}_0 > 1$. (For this case, we find $\mathcal{R}_0 \approx 1.93$ through numerical evaluation of equation 3.13). In contrast, with the optimal control implemented, the concentration of brucella decreases over time, and the initial oscillation decays away, eventually approaching a value very close to 0, at which time both controls u_1 and u_2 would stay at the minimum (see Figure 3.4). Meanwhile, Figure 3.7 depicts the numbers of exposed and infectious animals over time with and without the optimal control. The results clearly show that the optimal control strategy significantly reduces the exposed and

infectious animal populations (compared to the case with regular control), to a level close to 0 when t > 20 years. Similar patterns are observed for the autonomous model (see Figure 3.8), but without the oscillatory behaviors of the curves in both cases.

To explore the impact of the costs on the implementation of control strategies, we have also varied the values of the cost parameters W_1 and W_2 . Suppose that the vaccination and decontamination can be achieved with significantly lower costs, say $W_1 = 10$ and $W_2 = 1$. Figure 3.9 shows the optimal control profiles for $u_1(t)$ and $u_2(t)$ in this hypothetical case for the periodic model. We see that, again, both u_1 and u_2 start from their maximums, and they stay at the maximum strength for much longer periods of time than the previous case (compare to Figure 3.4), due to the reduced costs of the controls. Afterwards both u_1 and u_2 oscillate with time and eventually settle at the minimum $u_1 = u_2 = 1$. In contrast, consider that there are high costs associated with these controls, and assume that $W_1 = 10^6$ and $W_2 = 1000$. The optimal control profiles for $u_1(t)$ and $u_2(t)$ in this case are presented in Figure 3.10. As is shown, the very high value of W_1 forces u_1 to stay at the minimum $u_1 = 1$ for almost all the time. The profile of u_2 still starts from its maximum, due to the relatively lower value of W_2 . It, however, quickly evolves into a yearly oscillation which continues for a long period (approximately 31 years), partly to compensate the effect that the control of u_1 is minimum for all the time. The profile of u_2 finally decays to the minimal state $u_2 = 1$. Figures 3.11 and 3.12 show the concentration of brucella and the number of exposed animals in this case, where we clearly observe that even with the optimal control, both the bacterial concentration and the exposed animal population keep oscillating (though, at much lower levels than their regular control counterparts) all the time without approaching a minimum value, a result different from the cases with low costs of controls. In all these scenarios, the optimal control maintains a "best" balance between the costs and the outcomes (i.e., reducing the exposed and infectious animal populations). Thus, higher costs would yield a relatively weaker, and perhaps insufficient, control strategy, as illustrated by the last case.

3.5 Conclusion and discussion

We have conducted an analysis for the impacts of seasonality on blucellosis transmission. Our mathematical model is an extension of a previous autonomous model [30] into time-periodic environments. We analyzed the basic reproduction number, \mathcal{R}_0 , associated with our periodic blucellosis model, and established threshold results characterized by \mathcal{R}_0 regarding the disease dynamics: when $\mathcal{R}_0 < 1$, the disease-free equilibrium is globally asymptotically stable; when $\mathcal{R}_0 > 1$, the system is uniformly persistent, and there exists a positive periodic solution.

We have performed an optimal control study by examining two types of controls: animal vaccination and environmental decontamination. We conducted analysis and simulation for both the autonomous and periodic brucellosis models. Our optimal control aims to minimize the numbers of the exposed and infectious animals, meanwhile minimize the associated costs. Our results show that, in all the scenarios, the optimal control can greatly reduce the numbers of the exposed and infectious animals and keep these populations at low levels, a significantly better outcome compared to that with regular control (i.e., with minimal effort $u_1 = u_2 = 1$). We observe that the optimal control strategies strongly depend on the cost parameters. With low costs, both the vaccination and decontamination will be carried out at or close to their maximum strength for a sufficiently long period of time, so as to minimize the disease exposure and infection. With high costs, however, the controls have to be implemented with reduced, or even minimum, strength, to achieve an optimal balance between the costs and effects of the control.

Our analysis and results throughout the chapter highlight the difference between the autonomous and periodic models. With constant parameters, the autonomous model is not able to reflect the seasonal variation, which is an important factor in brucellosis dynamics. Extending the autonomous model to time-periodic environments makes the model more realistic, but at the same time adding significant challenges to its mathematical analysis. We have established the uniform persistence of the disease dynamics and the existence of a nontrivial periodic solution when $\mathcal{R}_0 > 1$. However, whether the periodic solution is unique and what is the stability property, remains unresolved in the present work, and we plan to pursue these tasks in our future research. In addition, our optimal control simulation to the periodic model also produces quite different results from those with the autonomous model. Particularly, the optimal control profiles for u_1 and u_2 both exhibit annual oscillations, a pattern consistent with the seasonal variation of the model parameters, as well as a practical means to reduce the costs of the control (in contrast to constantly staying at the maximum strength). Finally, depending on the cost parameters associated with the control, the optimal profiles of u_1 and u_2 exhibit different lengths and amplitudes of oscillations, before eventually settling at their minimum levels. Consequently, the concentration of brucella and the numbers of exposed and infectious animals over time either approach a minimal state very close to 0, or oscillate at a level above 0. These results could provide useful guidelines to animal production and public health administration in designing effective control strategies against brucellosis.

Finally, we acknowledge that modeling the transmission and spread of infectious diseases, particularly brucellosis, would be of greater importance to public health and agriculture with the aid of realistic infection data. Unfortunately, the scarcity of seasonal brucellosis data at present limits our ability to calibrate some important seasonally varied parameters in our periodic model. We expect to improve this study in our future work with the availability of such data.

Chapter 4

On the dynamics of brucellosis infection in bison population with vertical transmission and culling

4.1 Introduction

Brucellosis is a zoonotic bacterial infection that affects domesticated animals, wildlife and humans. Animals acquire the infection mainly through direct contact with infected animals or indirectly from the environment containing large quantities of bacteria discharged by infected individuals [64], whereas in human, common routes of infection include direct inoculation through cuts and abrasions in the skin or inhalation of infectious aerosols and ingestion of infectious unpasteurized milk or other dairy products [38]. Human to human transmission is extremely rare [64, 38].

Although, brucellosis has been effectively controlled in many developed countries the disease remains common in Mediterranean areas, the south and the center of America, Africa, Asia, Arab peninsula, Indian subcontinent and the Middle East [65]. Currently more than 500,000 new cases of the disease are reported annually [42], with incidence as high as 200 cases per 100,000 of the population in endemic countries [43].

Mathematical modeling, analysis and simulation for infectious diseases have proved to be an essential guiding tool that could give a sound direction to policy makers and public health administration on how to effectively prevent and control brucellosis transmission. In particular, Abatih et al. [38] proposed the following set of differential equations to model the transmission dynamics of brucellosis:

$$\begin{cases}
\frac{dS}{dt} = (a - \phi N)[S + R + I\rho(1 - e)] - mS + \delta R - \frac{\beta IS}{N}, \\
\frac{dI}{dt} = \frac{\beta IS}{N} + e\rho(a - \phi N)I - (m + \alpha + v)I, \\
\frac{dR}{dt} = vI - (m + \delta)R,
\end{cases} (4.1)$$

where S(t), I(t) and R(t) are the numbers of the susceptible, infectious and recovered bison population at time t, respectively. The total bison population at time t is N(t) = S(t) + I(t) + R(t). Model parameter a denotes birth rate, ϕ is the density dependent reduction in births, m is the natural mortality rate and it is assumed to be constant in all epidemiological classes, α is the disease-related death rate, δ is the rate of lost of resistance, v is the recovery rate, β is the transmission rate, e is the proportion of vertical transmission rate and ρ is the reduction of fecundity in infectious bison. Thus, ρe is the reduced birth rate. Here, the bison enter the susceptible class through birth from the susceptible and recovered class at the net per capita birth rate of $(a - \phi N)$ and from the infectious class at the overall per capita birth rate of $\rho(1 - e)(a - \phi N)$. The susceptible population is also augmented through lost of immunity by bison already in the recovered class at the per capita rate of δ .

Although, the contribution of this study and several other studies (see, for example [5, 30, 32, 31, 66, 67]) cannot be underestimated, there are some few questions that remain unanswered. Such questions include:

- (i) To what extent does animals in chronic state influence the spread and control of disease?
- (ii) What is the influence of seasonal variations on brucellosis dynamics?
- (iii) To what extent can optimal culling strategies be effective on minimizing disease burden?

First, effective control of any disease depends as much on a thorough understanding of all the epidemiological stages an infected human/animal will go through. In both human and animals, brucellosis ecology can be segmented as: acute (0-2)

months), sub-acute (3-12 months) and chronic (> 12 months) [68]. For animals in sub-acute stage, a small fraction may progress to become chronic while some may recover from the infection [68]. Further, it is worth noting that animals in chronic state show no clinical signs of the disease and majority of these animals would be non-pregnant animals [69]. Since chronically infected animals transmit the infection it is therefore essential to gain a better and more comprehensive understanding of effective ways to control the disease.

Second, like many other infectious diseases, brucellosis incidence exhibits strong seasonal fluctuations in temperate regions world over [27, 28, 70, 71]. Seasonal variations in environmental and climatic conditions have an influence on animal behavior which in-turn can be attributed to seasonality in brucellosis dynamics. For example, in Botswana incidences of brucellosis have been observed to be high during dry seasons compared to wet seasons. The seasonality of brucellosis in Botswana has been attributed to the fact that during the dry seasons a large population of animals will be concentrated along river-fronts whereas during the wet seasons, animals are often spread out across the landscape [70]. The seasonality of brucellosis in European countries has also be reported by other researchers who observed that > 70% of brucellosis cases occur from March to June, with the peak observed from May to June [71]. In addition, prior studies have shown that the survival of Brucella in the environment depends critically on humidity, temperature and exposure to UV light and for an ideal environment the bacteria can last for 135 days [27]. Such seasonal variations need to be incorporated in models that aim to inform animal managers and policy makers efficiency and effective ways to control the disease.

Third, since prevalence of brucellosis is high in developing nations where resources for public health are limited, it is crucial to devise control strategies that are cost effective, i.e. that allow to minimize disease burden at minimal cost. In practice there is need to understand trade-off between the cost (or the constraints) of implementing the strategies and the potential or expected economic losses that these control measures should avoid. In practice it is impractical, if not unethical to conduct a series of control-effort experiments among animals so as to determine a specific culling strategy that performs better, hence on can utilise epidemiological models to describe dynamics in the framework of the optimal control theory [63].

The aim of the present work is to formulate a mathematical model for brucellosis transmission and control that suits developing countries, where the disease is endemic and animal vaccination is an expensive intervention strategy. Our model can also be utilized to understand brucellosis transmission dynamics among wildlife, since prior studies suggest that vaccination of wildlife is impractical [72]. To that end, we will extend the model for brucellosis transmission proposed in [38] to include:

- (i) an additional epidemiological class that account for animals in chronic state,
- (ii) seasonal variation on disease transmission pathway,
- (iii) time dependent culling effort :-precisely, we will investigate the effects of optimal control strategies when culling is the only viable control strategy. Although brucellosis can be controlled by either vaccination or culling, in developing nations vaccines are often expensive or unavailable [72, 73] leaving culling as the only viable control strategy. In addition, the "test-and-slaughter" method which can be used to detect animals in chronic state has proved to be an expensive intervention strategy for brucellosis control in developing countries [73]. As a consequence, culling of clinically infected animals remains the only viable disease intervention strategy for developing countries.

The remainder of the chapter is organized as follows. In Section 4.2, we introduce the ODE bison-brucellosis model that incorporates chronic brucellosis. We then conduct a thorough epidemic and endemic analysis of the model. In Section 4.3, we present a non-autonomous bison-brucellosis model that incorporates seasonal variations. We examine the threshold value, and study the global stability of the disease-free periodic solution and the uniform persistence of the system. In Section 4.4, we investigate the influence of culling control on minimizing the spread of the disease, through both mathematical analysis and numerical simulation. We conclude the chapter in Section 4.5 with a brief discussion.

4.2 Brucellosis model without seasonal variations

4.2.1 Model construction

Motivated by model (4.1), we propose the following autonomous dynamical system to account for brucellosis transmission:

$$\begin{cases}
\frac{dS}{dt} = (a - \phi N)[S + R + (I + A)\rho(1 - e)] - mS + \delta R - \frac{\beta(I + \epsilon A)S}{N}, \\
\frac{dI}{dt} = \frac{\beta(I + \epsilon A)S}{N} + e\rho(a - \phi N)(I + A) - (m + \alpha + \gamma + v)I, \\
\frac{dA}{dt} = pvI - (m + \alpha)A, \\
\frac{dR}{dt} = (1 - p)vI - (m + \delta)R.
\end{cases} (4.2)$$

All model parameters are non-negative, and they retain the same definitions as in model (4.1). On formulating model (4.2) the following additional assumptions were made:

- Based on the ecological information about brucellosis, an animal can be regarded to be in chronic state if it has been infected with the disease for more than 12 months [68], thus our model assumes that all newborn calves are either susceptible or clinically infected, since the gestation period in animals is less than 12 months.
- Infected bison display clinical signs of the disease for v^{-1} days after which a fraction p move to chronic state (modelled by A(t)) and the complementary (1-p) recover from the infection.
- We assume that animals in chronic state have less bacteria load than those displaying clinical signs of the disease, hence parameter ϵ accounts for the reduction of infectivity of animals in chronic state in comparison to animals in the symptomatic class.
- Since brucellosis is endemic in countries with limited resources, only animals displaying clinical signs of the disease are culled at constant rate γ .

Table 4.1: Parameters and values

Symbo	ol Definition	Units	Value	Source
\overline{p}	Proportion of symptomatic animals that become chronic	c unit-less	0.5	Assumed
ρ	Reduction of fecundity in infectious bison	unit-less	0.5	[38]
ϕ	Density dependent reduction in birth	$year^{-1}$	0.00004	[38]
e	Proportion of vertical transmission	unit-less	0.9	[38]
m	Per capita disease free death rate	$year^{-1}$	0.07	[38]
β	Disease transmission rate	$year^{-1}$	0.05 - 10	[38]
δ	Rate of loss of resistance	$year^{-1}$	0.2	[38]
α	Disease related death rate	$year^{-1}$	0.05	[38]
ϵ	Modification factor	unitless	0.08	Assumed
a	Recruitment rate	$year^{-1}$	0.82	[38]
γ	Culling rate	${ m year}^{-1}$	0.4	[38]
v	Recovery rate	${ m year}^{-1}$	0.5	[38]
S(0)	Initial number of susceptible	animals	4050	[38]
I(0)	Initial infected animals	animals	450	[38]
A(0)	Initial carrier animals	animals	0	[38]
R(0)	Initial recovered animals	animals	0	[38]

It can easily be verified that the domain of biological interest

$$\Omega = \left\{ (S, R, I, A) \in \mathbb{R}_+^4 : S > 0, \ R \ge 0, \ I \ge 0, \ A \ge 0 \text{ and} \right.$$

$$S(t) + R(t) + I(t) + A(t) \le \frac{a - m}{\phi} \right\}, \tag{4.3}$$

is positively invariant and attracting with respect to model (4.2).

4.2.2 The reproduction number

The corresponding disease-free equilibrium (DFE) of system (4.2) is given by

$$\mathcal{E}^0: (S^0, R^0, I^0, A^0) = \left(\frac{a-m}{\phi}, 0, 0, 0\right),$$

and it exists provided a > m. The reproduction number \mathcal{R}_0 is a threshold parameter for the infectious disease and it is essential on determining the spread of the disease. According to the next generation matrix developed by van den Driessche and Watmough [50], we define the basic reproduction number of system (4.2) as

$$\mathcal{R}_0 = \frac{e\rho m(p\nu + m + \alpha)}{(m+\alpha)(m+\alpha+\gamma+\nu)} + \frac{\beta(\epsilon p\nu + m + \alpha)}{(m+\alpha)(m+\alpha+\gamma+\nu)}, \tag{4.4}$$

where $\frac{e\rho m(p\nu+m+\alpha)}{(m+\alpha)(m+\alpha+\gamma+\nu)}$ and $\frac{\beta(\epsilon p\nu+m+\alpha)}{(m+\alpha)(m+\alpha+\gamma+\nu)}$, represents the number of new infections generated through vertical transmission and direct contact, respectively.

4.2.3 Equilibria

Regarding the stability of the disease-free equilibrium \mathcal{E}^0 and endemic equilibrium \mathcal{E}^* , we have the following Theorem.

Theorem 4.2.1

- (i) If $\mathcal{R}_0 \leq 1$, the DFE is globally asymptotically stable.
- (ii) If $\mathcal{R}_0 > 1$, system (4.2) has a unique endemic equilibrium \mathcal{E}^* , which is globally asymptotically stable.

Proof of Theorem 4.2.1 (i)

Proof 6 In what follows, we will show that if $\mathcal{R}_0 \leq 1$ then system (4.2) has a disease-free equilibrium which is globally asymptotically stable (Theorem 4.2.1 (i).) Consider the Lyapunov functional

$$L(t) = \left[\frac{(\beta + e\rho m)k_2 + (\beta \epsilon + e\rho m)p\nu}{k_1 k_2} \right] I(t) + \left[\frac{\beta \epsilon + e\rho m}{k_2} \right] A(t)$$
 (4.5)

where $k_1 = (m + \alpha + \gamma + \nu)$, $k_2 = (m + \alpha)$. Taking the derivative of L(t) with respect to t along the solutions of (4.2) gives

$$\begin{split} \dot{L}(t) &= \left[\frac{(\beta + e\rho m)k_2 + (\beta \epsilon + e\rho m)p\nu}{k_1k_2}\right] \left[\frac{\beta(I + \epsilon A)S}{N}\right] - \beta(I + \epsilon A) \\ &+ \left[\frac{(\beta + e\rho m)k_2 + (\beta \epsilon + e\rho m)p\nu}{k_1k_2}\right] e\rho(a - \phi N)(I + A) - e\rho m(I + A), \\ &= \left[\frac{(\beta + e\rho m)k_2 + (\beta \epsilon + e\rho m)p\nu}{k_1k_2} \frac{S}{N} - 1\right] \beta(I + \epsilon A) \\ &+ \left[\frac{(\beta + e\rho m)k_2 + (\beta \epsilon + e\rho m)p\nu}{k_1k_2} \frac{(a - \phi N)}{m} - 1\right] e\rho m(I + A) \\ &\leq \left[\frac{(\beta + e\rho m)k_2 + (\beta \epsilon + e\rho m)p\nu}{k_1k_2} - 1\right] \left[\beta(I + \epsilon A) + e\rho m(I + A)\right] \end{split}$$

$$= \left[\mathcal{R}_0 - 1 \right] \left[\beta (I + \epsilon A) + e \rho m (I + A) \right]. \tag{4.6}$$

Therefore, $\dot{L} \leq 0$ as long as $\mathcal{R}_0 \leq 1$. When $\mathcal{R}_0 < 1$, $\dot{L} = 0$ yields I = A = 0. Then it can be easily observed from the system (4.2) that as $t \to \infty$, $S \to S^0 = N = \frac{a-m}{\phi}$ and R = 0. Hence, the only invariant set when $\dot{L} = 0$ is the singleton $\mathcal{E}^0 = (S^0, 0, 0, 0)$. It follows from Lasalle's Invariance Principle [46] that every solution of the system (4.2), with initial conditions in Ω , approaches \mathcal{E}^0 as $t \to \infty$. Thus, the DFE is a global attractor.

Proof of Theorem 4.2.1 (ii)

Proof 7 We will begin by demonstrating that system (4.2) admits a unique endemic equilibrium point whenever $\mathcal{R}_0 > 1$. One can reduce system (4.2) into three dimensional system by setting R = N - S - I - A to get

$$\begin{cases}
\frac{dS}{dt} = (a - \phi N)[N + (\rho(1 - e) - 1)(I + A)] - mS + \delta(N - S - I - A) \\
-\frac{\beta(I + \epsilon A)S}{N}, \\
\frac{dI}{dt} = \frac{\beta(I + \epsilon A)S}{N} + e\rho(a - \phi N)(I + A) - (m + \alpha + \gamma + v)I, \\
\frac{dA}{dt} = pvI - (m + \alpha)A.
\end{cases}$$
(4.7)

The endemic equilibrium of the system (4.7) is determined by equations

$$\begin{cases} (a - \phi N^*)[N^* + (\rho(1 - e) - 1)(I^* + A^*)] - mS^* + \delta(N^* - S^* - I^* - A^*) \\ -\frac{\beta(I^* + \epsilon A^*)S^*}{N^*} = 0, \\ \frac{\beta(I^* + \epsilon A^*)S^*}{N^*} + e\rho(a - \phi N^*)(I^* + A^*) - (m + \alpha + \gamma + v)I^* = 0, \\ pvI^* - (m + \alpha)A^* = 0. \end{cases}$$

$$(4.8)$$

From the last equation of (4.8) we have

$$I^* = \frac{(m+\alpha)}{pv}A^*, \quad I^* + A^* = M_1A^*, \quad \text{and} \quad I^* + \epsilon A^* = M_2A^*.$$
 (4.9)

with

$$M_1 = \frac{m + \alpha + pv}{pv}$$
, and $M_2 = \frac{m + \alpha + \epsilon pv}{pv}$. (4.10)

It follows from the first equations in (4.8) that

$$S^* = \frac{(a - \phi N^*)N^* + (a - \phi N^*)\rho M_1 A^* + \delta N^*}{(m + \delta + \frac{\beta}{N^*} M_2 A^*)}$$

$$+\frac{-(a-\phi N^*)\rho e M_1 A^* - (a-\phi N^*) M_1 A^* - \delta M_1 A^*}{(m+\delta + \frac{\beta}{N^*} M_2 A^*)},$$
 (4.11)

for $A^* \neq 0$, substituting equation (4.9) into the second equation in (4.8) yields

$$S^* = \frac{k_1 k_2 N^* - e\rho(a - \phi N^*) M_1 p v N^*}{\beta M_2 p v}.$$
 (4.12)

substituting (4.11) into (4.12) gives

$$F(A^*) = \frac{(a - \phi N^*)N^* + (a - \phi N^*)\rho M_1 A^* - (a - \phi N^*)\rho e M_1 A^*}{(m + \delta + \frac{\beta}{N} M_2 A^*)} + \frac{-(a - \phi N^*)M_1 A^* + \delta N^* - \delta M_1 A^*}{(m + \delta + \frac{\beta}{N} M_2 A^*)} + \frac{e\rho(a - \phi N^*)M_1 N^*}{\beta M_2} - \frac{k_1 k_2 N^*}{\beta M_2 \rho v} = 0.$$

$$(4.13)$$

Direct calculation for $A^* \geq 0$ shows

$$F'(A^*) = \frac{-\hbar_0(1-\rho) - [\hbar_0\rho e + \hbar_1 + \hbar_2 + \hbar_3]}{(m+\delta + \frac{\beta}{N^*}M_2A^*)^2},$$
(4.14)

with

$$hbar{h}_0 = (a - \phi N)(m + \delta)M_1, \quad \hbar_1 = \delta(m + \delta)M_1, \quad \hbar_2 = \beta(a - \phi N^*)M_2, \quad \hbar_3 = \beta\delta M_2.$$

Since $\rho \in [0,1]$ it implies that F'(A) < 0. Therefore the function F(A) is monotonic decreasing for A > 0, and it follows that

$$F(0) = N^* + \frac{e\rho m M_1 N^*}{\beta M_2} - \frac{k_1 k_2 N^*}{\beta M_2 p v} = \frac{N^* k_1 k_2}{p v \beta M_2} (\mathcal{R}_0 - 1). \tag{4.15}$$

Therefore, by monotonicity of a function F(A), there exists a unique positive root in the interval $(0, \frac{a-m}{\phi})$ when $\mathcal{R}_0 > 1$ and there is no positive root in the interval $(0, \frac{a-m}{\phi})$ when $\mathcal{R}_0 < 1$. Thus model (4.2) has a unique endemic equilibrium $\mathcal{E}^* = (S^*, I^*, A^*)$.

In what follows, we prove the second part of Theorem 4.2.1(ii), i.e, whenever $\mathcal{R}_0 > 1$, then the unique endemic equilibrium point \mathcal{E}^* of system (4.2) is globally asymptotically stable. To achieve this objective we will utilize the geometric approach originally proposed by Li and Muldowney [74]. For completeness, we first present the following result from [74].

Lemma 4.1 Consider a dynamical system $\frac{dX}{dt} = f(X)$, where $f: D \mapsto \mathbb{R}^n$ is a C^1 function and $D \subset \mathbb{R}^n$ is a simply connected domain. Assume that there exists a compact absorbing set $K \subset D$ and the system has a unique equilibrium point X^* in D. Then X^* is globally asymptotically stable in D if $\bar{q}_2 < 0$, where

$$\bar{q}_2 = \limsup_{t \to \infty} \sup_{X_0 \in K} \frac{1}{t} \int_0^t m(Q(X(s, X_0))) ds.$$

$$(4.16)$$

In equation (4.16), Q is a matrix-valued function defined as

$$Q = P_f P^{-1} + P J^{[2]} P^{-1} ,$$

where P(X) is a $\binom{n}{2} \times \binom{n}{2}$ matrix-valued C^1 function in D, P_f is the derivative of P (entry-wise) along the direction of f, and $J^{[2]}$ is the second additive compound matrix of the Jacobian J(X) = Df(X). Meanwhile, m(Q) is the Lozinskii measure of Q with respect to a matrix norm; i.e.,

$$m(Q) = \lim_{h \to 0^+} \frac{|\mathbb{I} + hQ| - 1}{h},$$

where \mathbb{I} represents the identity matrix.

Now we proceed to investigate the global stability of the endemic equilibrium point \mathcal{E}^* . It is easy to show that the Jacobian matrix of system (4.7) at \mathcal{E}^* is

$$\mathcal{J} = \begin{bmatrix}
d_{11} & d_{12} & -(a - \phi N^*) + (a - \phi N^*)\rho(1 - e) - \delta - \frac{\beta \epsilon S^*}{N^*} \\
\frac{\beta(I^* + \epsilon A^*)}{N^*} & d_{22} & \frac{\beta \epsilon S^*}{N^*} + e\rho(a - \phi N^*) \\
0 & pv & d_{33}
\end{bmatrix}, (4.17)$$

with

$$d_{11} = -m - \delta - \frac{\beta(I^* + \epsilon A^*)}{N^*},$$

$$d_{12} = -(a - \phi N^*) + (a - \phi N^*)\rho(1 - e)$$

$$-\delta - \frac{\beta S^*}{N^*},$$

$$d_{22} = \frac{\beta S^*}{N^*} + e\rho(a - \phi N^*) - (m + \alpha + \gamma + v), \quad d_{33} = -(m + \alpha),$$

and the associated second compound matrix is

$$\mathcal{J}^{[2]} = \begin{bmatrix} \chi_1 & \frac{\beta \epsilon S^*}{N^*} + e\rho(a - \phi N^*) & (a - \phi N^*) - (a - \phi N^*)\rho(1 - e) + \delta + \frac{\beta \epsilon S^*}{N^*} \\ pv & \chi_2 & -(a - \phi N^*) + (a - \phi N^*)\rho(1 - e) - \delta - \frac{\beta S^*}{N^*} \\ 0 & \frac{\beta(I^* + \epsilon A^*)}{N^*} & \chi_3 \end{bmatrix},$$

with

$$\chi_{1} = -2m - \alpha - \gamma - \delta - v + e\rho(a - \phi N^{*}) + \frac{\beta S^{*}}{N^{*}} - \frac{\beta(I^{*} + \epsilon A^{*})}{N^{*}},
\chi_{2} = -2m - \alpha - \delta - \frac{\beta(I^{*} + \epsilon A^{*})}{N^{*}},
\chi_{3} = -2m - 2\alpha - \gamma - v + \frac{\beta S^{*}}{N^{*}} + e\rho(a - \phi N^{*}).$$
(4.18)

Set, $H = diag\left[1, \frac{I^*}{A^*}, \frac{I^*}{A^*}\right]$, then

$$H_F H^{-1} = diag \left[0, \frac{\dot{I}}{I^*} - \frac{\dot{A}}{A^*}, \frac{\dot{I}}{I^*} - \frac{\dot{A}}{A^*} \right],$$

and $H\mathcal{J}^{[2]}H^{-1}$ is

$$\begin{bmatrix} \chi_1 & \frac{A^*}{I^*} (\frac{\beta \epsilon S^*}{N^*} + e\rho(a - \phi N^*)) & \frac{A^*}{I^*} (a + \frac{\beta \epsilon S^*}{N^*} + \delta - \phi N^* - (1 - e)\rho(a - \phi N^*)) \\ \frac{I^*pv}{A^*} & \chi_2 & -a - \frac{\beta S^*}{N^*} - \delta + (1 - e)\rho(a - \phi N^*) + \phi N^* \\ 0 & \frac{\beta(I^* + \epsilon A^*)}{N^*} & \chi_3 \end{bmatrix}.$$
(4.19)

The matrix $Q = H_F H^{-1} + H \mathcal{J}^{[2]} H^{-1}$ can be written in the block form as follows:

$$Q = \begin{bmatrix} Q_{11} & Q_{12} \\ Q_{21} & Q_{22} \end{bmatrix}$$

in which

$$Q_{11} = -(2m + \alpha + \gamma + \delta + v) + e\rho(a - \phi N^*) + \frac{\beta S^*}{N^*} - \frac{\beta (I^* + \epsilon A^*)}{N^*},$$

$$Q_{12} = \left[\frac{A^*}{I^*} \left(\frac{\beta \epsilon S^*}{N^*} + e\rho(a - \phi N^*)\right) \left(\frac{\beta \epsilon S^*}{N^*} + e\rho(a - \phi N^*) - [\phi N^* + \rho(a - \phi N^*) - (\phi N^*) - (\phi N^*) - (\phi N^*)\right) - (\phi N^*) - (\phi N^*)\right],$$

$$Q_{21} = \begin{bmatrix} pv \frac{I^*}{A^*} \\ 0 \end{bmatrix}, \quad Q_{22} = \begin{bmatrix} \chi_2 + \frac{\dot{I}}{I} - \frac{\dot{A}}{A} & -a - \frac{\beta S^*}{N^*} - \delta + (1 - e)\rho(a - \phi N^*) + \phi N^* \\ \frac{\beta(I^* + \epsilon A^*)}{N^*} & \chi_3 + \frac{\dot{I}}{I} - \frac{\dot{A}}{A} \end{bmatrix}.$$

We now define the vector norm \mathbb{R}^3 as

$$|(y_1, y_2, y_3)| = \max\{|y_1|, |y_2|, |y_3|\},\$$

for any vector $(y_1, y_2, y_3) \in \mathbb{R}^3$. Let η denote the Lozinskii measure with respect to this norm. By direct calculation one gets

$$\eta(Q) \le \sup\{g_1, g_2\}$$

with

$$g_1 = \eta_1(Q_{11}) + |Q_{12}|,$$

$$g_2 = |Q_{21}| + \eta_1(Q_{22}),$$

where $|Q_{12}|$ and $|Q_{21}|$ are matrix norms with respect to L_1 vector norm, and η_1 denotes the Lozinskii measure with respect to the L_1 norm. Specifically

$$\eta_{1}(Q_{11}) = -(2m + v + \alpha + \gamma + \delta) + \frac{\beta S^{*}}{N^{*}} - \frac{\beta (I^{*} + \epsilon A^{*})}{N^{*}} + e\rho(a - \phi N^{*}),
\eta_{1}(Q_{22}) = -(2m + \alpha + \delta) + \frac{\dot{I}}{I^{*}} - \frac{\dot{A}}{A^{*}}
+ \sup \left\{ 0, \rho(a - \phi N^{*}) + \phi N^{*} - (a + v + \alpha + \gamma) \right\}.$$

Therefore,

$$g_{1} = -(2m + v + \alpha + \gamma + \delta) + \frac{\beta S^{*}}{N^{*}} - \frac{\beta (I^{*} + \epsilon A^{*})}{N^{*}} + e\rho(a - \phi N^{*}) + \left[\frac{\beta \epsilon S^{*}}{N^{*}} + e\rho(a - \phi N^{*})\right] \frac{A^{*}}{I^{*}}.$$

From the second equation of (4.7) we have

$$\left[\frac{\beta \epsilon S^*}{N^*} + e\rho(a - \phi N^*)\right] \frac{A^*}{I^*} = \frac{\dot{I}}{I^*} - \frac{\beta S^*}{N^*} - e\rho(a - \phi N^*) + (m + \alpha + \gamma + v).$$

Thus,

$$g_1 = \frac{\dot{I}}{I^*} - (m+\delta) - \frac{\beta(I^* + \epsilon A^*)}{N^*} \le \frac{\dot{I}}{I^*} - (m+\delta).$$

Similarly

$$g_2 = pv \frac{I^*}{A^*} - 2m - \alpha - \delta + \frac{\dot{I}}{I^*} - \frac{\dot{A}}{A^*} + \sup \left\{ 0, \rho(a - \phi N^*) + \phi N^* - (a + v + \alpha + \gamma) \right\},$$

Using the relation of the last equation in (4.7)

$$\frac{\dot{A}}{A^*} = pv \frac{I^*}{A^*} - (m+\alpha),$$

we have

$$g_2 = \frac{\dot{I}}{I^*} - (m+\delta) + \sup \left\{ 0, \rho(a - \phi N^*) + \phi N^* - (a+v+\alpha+\gamma) \right\} \le \frac{\dot{I}}{I^*} - (m+\delta).$$

Since $N^* \leq \frac{a-m}{\phi}$ one can easily deduce that $\rho(a-\phi N^*) + \phi N^* - (a+v+\alpha+\gamma) \leq 0$. Therefore

$$\eta(Q) \le \frac{\dot{I}}{I^*} - (m + \delta).$$

Since $0 \le I(t) \le N(t)$, there exists T > 0 such that when t > T, $\frac{\ln I(t) - \ln I(0)}{t} < \frac{(m+\delta)}{2}$. As a result

$$\frac{1}{t} \int_0^t \eta(s) dt \le \frac{1}{t} \int_0^t \left[\frac{\dot{I}(s)}{I(s)} - (m+\delta) \right] ds = \frac{\ln I(t) - \ln I(0)}{t} - (m+\delta) \le -\frac{(m+\delta)}{2}.$$

which implies that $\bar{q}_2 \leq -\frac{(m+\delta)}{2} < 0$. This completes the proof.

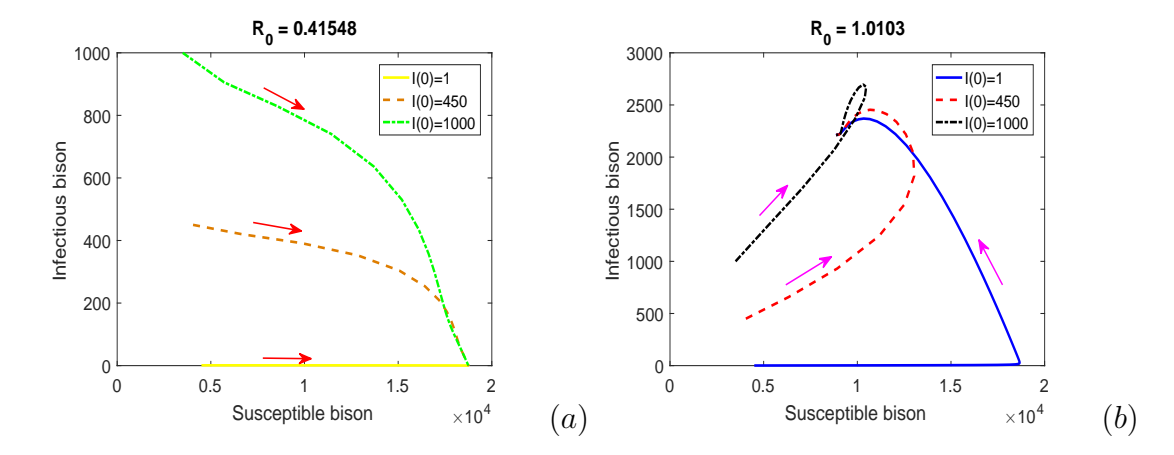


Figure 4.1: Phase portrait depicting the global stability of (a) the disease-free equilibrium \mathcal{E}^0 which exists for $\mathcal{R}_0 \leq 1$, here we set $\beta = 0.28$ to get $\mathcal{R}_0 = 0.41548$ (b) the endemic equilibrium point which exists whenever $\mathcal{R}_0 > 1$, note that we set $\beta = 0.8$ to obtain $\mathcal{R}_0 = 1.0103$. The numerical results depicted in (a) supports that analytical findings in Theorem 4.2.1 (i), that whenever $\mathcal{R}_0 < 1$ then system (4.2) has a globally asymptotically stable disease-free equilibrium. Similarly, plot (b) demonstrate the analytical predictions in Theorem 4.2.1 (ii) that if $\mathcal{R}_0 > 1$, system (4.2) has a unique endemic equilibrium \mathcal{E}^* , which is globally asymptotically stable.

Using the parameter values in Table 4.1, we conduct some numerical simulations in order to verify Theorem 4.2.1 (see, Figure 4.1). In Figure 4.1(a) we set $\beta = 0.28$ to obtain $\mathcal{R}_0 = 0.41548$ and varied the initial conditions. The simulation results clearly show that when $\mathcal{R}_0 < 1$, system (4.2) has a globally stable disease-free equilibrium with $S \approx 1.85 \times 10^4$ and I = 0. This result is in agreement with the analytical predictions in Theorem 4.2.1 (i).

In Figure 4.1 (b), we set $\beta = 1.08$ to get $\mathcal{R}_0 = 1.3305$ and varied the initial conditions. The numerical results demonstrate that when $\mathcal{R}_0 > 1$ all solutions for system (4.2) in the plane I vs S converge to endemic endemic equilibrium with $S \approx 8870.715$ and $I \approx 2211.848$. This result support the analytical result of Theorem 4.2.1 (ii) which states that whenever $\mathcal{R}_0 > 1$, system (4.2) admits a unique endemic equilibrium \mathcal{E}^* , which is globally asymptotically stable.

4.3 Brucellosis model with seasonal variations

4.3.1 Model construction

As highlighted earlier, incidences of brucellosis in both developed and developing countries exhibit seasonal variations, with high incidences observed in certain months of the year. In order to incorporate seasonal variations into our basic model (4.2) we modelled the contact rate by the following periodic function $\beta(t) = \beta_0(1 + \beta_1 \cos \omega t)$, where β_0 denotes the basic contact rate without seasonal forcing, $0 \le \beta_1 \le 1$ denotes the magnitude of seasonal fluctuations, $\omega = \frac{2\pi}{12}$ corresponds to a one year period. Using the same parameter and class names as in system (4.2), the system of differential equations describing our model with seasonal variations is:

$$\begin{cases}
\frac{dS}{dt} &= (a - \phi N)[S + R + (I + A)\rho(1 - e)] - mS + \delta R - \frac{\beta(t)(I + \epsilon A)S}{N}, \\
\frac{dI}{dt} &= \frac{\beta(t)(I + \epsilon A)S}{N} + e\rho(a - \phi N)(I + A) - (m + \alpha + \gamma + v)I, \\
\frac{dA}{dt} &= pvI - (m + \alpha)A, \\
\frac{dR}{dt} &= (1 - p)vI - (m + \delta)R.
\end{cases}$$
(4.20)

4.3.2 The reproduction number

One can easily verify that the disease-free equilibrium of system (4.20) is

$$\mathcal{E}^{0} = \left(S^{0} = \frac{a-m}{\phi}, 0, 0, 0\right)$$

and it is the same as the for the autonomous system (4.2). In what follows we now introduce the basic reproduction number by applying the next-generation method. Thus, we define matrices F(t) and V(t) (evaluated at the disease-free equilibrium) as

$$F(t) = \begin{bmatrix} \beta(t) + em & \beta(t)\epsilon + e\rho m \\ 0 & 0 \end{bmatrix} \text{ and } V(t) = \begin{bmatrix} k_1 & 0 \\ -pv & k_2 \end{bmatrix}.$$

In order to define the basic reproduction number of this non-autonomous model, we follow the work of Wang and Zhao [55]. They introduced the next-infection

operator L for a model in periodic environments by

$$(L\psi)(t) = \int_0^\infty Y(t, t-s)F(t-s)\psi(t-s)ds, \tag{4.21}$$

where $Y(t,s), t \geq s$, is the evolution operator of the linear ω -periodic system dy/dt = -V(t)y and $\psi(t)$, the initial distribution of infectious individuals, is ω -periodic and nonnegative. The basic reproduction number is then defined as the spectral radius of the next-infection operator,

$$R_0 = \rho(L). \tag{4.22}$$

For our model (4.20), the evolution operator can be determined by solving the system of differential equations dy/dt = -V(t)y with the initial condition $Y(s,s) = I_{2\times 2}$; thus, we obtain

$$Y(t,s) = \begin{bmatrix} e^{-k_1(t-s)} & 0\\ \frac{pv}{(\gamma+v)} [e^{-k_2(t-s)} - e^{-k_1(t-s)}] & e^{-k_2(t-s)} \end{bmatrix}$$
(4.23)

The basic reproduction number defined in Equation (4.22) can be numerically evaluated by using, for example, the method described in [56].

4.3.3 Threshold dynamics

Using the basic reproduction number R_0 , we aim to establish the threshold type result, stated in the theorem below, for the periodic model (4.20). To that end, we first note that \mathbb{R}_+ is positively invariant for the following equation:

$$\dot{S}(t) = (a - \phi N)[S + R + (I + A)\rho(1 - e)] - mS + \delta R - \frac{\beta(t)(I + \epsilon A)S}{N}, \quad (4.24)$$

and that S^0 is the unique equilibrium solution which is globally attractive in \mathbb{R}_+ .

Theorem 4.3.1

- (i) If $R_0 < 1$, then the disease-free equilibrium \mathcal{E}_0 of system (4.20) is globally asymptotically stable;
- (ii) If $R_0 > 1$, then system (4.20) admits at least one positive ω -periodic solution, and solutions of system (4.20) are uniformly persistent.

Proof of Theorem 4.3.1

Proof 8 If (S(t), R(t), I(t), A(t)) is a non-negative solution of (4.20), then we have

$$\dot{S}(t) \le (a - \phi N)[S + R + (I + A)\rho(1 - e)] - mS + \delta R - \frac{\beta(t)(I + \epsilon A)S}{N}, \quad (4.25)$$

Note that any nonnegative solution S(t) of system (4.24) approaches S^0 as $t \to \infty$. It then follows from the standard comparison theorem (see, e.g., [75, Theorem A.4]) that for any $\epsilon' > 0$, there is a T > 0 such that

$$S(t) < S^0 + \epsilon', \text{ for } t > T. \tag{4.26}$$

Thus, for t > T, we have

$$\dot{I}(t) \le \frac{\beta(t)(I + \epsilon A)(S^0 + \epsilon')}{N} + e\rho(a - \phi N)(I + A) - (m + \alpha + \gamma + v)I,$$

$$\dot{A}(t) \le pvI - (m + \alpha)A.$$
(4.27)

Define

$$F_{\epsilon'}(t) = \begin{bmatrix} \frac{\beta(t)}{N} (S^0 + \epsilon') & \frac{\beta(t)\epsilon}{N} (S^0 + \epsilon') \\ 0 & 0 \end{bmatrix}.$$

By [55, Thorem 2.2], we have $R_0 < 1 \iff \rho(\phi_{F-V}(\omega)) < 1$, where $\rho(\phi_{F-V}(\omega))$ is the spectral radius of $\phi_{F-V}(\omega)$, and $\phi_{F-V}(\omega)$ is the monodromy matrix of the linear ω -periodic system dy/dt = (F-V)y. Then we can set ϵ' sufficiently small such that $\rho(\phi_{F_{\epsilon'}-V}(\omega)) < 1$. As a consequence, the trivial solution (0,0) of the following linear ω -periodic system , and from the last equation of system(4.20) it is straight forward to observe that $\lim_{t\to\infty} R(t) = 0$

$$\dot{I}(t) = \frac{\beta(t)(I + \epsilon A)(S^0 + \epsilon')}{N} + e\rho(a - \phi N)(I + A) - (m + \alpha + \gamma + v)I,$$

$$\dot{A}(t) = pvI - (m + \alpha)A.$$
(4.28)

is globally asymptotically stable. Again by the comparison theorem, we know that $I(t) \to 0, A(t) \to 0$ as $t \to \infty$. Finally, the first equation of system (4.20) imply that $S(t) \to S^0$ as $t \to \infty$. This proves the result in part (i).

Now we consider the case $R_0 > 1$. We define $X = \mathbb{R}^4_+$, $X_0 = \mathbb{R}^2_+ \times Int(\mathbb{R}^2_+)$, $\partial X_0 = X \setminus X_0$, It is easy to see that both X and X_0 are positively invariant. Let $P : \mathbb{R}^4_+ \to X_0$

 \mathbb{R}^4_+ be the Poincaré map associated with system (4.20); that is, $P(x_0) = u(\omega, x_0)$ for all $x_0 \in \mathbb{R}^4_+$, where $u(t, x_0)$ is the unique solution of (4.20) with $u(0, x_0) = x_0$. Set

$$M_{\partial} = \{ (S(0), R(0), I(0), A(0)) \in \partial X_0 : P^m(S(0), R(0), I(0), A(0)) \in \partial X_0, \ \forall m \ge 0 \},$$

$$M = \{(S, R, I, A) : S \ge 0, R = 0, I = 0, A = 0\}.$$

We first show that

$$M_{\partial} = M. \tag{4.29}$$

Clearly, $M \subseteq M_{\partial}$. For any $(S(0), R(0), I(0), A(0)) \in \partial X_0 \backslash M$, if A(0) > 0, I(0) = 0, then $\dot{I}(0) > 0$. if I(0) > 0, A(0) = 0, then $\dot{A}(0) > 0$. Thus, we have

$$(S(t), R(t), I(t), A(t)) \notin \partial X_0$$

for $0 < t \ll 1$. By the positive invariance of X_0 , we know that

$$P^{m}(S(0), R(0), I(0), A(0)) \notin \partial X_{0}$$

for $m \ge 1$, hence $(S(0), R(0), I(0), A(0)) \notin M_{\partial}$, and thus (4.29) holds.

Now consider the fixed point $M_0 = (S^0, 0, 0, 0)$ of the Poincaré map P. Define $W^S(M_0) = \{x_0 : P^m(x_0) \to M_0, m \to \infty\}$. From system(4.20), it is easy to observe that when A = I = 0, we have $R \to 0$ We show that

$$W^S(M_0) \cap X_0 = \emptyset. (4.30)$$

Based on the continuity of solutions with respect to the initial conditions, for any $\epsilon' > 0$, there exists $\delta > 0$ small enough such that for all $(S(0), R(0), I(0), A(0)) \in X_0$ with $||(S(0), R(0), I(0), A(0)) - M_0|| \leq \delta$, we have

$$||u(t, (S(0), R(0), I(0), A(0))) - u(t, M_0)|| < \epsilon', \quad \forall t \in [0, \omega].$$
 (4.31)

To obtain (4.30), we claim that

$$\lim_{m \to \infty} \sup_{l \to \infty} ||P^{m}(S(0), R(0), I(0), A(0)) - M_{0}|| \ge \delta, \quad \forall (S(0), R(0), I(0), A(0)) \in X_{0}.$$
(4.32)

We prove this claim by contradiction; that is, we suppose

$$\lim_{m \to \infty} \sup_{n \to \infty} ||P^m(S(0), R(0), I(0), A(0)) - M_0|| < \delta$$

for some $(S(0), R(0), I(0), A(0)) \in X_0$. Without loss of generality, we assume that

$$||P^m(S(0), R(0), I(0), A(0)) - M_0|| < \delta, \quad \forall m \ge 0.$$

Thus,

$$||u(t, P^m(S(0), R(0), I(0, A(0))) - u(t, M_0)|| < \epsilon', \quad \forall t \in [0, \omega] \text{ and } m \ge 0.$$
 (4.33)

Moreover, for any $t \geq 0$, we write $t = t_0 + k\omega$ with $t_0 \in [0, \omega)$ and $k = [t/\omega]$, the greatest integer less than or equal to t/ω . Then we obtain

$$||u(t, (S(0), R(0), I(0), A(0))) - u(t, M_0)||$$

$$= ||u(t_0, P^m(S(0), R(0), I(0), A(0))) - u(t_0, M_0)|| < \epsilon$$

'for any $t \geq 0$. Let (S(t), R(t), I(t), A(0)) = u(t, (S(0), R(0), I(0), A(0))). It follows that $-\epsilon' < S(t) - S^0 < \epsilon', 0 < I(t) < \epsilon', \text{ and } 0 < A(t) < \epsilon'.$ Again based on [55, Thorem 2.2], $R_0 > 1$ if and only if $\rho(\Phi_{F-V}(\omega)) > 1$. Thus, for ϵ' small enough, we have $\rho(\Phi_{F'_{\epsilon}-V}(\omega)) > 1$ which immediately yields the contradiction as

$$\lim_{t \to \infty} I(t) = \infty \quad \lim_{t \to \infty} A(t) = \infty.$$

Let $P_1: \mathbb{R}_+ \longrightarrow \mathbb{R}_+$ be the Poincareé map associated with (4.24). Then S^0 is globally attractive in $\mathbb{R}_+ \setminus \{0\}$ for P_1 . It follows that M_0 is isolated invariant set in X, and notice that $W^S(M_0) \cap X_0 = \emptyset$. Hence, every orbit in M_0 converges to M_0 and M_0 is acyclic in M_0 . By [58, Thorem 1.3.1], for a stronger repelling property of ∂X_0 , we conclude that P is uniformly persistent with respect to $(X_0, \partial X_0)$, which implies the uniform persistence of the solutions of system (4.20) with respect to $(X_0, \partial X_0)$ [58, Thorem 3.1.1]. Consequently, based on [58, Theorem 1.3.6], the Poincaré map P has a fixed point $(\bar{S}(0), \bar{R}(0), \bar{I}(0), \bar{A}(0)) \in X_0$, and it can be easily seen that $\bar{S}(0) \neq 0$. Thus, $(\bar{S}(0), \bar{R}(0), \bar{I}(0, \bar{A}(0)) \in Int(\mathbb{R}^4_+)$ and

$$(\bar{S}(t), \bar{R}(t), \bar{I}(t), \bar{A}(0)) = u(t, (\bar{S}(0), \bar{R}(0), \bar{I}(0), \bar{A}(0)))$$

is a positive ω -periodic solution of the system.

4.4 Optimal control

Our goal here is to determine an optimal culling strategy that will minimize the total disease burden, while minimizing the cost of implementing such a strategy. Due to limitedness of resources in most brucellosis endemic areas, we assume that culling of clinically infected animals is the only viable intervention strategy since it is associated with low costs.

4.4.1 Formulation

To determine the optimal culling strategy, we modify model (4.2) by letting $\gamma = u(t)$ and this results in the following system

$$\begin{cases} \frac{dS}{dt} &= (a - \phi N(t))[S(t) + R(t) + (I(t) + A(t))\rho(1 - e)] - mS(t) + \delta R(t) \\ &- \frac{\beta(I(t) + \epsilon A(t))S(t)}{N(t)}, \\ \frac{dI}{dt} &= \frac{\beta[I(t) + \epsilon A(t)]S(t)}{N(t)} + e\rho(a - \phi N(t))(I(t) + A(t)) \\ &- (m + \alpha + u(t) + v)I(t) \\ \frac{dA}{dt} &= pvI(t) - (m + \alpha)A(t), \\ \frac{dR}{dt} &= (1 - p)vI(t) - (m + \delta)R(t). \end{cases}$$
(4.34)

Remark: Note that in the formulation of our optimality system, parameter β , can be either constant, for the autonomous model (4.2), or periodic function as in system (4.20).

We consider the following objective functional

$$J(u(t)) = \int_0^T \left[C_1 I(t) + C_2 A(t) - C_3 S(t) + C_4 u(t) \right] dt.$$
 (4.35)

where C_i (i = 1, 2, 3, 4) represents the appropriate positive balancing constants. The objective is to minimize the total number of infected animals (both clinical and chronic) and maximize the total number of susceptible population, while also minimizing the cost of implementation. In addition, our objective functional (4.35) assumes that there is a linear relationship between the costs and the number of clinically infected animals to be culled. The control set is defined as

$$Q = \{ u(t) \mid 0 \le U_1 \le u(t) \le U_2 \le 1, 0 \le t \le T \}.$$
 (4.36)

where U_1 and U_2 denote the lower and upper bounds of culling efforts, respectively. These bounds reflect practical limitation of resources to implement the control in a given time horizon. By utilizing the Pontryagin's maximum Principle [63], we have the following Hamiltonian function H:

$$H(t) = C_{1}I(t) + C_{2}A(t) - C_{3}S(t) + C_{4}u(t)$$

$$+\lambda_{1}(t) \left[(a - \phi N(t))[S(t) + R(t) + (I(t) + A(t))\rho(1 - e)] - mS(t) + \delta R(t) \right]$$

$$-\frac{\beta(I(t) + \epsilon A(t))S(t)}{N(t)} \Big]$$

$$+\lambda_{2}(t) \left[\frac{\beta(I(t) + \epsilon A(t))S(t)}{N(t)} + e\rho(a - \phi N(t))(I(t) + A(t)) \right]$$

$$-(m + \alpha + u(t) + v)I \Big]$$

$$+\lambda_{3}(t) \left[pvI(t) - (m + \alpha)A(t) \right]$$

$$+\lambda_{4}(t) \left[(1 - p)v(t)I - (m + \delta)R(t) \right].$$

It is known that, if the Hamiltonian is linear in the control variable u(t) then it can be difficult to solve for the optimal solutions u^* from the optimality equation [61, 72, 76]. For mathematical convenience, in our optimal control analysis we assume $a = m + \phi N + \alpha (I + A)N^{-1}$. Thus the total population N is constant. We can also treat the non-constant population case by these techniques, but we choose to present the constant population case here.

Given an optimal control $u^*(t)$, there exists adjoint functions, $\lambda_i(t)$, for i = 1, 2, 3, 4, corresponding to the states S, I, A, and R respectively satisfying

$$\frac{d\lambda_1(t)}{dt} = -\frac{\partial H}{\partial S}, \quad \frac{d\lambda_2(t)}{dt} = -\frac{\partial H}{\partial I}, \quad \frac{d\lambda_3(t)}{dt} = -\frac{\partial H}{\partial A}, \quad \frac{d\lambda_4(t)}{dt} = -\frac{\partial H}{\partial B}, \quad (4.37)$$

such that

$$\frac{d\lambda_1(t)}{dt} = -\left[-C_3 + \lambda_1(t)\left((a - \phi N(t)) - m - \frac{\beta(I(t) + \epsilon A(t))}{N(t)}\right) + \lambda_2(t)\left(\frac{\beta(I(t) + \epsilon A(t))}{N(t)}\right)\right],$$

$$\frac{d\lambda_2(t)}{dt} = -\left[C_1 + \lambda_1(t)\left((a - \phi N(t))\rho(1 - e) - \frac{\beta S(t)}{N(t)}\right) + \lambda_2(t)\left(\frac{\beta S(t)}{N(t)} + e\rho(a - \phi N(t)) - (m + \alpha + u(t) + v)\right) + \lambda_3(t)pv$$

$$+\lambda_4(t)(1-p)v\Big],$$

$$\frac{d\lambda_3(t)}{dt} = -\Big[C_2 + \lambda_1(t)\left((a-\phi N(t))\rho(1-e) - \frac{\beta\epsilon S(t)}{N(t)}\right) + \lambda_2(t)\left(\frac{\beta\epsilon S(t)}{N(t)} + e\rho(a-\phi N(t))\right) - \lambda_3(t)(m+\alpha)\Big],$$

$$\frac{d\lambda_4(t)}{dt} = -\Big[\lambda_1(t)\left((a-\phi N(t)) + \delta\right) - \lambda_4(t)(m+\delta)\Big],$$

where $\lambda_i(T) = 0$ for i = 1, 2, 3, 4, are transversality conditions.

The Hamiltonian H is minimized with respect to the control variable at u^* . Since the Hamiltonian is linear in the control, we need to determine if the optimal control is bang-bang (at its lower or upper bound), singular or a combination. The singular case could occur if the slope or the switching function

$$\frac{\partial H}{\partial u} = C_4 - \lambda_2(t)I(t), \tag{4.38}$$

is zero on non-trivial interval of time. Note that the optimal control would be at it its upper or lower bound according to:

$$\frac{\partial H}{\partial u} < 0$$
, or $\frac{\partial H}{\partial u} > 0$.

Since the behaviour of the control can be determined from the switching function $\frac{\partial H}{\partial u}$, we now investigate the singular case by letting $\frac{\partial H}{\partial u} = 0$, on some non-trivial interval. In this case we calculate $\frac{d}{dt} \left(\frac{\partial H}{\partial u} \right) = 0$ and then we will show that the control is not present in that equation. Thus

$$\frac{d}{dt} \left(\frac{\partial H}{\partial u} \right) = \frac{d}{dt} [C_4 - \lambda_2 I]$$

$$= \left[C_1 + \lambda_1 (a - \phi N) \rho (1 - e) + \lambda_3 p v + \lambda_4 (1 - p) v \right] I$$

$$-\beta (\lambda_1 I + \epsilon \lambda_2 A) N^{-1} S - \lambda_2 e \rho (a - \phi N) A. \tag{4.39}$$

It is evident that the control term is not present in equation (4.39), hence we need to differentiate the switching function, that is., $\frac{d^2}{dt^2} \left(\frac{\partial H}{\partial u} \right) = 0$, in order to determine if the control term now exists and if not we will keep on differentiating until the control term appear. After differentiating the switching function we obtained

$$\frac{d^2}{dt^2} \left(\frac{\partial H}{\partial u} \right) = \Psi_1(t)u(t) + \Psi_2(t), \tag{4.40}$$

where,

$$\begin{split} \Psi_{1}(t) &= -\left[C_{1} + (a - \phi N)\rho(1 - e)\lambda_{1} + pv\lambda_{3} + (1 - p)v\lambda_{4}\right]I - \left[e\rho(a - \phi N)\lambda_{2}\right]A \\ &- \beta \epsilon N^{-1}\lambda_{2}SA + \beta N^{-1}\lambda_{1}SI, \\ \Psi_{2}(t) &= \left[C_{3}(a - \phi N)\rho(1 - e) - C_{2}pv + C_{1}e\rho(a - \phi N) - C_{1}(m + \alpha + v)\right]I \\ &- \left[\left(a - \phi N\right)\rho(1 - e)(\alpha + v + pv + (a - \phi N)(1 - e\rho))\lambda_{1} \right. \\ &+ \left(1 - p\right)v(a - \phi N + \delta)\right)\lambda_{1}\right]I - \left[\left(a - \phi N\right)\rho(2pve + \beta N^{-1}(1 - e)I\right)\lambda_{2}\right]I \\ &+ \left[pv(e\rho(a - \phi N) - v)\lambda_{3}\right]I + \left[(1 - p)v(\delta - \alpha - v + e\rho(a - \phi N))\lambda_{4}\right]I \\ &- \beta N^{-1}(a - \phi N)\rho(1 - e)\lambda_{1}AI + \beta \epsilon N^{-1}(a - \phi N)\rho(1 - e)\left[\lambda_{1} - 2\lambda_{2}\right]AI \\ &- \beta N^{-1}\left[(a - \phi N + \delta)\lambda_{1}\right]RI + \beta N^{-1}\left[C_{1} - C_{3} + \left(pv\epsilon + (a - \phi N)\rho(1 - 2e) - \beta SN^{-1} + (m + \alpha + v)\right)\lambda_{1}\right]SI + \beta N^{-1}\left[\left(\beta N^{-1}I - 2pv\epsilon + 2\beta\epsilon N^{-1}A\right)\lambda_{2} \right. \\ &+ \left.\left(\lambda_{3} - \lambda_{4}\right)pv + v\lambda_{4}\right]SI - \beta\epsilon N^{-1}\left[(a - \phi N + \delta)\lambda_{2}\right]RA \\ &+ \beta N^{-1}\left[2C_{1}\epsilon + 2\left((a - \phi N)\rho(\epsilon - e\epsilon - e) - \beta\epsilon N^{-1}S\right)\lambda_{1}\right]SA \\ &+ \beta N^{-1}\left[\left((a - \phi N)(e\rho + \epsilon(e\rho - 1)) - \epsilon(v - m) + \epsilon\beta N^{-1}\left(S + \epsilon A\right)\right)\lambda_{2} \right. \\ &+ 2v\epsilon(p(\lambda_{3} - \lambda_{4}) + \lambda_{4})\right]SA + \left[2C_{1}e\rho(a - \phi N) + 2(a - \phi N)^{2}\rho^{2}e(1 - e)\lambda_{1} \right. \\ &+ e\rho(a - \phi N)(e\rho(a - \phi N) - v)\lambda_{2}\right]A + \left[\beta\epsilon N^{-1}(a - \phi N)\rho(1 - e)A\lambda_{2} \right. \\ &+ 2e\rho(a - \phi N)v\left(p(\lambda_{3} - \lambda_{4}) + \lambda_{4}\right)A. \end{split}$$

We can solve (4.40) for the singular control as $u_{\text{singular}}(t) = -\frac{\Psi_2(t)}{\Psi_1(t)}$, if $\Psi_1(t) \neq 0$ and $U_1 \leq -\frac{\Psi_2(t)}{\Psi_1(t)} \leq U_2$. To check generalized Legendre-Clebsch condition for the singular control to be optimal, we require $\frac{d}{du}\frac{d^2}{dt^2}\left(\frac{\partial H}{\partial u}\right) = \Psi_1(t)$ to be negative [77]. For our minimization problem, our control characterization is as follows:

if
$$\frac{\partial H}{\partial u} < 0$$
 at t then $u^*(t) = U_2$,
if $\frac{\partial H}{\partial u} > 0$ at t then $u^*(t) = U_1$,
if $\frac{\partial H}{\partial u} < 0$ at t then $u_{\text{singular}}(t) = -\frac{\Psi_2}{\Psi_1}$

Thus, our control is optimal at t provided $\Psi_1(t) < 0$ and $U_1 \le -\frac{\Psi_2(t)}{\Psi_1} \le U_2$.

4.4.2 Numerical results

In this section, we utilize the forward-backward sweep method [61] together with parameters values in Table 4.1 and 4.2 to determine numerical solutions of our optimality system. We assume that the minimization of the clinically infected bison population has the same importance/weight as that of the chronically infected bison population., that is, $C_1 = C_2$. Further, for simplicity in our numerical computations we set $C_1 = C_2 = C_3 = 0.1$.

Table 4.2: Additional model parameters and their values

Symbo	l Definition	Value	Units	Source
$\overline{\beta_0}$	Averaged disease transmission rate	0.75	$year^{-1}$	[38]
β_1	Amplitude of oscillation in $\beta(t)$	0.8	unit-less	[31]
U_1	Lower bound of control $u(t)$	0.1	unit-less	Assumed
U_2	Upper bound of control $u(t)$	0.8	unit-less	Assumed
a	Recruitment rate	$year^{-1}$	0.255	Computed

The total number of new infections in this study are given by

$$T_B = \int_0^T \left[\beta(I + \epsilon A)SN^{-1} + e\rho(a - \phi N)(I + A) \right] dt, \tag{4.42}$$

and the total cost associated with the implementation of the control is given by objective functional J (4.35). In subsequent discussion, we will present the values for the total number of new infections and J for both periodic and non-period environments.

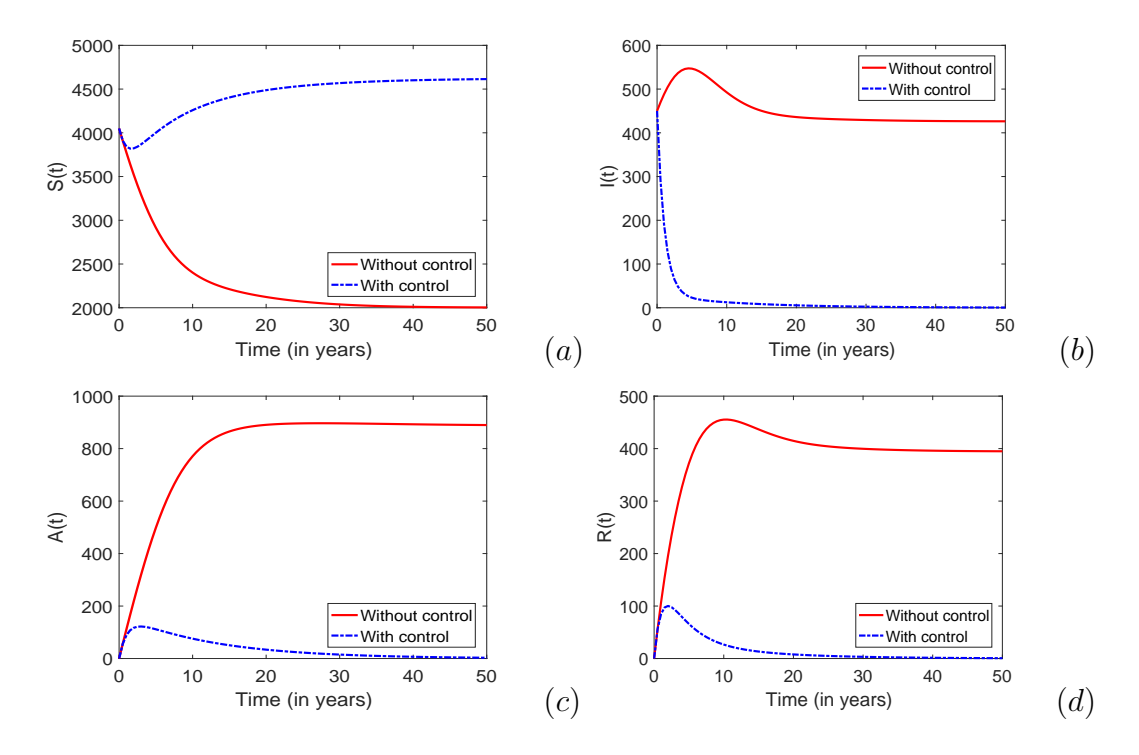


Figure 4.2: Simulation results of the autonomous model with and without the control (a) susceptible animals (b) clinically infected animals (c) chronically infected animals (d) recovered animals. The dotted blue and solid red curves in all the figures represent the total population over a 50 year period with and without control, respectively. The time varying optimal culling associated with these figures is shown in Figure 4.3. Note that the basic reproduction number $\mathcal{R}_0 = 1.576$, $\beta = 0.35$ and $C_4 = 10$.

Figure 4.2 shows the effects of optimal culling on long-term brucellosis dynamics for the autonomous model, with the cost parameter $C_4 = 10$ and the basic reproduction number $\mathcal{R}_0 = 1.5679$. The results clearly demonstrate that optimal culling can significantly reduce the populations of clinically infected, chronic and recovered animals to a level close to zero when t > 30 years. In addition, we also note that, with the optimal control implemented, the total population of susceptible animals increase over time and converges to the carrying capacity N = 4500 when $t \geq 30$ years. This result demonstrates the existence of a globally stable disease-free equilibrium as guaranteed by Theorem 4.2.1 (i). In contrast, without the implementation of optimal culling, the susceptible population decreases over time and converges to N = 2000 when t > 30 years. This result demonstrates the existence of a globally stable endemic equilibrium for $\mathcal{R}_0 > 1$ as guaranteed by Theorem 4.2.1

(ii). Furthermore, the total number of new infections over the entire time horizon is $T_B = 1.0904 \times 10^4$ and the total cost is $J = 5.8260 \times 10^4$.

Figure 4.3 (a) shows the optimal control profile for the autonomous model with the cost parameter (a) $C_4 = 10$, (b) $C_4 = 100$, and the basic reproduction number $\mathcal{R}_0 = 1.5679$. As we can observe, in (a) u starts from the maximum initially (u = 0.8) and stays there for approximately 26 years, followed by a switch to its minimum (u = 0.1) where it remains till the final time. To investigate the impact of the costs on the implementation of optimal culling, we set $C_4 = 100$ (implies higher costs) and generated the simulation results presented in Figure 4.3 (b). It is evident that with higher costs u stays at its maximum for a very short period of time (approximately 7 years) before it switches to its minimum where it remains till the final time. With higher costs the total number of new infections generated $T_B = 1.0903 \times 10^4$ and the total cost is $J = 6.4942 \times 10^4$. In addition, the optimal control graphs for higher costs (not included) are almost the same as in Figure 4.2. We present the values of the total number of new infections in the presence and absence of optimal control in Table 4.3.

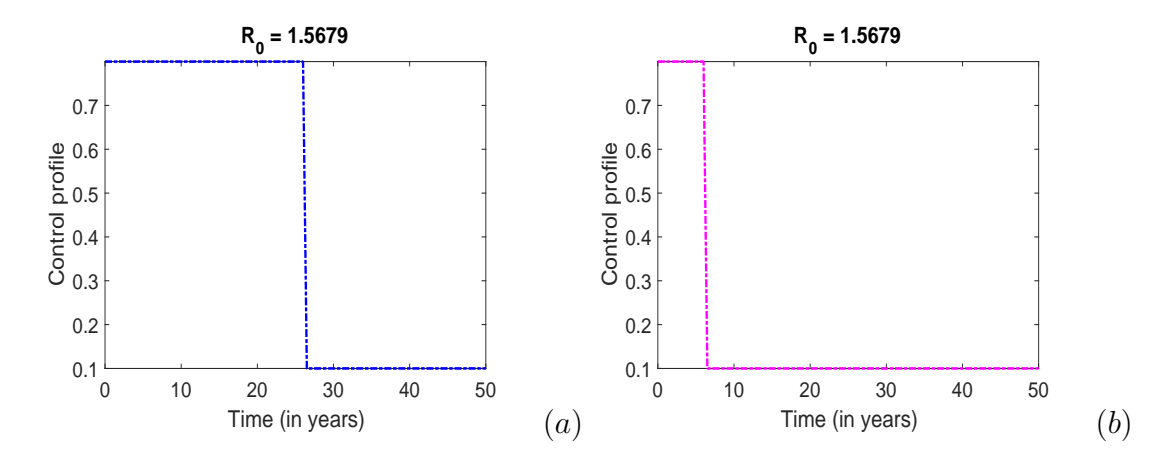


Figure 4.3: Simulation results showing the control profile for the autonomous model, over a period of 50 years, with (a) $C_4 = 10$ and (b) $C_4 = 100$. We can observe that in all cases the control profile admits a bang-bang solution with one switch.

Figure 4.4 shows the optimal control graphs for the time-periodic model, with same values for the cost parameters, as the autonomous model, i.e. $C_4 = 10$. From these simulation results, we see that with and without control, in all cases the population of animals oscillates with time and this corresponds to the annual periodic

Table 4.3: The total number of newly infected animals over 50 years and the total cost J with respect to different control strategies for the autonomous model with $\mathcal{R}_0 = 1.5679$.

Strategies	T_B	Infections averted	J
No control	1.4296×10^4		
Optimal control with $C_4 = 10$, $\beta = 0.75$	1.0904×10^4	3.392×10^{3}	5.8260×10^{4}
Optimal control with $C_4 = 100, \beta = 0.75$	1.0903×10^4	3.393×10^{3}	6.4942×10^4

oscillation of contact rate $\beta(t)$. We also note that the amplitude of oscillations is more pronounced when there is no control compared to a scenario when there is a control. With seasonality, the total number of new infections is 1.5455×10^3 and the corresponding total cost is 5.5017×10^4 . In addition, we see that the optimal control strategy significantly reduces the infected population to levels close to zero over time. Also note that when seasonal variations are incorporated into the model the total number of new infections generated over the entire period (50 years) is less compared to when there are no seasonal variations. This results concur with earlier findings in [31, 53], that the total disease burden is usually overestimated whenever non-periodic models are used to explore transmission dynamics for diseases that are influenced by seasonal variations.

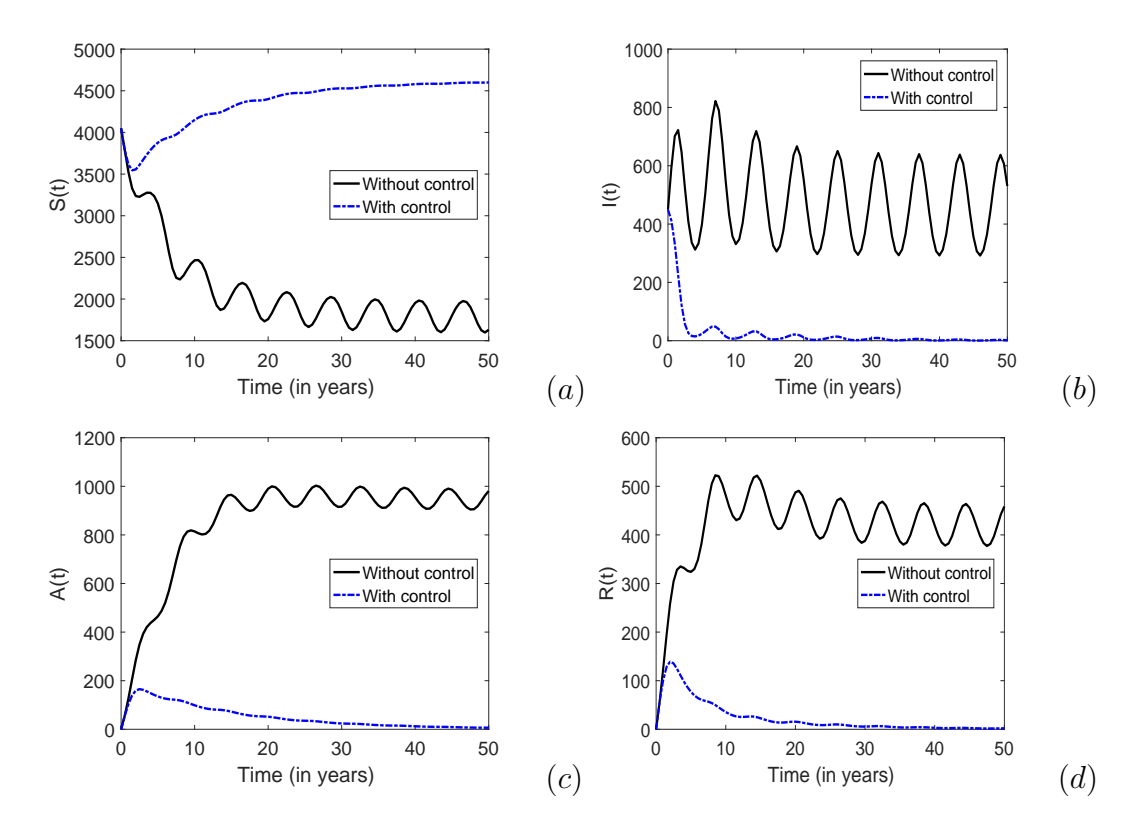


Figure 4.4: Simulation results of the non-autonomous model with and without the control (a) susceptible animals (b) clinically infected animals (c) chronically infected animals (d) recovered animals. The dotted blue and solid black curves represent the total population, with and without control, respectively. The time varying optimal culling associated with these figures is shown in Figure 4.5. Note that the basic reproduction number $\mathcal{R}_0 = 1.312$ and $C_4 = 10$.

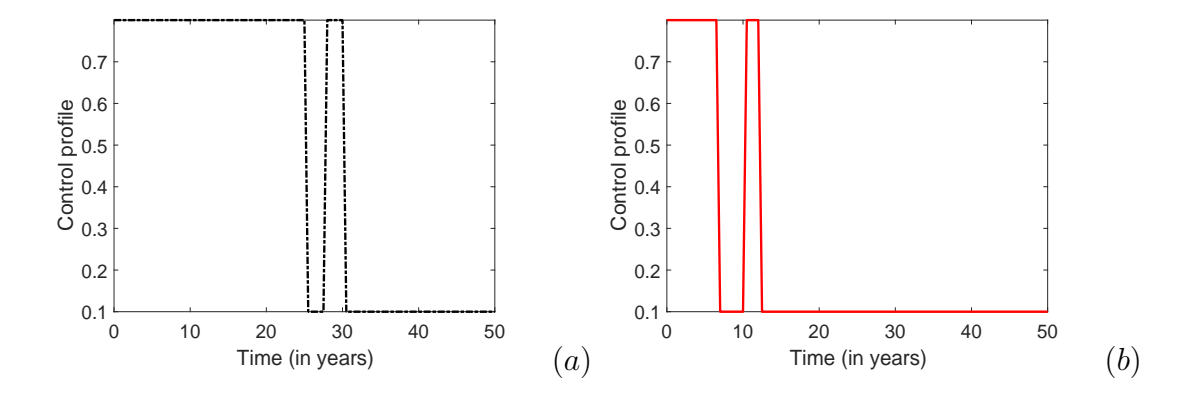


Figure 4.5: Simulation results showing the control profile for the non-autonomous model, over a period of 50 years, with (a) $C_4 = 10$ and (b) $C_4 = 100$. We can observe that in both scenarios the control profile exhibits a bang-bang solution with more than one switch.

Figure 4.5 depicts the control profile for system (4.34) when seasonal variations are incorporated. As we can note, Figure 4.5 (a) in the control profile for u starts from the maximum initially and stays there for approximately 26 years, followed by a switch to the minimum where it stays for a year and then it switches back to the maximum where it stays for a year before its final switch to the minimum, where it remains until the final time. In Figure 4.5 (b), we note that when the costs are high $C_4 = 100$ the control profile exhibits the same behavior as when the costs are low $C_4 = 10$. We note however, that with high costs, the control efforts need to be implemented with reduced, or even minimum, strength, to achieve an optimal balance between the costs and effects of the control. Numerical illustrations in Figure 4.5 also demonstrated non-uniqueness ("bang-bang" form), of the optimal control, a feature which is largely associated with problems with a linearly dependent control function. Bang-bang solutions provides a lower bound on the cost that can be achieved by optimal control in real problems.

We present the values of the total number of new infections in the presence and absence of optimal control in Table 4.4 for a non-autonomous case, that is, $\beta = \beta(t)$.

Results in Table 4.3 and 4.4 demonstrates that a periodic model is associated with less number of new infections compared to a non-periodic one, even though the averaged transmission rate β_0 (for the periodic model) is equivalent to the transmission rate for the autonomous model, $\beta_0 = 0.75$.. These findings highlights that the risk of infection will be overestimated whenever the basic reproduction number for

Table 4.4: The total number of newly infected animals over 50 years and the total cost J with respect to different control strategies for the non-autonomous model with $\mathcal{R}_0 = 1.312$.

Strategies	T_B	Infections averted	J
No control	1.9568×10^{4}		
Optimal control with $C_4 = 10$, $\beta = \beta(t)$	1.5455×10^{3}	1.8022×10^4	5.5017×10^4
Optimal control with $C_4 = 100, \beta = \beta(t)$	1.1661×10^4	1.1474×10^6	7.907×10^{3}

the autonomous models is used to estimate the power of the disease to invade the population in a seasonal environment. The results established here are in agreement with findings from [31, 53].

4.5 Concluding remarks

To investigate the effects of culling on the transmission dynamics of brucellosis among bison population, two mathematical models were developed and analyzed. The first model, an autonomous one, accounted for brucellosis transmission in non-periodic environments while the second model, a periodic one, models brucellosis transmission in periodic environments. For both the periodic and non-periodic model, we computed the basic reproduction number \mathcal{R}_0 and demonstrated that it is a sharp threshold for brucellosis transmission dynamics in both environments.

We also investigated the impact of time dependent culling efforts on the spread and control of brucellosis. Thus, we formulated an optimal control problem with the goal of minimizing the total number of infected (clinical and chronic) animals and maximize the total number of susceptible and recovered population, while also minimizing the cost of control. Our results have shown that, in all the scenarios, optimal culling efforts can significantly reduce the total population of infected animals to a level close to zero, while the susceptible population will be maximized to the maximum carrying capacity. After the incorporation of seasonal variations, disease dynamics oscillated with time and this corresponds to the annual periodic oscillations of contact rate. Further, we note that a periodic model is associated with less number of new infections compared to a non-periodic one. This scenario

was also observed in [53, 31]. Moreover, the control profiles for both models exhibits a bang-bang solution, with a finite number of switches. Precisely, the control profile for an autonomous model has one switch while the control profile for the periodic model has three switches. In addition, we also noted that, with low costs optimal culling efforts can be implemented at maximum strength for a long period of time. Overall, our results have shown that optimal culling could significantly control the spread of brucellosis in both periodic and non-periodic environments.

This work clearly demonstrated the value of optimal control theory as a tool to determine effective ways of controlling the spread of brucellosis in both periodic and non-periodic environments.

Chapter 5

Modeling the spatiotemporal variations in brucellosis transmission

5.1 Introduction

Brucellosis, an infectious bacterial disease, is one of the world's major zoonoses. Caused by various species of the bacteria Brucella [4], the disease can be transmitted to animals and humans with exposure to infected animals or ingestion of contaminated water, food, and dust, etc [2]. In animals, especially among sheep and goats, brucellosis mainly affects the reproduction process and can lead to fertility problems and abortion, and reduce the survival of newborns [8]. In humans, mortality is negligible, but the illness can last for several years [14], characterized by such symptoms as intermittent fever, headache, fatigue, joint and bone pain, psychosis, and disturbance [6].

Currently there are more than 500,000 new cases of brucellosis reported annually and the disease remains endemic in many areas of the world, including Spain, Latin America, the Middle East, and Africa [1, 2]. Among these, the majority of brucellosis cases are found in sub-Sahara Africa, where Ethiopia, Chad, Tanzania, Nigeria, Uganda, Kenya, Zimbabwe and Somalia have been reporting persistence of brucellosis in humans attributed to the infection of domestic cattle, camels, goats

and sheep [3]. With large pastoral communities, and the demand for meat and livestock products to double by 2050, brucellosis poses a major threat to the public health and economic growth of the region and demands serious control efforts.

Mathematical modeling, analysis and simulation offer a useful means to understand the transmission and spread of brucellosis so that effective disease control measures could be designed. A few mathematical models have been published in recent years to investigate brucellosis dynamics. For example, Hou and co-workers [30] employed a system of ordinary differential equations (ODEs) to model the transmission of brucellosis and the effects of vaccination on brucellosis prevention and intervention. Lolika et al. [31] proposed a brucellosis model and conducted an optimal control study on the use of animal vaccination and environmental decontamination as disease control measures against brucellosis infection. Li et al. [32] proposed a model to investigate the transmission of brucellosis among sheep and from sheep to humans, and their findings indicated that a combination of intervention methods (such as prohibiting mixed feeding, vaccination, and detection and elimination) is useful in controlling human brucellosis.

Despite these efforts, however, several challenges remain in the mathematical modeling of brucellosis. First, different places likely have different geographic, ecological and environmental structures, and animals living in various locations likely exhibit different contact and communication patterns. In particular, animals make regular migration from one place to another, which directly contributes to the disease spread. So far these differences of the transmission dynamics have not been taken into account, leading to inadequate understanding of the influence of the spatial factors in the transmission and spread of brucellosis. Another limitation in brucellosis modeling is that the impact of seasonal variation is insufficiently addressed. In fact, like many other infectious diseases, brucellosis is significantly influenced by seasonal changes, and prior field studies have already demonstrated a strong correlation between brucellosis outbreaks and seasonal oscillations [26, 27, 28]. For example, a recent analysis of brucellosis datasets in a few countries [26] reveals that there is a marked seasonal variation in the incidence of acute brucellosis, with most cases occurring in the spring and summer. Factors such as periodic changes in temperature, seasonal precipitation which directly affects the availability of forage, environmental fluctuations in humidity and exposure to UV light which impact the survival of *Brucella*, and seasonal rituals in Africa which are associated with animal migration and slaughtering, all contribute to seasonal fluctuations in the transmission and spread of brucellosis.

Such spatial and temporal heterogeneities have strong impacts on the dynamics of brucellosis that are not captured by homogeneous, autonomous differential equation models. In the present study, we will make a first step toward integrating the spatial and seasonal variations into a single framework for a comprehensive modeling of brucellosis dynamics. To that end, we propose a two-patch deterministic model, where each patch has distinct populations and infection characteristics, to study the transmission of brucellosis among animals. In each patch, the animal population is subdivided into the susceptible and the infected compartments; meanwhile, another compartment is introduced to represent the concentration of the pathogen (i.e., Brucella) in the environment. Both the indirect (i.e., environment-to-host) and direct (i.e., host-to-host) transmission routes are considered in our model, representing the multiple pathways in the force of infection for brucellosis. Animals may move from one patch to the other, representing their migration in space. Additionally, we will incorporate the effects of seasonal oscillation by employing time-periodic model parameters, which leads to a non-autonomous patchy ODE system.

We organize the remainder of this chapter as follows. In Section 5.2, we first introduce our two-patch model in the autonomous form, where each model parameter is fixed as a constant, and then conduct a thorough equilibrium analysis for this model. In Section 5.3, we extend the autonomous model to a periodic two-patch model and analyze the threshold dynamics. In Section 5.4, we use numerical simulation results to validate our analytical predictions. Finally, we conclude the chapter with some discussion in Section 5.5.

5.2 A two-patch autonomous model

We consider the spatial spread of brucellosis in an environment of two patches, where brucellosis can spread from one patch to the other due to animal movement, particularly, through migration. We further assume a unidirectional form of migration; that is, animals move from patch 1 to patch 2. Let S_j and I_j (j=1,2) denote the number of susceptible and infectious animals, respectively, in each patch. Meanwhile, we introduce another compartment B_j that represents the population of the free-living pathogen (i.e., Brucella) in the environment. The Brucella population can be replenished by infectious hosts that excrete the pathogen to the environment. In contrast, the natural decay of the pathogen and the decontamination practices reduce the environmental persistence of the pathogen. Susceptible animals become infected (and infectious) either by adequate contacts with infectious animals or the contaminated environment. The following system of ordinary differential equations (ODEs) describe the brucellosis transmission dynamics:

$$\begin{cases}
\dot{S}_{1}(t) = A_{1} - (\alpha_{1}I_{1} + \beta_{1}B_{1})S_{1} - (\theta_{S} + \mu_{1})S_{1}, \\
\dot{I}_{1}(t) = (\alpha_{1}I_{1} + \beta_{1}B_{1})S_{1} - (\theta_{I} + c_{1} + \mu_{1})I_{1}, \\
\dot{B}_{1}(t) = \phi_{1}I_{1} - d_{1}B_{1}, \\
\dot{S}_{2}(t) = A_{2} - (\alpha_{2}I_{2} + \beta_{2}B_{2})S_{2} - \mu_{2}S_{2} + \theta_{S}S_{1}, \\
\dot{I}_{2}(t) = (\alpha_{2}I_{2} + \beta_{2}B_{2})S_{2} - (\mu_{2} + c_{2})I_{2} + \theta_{I}I_{1}, \\
\dot{B}_{2}(t) = \phi_{2}I_{2} - d_{2}B_{2},
\end{cases} (5.1)$$

where all model parameters are non-negative. The parameter A_j (j=1,2) is the constant recruitment rate for animals in each patch, μ_j is the natural animal death rate, α_j and β_j denote the host-to-host and environment-to-host disease transmission rates, respectively. The mean infectious period for animals in each patch is denoted by c_j^{-1} . For the pathogen population, ϕ_j denotes the pathogen shedding rate, and d_j is the pathogen removal rate that includes the effects of both the natural decay and the decontamination practices. In addition, we assume that the susceptible and infectious animals migrate from patch 1 to patch 2 at rates θ_S and θ_I , respectively.

5.2.1 Feasible region

Let $N(t) = S_1(t) + I_1(t) + S_2(t) + I_2(t)$. Adding all equations for animal individuals in (5.1)

$$\dot{N} = A_1 + A_2 - \mu_1(S_1 + I_1) - \mu_2(S_2 + I_2) - c_1I_1 - c_2I_2 \le A_1 + A_2 - \min(\mu_1, \mu_2)N$$

which implies that

$$\limsup_{t \to \infty} N(t) \le \frac{(A_1 + A_2)}{\min(\mu_1, \mu_2)}.$$

From the pathogen equation in (5.1) leads

$$\frac{dB_j}{dt} = \phi_j I_j - d_j B_j \le \frac{\phi_j (A_1 + A_2)}{\min(\mu_1, \mu_2)} - d_j B_j$$

giving

$$\limsup_{t \to \infty} B_j \le \frac{\phi_j(A_1 + A_2)}{\min(\mu_1, \mu_2) d_j}$$

then the domain of biological interest

$$\Gamma = \left\{ (S_1, I_1, B_1, S_2, I_2, B_2) \in \mathbb{R}_+^6 : S_j \leq S_j^0, B_j \leq \frac{\phi_j(A_1 + A_2)}{d_j \mu_j}, j = 1, 2; \\ N(t) \leq \frac{(A_1 + A_2)}{\min(\mu_1, \mu_2)} \right\}$$

is positively invariant and attracting all orbits with respect to the model (5.1).

5.2.2 Disease-free equilibrium

A disease-free equilibrium refers to the equilibrium that exists when there is no disease (that is $S_1 = S_1^0 > 0$, $S_2 = S_2^0 > 0$, $I_1^0 = I_2^0 = B_1^0 = B_2^0 = 0$). The disease-free equilibrium is determined by equations:

$$\begin{cases}
A_{1} - (\alpha_{1}I_{1} + \beta_{1}B_{1})S_{1} - (\theta_{S} + \mu_{1})S_{1} &= 0 \\
(\alpha_{1}I_{1} + \beta_{1}B_{1})S_{1} - (\theta_{I} + c_{1} + \mu_{1})I_{1} &= 0 \\
\phi_{1}I_{1} - d_{1}B_{1} &= 0 \\
A_{2} - (\alpha_{2}I_{2} + \beta_{2}B_{2})S_{2} - \mu_{2}S_{2} + \theta_{S}S_{1} &= 0 \\
(\alpha_{2}I_{2} + \beta_{2}B_{2})S_{2} - (\mu_{2} + c_{2})I_{2} + \theta_{I}I_{1} &= 0 \\
\phi_{2}I_{2} - d_{2}B_{2} &= 0.
\end{cases} (5.2)$$

A disease-free equation (5.2) yields

$$\begin{cases}
A_1 - (\theta_S + \mu_1) S_1^0 = 0, \\
A_2 - \mu_2 S_2^0 + \theta_S S_1^0 = 0.
\end{cases}$$
(5.3)

solving system (5.3) for S_1^0 and S_2^0 implies that system (5.1) has an evident disease-free equilibrium (DFE) given by

$$\mathcal{E}^{0} = \left(S_{1}^{0}, I_{1}^{0}, B_{1}^{0}, S_{2}^{0}, I_{2}^{0}, B_{2}^{0}\right) = \left(\frac{A_{1}}{\theta_{S} + \mu_{1}}, 0, 0, \frac{\theta_{S} A_{1} + (\theta_{S} + \mu_{1}) A_{2}}{\mu_{2}(\theta_{S} + \mu_{1})}, 0, 0\right). \tag{5.4}$$

5.2.3 The reproduction number

The basic reproduction number, denoted \mathcal{R}_0 , measures the average number of secondary infections generated by a single infectious case in a fully susceptible population during its average infectious period [50]. The reproduction number is commonly regarded as a threshold quantity for the disease dynamics, essential in determining the transmission and spread of the disease. Using the next-generation matrix notations in [50], the non-negative matrix F that denotes the generation of new infection and the non-singular matrix V that denotes the disease transfer among compartments, are respectively given by

$$F = \begin{bmatrix} \alpha_1 S_1^0 & \beta_1 S_1^0 & 0 & 0 \\ 0 & 0 & 0 & 0 \\ 0 & 0 & \alpha_2 S_2^0 & \beta_2 S_2^0 \\ 0 & 0 & 0 & 0 \end{bmatrix},$$
 and
$$V = \begin{bmatrix} (c_1 + \theta_I + \mu_1) & 0 & 0 & 0 \\ -\phi_1 & d_1 & 0 & 0 \\ -\theta_I & 0 & (c_2 + \mu_2) & 0 \\ 0 & 0 & -\phi_2 & d_2 \end{bmatrix}.$$
 (5.5)

Let us use \mathcal{R}_i to denote the reproduction number associated with patch i (i = 1, 2), where

$$\mathcal{R}_1 = \frac{(\alpha_1 d_1 + \beta_1 \phi_1) A_1}{d_1(\theta_S + \mu_1)(c_1 + \theta_I + \mu_1)}, \quad \mathcal{R}_2 = \frac{(\alpha_2 d_2 + \beta_2 \phi_2)(\theta_S A_1 + (\theta_S + \mu_1) A_2)}{d_2 \mu_2(\theta_S + \mu_1)(\mu_2 + c_2)}. \quad (5.6)$$

Biologically, \mathcal{R}_1 and \mathcal{R}_2 represent the disease risks for patches 1 and 2, respectively. We observe that, based on our assumption of the unidirectional animal movement, \mathcal{R}_1 does not depend on the properties of patch 2, whereas \mathcal{R}_2 depends on some characteristics of patch 1. In particular, the disease risk for patch 2 has been increased due to the animal migration from patch 1.

From (5.5), we know that the basic reproduction number \mathcal{R}_0 for the entire system is determined by the spectral radius of the next-generation matrix FV^{-1} . It then follows that

$$\mathcal{R}_0 = \max(\mathcal{R}_1, \, \mathcal{R}_2), \tag{5.7}$$

showing that the disease risk for the entire system depends on that associated with each of the two patches.

5.2.4 Global stability of the disease-free equilibrium

From the work in [50], we know that the DFE is locally asymptotically stable when $\mathcal{R}_0 < 1$, and unstable when $\mathcal{R}_0 > 1$. Indeed, we can establish a stronger result regarding the global dynamics of the DFE.

Theorem 5.2.1 If $\mathcal{R}_0 \leq 1$, the DFE is globally asymptotically stable in Γ . If $\mathcal{R}_0 > 1$, the system is uniformly persistent.

Proof 9 Let $\mathcal{Y}(t) = (I_1, B_1, I_2, B_2)$. Since

$$\begin{cases}
\dot{I}_{1}(t) = (\alpha_{1}I_{1} + \beta_{1}B_{1})S_{1} - (\theta_{I} + c_{1} + \mu_{1})I_{1}, \\
\dot{B}_{1}(t) = \phi_{1}I_{1} - d_{1}B_{1}, \\
\dot{I}_{2}(t) = (\alpha_{2}I_{2} + \beta_{2}B_{2})S_{2} - (\mu_{2} + c_{2})I_{1} + \theta_{I}I_{1}, \\
\dot{B}_{2}(t) = \phi_{2}I_{2} - d_{2}B_{2},
\end{cases} (5.8)$$

it follows that

$$\dot{\mathcal{Y}}(t) \le (F - V)\mathcal{Y},$$

where F and V are defined in (5.5). Motivated by [78], we define a Lyapunov function as follows

$$\mathcal{L} = w^T V^{-1} \mathcal{Y}.$$

Differentiating \mathcal{L} along solutions of (5.1), we have

$$\dot{\mathcal{L}}(t) = w^T V^{-1} \dot{\mathcal{Y}}
\leq w^T V^{-1} (F - V) \mathcal{Y}
= (\mathcal{R}_0 - 1) w^T \mathcal{Y} \leq 0, \quad \text{if } \mathcal{R}_0 \leq 1.$$

It can be easily verified that the largest invariant subset of Γ where $\dot{\mathcal{L}}=0$ is the singleton $\{\mathcal{E}^0\}$. Therefore, by LaSalle's invariance principle [46], \mathcal{E}^0 is globally asymptotically stable in Γ when $\mathcal{R}_0 \leq 1$.

If $\mathcal{R}_0 > 1$, then by continuity, $\dot{\mathcal{L}} > 0$ in a neighborhood of \mathcal{E}^0 in $\mathring{\Gamma}$. Solutions in $\mathring{\Gamma}$ sufficiently close to \mathcal{E}^0 move away from the DFE, implying that the DFE is unstable. Using a uniform persistence result from [79] and an argument as in the proof of Proposition 3.3 of [80], it can be shown that when $\mathcal{R}_0 > 1$, the instability of the DFE implies the uniform persistence of the model (5.1).

The result in Theorem 5.2.1 shows that $\mathcal{R}_0 = 1$ is a sharp threshold for disease dynamics: the disease will die out when $\mathcal{R}_0 \leq 1$, whereas the disease will persist when $\mathcal{R}_0 > 1$ (we refer to [27, 81, 82] for more details on the persistence theory). Next, we turn to the analysis of the nontrivial equilibria of the system and their dynamical properties.

5.2.5 Nontrivial equilibria

Any nontrivial equilibrium $(S_1, I_1, B_1, S_2, I_2, B_2)$ for system (5.1) satisfies the following algebraic equations:

$$A_1 = (\alpha_1 I_1 + \beta_1 B_1 + \theta_S + \mu_1) S_1, \tag{5.9}$$

$$(\alpha_1 I_1 + \beta_1 B_1) S_1 = (\theta_I + c_1 + \mu_1) I_1, \tag{5.10}$$

$$d_1 B_1 = \phi_1 I_1, \tag{5.11}$$

$$A_2 = (\alpha_2 I_2 + \beta_2 B_2 + \mu_2) S_2 - \theta_S S_1, \tag{5.12}$$

$$(\alpha_2 I_2 + \beta_2 B_2) S_2 = (\mu_2 + c_2) I_2 - \theta_I I_1, \tag{5.13}$$

$$d_2 B_2 = \phi_2 I_2. (5.14)$$

We have $B_1 = \frac{\phi_1}{d_1} I_1$ from equation (5.12), and plug it into (5.11) to obtain

$$\left(\alpha_1 + \frac{\beta_1 \phi_1}{d_1}\right) I_1 S_1 = (\theta_I + c_1 + \mu_1) I_1.$$
 (5.15)

If $I_1 = 0$, then $B_1 = 0$, $S_1 = \frac{A_1}{\theta_S + \mu_1} := \widetilde{S}_1$, where $\widetilde{S}_1 = S_1^0$. Combining (5.14) and (5.15), we obtain

$$\frac{\alpha_2 d_2 + \beta_2 \phi_2}{d_2} I_2 S_2 = (\mu_2 + c_2) I_2. \tag{5.16}$$

Notice that I_2 must be positive for a nontrivial equilibrium (since $I_1 = 0$ already). It then yields

$$S_2 = \frac{d_2(\mu_2 + c_2)}{\alpha_2 d_2 + \beta_2 \phi_2} := \widetilde{S}_2.$$
 (5.17)

By substituting equations (5.14) and (5.17) into (5.13), we have

$$I_2 = \frac{d_2\mu_2(\mathcal{R}_2 - 1)}{\alpha_2d_2 + \beta_2\phi_2} := \widetilde{I_2}, \quad B_2 = \frac{\phi_2\mu_2(\mathcal{R}_2 - 1)}{\alpha_2d_2 + \beta_2\phi_2} := \widetilde{B_2}.$$

Therefore, we conclude that there exists a nontrivial boundary equilibrium

$$\mathcal{E}_1 = (\widetilde{S}_1, 0, 0, \widetilde{S}_2, \widetilde{I}_2, \widetilde{B}_2) \tag{5.18}$$

for system (5.1) if and only if $\mathcal{R}_2 > 1$.

Next, we consider the case $I_1 = I_1^* > 0$. We can calculate $S_1 = S_1^*$ directly from (5.15), which yields

$$S_1^* = \frac{d_1(\theta_I + c_1 + \mu_1)}{\alpha_1 d_1 + \beta_1 \phi_1}. (5.19)$$

Then substitution of equation (5.19) into (5.10) yields

$$I_1^* = \frac{d_1(\theta_I + c_1 + \mu_1)}{\alpha_1 d_1 + \beta_1 \phi_1} (\mathcal{R}_1 - 1). \tag{5.20}$$

Clearly, $I_1^* > 0$ if and only if $\mathcal{R}_1 > 1$. Subsequently, $B_1 = B_1^* = \frac{\phi_1}{d_1} I_1^*$ is uniquely determined by I_1^* . Meanwhile, equations (5.13), (5.14) and (5.15) can be reduced to two equations:

$$A_2 = \left(\frac{\alpha_2 d_2 + \beta_2 \phi_2}{d_2} I_2 + \mu_2\right) S_2 - \theta_S S_1^*, \tag{5.21}$$

$$\frac{\alpha_2 d_2 + \beta_2 \phi_2}{d_2} I_2 S_2 = (\mu_2 + c_2) I_2 - \theta_I I_1^*. \tag{5.22}$$

Combining (5.21) and (5.22) and canceling out S_2 , we have

$$\frac{\alpha_2 d_2 + \beta_2 \phi_2}{d_2} (\mu_2 + c_2) I_2^2 + \left[\mu_2 (\mu_2 + c_2) - \frac{\alpha_2 d_2 + \beta_2 \phi_2}{d_2} (A_2 + \theta_S S_1^* + \theta_I I_1^*) \right] I_2$$
$$-\mu_2 \theta_I I_1^* = 0,$$

which indicates that I_2 has a unique positive solution $I_2^* > 0$ since $\frac{\alpha_2 d_2 + \beta_2 \phi_2}{d_2} (\mu_2 + c_2) > 0$ and $\mu_2 \theta_I I_1^* > 0$. Consequently, $S_2^* = \frac{A_2 + \theta_S S_1^*}{r_2 I_2^* + \mu_2}$ and $B_2^* = \frac{\phi_2}{d_2} I_2^*$ are uniquely decided by I_2^* . Therefore, we have a positive endemic equilibrium

$$\mathcal{E}_2 = (S_1^*, I_1^*, B_1^*, S_2^*, I_2^*, B_2^*) \tag{5.23}$$

for system (5.1) if and only if $\mathcal{R}_1 > 1$.

Now we may summarize the above analysis by the following theorem.

Theorem 5.2.2

If $\mathcal{R}_0 = \max\{\mathcal{R}_1, \mathcal{R}_2\} \leq 1$, then system (5.1) only has the trivial, disease-free equilibrium \mathcal{E}^0 .

If $\mathcal{R}_0 = \max\{\mathcal{R}_1, \mathcal{R}_2\} > 1$, then in addition to the DFE \mathcal{E}^0 , nontrivial equilibria exist:

- 1) If $\mathcal{R}_1 \leq 1$, $\mathcal{R}_2 > 1$, there is only a nontrivial boundary equilibrium \mathcal{E}_1 in Γ .
- 2) If $\mathcal{R}_1 > 1$, $\mathcal{R}_2 \leq 1$, there is only a positive endemic equilibrium \mathcal{E}_2 in Γ .
- 3) If $\mathcal{R}_1 > 1$, $\mathcal{R}_2 > 1$, both the boundary equilibrium \mathcal{E}_1 and the endemic equilibrium \mathcal{E}_2 exist in Γ .

5.2.6 Local and global dynamics

We proceed to investigate the dynamical behavior of the nontrivial equilibria. The following result characterizes the local dynamics of the boundary equilibrium \mathcal{E}_1 .

Theorem 5.2.3

- (ii) If $\mathcal{R}_1 < 1$ and $\mathcal{R}_2 > 1$, then \mathcal{E}_1 is locally asymptotically stable.
- (i) If $\mathcal{R}_1 > 1$ and $\mathcal{R}_2 > 1$, then \mathcal{E}_1 is unstable.

Proof 10 Linearizing the system (5.1) at the boundary equilibrium \mathcal{E}_1 , we obtain the Jacobian matrix $J = \begin{bmatrix} \widetilde{J}_1 & 0 \\ \widetilde{J}_* & \widetilde{J}_2 \end{bmatrix}$, where

$$\widetilde{J}_{1} = \begin{bmatrix}
-(\theta_{S} + \mu_{1}) & -\alpha_{1}\widetilde{S}_{1} & -\beta_{1}\widetilde{S}_{1} \\
0 & \alpha_{1}\widetilde{S}_{1} - (\theta_{I} + c_{1} + \mu_{1}) & \beta_{1}\widetilde{S}_{1} \\
0 & \phi_{1} & -d_{1}
\end{bmatrix},$$

$$\widetilde{J}_2 = \begin{bmatrix} -(\alpha_2 \widetilde{I}_2 + \beta_2 \widetilde{B}_2 + \mu_2) & -\alpha_2 \widetilde{S}_2 & -\beta_2 \widetilde{S}_2 \\ \alpha_2 \widetilde{I}_2 + \beta_2 \widetilde{B}_2 & \alpha_1 \widetilde{S}_2 - (\mu_2 + c_2) & \beta_2 \widetilde{S}_2 \\ 0 & \phi_2 & -d_2 \end{bmatrix}.$$

It is easy to verify that the characteristic polynomial of J is $\det(\lambda I - J) = \det(\lambda I - \widetilde{J}_1) \det(\lambda I - \widetilde{J}_2)$, and

$$\det(\lambda I - \widetilde{J}_1) = \lambda^3 + x_1 \lambda^2 + y_1 \lambda + z_1,$$

$$\det(\lambda I - \widetilde{J}_2) = \lambda^3 + x_2 \lambda^2 + y_2 \lambda + z_2,$$

where

$$x_{1} = d_{1} + Y_{1} + X_{1} \left(1 - \frac{\alpha_{1} d_{1}}{Z_{1}} \mathcal{R}_{1} \right),$$

$$y_{1} = Y_{1} \left(d_{1} + X_{1} \left(1 - \frac{\alpha_{1} d_{1}}{Z_{1}} \mathcal{R}_{1} \right) \right) + d_{1} X_{1} (1 - \mathcal{R}_{1}),$$

$$z_{1} = d_{1} X_{1} Y_{1} (1 - \mathcal{R}_{1}),$$

$$x_{2} = d_{2} + \mu_{2} \mathcal{R}_{2} + \frac{\beta_{2} \phi_{2}}{Z_{2}} X_{2},$$

$$y_{2} = \mu_{2} X_{2} (\mathcal{R}_{2} - 1) + \mu_{2} X_{2} \frac{\beta_{2} \phi_{2}}{Z_{2}} + d_{2} \mu_{2} \mathcal{R}_{2},$$

$$z_{2} = \mu_{2} d_{2} X_{2} (\mathcal{R}_{2} - 1),$$

with

$$X_{1} = \theta_{I} + c_{1} + \mu_{1},$$

$$Y_{1} = \theta_{S} + \mu_{1},$$

$$Z_{1} = \alpha_{1}d_{1} + \beta_{1}\phi_{1},$$

$$X_{2} = \mu_{2} + c_{2},$$

$$Z_{2} = \alpha_{2}d_{2} + \beta_{2}\phi_{2}.$$

Clearly, if $\mathcal{R}_1 > 1$ and $\mathcal{R}_2 > 1$, then $z_1 < 0$, and there exists an eigenvalue of J that has a positive real part. Hence \mathcal{E}_1 is unstable in this case. On the other hand, $x_1, y_1, z_1, x_2, y_2, z_2$ are all positive when $\mathcal{R}_1 < 1$ and $\mathcal{R}_2 > 1$. Furthermore, we have $x_1y_1 > z_1$ and $x_2y_2 > z_2$, since $x_1 > Y_1, y_1 > d_1X_1(1 - \mathcal{R}_1)$ and $x_2 > d_2, y_2 > \mu_2X_2(\mathcal{R}_2 - 1)$. It follows from the Routh-Hurwitz criterion that \mathcal{E}_1 is locally asymptotically stable if $\mathcal{R}_1 < 1$ and $\mathcal{R}_2 > 1$.

We already know that the disease-free equilibrium \mathcal{E}_0 is unstable when there exist nontrivial equilibria; i.e., when $\mathcal{R}_0 > 1$. Theorem 5.2.3 shows that when \mathcal{E}_1 is the only nontrivial equilibrium, it must be (locally) stable; and when both \mathcal{E}_1 and \mathcal{E}_2 exist, \mathcal{E}_1 becomes unstable. This, consequently, implies that the endemic equilibrium \mathcal{E}_2 is stable whenever it exists. The local stability of \mathcal{E}_2 can be similarly analyzed by examining its characteristic polynomial and using the Routh-Hurwitz criterion, though the algebraic manipulation becomes extremely tedious. Instead of

engaging the (somehow unnecessary) algebraic complications, we proceed to establish the stronger results regarding the global asymptotic stabilities of both \mathcal{E}_1 and \mathcal{E}_2 . To that end, we introduce two more assumptions:

(C1) sup $(S_1) \leq \frac{\theta_I + c_1}{2\alpha_1}$.

(C2) sup
$$(S_2) \leq \frac{c_2}{2\alpha_2}$$
.

These conditions provide additional regulations on the upper bounds of the susceptible populations in both patches to ensure global stability. In particular, if $S_1^0 \leq \frac{\theta_I + c_1}{2\alpha_1}$ and $S_2^0 \leq \frac{c_2}{2\alpha_2}$, then (C1) and (C2) will be automatically satisfied.

We will follow the geometric approach originally proposed by Li and Muldowney [74] to investigate the global asymptotic stabilities of the nontrivial equilibria. For completeness, we first present the following result from [74].

Lemma 5.1 Consider a dynamical system $\frac{dX}{dt} = f(X)$, where $f: D \mapsto \mathbb{R}^n$ is a C^1 function and $D \subset \mathbb{R}^n$ is a simply connected domain. Assume that there exists a compact absorbing set $K \subset D$ and the system has a unique equilibrium point X^* in D. Then X^* is globally asymptotically stable in D if $\bar{q}_2 < 0$, where

$$\bar{q}_2 = \limsup_{t \to \infty} \sup_{X_0 \in K} \frac{1}{t} \int_0^t m(Q(X(s, X_0))) ds.$$
 (5.24)

In equation (5.24), Q is a matrix-valued function defined as

$$Q = P_f P^{-1} + P J^{[2]} P^{-1} , (5.25)$$

where P(X) is a $\binom{n}{2} \times \binom{n}{2}$ matrix-valued C^1 function in D, P_f is the derivative of P (entry-wise) along the direction of f, and $J^{[2]}$ is the second additive compound matrix of the Jacobian J(X) = Df(X). Meanwhile, m(Q) is the Lozinskii measure of Q with respect to a matrix norm; i.e.,

$$m(Q) = \lim_{h \to 0^+} \frac{|\mathbb{I} + hQ| - 1}{h},$$
 (5.26)

where \mathbb{I} represents the identity matrix.

Now we are ready to prove the following global stability result.

Theorem 5.2.4

(i) If $\mathcal{R}_1 > 1$, then the endemic equilibrium \mathcal{E}_2 exists and is global asymptotically stable, provided that the assumptions (C1) and (C2) hold.

(ii) If $\mathcal{R}_1 < 1$ and $\mathcal{R}_2 > 1$, then the boundary equilibrium \mathcal{E}_1 is global asymptotically stable.

Proof 11 We apply the geometric approach, summarized in Lemma 5.1, to analyse the global stabilities.

(i). Note that patch 1 does not depend on patch 2 and that the endemic equilibrium of patch 1 is (uniquely) represented by the first three components of \mathcal{E}_2 ; i.e., $\mathcal{E}_2^{(1)} = (S_1^*, I_1^*, B_1^*)$. This indicates that the global stability of $\mathcal{E}_2^{(1)}$ in patch 1 can be analyzed independently, based on the first three equations in system (5.1). Thus we will first prove that $\mathcal{E}_2^{(1)}$ is globally asymptotically stable in patch 1, using the geometric approach.

By direct calculation, we find that the Jacobian matrix of the linearized subsystem in patch 1 is

$$J_{1} = \begin{bmatrix} -(\alpha_{1}I_{1} + \beta_{1}B_{1} + Y_{1}) & -\alpha_{1}S_{1} & -\beta_{1}S_{1} \\ \alpha_{1}I_{1} + \beta_{1}B_{1} & \alpha_{1}S_{1} - X_{1} & \beta_{1}S_{1} \\ 0 & \phi_{1} & -d_{1} \end{bmatrix},$$

and the associated second additive compound matrix $J_1^{[2]}$ is

$$\begin{bmatrix} \alpha_1 S_1 - (\alpha_1 I_1 + \beta_1 B_1 + Y_1 + X_1) & \beta_1 S_1 & \beta_1 S_1 \\ \phi_1 & -(\alpha_1 I_1 + \beta_1 B_1 + Y_1 + d_1) & -\alpha_1 S_1 \\ 0 & \alpha_1 I_1 + \beta_1 B_1 & \alpha_1 S_1 - X_1 - d_1 \end{bmatrix}.$$

Define $P_1 = diag\left[1, \frac{I_1}{B_1}, \frac{I_1}{B_1}\right]$ and let F_1 denote the vector field of patch 1, then

$$P_{1F_1}P_1^{-1} = diag\left[0, \frac{\dot{I_1}}{I_1} - \frac{\dot{B_1}}{B_1}, \frac{\dot{I_1}}{I_1} - \frac{\dot{B_1}}{B_1}\right],$$

and $P_1 J_1^{[2]} P_1^{-1}$ is given by

$$\begin{bmatrix} \alpha_1 S_1 - (\alpha_1 I_1 + \beta_1 B_1 + Y_1 + X_1) & \beta_1 S_1 \frac{B_1}{I_1} & \beta_1 S_1 \frac{B_1}{I_1} \\ \frac{I_1}{B_1} \phi_1 & -(\alpha_1 I_1 + \beta_1 B_1 + Y_1 + d_1) & -\alpha_1 S_1 \\ 0 & \alpha_1 I_1 + \beta_1 B_1 & \alpha_1 S_1 - X_1 - d_1 \end{bmatrix}.$$

The matrix $Q^{(1)} := P_{1F_1}P_1^{-1} + P_1J_1^{[2]}P_1^{-1}$ can be written in the block form as follows

$$Q^{(1)} = \begin{bmatrix} Q_{11}^{(1)} & Q_{12}^{(1)} \\ Q_{21}^{(1)} & Q_{22}^{(1)} \end{bmatrix},$$

where

$$Q_{11}^{(1)} = \alpha_1 S_1 - (\alpha_1 I_1 + \beta_1 B_1 + Y_1 + X_1),$$

$$Q_{12}^{(1)} = \left[\beta_1 S_1 \frac{B_1}{I_1}, \beta_1 S_1 \frac{B_1}{I_1}\right],$$

$$Q_{21}^{(1)} = \left[\frac{I_1}{B_1} \phi_1, 0\right]^T,$$

$$Q_{22}^{(1)} = \begin{bmatrix} -(\alpha_1 I_1 + \beta_1 B_1 + Y_1 + d_1) + \frac{\dot{I_1}}{I_1} - \frac{\dot{B_1}}{B_1} & -\alpha_1 S_1 \\ \alpha_1 I_1 + \beta_1 B_1 & \alpha_1 S_1 - X_1 - d_1 + \frac{\dot{I_1}}{I_1} - \frac{\dot{B_1}}{B_1} \end{bmatrix}.$$

We now define the vector norm for any $(x_1, x_2, x_3) \in \mathbb{R}^3$ as

$$|(x_1, x_2, x_3)| = \max(|x_1|, |x_2| + |x_3|).$$

Let m denote the Lozinskii measure with respect to this norm. By direct calculation, we find

$$m\left(Q^{(1)}\right) = \sup\left(g_1^{(1)}, g_2^{(1)}\right)$$

with $g_1^{(1)} = m_1 \left(Q_{11}^{(1)}\right) + \left|Q_{12}^{(1)}\right|$, $g_2^{(1)} = \left|Q_{21}^{(1)}\right| + m_1 \left(Q_{22}^{(1)}\right)$, where $\left|Q_{12}^{(1)}\right|$ and $\left|Q_{21}^{(1)}\right|$ are the matrix norms induced by the L_1 norm, and m_1 denotes the Lozinskii measure with respect to the L_1 norm. Specifically,

$$g_1^{(1)} = \alpha_1 S_1 - (\alpha_1 I_1 + \beta_1 B_1 + Y_1 + X_1) + \beta_1 S_1 \frac{B_1}{I_1},$$

$$g_2^{(1)} = -Y_1 + \frac{\dot{I}_1}{I_1} + \sup(0, 2\alpha_1 S_1 - X_1 + Y_1).$$

Observing that $\frac{\dot{I}_1}{I_1} = (\alpha_1 S_1 + \beta_1 S_1 \frac{B_1}{I_1}) - X_1$ and using assumption (C1), we have

$$g_1^{(1)} = \frac{\dot{I}_1}{I_1} - (\alpha_1 I_1 + \beta_1 B_1 + Y_1) \le \frac{\dot{I}_1}{I_1} - \mu_1,$$

$$g_2^{(1)} \le \frac{\dot{I}_1}{I_1} - \mu_1.$$

Hence $m(Q^{(1)}) \leq \frac{\dot{I_1}}{I_1} - \mu_1$. In view of $0 \leq I_1(t) \leq N(t) \leq \frac{A_1 + A_2}{\min(\mu_1, \mu_2)}$, if t is large enough, then

$$\frac{\ln(I_1(t)) - \ln(I_1(0))}{t} \le \frac{\mu_1}{2}.$$

Consequently,

$$\frac{1}{t} \int_0^t m(Q^{(1)}) ds \le \frac{1}{t} \int_0^t (\frac{\dot{I}_1}{I_1} - \mu_1) ds = \frac{\ln(I_1(t)) - \ln(I_1(0))}{t} - \mu_1 \le -\frac{\mu_1}{2}$$

for t sufficiently large. Therefore, we obtain

$$\bar{q}_2^{(1)} := \limsup_{t \to \infty} \frac{1}{t} \int_0^t m(Q^{(1)}) ds \le -\frac{\mu_1}{2} < 0,$$

which shows that $\mathcal{E}_2^{(1)}$ is globally asymptotically stable in patch 1.

Thus, to establish the global asymptotic stability of \mathcal{E}_2 in the entire domain, it is sufficient to show that the endemic equilibrium of patch 2; i.e., $\mathcal{E}_2^{(2)} = (S_2^*, I_2^*, B_2^*)$, is globally asymptotically stable in patch 2 under the condition $(S_1, I_1, B_1) = (S_1^*, I_1^*, B_1^*)$. This can be proved in a similar way and details are provided below.

For patch 2, the Jacobian matrix of the linearized subsystem is

$$J_2 = \begin{bmatrix} -(\alpha_2 I_2 + \beta_2 B_2 + \mu_2) & -\alpha_2 S_2 & -\beta_2 S_2 \\ \alpha_2 I_2 + \beta_2 B_2 & \alpha_2 S_2 - X_2 & \beta_2 S_2 \\ 0 & \phi_2 & -d_2 \end{bmatrix},$$

and the associated second additive compound matrix is $J_2^{[2]}$

$$\begin{bmatrix} \alpha_2 S_2 - (\alpha_2 I_2 + \beta_2 B_2 + \mu_2 + X_2) & \beta_2 S_2 & \beta_2 S_2 \\ \phi_2 & -(\alpha_2 I_2 + \beta_2 B_2 + \mu_2 + d_2) & -\alpha_2 S_2 \\ 0 & \alpha_2 I_2 + \beta_2 B_2 & \alpha_2 S_2 - X_2 - d_2 \end{bmatrix}.$$

Also define $P_2 = diag\left[1, \frac{I_2}{B_2}, \frac{I_2}{B_2}\right]$ and let F_2 denote the vector field of patch 2, then

$$P_{2F_2}P_2^{-1} = diag \left[0, \frac{\dot{I}_2}{I_2} - \frac{\dot{B}_2}{B_2}, \frac{\dot{I}_2}{I_2} - \frac{\dot{B}_2}{B_2} \right],$$

and $P_2J_2^{[2]}P_2^{-1}$ is given by

$$\begin{bmatrix} \alpha_2 S_2 - (\alpha_2 I_2 + \beta_2 B_2 + \mu_2 + X_2) & \beta_2 S_2 \frac{B_2}{I_2} & \beta_2 S_2 \frac{B_2}{I_2} \\ \frac{I_2}{B_2} \phi_2 & -(\alpha_2 I_2 + \beta_2 B_2 + \mu_2 + d_2) & -\alpha_2 S_2 \\ 0 & \alpha_2 I_2 + \beta_2 B_2 & \alpha_2 S_2 - X_2 - d_2 \end{bmatrix}.$$

The matrix $Q^{(2)}:=P_{2F_2}P_2^{-1}+P_2J_2^{[2]}P_2^{-1}$ can be written in the block form as follows

$$Q^{(2)} = \begin{bmatrix} Q_{11}^{(2)} & Q_{12}^{(2)} \\ Q_{21}^{(2)} & Q_{22}^{(2)} \end{bmatrix},$$

where

$$Q_{11}^{(2)} = \alpha_2 S_2 - (\alpha_2 I_2 + \beta_2 B_2 + \mu_2 + X_2),$$

$$Q_{12}^{(2)} = \left[\beta_2 S_2 \frac{B_2}{I_2}, \beta_2 S_2 \frac{B_2}{I_2}\right],$$

$$Q_{21}^{(2)} = \left[\frac{I_2}{B_2} \phi_2, 0\right]^T,$$

$$Q_{22}^{(2)} = \begin{bmatrix} -(\alpha_2 I_2 + \beta_2 B_2 + \mu_2 + d_2) + \frac{I_2}{I_2} - \frac{B_2}{B_2} & -\alpha_2 S_2 \\ \alpha_2 I_2 + \beta_2 B_2 & \alpha_2 S_2 - X_2 - d_2 + \frac{I_2}{I_2} - \frac{B_2}{B_2} \end{bmatrix}.$$

Then we have $m(Q^{(2)}) = \sup(g_1^{(2)}, g_2^{(2)})$, where

$$g_1^{(2)} = \alpha_2 S_2 - (\alpha_2 I_2 + \beta_2 B_2 + \mu_2 + X_2) + \beta_2 S_2 \frac{B_2}{I_2},$$

$$g_2^{(2)} = -\mu_2 + \frac{\dot{I}_2}{I_2} + \sup(0, 2\alpha_2 S_2 - c_2).$$

Since $\frac{\dot{I}_2}{I_2} = (\alpha_2 S_2 + \beta_2 S_2 \frac{B_2}{I_2}) - X_2 + \theta_I \frac{I_1^*}{I_2}$ and the assumption (C2) holds, we have

$$g_1^{(2)} = \frac{\dot{I}_2 - \theta_I I_1^*}{I_2} - (\alpha_2 I_2 + \beta_2 B_2 + \mu_2) \le \frac{\dot{I}_2}{I_2} - \mu_2,$$

$$g_2^{(2)} \le \frac{\dot{I}_2}{I_2} - \mu_2,$$

Hence $m(Q^{(2)}) \leq \frac{\dot{I}_2}{I_2} - \mu_2$. Also notice that $0 \leq I_2(t) \leq N(t) \leq \frac{A_1 + A_2}{\min(\mu_1, \mu_2)}$. Then

$$\frac{\ln(I_2(t)) - \ln(I_2(0))}{t} \le \frac{\mu_2}{2}$$

if t is large enough. Therefore,

$$\frac{1}{t} \int_0^t m(Q^{(2)}) ds \le \frac{1}{t} \int_0^t (\frac{\dot{I}_2}{I_2} - \mu_2) ds = \frac{\ln(I_2(t)) - \ln(I_2(0))}{t} - \mu_2 \le -\frac{\mu_2}{2}$$

for t sufficiently large. This implies $\bar{q}_2^{(2)} := \limsup_{t \to \infty} \frac{1}{t} \int_0^t m(Q^{(2)}) ds \le -\frac{\mu_2}{2} < 0$ which establishes the global stability of $\mathcal{E}_2^{(2)}$ in patch 2. Consequently, the proof of the global asymptotic stability of \mathcal{E}_2 in Γ is complete.

(ii). If $\mathcal{R}_1 < 1$ and $\mathcal{R}_2 > 1$, there is only one nontrivial equilibrium \mathcal{E}_1 and we may write $\mathcal{E}_1 = (\mathcal{E}_1^{(1)}, \mathcal{E}_1^{(2)})$, where $\mathcal{E}_1^{(1)} = (\widetilde{S}_1, 0, 0)$ is the disease-free equilibrium of patch 1, and $\mathcal{E}_2^{(2)} = (\widetilde{S}_2, \widetilde{I}_2, \widetilde{B}_2)$ is the unique positive equilibrium of patch 2

under the condition $(S_1, I_1, B_1) = (\widetilde{S}_1, 0, 0)$. Similar to the proof of Theorem 5.2.1 and Theorem 5.2.4 (i), it can be easily verified that $\mathcal{E}_1^{(1)}$ is globally asymptotically stable in patch 1, and $\mathcal{E}_1^{(2)}$ is globally asymptotically stable in patch 2 provided that $(S_1, I_1, B_1) = (\widetilde{S}_1, 0, 0)$. Hence we conclude that \mathcal{E}_1 is globally asymptotically.

5.3 A two-patch periodic model

Having thoroughly analyzed the dynamics of the autonomous model, we now incorporate the seasonal variation into our modeling framework. As mentioned before, brucellosis exhibits a strong seasonal pattern, with concentrated mortality and morbidity burden in a few months each year. These seasonal fluctuations could be represented by periodic changes in the various contact and transmission rates in our model.

For illustration, let us consider the temporal oscillation of the direct (i.e., host-to-host) and indirect (i.e., environment-to-host) transmission rates. We define

$$\beta_{j}(t) = \beta_{j0} \left[1 + a_{1} \cos \left(\frac{\pi t}{6} \right) \right], \quad j = 1, 2$$

$$\alpha_{j}(t) = \alpha_{j0} \left[1 + a_{2} \cos \left(\frac{\pi t}{6} \right) \right], \quad j = 1, 2$$

where α_{j0} and β_{j0} denote the respective time-averaged (or, basic) transmission rates. Meanwhile, we represent the pathogen shedding rate by

$$\phi_j(t) = \phi_{j0} \left[1 + a_3 \cos\left(\frac{\pi t}{6}\right) \right], \quad j = 1, 2$$

where ϕ_{j0} denotes the basic shedding rate in the absence of seasonal forcing. Note that $0 \le a_k \le 1$ (k = 1, 2, 3) denote the magnitude of seasonal fluctuations for these three parameters. For simplicity, we assume that all other model parameters are the same as defined in system (5.1). Our new two-patch system incorporating both spatial and seasonal variations is thus given by

$$\begin{cases}
\dot{S}_{1}(t) &= A_{1} - [\alpha_{1}(t)I_{1} + \beta_{1}(t)B_{1}]S_{1} - [\theta_{S} + \mu_{1}]S_{1}, \\
\dot{I}_{1}(t) &= [\alpha_{1}(t)I_{1} + \beta_{1}(t)B_{1}]S_{1} - [\theta_{I} + c_{1} + \mu_{1}]I_{1}, \\
\dot{B}_{1}(t) &= \phi_{1}(t)I_{1} - d_{1}B_{1}, \\
\dot{S}_{2}(t) &= A_{2} - [\alpha_{2}(t)I_{2} + \beta_{2}(t)B_{2}]S_{2} - \mu_{2}S_{2} + \theta_{S}S_{1}, \\
\dot{I}_{2}(t) &= [\alpha_{2}(t)I_{2} + \beta_{2}B_{2}(t)]S_{2} - (\mu_{2} + c_{2})I_{2} + \theta_{I}I_{1}, \\
\dot{B}_{2}(t) &= \phi_{2}(t)I_{2} - d_{2}B_{2}.
\end{cases} (5.27)$$

It again can be easily verified that system (5.27) has a unique and bounded solution with any initial value $(S_j(0), I_j(0), B_j(0)) \in \Gamma$, and that the compact set Γ is positively invariant with respect to system (5.27).

5.3.1 The reproduction number

It is straightforward to see that $\mathcal{E}^0 = (S_1^0, 0, 0, S_2^0, 0, 0)$ remains the disease-free equilibrium for the model (5.27). Thus, we can similarly introduce the next-generation matrices F(t) and V(t) (evaluated at the disease-free equilibrium) as

$$F(t) = \begin{bmatrix} \alpha_1(t)S_1^0 & \beta_1(t)S_1^0 & 0 & 0\\ 0 & 0 & 0 & 0\\ 0 & 0 & \alpha_2(t)S_2^0 & \beta_2(t)S_2^0\\ 0 & 0 & 0 & 0 \end{bmatrix},$$
 and
$$V(t) = \begin{bmatrix} (c_1 + \theta_I + \mu_1) & 0 & 0 & 0\\ -\phi_1(t) & d_1 & 0 & 0\\ -\theta_I & 0 & (c_2 + \mu_2) & 0\\ 0 & 0 & -\phi_2(t) & d_2 \end{bmatrix}$$

In order to define the basic reproduction number of this non-autonomous model, we follow the work of Wang and Zhao [55]. They introduced the next-infection operator L for a model in periodic environments by

$$(L\phi)(t) = \int_0^\infty Y(t, t-s)F(t-s)\phi(t-s)ds, \tag{5.28}$$

where $Y(t,s), t \geq s$, is the evolution operator of the linear ω -periodic system dy/dt = -V(t)y and $\phi(t)$, the initial distribution of infectious individuals, is ω -periodic and

nonnegative. The basic reproduction number is then defined as the spectral radius of the next-infection operator,

$$R_0 = \rho(L). \tag{5.29}$$

For our model (5.27), the evolution operator can be determined by solving the system of differential equations dy/dt = -V(t)y with the initial condition $Y(s,s) = I_{4\times 4}$; thus, we obtain

$$Y(t,s) = \begin{bmatrix} y_{11}(t,s) & 0 & 0 & 0 \\ y_{21}(t,s) & y_{22}(t,s) & 0 & 0 \\ y_{31}(t,s) & 0 & y_{33}(t,s) & 0 \\ y_{41}(t,s) & 0 & y_{43}(t,s) & y_{44}(t,s) \end{bmatrix}$$
(5.30)

where

$$y_{11}(t,s) = e^{-(c_1+\theta_I+\mu_1)(t-s)},$$

$$y_{21}(t,s) = \phi_{10}e^{-d_1t}\int_s^t e^{d_1x}\left(1+a_3\cos\left(\frac{\pi x}{6}\right)\right)y_{11}(x,s)dx,$$

$$y_{31}(t,s) = \theta_I e^{-(c_2+\mu_2)t}\int_s^t e^{(c_2+\mu_2)x}y_{11}(x,s)dx,$$

$$y_{41}(t,s) = \phi_{20}e^{-d_2t}\int_s^t e^{d_2x}\left(1+a_3\cos\left(\frac{\pi x}{6}\right)\right)y_{31}(x,s)dx,$$

$$y_{22}(t,s) = e^{-d_1(t-s)},$$

$$y_{33}(t,s) = e^{-(c_2+\mu_2)(t-s)},$$

$$y_{43}(t,s) = \phi_{20}e^{-d_2t}\int_s^t e^{d_2x}\left(1+a_3\cos\left(\frac{\pi x}{6}\right)\right)y_{33}(x,s)dx,$$

$$y_{44}(t,s) = e^{-d_2(t-s)}.$$

The basic reproduction number defined in Equation (5.29) can be numerically evaluated by using, for example, the method described in [56].

5.3.2 Threshold dynamics

Using the basic reproduction number R_0 , we aim to establish the threshold type result, stated in the theorem below, for the periodic model (5.27). To that end, we first note that \mathbb{R}^2_+ is positively invariant for the following cooperative system:

$$\begin{cases}
\dot{S}_1(t) = A_1 - (\theta_S + \mu_1)S_1, \\
\dot{S}_2(t) = A_2 - \mu_2S_2 + \theta_SS_1,
\end{cases} (5.31)$$

and that (S_1^0, S_2^0) is the unique equilibrium solution which is globally attractive in \mathbb{R}^2_+ .

Theorem 5.3.1

- (i) If $R_0 < 1$, then the disease-free equilibrium \mathcal{E}_0 of system (5.27) is globally asymptotically stable;
- (ii) If $R_0 > 1$, then system (5.27) admits at least one positive ω -periodic solution, and solutions of system (5.27) are uniformly persistent.

Proof 12 If $(S_1(t), I_1(t), B_1(t), S_2(t), I_2(t), B_2(t))$ is a nonnegative solution of (5.27), then we have

$$\begin{cases}
\dot{S}_1(t) \le A_1 - (\theta_S + \mu_1)S_1, \\
\dot{S}_2(t) \le A_2 - \mu_2 S_2 + \theta_S S_1.
\end{cases}$$
(5.32)

Note that any nonnegative solution $(S_1(t), S_2(t))$ of system (5.31) approaches (S_1^0, S_2^0) as $t \to \infty$. It then follows from the standard comparison theorem (see, e.g., [75, Theorem A.4]) that for any $\epsilon > 0$, there is a T > 0 such that

$$S_i(t) < S_i^0 + \epsilon, \quad i = 1, 2, \text{ for } t > T.$$
 (5.33)

Thus, for t > T, we have

$$\dot{I}_1(t) \leq [\alpha_1(t)I_1 + \beta_1(t)B_1](S_1^0 + \epsilon) - [\theta_I + c_1 + \mu_1]I_1, \tag{5.34}$$

$$\dot{B}_1(t) \leq \phi_1(t)I_1 - d_1B_1,$$

$$\dot{I}_2(t) \leq [\alpha_2(t)I_2 + \beta_2B_2(t)](S_2^0 + \epsilon) - [\mu_2 + c_2]I_2 + \theta_I I_1,$$
(5.35)

$$\dot{I}_2(t) \leq [\alpha_2(t)I_2 + \beta_2 B_2(t)](S_2^0 + \epsilon) - [\mu_2 + c_2]I_2 + \theta_I I_1,$$
 (5.36)

$$\dot{B}_2(t) \leq \phi_2(t)I_2 - d_2B_2. \tag{5.37}$$

Define

$$F_{\epsilon}(t) = \begin{bmatrix} \alpha_1(t)(S_1^0 + \epsilon) & \beta_1(t)(S_1^0 + \epsilon) & 0 & 0\\ 0 & 0 & 0 & 0\\ 0 & 0 & \alpha_2(t)(S_2^0 + \epsilon) & \beta_2(t)(S_2^0 + \epsilon)\\ 0 & 0 & 0 & 0 \end{bmatrix}.$$

By [55, Thorem 2.2], we have $R_0 < 1 \iff \rho(\phi_{F-V}(\omega)) < 1$, where $\rho(\phi_{F-V}(\omega))$ is the spectral radius of $\phi_{F-V}(\omega)$, and $\phi_{F-V}(\omega)$ is the monodromy matrix of the linear ω -periodic system dy/dt = (F - V)y. Then we can set ϵ sufficiently small such that $\rho(\phi_{F_{\epsilon}-V}(\omega)) < 1$. As a consequence, the trivial solution (0,0,0,0) of the following linear ω -periodic system

$$\dot{I}_1(t) = [\alpha_1(t)I_1 + \beta_1(t)B_1](S_1^0 + \epsilon) - [\theta_I + c_1 + \mu_1]I_1, \tag{5.38}$$

$$\dot{B}_1(t) = \phi_1(t)I_1 - d_1B_1, \tag{5.39}$$

$$\dot{I}_2(t) = [\alpha_2(t)I_2 + \beta_2 B_2(t)](S_2^0 + \epsilon) - [\mu_2 + c_2]I_2 + \theta_I I_1, \qquad (5.40)$$

$$\dot{B}_2(t) = \phi_2(t)I_2 - d_2B_2, \tag{5.41}$$

is globally asymptotically stable. Again by the comparison theorem, we know that $I_i(t) \to 0$, $B_i(t) \to 0$ as $t \to \infty$ for i = 1, 2. Finally, the first and fourth equations of system (5.27) imply that $S_i(t) \to S_i^0$ as $t \to \infty$ for i = 1, 2. This proves the result in part (i).

Now we consider the case $R_0 > 1$. We define $X = \mathbb{R}^6_+$, $X_0 = \mathbb{R}^2_+ \times Int(\mathbb{R}^4_+)$, $\partial X_0 = X \setminus X_0$, and denote $S(t) = (S_1(t), S_2(t))$, $I(t) = (I_1(t), I_2(t))$, $B(t) = (B_1(t), B_2(t))$. It is easy to see that both X and X_0 are positively invariant. Let $P : \mathbb{R}^6_+ \to \mathbb{R}^6_+$ be the Poincaré map associated with system (5.27); that is, $P(x_0) = u(\omega, x_0)$ for all $x_0 \in \mathbb{R}^6_+$, where $u(t, x_0)$ is the unique solution of (5.27) with $u(0, x_0) = x_0$. Set

$$M_{\partial} = \{ (S(0), I(0), B(0)) \in \partial X_0 : P^m(S(0), I(0), B(0)) \in \partial X_0, \forall m \ge 0 \},$$

$$M = \{(S, I, B) : S \ge 0, I = (0, I_2), B = (0, B_2), I_2 \ge 0, B_2 \ge 0\}.$$

We first show that

$$M_{\partial} = M. \tag{5.42}$$

Clearly, $M \subseteq M_{\partial}$. For any $(S(0), I(0), B(0)) \in \partial X_0 \backslash M$, if $I_1(0) > 0, I_2(0) = 0, B(0) = 0$, then $\dot{B}_1(0) = \phi_1(0)I_1(0) > 0, \dot{I}_2(0) = \theta_I(0)I_1(0) > 0$. It follows that $I(t) > 0, B_1(t) > 0$ for $0 < t \ll 1$, hence $\dot{B}_2(t) > 0$ for $0 < t \ll 1$, which implies B(t) > 0 for $0 < t \ll 1$. If $B_1(0) > 0, I_1(0) = 0$, then $\dot{I}_1(0) = \alpha_1(0)B_1(0)S_1(0) > 0$, we can still obtain I(t) > 0, B(t) > 0 for $0 < t \ll 1$. Thus, we have $(S(t), I(t), B(t)) \notin \partial X_0$ for $0 < t \ll 1$. By the positive invariance of X_0 , we know that $P^m(S(0), I(0), B(0)) \notin \partial X_0$ for $m \ge 1$, hence $(S(0), I(0), B(0)) \notin M_{\partial}$, and thus (5.42) holds.

Now consider the fixed point $M_0 = (S^0, 0, 0)$ of the Poincaré map P, where $S^0 = (S_1^0, S_2^0)$. Define $W^S(M_0) = \{x_0 : P^m(x_0) \to M_0, m \to \infty\}$. We show that

$$W^S(M_0) \cap X_0 = \emptyset. \tag{5.43}$$

Based on the continuity of solutions with respect to the initial conditions, for any $\epsilon > 0$, there exists $\delta > 0$ small enough such that for all $(S(0), I(0), B(0)) \in X_0$ with $||(S(0), I(0), B(0)) - M_0|| \le \delta$, we have

$$||u(t, (S(0), I(0), B(0)) - u(t, M_0)|| < \epsilon, \quad \forall t \in [0, \omega].$$
 (5.44)

To obtain (5.43), we claim that

$$\limsup_{m \to \infty} ||P^m(S(0), I(0), B(0)) - M_0|| \ge \delta, \quad \forall (S(0), I(0), B(0)) \in X_0.$$
 (5.45)

We prove this claim by contradiction; that is, we suppose

$$\limsup_{m \to \infty} ||P^m(S(0), I(0), B(0)) - M_0|| < \delta$$

for some $(S(0), I(0), B(0)) \in X_0$. Without loss of generality, we assume that $||P^m(S(0), I(0), B(0)) - M_0|| < \delta$, $\forall m \geq 0$. Thus,

$$||u(t, P^m(S(0), I(0), B(0)) - u(t, M_0)|| < \epsilon, \quad \forall t \in [0, \omega] \text{ and } m \ge 0.$$
 (5.46)

Moreover, for any $t \geq 0$, we write $t = t_0 + k\omega$ with $t_0 \in [0, \omega)$ and $k = [t/\omega]$, the greatest integer less than or equal to t/ω . Then we obtain

$$||u(t, (S(0), I(0), B(0)) - u(t, M_0)|| = ||u(t_0, P^m(S(0), I(0), B(0)) - u(t_0, M_0)|| < \epsilon$$
(5.47)

for any $t \geq 0$. Let (S(t), I(t), B(t)) = u(t, (S(0), I(0), B(0))). It follows that $-\epsilon < S(t) - S^0 < \epsilon, 0 < I(t) < \epsilon$ and $0 < B(t) < \epsilon$. Again based on [55, Thorem 2.2], $R_0 > 1$ if and only if $\rho(\Phi_{F-V}(\omega)) > 1$. Thus, for ϵ small enough, we have $\rho(\Phi_{F_{\epsilon}-V}(\omega)) > 1$ which immediately yields the contradiction as

$$\lim_{t \to \infty} I_i(t) = \infty, \quad \lim_{t \to \infty} B_i(t) = \infty, \quad i = 1, 2.$$

Let $P_1: \mathbb{R}^2_+ \longrightarrow \mathbb{R}^2_+$ be the Poincaré map associated with (5.31). Then S^0 is globally attractive in $\mathbb{R}^2_+ \setminus \{0\}$ for P_1 . It follows that M_0 is isolated invariant set in

X, and notice that $W^S(M_0) \cap X_0 = \emptyset$. Hence, every orbit in M_∂ converges to M_0 and M_0 is acyclic in M_∂ . By [58, Thorem 1.3.1], for a stronger repelling property of ∂X_0 , we conclude that P is uniformly persistent with respect to $(X_0, \partial X_0)$, which implies the uniform persistence of the solutions of system (5.27) with respect to $(X_0, \partial X_0)$ [58, Thorem 3.1.1]. Consequently, based on [58, Theorem 1.3.6], the Poincaré map P has a fixed point $(\bar{S}(0), \bar{I}(0), \bar{B}(0)) \in X_0$, and it can be easily seen that $\bar{S}(0) \neq 0$. Thus, $(\bar{S}(0), \bar{I}(0), \bar{B}(0)) \in Int(\mathbb{R}^6_+)$ and $(\bar{S}(t), \bar{I}(t), \bar{B}(t)) = u(t, (\bar{S}(0), \bar{I}(0), \bar{B}(0)))$ is a positive ω -periodic solution of the system.

5.4 Numerical results

In this section, we conduct some numerical simulation in order to verify our analytical findings. We list the model parameters and their numerical values in Table 5.1.

Table 5.1: Parameters and their values

Symbo	l Definition	Value	Unit	Source
$\overline{c_j}$	Elimination rate due to brucellosis, $(j = 1, 2)$	0.15	$year^{-1}$	[30]
α_{j0}	Averaged direct transmission rate, $(j = 1, 2)$	1.48×10^{-8}	$animal^{-1}year^{-1}$	[30]
β_{j0}	Averaged indirect transmission rate, $(j = 1, 2)$	1.7×10^{-10}	$pathogen^{-1}year^{-1}$	[30]
ϕ_{j0}	Averaged brucella shedding rate, $(j = 1, 2)$	15	$pathogen\ animal^{-1}$	[30]
			$year^{-1}$	
θ_S	Averaged susceptible animals migration rate	Varied	$year^{-1}$	-
$ heta_I$	Averaged infectious animals migration rate	Varied	$year^{-1}$	-
a_1	Amplitude of oscillation in $\beta_j(t)$, $(j = 1, 2)$	0.8	-	Assumed
a_2	Amplitude of oscillation in $\alpha_j(t)$, $(j = 1, 2)$	0.8	-	Assumed
a_3	Amplitude of oscillation in $\phi_j(t)$, $(j = 1, 2)$	0.8	-	Assumed
a_4	Amplitude of oscillation in $\theta_S(t)$	0.8	-	Assumed
a_5	Amplitude of oscillation in $\theta_I(t)$	0.8	-	Assumed
μ_j	Natural elimination rate, $(j = 1, 2)$	0.22	$year^{-1}$	[30]
A_j	Recruitment rate, $(j = 1, 2)$	11629200	$animals\ year^{-1}$	[30]
d_{j}	Pathogen decay rate, $(j = 1, 2)$	3.6	$year^{-1}$	[30]
$S_j(0)$	Initial number of susceptible, $(j = 1, 2)$	5.185×10^{7}	animals	[30]
$I_j(0)$	Initial infected animals, $(j = 1, 2)$	1.33×10^6	animals	[30]
$B_j(0)$	Initial load of $brucella$, $(j = 1, 2)$	6×10^6	pathogens	[30]

Using the parameter values in Table 5.1, we first perform a numerical study on the autonomous model (5.1). Our main analytical result, Theorem 5.2.4, states the global asymptotic stability of the two nontrivial equilibria, \mathcal{E}_1 and \mathcal{E}_2 . Numerically, we vary the animal migration rates θ_S and θ_I so as to generate different values of \mathcal{R}_1 and \mathcal{R}_2 . For each of these scenarios, we pick a number of initial conditions and conduct separate simulations to system (5.1). Figure 5.1 illustrates a case where we set $\theta_S = \theta_I = 0.2$ which results in $\mathcal{R}_1 \doteq 0.75 < 1$, $\mathcal{R}_2 \doteq 3.27 > 1$, and all solution curves converge to the equilibrium $\mathcal{E}_1 \doteq (2.77 \times 10^7, 0, 0, 2.39 \times 10^7, 3.22 \times 10^7, 1.34 \times 10^8)$ over time. The same convergence pattern is observed throughout the regime $\mathcal{R}_1 < 1$, $\mathcal{R}_2 > 1$, though \mathcal{E}_1 changes as θ_S and θ_I vary. In contrast, Figure 5.2 illustrates that when we set $\theta_S = \theta_I = 0.1$ which results in $\mathcal{R}_1 \doteq 1.2 > 1$, all solution curves converge to the equilibrium $\mathcal{E}_2 \doteq (3.03 \times 10^7, 4.11 \times 10^6, 1.71 \times 10^7, 2.29 \times 10^7, 2.71 \times 10^7, 1.13 \times 10^8)$. As θ_S and θ_I vary, \mathcal{E}_2 also changes but the same type of convergence to \mathcal{E}_2 is numerically observed for all $\mathcal{R}_1 > 1$. These results demonstrate the analytical predictions in Theorem 5.2.4.

Next, we turn to the periodic model (5.27) and numerically demonstrate the threshold dynamics result in Theorem 5.3.1. Figure 5.3 plots the time evolution of two infection curves, I_1 for patch 1 and I_2 for patch 2, when $R_0 < 1$. We clearly observe that both curves approaches the disease-free equilibrium \mathcal{E}_0 (where $I_1 = I_2 = 0$) over time. Though not shown here, the same pattern is observed when we vary the initial conditions for I_1 and I_2 , an evidence for the global asymptotic stability of \mathcal{E}_0 when $R_0 < 1$. Figure 5.4, on the other hand, illustrates the case with $R_0 > 1$. We observe that each infection curve converges to a periodic solution with a period $\omega = 12$ months, highlighting the persistence of the infection when $R_0 > 1$. Particularly, we note that the infection curve I_2 stays at a much higher level and exhibits a much stronger oscillation than those with the curve I_1 , showing a higher disease prevalence and risk associated with patch 2 due to the animal migration. This result indicates that in a (simple) population system of two patches where animals migrate from patch 1 to patch 2, with otherwise identical characteristics between the two patches, more prevention and intervention efforts should be devoted to patch 2 in order to control brucellosis outbreaks. Furthermore, such disease control strategies should take into account the seasonal fluctuations of brucellosis so

as to make best use of available resources.

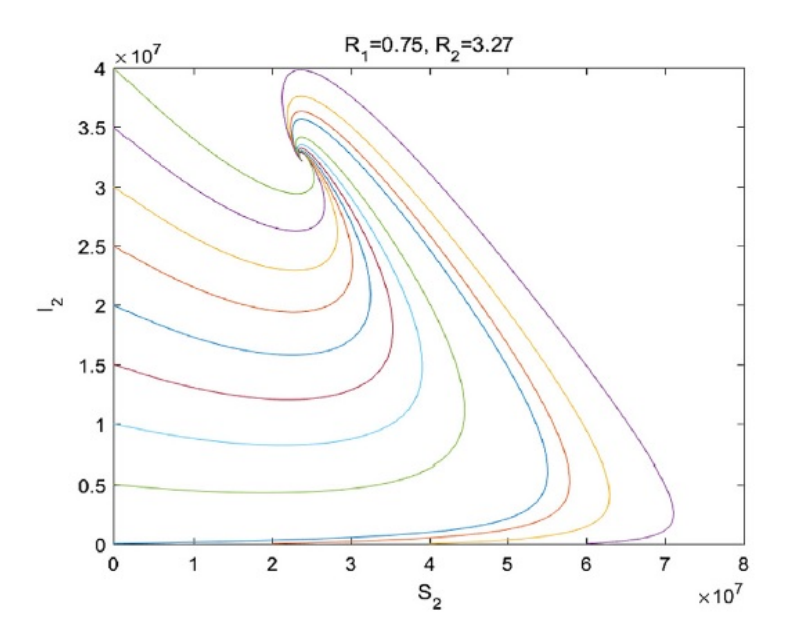


Figure 5.1: Phase portrait illustrating the global stability of \mathcal{E}_1 for system (5.1) in the S_2 - I_2 plane with $\mathcal{R}_1 < 1$, $\mathcal{R}_2 > 1$. Each curve in the plot corresponds to a different initial condition, and all these curves converge to the equilibrium \mathcal{E}_1 (where $S_2 \doteq 2.39 \times 10^7$, $I_2 \doteq 3.22 \times 10^7$) over time.

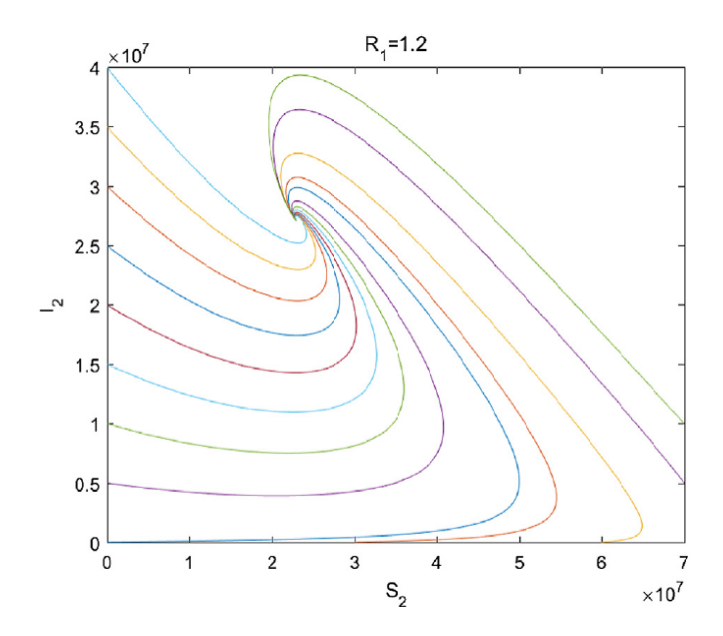


Figure 5.2: Phase portrait illustrating the global stability of \mathcal{E}_2 for system (5.1) in the S_2 - I_2 plane with $\mathcal{R}_1 > 1$. Each curve in the plot corresponds to a different initial condition, and all these curves converge to the equilibrium \mathcal{E}_2 (where $S_2 \doteq 2.29 \times 10^7$, $I_2 \doteq 2.71 \times 10^7$) over time

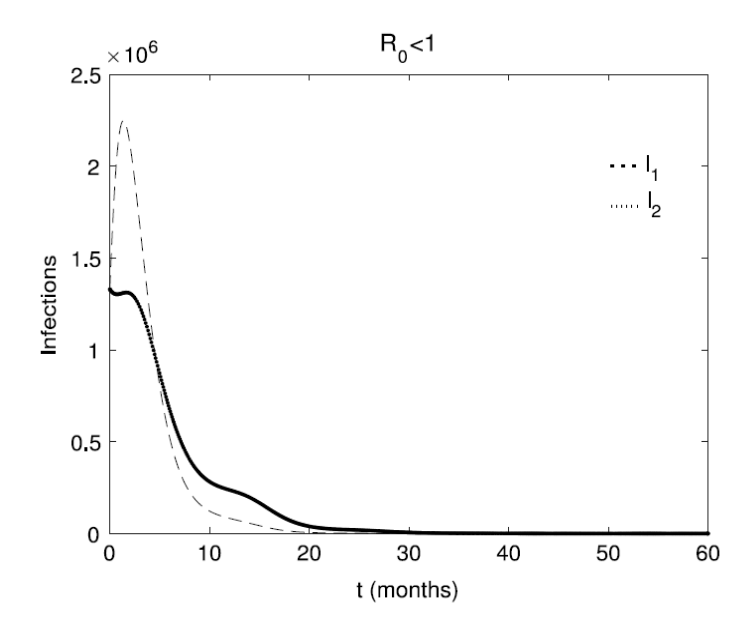


Figure 5.3: The infection curves for the two patches associated with system (5.27) when $R_0 < 1$. Both curves converge to the disease-free equilibrium \mathcal{E}_0 over time.

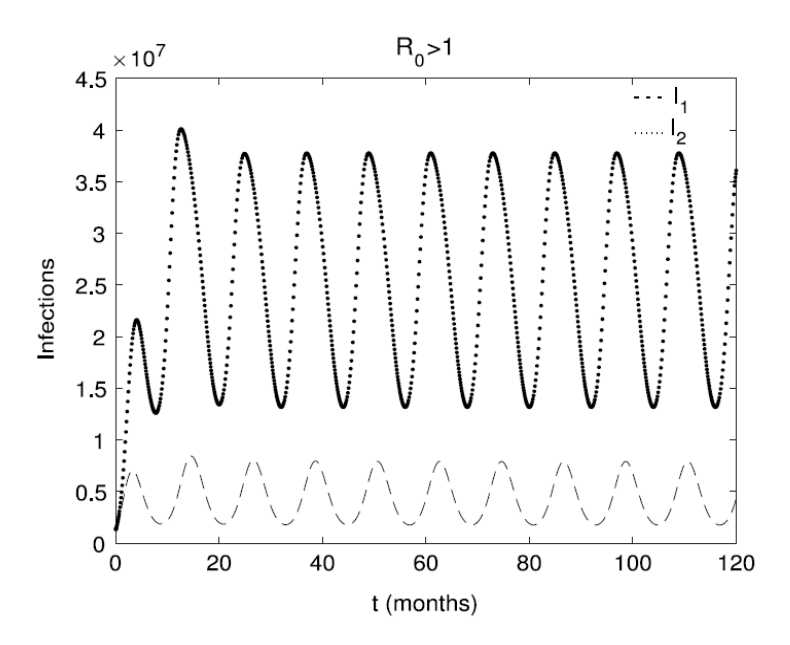


Figure 5.4: The infection curves for the two patches associated with system (5.27) when $R_0 > 1$. Each curve converges to a periodic oscillation with a period $\omega = 12$ months.

5.5 Conclusion and discussion

We have proposed a new mathematical modeling framework for the dynamics of brucellosis, incorporating multiple transmission pathways and both spatial and temporal heterogeneities. As a demonstration of this framework, we have focused on a two-patch model throughout this chapter. We started our analysis on the two-patch model with fixed coefficients (an autonomous system) where detailed results were obtained, showing the rich dynamics of brucellosis transmission due to the spatial variation. In particular, we have thoroughly characterized the multiple equilibria of the system and their stabilities, using the reproduction numbers associated with the model. In the second part of this study, we extended our model to a time-periodic environment that represents seasonal oscillation. We then calculated the basic reproduction number, R_0 , for this periodic two-patch model and established the threshold result: when $R_0 < 1$, the disease-free equilibrium is globally stable; when $R_0 > 1$, the disease is uniformly persistent.

For our autonomous model, we were able to completely determine its local and global dynamics. Particularly, we applied the geometric approach to prove the global

asymptotic stability of the nontrivial equilibria. For the periodic two-patch model, however, the dynamics are more complex. Although we were able to establish the uniform persistence result, we have not resolved the stabilities of the nontrivial periodic orbits when $R_0 > 1$ and that remains an interesting topic for our future research. Nevertheless, our current study demonstrates that the incorporation of spatial and temporal variations leads to rich and complex dynamics that are distinct from those observed from prior models based on homogeneous environments. Our results also indicate that the prevention and intervention strategies need to take into account the spatial and temporal heterogeneities in order to effectively control brucellosis while optimize the use of available resources.

Our current study on the spatial modeling of brucellosis is based on the patch structure, and we plan to extend this work to a more general setting with an arbitrary number of patches. We expect that many results presented in this chapter can be similarly established for the general spatial setting. On the other hand, a different approach to model spatial heterogeneity is to utilize partial differential equations (PDEs), for example, by adding diffusion terms to an ODE model so as to represent the movement and dispersal of the animals and the pathogen, and by adding convection terms to represent the migration of animals. Seasonal variation can be similarly incorporated by considering periodic model parameters, resulting in a periodic PDE system. Such a periodic PDE model can be possibly analyzed using techniques recently proposed by Zhao and co-workers [83, 84, 85]. In particular, the basic reproduction number can still be defined which can be used to investigate the threshold properties of the model. It will be very interesting to compare the threshold dynamics from these two modeling approaches: one based on multi-patch periodic ODEs and the other based on Periodic PDEs.

Chapter 6

On the role of short-term animal movements on the persistence of brucellosis

6.1 Introduction

Brucellosis, a highly contagious zoonotic disease, remains a significant public health threat worldwide. It is estimated that more than 500,000 new cases of the disease are reported annually [42], with incidence as high as 200 cases per 100,000 of the population in most endemic countries [43]. Majority of brucellosis infections occur in: the sub-Sahara Africa in countries such as Ethiopia, Chad, Tanzania, Nigeria, Uganda, Kenya, Zimbabwe and Somalia due to high level of pastoralism; the Middle East, Spain, Latin America and Asia-in particular South-east Asia where factors such as pastoral farming practices, beliefs and lack of bio-security have been attributed to persistence of the disease [44]. Since human transmission of brucellosis is considered to be negligible [3], measures to effectively control brucellosis in humans ultimately require a thorough control of the disease among domestic cattle, camels, goats and sheep.

Transmission and control of brucellosis in both human and animal population remains a complex phenomena that possibly involve the type of farming practised in the area, economic, geographic and environmental structures, as well as the intrinsic disease biology and ecology. In particular, animal movement plays crucial role on transmission and control of the disease. For example, in communal farming zones animal movements are highly uncontrolled compared to private farming. Prior studies have demonstrated that, on a daily basis, a single cattle herd in a communal farming zone has the potential to mix with at least five heterogeneous herds at both the communal grazing and watering points. Since livestock management varies from one farmer to another, it is evident that understanding the volume of these movements and the risks associated with them is fundamental in elucidating the epidemiology and control of animal diseases.

Mathematical models have proved to be important tools that can aid our understanding as well as provide solutions to phenomena which are complex to measure in the field. Recently a number of mathematical models have been proposed to explore brucellosis transmission and control, see for instance [31, 32, 38, 66, 86, 87, 67]. For example, Dobson and Meagherin [86] used nonlinear ordinary differential equations to describe brucellosis transmission among the bison population in the Yellowstone National Park (YNP). Abatih et al. [38] mathematically analyzed the brucellosis model proposed in [86]. Lolika et al. [31] applied a non-autonomous model to discuss the effects of optimal vaccination and environmental decontamination on long-term brucellosis dynamics among cattle in periodic environments. Yang et al. [66] developed a two-patch model with risk heterogeneity in which animals immigrated between two different risk environments. Their work utilized a Eulerian approach for mobility. However, the Eulerian approach has some limitations, for instance it neither incorporates the concept of residence times nor the effective population size. Here the term residence times refers to the average proportion of daily time an animal spends in a given patch. Therefore to gain a better and more comprehensive understanding of effects of animals movements on brucellosis dynamics, a model should incorporate a Lagrangian approach- which is capable of accounting for the effects of residence times and the effective population size per patch.

In this chapter, we consider a dynamical model to describe the role of shortterm animal movements on the persistence of brucellosis. The proposed two-patch model incorporates all the relevant biological and ecological factors as well as shortterm animal movements which are modeled using the Lagrangian approach. For the purpose of distinction between the hosts, we assumed that patch 1 is a high risk environment, that is, brucellosis control measures in this patch are poorly managed. The reverse is assumed for patch 2. Thus, disease transmission in patch 1 is assumed to be higher relative to patch 2. Further, disease transmission is assumed to occur through direct contact and vertical transmission. In addition, since vaccines are often unavailable or expensive to farmers in communal farming zones we assumed that a more sensible approach to control the spread of the disease is culling of infected animals.

6.2 Modeling framework

We developed a mathematical model to study the transmission and control of brucellosis within an environment defined by two-patches of heterogeneous risk. Our model is a modification of the one developed in [38]. Precisely, the model in [38] is a single-patch framework.

Let $N_i(t)$ represent the total population of animals in patch i at time t, i = 1, 2. We assume that animals of Patch i spend $p_{ij} \in [0, 1]$ time in Patch j, with $\sum_{j=1}^{2} p_{ij} = 1$, for each i. Thus, animals of Patch 1 spends, on the average, the proportion p_{11} of their time in residency in patch 1 and the proportion p_{12} of their time in patch 2 such that $p_{11} + p_{12} = 1$.

Similarly, animals of patch 2 spend the proportion p_{22} of their time in patch 2 and $p_{21} = 1 - p_{22}$ in patch 1. Therefore, at time t, the effective population in patch 1 is $p_{11}N_1 + p_{21}N_2$ while the effective population of patch 2, at time t is $p_{12}N_1 + p_{22}N_2$. Susceptible animals of patch 1 (S_1) could be infected contagiously, in patch 1 (if currently in patch 1, that is., $p_{11}S_1$) or in patch 2 (if currently in patch 2, that is., $p_{12}S_1$). It follows from the above discussion that the effective proportion of infectious individual in patch 1 is

$$\frac{p_{11}I_1 + p_{21}I_2}{p_{11}N_1 + p_{21}N_2}.$$

Consequently the effective proportion of infectious individual in patch 2 is

$$\frac{p_{12}I_1 + p_{22}I_2}{p_{12}N_1 + p_{22}N_2}.$$

The following system of ordinary differential equations (ODES) account for the brucellosis dynamics in two patches:

$$\begin{cases}
\frac{dS_{i}}{dt} = \mu_{i}(N_{i} - e_{i}I_{i}) - \sum_{j=1}^{2} \beta_{j}p_{ij}S_{i} \frac{\sum_{k=1}^{2} p_{kj}I_{k}}{\sum_{k=1}^{2} p_{kj}N_{k}} - \mu_{i}S_{i} + \delta_{i}R_{i}, \\
\frac{dI_{i}}{dt} = \mu_{i}e_{i}I_{i} + \sum_{j=1}^{2} \beta_{j}p_{ij}S_{i} \frac{\sum_{k=1}^{2} p_{kj}I_{k}}{\sum_{k=1}^{2} p_{kj}N_{k}} - (\mu_{i} + \alpha_{i})I_{i}, \\
\frac{dR_{i}}{dt} = \alpha_{i}I_{i} - (\mu_{i} + \delta_{i})R_{i}.
\end{cases} (6.1)$$

Where the variables $S_i(t)$, $I_i(t)$ and $R_i(t)$ represents the susceptible, infectious and recovered population, μ_i is recruitment rate of animals and it is assumed to be equal to natural death rate of animals, thus, μ_i^{-1} represents the animal's commercial lifespan, e_i ($0 \le e_i \le 1$) denotes a proportion of new recruits that are infected with brucellosis and the complementary proportion $(1 - e_i)$ represents those that are susceptible to infection, β_i denotes the disease transmission, α_i is the recovery rate, δ_i denotes immunity waning rate. Disease related mortality is considered negligible. Thus, the total population is constant and is given by $N_i(t) = S_i(t) + I_i(t) + R_i(t)$.

Table 6.1: Parameters and values

Symbol Definition			Value Source					
$\overline{p_{ij}}$	Proportion of time that animals of patch i spend in patch j unit-less varies							
β_1	Susceptibility to brucellosis invasion in patch 1	$year^{-1}$	1.63	[38]				
β_2	Susceptibility to brucellosis invasion in patch 2	$year^{-1}$	0.75	[38]				
e_1	Proportion of vertical transmission in patch 1	unit-less	0.9	[38]				
e_2	Proportion of vertical transmission in patch 2	unit-less	0.4	[38]				
μ_i	Recruitment rate in patch i $(i = 1, 2)$	$year^{-1}$	0.04	[38]				
δ_i	Rate of loss of resistance in patch i $(i = 1, 2)$	$year^{-1}$	0.2	[38]				
α_i	Recovery rate in patch i $(i = 1, 2)$	$year^{-1}$	0.5	[38]				
$S_i(0)$	Initial number of susceptible in patch i $(i = 1, 2)$	animals	4050	[38]				
$I_i(0)$	Initial infected animals in patch i $(i = 1, 2)$	animals	450	[38]				
$R_i(0)$	Initial recovered animals in patch i $(i = 1, 2)$	animals	0	[38]				

It can easily be verified that the domain of biological interest

$$\Omega = \left\{ (S_i, I_i, R_i) \in \mathbb{R}_+^6 | S_i + I_i + R_i \le N_i \right\}$$
(6.2)

is positively invariant and attracting with respect to model (6.1).

6.3 Disease dynamics for a single patch

If only a single patch, that is, i = 1, is considered then system (6.1) reduces to

$$\begin{cases}
\frac{dS_1}{dt} = \mu_1(N_1 - e_1I_1) - \frac{\beta_1I_1S_1}{N_1} - \mu_1S_1 + \delta_1R_1, \\
\frac{dI_1}{dt} = \frac{\beta_1I_1S_1}{N_1} + e_1\mu_1I_1 - (\mu_1 + \alpha_1)I_1, \\
\frac{dR_1}{dt} = \alpha_1I_1 - (\mu_1 + \delta_1)R_1.
\end{cases} (6.3)$$

System (6.3) is isomorphic to the model proposed by Dobson and Meagherin [86] and analysed by Abatih et al. [38]. As highlighted in [38], model (6.1) is well defined supporting a sharp threshold property, namely, the disease dies out if the basic reproduction number \mathcal{R}_{01} is less than unity, persisting whenever $\mathcal{R}_{01} > 1$ where $\mathcal{R}_{01} = \frac{(\beta_1 + e_1 \mu_1)}{(\alpha_1 + \mu_1)}$.

6.4 The reproduction number

The disease-free equilibrium \mathcal{E}^0 of system (6.1) is

$$\mathcal{E}^0: (S_1^0, S_2^0, I_1^0, I_2^0, R_1^0, R_2^0) = (N_1, N_2, 0, 0, 0, 0).$$

The basic reproduction number, denoted by \mathcal{R}_0 is an integral quantity in epidemiological model. It accounts for the average number of secondary infections generated by a single infectious animal introduced in a fully susceptible population during its average infectious period [50]. We utilized the next generation matrix approach [50] to determine \mathcal{R}_0 . We begin with those equations of model (6.1) that account for the production of new infections. We term this system (6.4) the infected subsystem:

$$\begin{cases}
\frac{dI_1}{dt} = \mu_1 e_1 I_1 + \beta_1 p_{11} S_1 \frac{p_{11} I_1 + p_{21} I_2}{p_{11} N_1 + p_{21} N_2} + \beta_2 p_{12} S_1 \frac{p_{12} I_1 + p_{22} I_2}{p_{12} N_1 + p_{22} N_2} - (\mu_1 + \alpha_1) I_1, \\
\frac{dI_2}{dt} = \mu_2 e_2 I_2 + \beta_1 p_{21} S_2 \frac{p_{11} I_1 + p_{21} I_2}{p_{11} N_1 + p_{21} N_2} + \beta_2 p_{22} S_2 \frac{p_{12} I_1 + p_{22} I_2}{p_{12} N_1 + p_{22} N_2} - (\mu_2 + \alpha_2) I_2.
\end{cases} (6.4)$$

Using the next-generation matrix notations in [50], the non-negative matrix \mathcal{F} that represents the generation of new infection and the non-singular matrix \mathcal{V} that denotes the disease transfer among compartments, are respectively given by

$$\mathcal{F} = \begin{bmatrix} e_1 \mu_1 + \frac{p_{11}^2 \beta_1 N_1}{p_{11} N_1 + p_{21} N_2} + \frac{p_{12}^2 \beta_2 N_1}{p_{12} N_1 + p_{22} N_2} & \frac{p_{11} p_{21} \beta_1 N_1}{p_{11} N_1 + p_{21} N_2} + \frac{p_{12} p_{22} \beta_2 N_1}{p_{12} N_1 + p_{22} N_2} \\ \frac{p_{11} p_{21} \beta_1 N_2}{p_{11} N_1 + p_{21} N_2} + \frac{p_{12} p_{22} \beta_2 N_2}{p_{12} N_1 + p_{22} N_2} & e_2 \mu_2 + \frac{p_{21}^2 \beta_1 N_2}{p_{11} N_1 + p_{21} N_2} + \frac{p_{22}^2 \beta_2 N_2}{p_{12} N_1 + p_{22} N_2} \end{bmatrix}$$

$$= \begin{bmatrix} m_{11} & m_{12} \\ m_{21} & m_{22} \end{bmatrix},$$
and,
$$\mathcal{V} = \begin{bmatrix} (\mu_1 + \alpha_1) & 0 \\ 0 & (\mu_2 + \alpha_2) \end{bmatrix} = \begin{bmatrix} \hbar_1 & 0 \\ 0 & \hbar_2 \end{bmatrix}.$$
(6.5)

Then \mathcal{R}_0 , which corresponds to the dominant eigenvalue of the matrix \mathcal{FV}^{-1} , is given by

$$\mathcal{R}_0 = \rho(\mathcal{F}\mathcal{V}^{-1}) = \frac{m_{11}\hbar_2 + m_{22}\hbar_1 + \sqrt{(m_{11}\hbar_2 - m_{22}\hbar_1)^2 + 4m_{12}m_{21}\hbar_1\hbar_2}}{2\hbar_1\hbar_2}$$

after some algebraic manipulations, we have the following results

$$\mathcal{R}_{0} = \frac{1}{2} \left[\left(\frac{m_{11}}{\hbar_{1}} + \frac{m_{22}}{\hbar_{2}} \right) + \sqrt{\left(\frac{m_{11}}{\hbar_{1}} + \frac{m_{22}}{\hbar_{2}} \right)^{2} + \frac{4m_{12}m_{21}}{\hbar_{1}\hbar_{2}}} \right], \quad (6.6)$$

with

$$m_{11} = e_{1}\mu_{1} + \frac{p_{11}^{2}\beta_{1}N_{1}}{p_{11}N_{1} + p_{21}N_{2}} + \frac{p_{12}^{2}\beta_{2}N_{1}}{p_{12}N_{1} + p_{22}N_{2}},$$

$$m_{12} = \frac{p_{11}p_{21}\beta_{1}N_{1}}{p_{11}N_{1} + p_{21}N_{2}} + \frac{p_{12}p_{22}\beta_{2}N_{1}}{p_{12}N_{1} + p_{22}N_{2}},$$

$$m_{21} = \frac{p_{11}p_{21}\beta_{1}N_{2}}{p_{11}N_{1} + p_{21}N_{2}} + \frac{p_{12}p_{22}\beta_{2}N_{2}}{p_{12}N_{1} + p_{22}N_{2}},$$

$$m_{22} = e_{2}\mu_{2} + \frac{p_{21}^{2}\beta_{1}N_{2}}{p_{11}N_{1} + p_{21}N_{2}} + \frac{p_{22}^{2}\beta_{2}N_{2}}{p_{12}N_{1} + p_{22}N_{2}},$$

$$\hbar_{1} = (\mu_{1} + \alpha_{1}), \quad \hbar_{2} = (\mu_{2} + \alpha_{2}).$$

We can write (6.6) as follows

$$\mathcal{R}_0 = \frac{1}{2} \left[\left(\mathcal{R}_{01} + \mathcal{R}_{02} \right) + \sqrt{\left(\mathcal{R}_{01} - \mathcal{R}_{02} \right)^2 + \frac{4m_{12}m_{21}}{\hbar_1\hbar_2}} \ \right]$$

where \mathcal{R}_{0i} (i=1,2) represents the disease risks for patches 1 and 2 in the absence of animal mobility. From (6.6) we can observe that the basic reproduction number is influenced by short-term animal dispersal.

To investigate the effects of short-term animal dispersal on the generation of new infections, we compute the values of the basic reproduction number using a residence-time matrix in Table 6.2. More precisely, the residence-time matrix configuration incorporates the coupling intensity and mobility patterns. For instance, weak coupling implies that most animals stay in their own patch while strong coupling implies that certain proportions of animals move to the other patch. Mobility patterns represents the symmetry of animal movement between the two patches. For example, symmetric mobility represents a scenario when an equal ratio of animals move from patch 1 to patch 2 and vice-versa. However, if the ratio of animals that move between the two patches is not equal then the mobility pattern is asymmetric. Note that the total population of animals in the two patches is assumed to be the same.

Table 6.2: Association between the basic reproduction number and the residencetime matrix

	Description	\mathcal{R}_0
1	Weak symmetric coupling $p_{11} = 0.99$, $p_{12} = 0.01$, $p_{21} = 0.01$, $p_{22} = 0.99$	3.03
2	Strong symmetric coupling $p_{11} = 0.7$, $p_{12} = 0.3$, $p_{21} = 0.3$, $p_{22} = 0.7$	2.31
3	Weak asymmetric coupling $p_{11} = 0.9$, $p_{12} = 0.1$, $p_{21} = 0.001$, $p_{22} = 0.999$	2.80
4	Strong asymmetric coupling $p_{11} = 0.7$, $p_{12} = 0.3$, $p_{21} = 0.001$, $p_{22} = 0.999$	2.36

Results in Table 6.2 demonstrate that the basic reproduction number will be always high when coupling intensity is weak, that is, when most animal stay in their patch. Further, the highest value of the basic reproduction number occurs when the mobility pattern is symmetric. Using parameters values in Table 6.1, we calculated the reproduction numbers for patch 1 and 2 in the absence of animal dispersal and we obtained $\mathcal{R}_{01} = 1.4$ and $\mathcal{R}_{02} = 0.05$. We can observe that, based on our assumption that patch 1 is high risk, the highest reproduction number came from this patch. In addition, we can observe that whenever there is animal mobility the disease transmission risk increases globally than locally, for instance, in the absence of animal mobility we expect brucellosis to die off in patch 2. It is worth noting that results in Table 6.2 shows that when animal mobility increases the basic reproduction number decreases, however, for all the cases demonstrated in Table 6.2 it will never drop below 1. Hence under our assumption we can conclude that effective brucellosis control will always be difficult to attain whenever there is animal

mobility.

6.5 Disease invasion and persistence

From the work in [50], we know that the DFE is locally asymptotically stable when $\mathcal{R}_0 < 1$, and unstable when $\mathcal{R}_0 > 1$. Indeed, we can establish a stronger result regarding the global dynamics of the DFE.

Theorem 6.5.1 If $\mathcal{R}_0 \leq 1$, the DFE is globally asymptotically stable in Ω . If $\mathcal{R}_0 > 1$, the system is uniformly persistent.

Proof 13 Let $\mathcal{Y}(t) = (I_1, I_2)$. Since

$$\begin{cases}
\frac{dI_1}{dt} = \mu_1 e_1 I_1 + \beta_1 p_{11} S_1 \frac{p_{11} I_1 + p_{21} I_2}{p_{11} N_1 + p_{21} N_2} + \beta_2 p_{12} S_1 \frac{p_{12} I_1 + p_{22} I_2}{p_{12} N_1 + p_{22} N_2} - (\mu_1 + \alpha_1) I_1, \\
\frac{dI_2}{dt} = \mu_2 e_2 I_2 + \beta_1 p_{21} S_2 \frac{p_{11} I_1 + p_{21} I_2}{p_{11} N_1 + p_{21} N_2} + \beta_2 p_{22} S_2 \frac{p_{12} I_1 + p_{22} I_2}{p_{12} N_1 + p_{22} N_2} - (\mu_2 + \alpha_2) I_2,
\end{cases} (6.7)$$

it follows that

$$\dot{\mathcal{U}}(t) \leq (\mathcal{F} - \mathcal{V})\mathcal{Y},$$

where \mathcal{F} and \mathcal{V} are defined in (6.5). Motivated by [78], we define a Lyapunov function as follows

$$\mathcal{U} = w^T \mathcal{V}^{-1} \mathcal{Y}.$$

Differentiating \mathcal{U} along solutions of (6.1), we have

$$\dot{\mathcal{U}}(t) = w^T \mathcal{V}^{-1} \dot{\mathcal{Y}}
\leq w^T V^{-1} (\mathcal{F} - \mathcal{V}) \mathcal{Y}
= (\mathcal{R}_0 - 1) w^T \mathcal{Y} \leq 0, \quad \text{if } \mathcal{R}_0 \leq 1.$$

It can be easily verified that the largest invariant subset of Ω where $\dot{\mathcal{U}}=0$ is the singleton $\{\mathcal{E}^0\}$. Therefore, by LaSalle's invariance principle [46], \mathcal{E}^0 is globally asymptotically stable in Ω when $\mathcal{R}_0 \leq 1$.

If $\mathcal{R}_0 > 1$, then by continuity, $\dot{\mathcal{U}} > 0$ in a neighbourhood of \mathcal{E}^0 in $\mathring{\Omega}$. Solutions in $\mathring{\Omega}$ sufficiently close to \mathcal{E}^0 move away from the DFE, implying that the DFE is unstable. In what follows we demonstrate that if $\mathcal{R}_0 > 1$, then the disease persists and a unique endemic equilibrium point exists.

6.6 Uniform persistence

System (6.1) is said to be uniformly persistent in the interior $\mathring{\Omega}$ if there exists a constant $\eta_0 > 0$ such that

$$\liminf_{t \to \infty} S_i(t) \ge \eta_0, \qquad \liminf_{t \to \infty} I_i(t) \ge \eta_0, \qquad \liminf_{t \to \infty} R_i(t) \ge \eta_0$$

provided that $(S_1(0), S_2(0), I_1(0), I_2(0), R_1(0), R_2(0)) \in \mathring{\Omega}$. Biologically, a uniform persistent system indicates that the infection persists for a long period of time. Thus we have the following result.

Theorem 6.6.1 If $\mathcal{R}_0 > 1$, then the DFE is unstable and system (6.1) is uniformly persistent in $\mathring{\Omega}$.

Proof 14 Let $X = \Omega$, $x = (S_1, S_2, I_1, I_2, R_1, R_2)$ and $X_0 = \{x \in X | I_1 + I_2 > 0\}$. Hence, $\partial X_0 = X \setminus X_0 = \{x \in X | I_1 = I_2 = 0\}$. Let ψ_t be semi-flow induced by the solutions of (6.1) and $M_{\partial} = \{x \in \partial X_0 | \psi_t x \in \partial X_0, t \geq 0\}$. By (6.2), we have $\psi_t X_0 \subset X_0$ and ψ_t is bounded in X_0 . Therefore a global attractor for ψ_t exists. The disease- free equilibrium is the unique equilibrium on the manifold ∂X_0 and is globally asymptotically stable on ∂X_0 . Moreover $\cup_{x \in M_{\partial}} \omega(x) = \{\mathcal{E}^0\}$ and no subset of M forms a cycle in ∂X_0 . Finally since the disease- free equilibrium is unstable on X_0 if $\mathcal{R}_0 > 1$, we deduce that System (6.1) is uniformly persistent by using a result from [58] (Theorem 1.3.1 and Remark 1.3.1). This completes the proof of Theorem 6.6.1.

Theorem 6.6.2 If $\mathcal{R}_0 > 1$ System (6.1) has a unique equilibrium \mathcal{E}^* , which is globally asymptotically stable.

Proof 15 We can reduce system (6.1) into four dimensional system by setting $R_i = N_i - S_i - I_i$ to get

$$\begin{cases}
\frac{dS_i}{dt} = \mu_i (N_i - e_i I_i) - \sum_{j=1}^2 \beta_j p_{ij} S_i \frac{\sum_{k=1}^2 p_{kj} I_k}{\sum_{k=1}^2 p_{kj} N_k} - \mu_i S_i + \delta_i (N_i - S_i - I_i), \\
\frac{dI_i}{dt} = \mu_i e_i I_i + \sum_{j=1}^2 \beta_j p_{ij} S_i \frac{\sum_{k=1}^2 p_{kj} I_k}{\sum_{k=1}^2 p_{kj} N_k} - (\mu_i + \alpha_i) I_i,
\end{cases}$$
(6.8)

We will use a result by Hethcote and Thieme in [88] to prove the uniqueness of the endemic equilibrium. An endemic equilibrium (S_i^*, I_i^*) satisfies:

$$\begin{cases}
\mu_{i}(N_{i} - e_{i}I_{i}^{*}) - \sum_{j=1}^{2} \beta_{j}p_{ij}S_{i}^{*} \frac{\sum_{k=1}^{2} p_{kj}I_{k}^{*}}{\sum_{k=1}^{2} p_{kj}N_{k}} - \mu_{i}S_{i}^{*} + \delta_{i}(N_{i} - S_{i}^{*} - I_{i}^{*}) &= 0, \\
\mu_{i}e_{i}I_{i}^{*} + \sum_{j=1}^{2} \beta_{j}p_{ij}S_{i}^{*} \frac{\sum_{k=1}^{2} p_{kj}I_{k}^{*}}{\sum_{k=1}^{2} p_{kj}N_{k}} - (\mu_{i} + \alpha_{i})I_{i}^{*} &= 0, \\
(6.9)
\end{cases}$$

The first equation of (6.9) gives

$$\begin{cases} S_i^* = \frac{\mu_i(N_i - e_i I_i^*) + \delta_i(N_i - I_i^*)}{\sum_{j=1}^2 \beta_j p_{ij} \frac{\sum_{k=1}^2 p_{kj} I_k^*}{\sum_{k=1}^2 p_{kj} N_k} + (\mu_i + \delta_i)} \end{cases}$$
(6.10)

Hence from the last equation of (6.9) we deduce that

$$\begin{cases}
I_i^* = \frac{\mu_i(N_i - e_i I_i^*) + \delta_i(N_i - I_i^*)}{\sum_{j=1}^2 \beta_j p_{ij} \sum_{k=1}^2 p_{kj} I_k^*} \times \frac{\sum_{j=1}^2 \beta_j p_{ij} \frac{\sum_{k=1}^2 p_{kj} I_k^*}{\sum_{k=1}^2 p_{kj} N_k}}{\mu_i (1 - e_i) + \alpha_i}
\end{cases} (6.11)$$

Let

$$H(x) = \begin{bmatrix} \frac{\mu_1(N_1 - e_1I_1^*) + \delta_1(N_1 - I_1^*)}{\sum_{j=1}^2 \beta_j p_{1j} \frac{\sum_{k=1}^2 p_{kj}I_k^*}{\sum_{k=1}^2 p_{kj}N_k} + (\mu_1 + \delta_1)} \times \frac{\sum_{j=1}^2 \beta_j p_{1j} \frac{\sum_{k=1}^2 p_{kj}I_k^*}{\sum_{k=1}^2 p_{kj}N_k}}{\mu_1(1 - e_1) + \alpha_1} \\ \frac{\mu_2(N_2 - e_2I_2^*) + \delta_2(N_2 - I_2^*)}{\sum_{j=1}^2 \beta_j p_{2j} \frac{\sum_{k=1}^2 p_{kj}I_k^*}{\sum_{k=1}^2 p_{kj}N_k}} \times \frac{\sum_{j=1}^2 \beta_j p_{2j} \frac{\sum_{k=1}^2 p_{kj}I_k^*}{\sum_{k=1}^2 p_{kj}N_k}}{\mu_2(1 - e_2) + \alpha_2} \end{bmatrix}$$

where $x = (I_1^*, I_2^*)$. The function H(x) is continuous, bounded, differentiable and $H(0_{\mathbb{R}^2}) = 0_{\mathbb{R}^2}$. The function H is monotone if the corresponding Jacobian matrix is Metzler, that is all off-diagonal entries are nonnegative. We have the derivative of H(x)

$$\dot{H}(x) = \begin{bmatrix} \mathcal{J}_1(x) & \mathcal{J}_2(x) \\ \mathcal{J}_3(x) & \mathcal{J}_4(x) \end{bmatrix}$$

Where

$$\mathcal{J}_{1}(x) = \frac{1}{(\mu_{1}(1-e_{1})+\alpha_{1})\left(\sum_{j=1}^{2}\beta_{j}p_{1j}\frac{\sum_{k=1}^{2}p_{kj}I_{k}^{*}}{\sum_{k=1}^{2}p_{kj}N_{k}}+(\mu_{1}+\delta_{1})\right)}\left[(\mu_{1}(N_{1}-e_{1}I_{1}^{*})+\delta_{1}(N_{1}-I_{1}^{*}))\left(\frac{(p_{11})^{2}\beta_{1}}{\sum_{k=1}^{2}p_{k1}N_{k}}+\frac{(p_{12})^{2}\beta_{2}}{\sum_{k=1}^{2}p_{k2}N_{k}}\right)\left(1-\sum_{j=1}^{2}\beta_{j}p_{1j}\frac{\sum_{k=1}^{2}p_{kj}I_{k}^{*}}{\sum_{k=1}^{2}p_{kj}N_{k}}\right)-(\delta_{1}+e_{1}\mu_{1})\sum_{j=1}^{2}\beta_{j}p_{1j}\frac{\sum_{k=1}^{2}p_{kj}I_{k}^{*}}{\sum_{k=1}^{2}p_{kj}N_{k}}\right] (6.12)$$

$$\mathcal{J}_{2}(x) = \frac{(\mu_{1}(N_{1} - e_{1}I_{1}^{*}) + \delta_{1}(N_{1} - I_{1}^{*})) \left(\frac{p_{11}p_{21}\beta_{1}}{\sum_{k=1}^{2}p_{k1}N_{k}} + \frac{p_{12}p_{22}\beta_{2}}{\sum_{k=1}^{2}p_{k2}N_{k}}\right)}{(\mu_{1}(1 - e_{1}) + \alpha_{1}) \left(\sum_{j=1}^{2}\beta_{j}p_{1j}\frac{\sum_{k=1}^{2}p_{kj}I_{k}^{*}}{\sum_{k=1}^{2}p_{kj}N_{k}} + (\mu_{1} + \delta_{1})\right)} \left[1 - \frac{\sum_{j=1}^{2}\beta_{j}p_{1j}\frac{\sum_{k=1}^{2}p_{kj}I_{k}^{*}}{\sum_{k=1}^{2}p_{kj}N_{k}}}{\left(\sum_{j=1}^{2}\beta_{j}p_{1j}\frac{\sum_{k=1}^{2}p_{kj}I_{k}^{*}}{\sum_{k=1}^{2}p_{kj}N_{k}} + (\mu_{1} + \delta_{1})\right)}\right]$$
(6.13)

$$\mathcal{J}_{3}(x) = \frac{(\mu_{2}(N_{2} - e_{2}I_{2}^{*}) + \delta_{2}(N_{2} - I_{2}^{*})) \left(\frac{p_{11}p_{21}\beta_{1}}{\sum_{k=1}^{2} p_{k1}N_{k}} + \frac{p_{12}p_{22}\beta_{2}}{\sum_{k=1}^{2} p_{k2}N_{k}}\right)}{(\mu_{2}(1 - e_{2}) + \alpha_{2}) \left(\sum_{j=1}^{2} \beta_{j}p_{2j}\frac{\sum_{k=1}^{2} p_{kj}I_{k}^{*}}{\sum_{k=1}^{2} p_{kj}N_{k}} + (\mu_{2} + \delta_{2})\right)} \left[1 - \frac{\sum_{j=1}^{2} \beta_{j}p_{2j}\frac{\sum_{k=1}^{2} p_{kj}I_{k}^{*}}{\sum_{k=1}^{2} p_{kj}N_{k}}}{\left(\sum_{j=1}^{2} \beta_{j}p_{2j}\frac{\sum_{k=1}^{2} p_{kj}I_{k}^{*}}{\sum_{k=1}^{2} p_{kj}N_{k}} + (\mu_{2} + \delta_{2})\right)}\right]$$

$$(6.14)$$

$$\mathcal{J}_{4}(x) = \frac{1}{(\mu_{2}(1 - e_{2}) + \alpha_{2}) \left(\sum_{j=1}^{2} \beta_{j} p_{2j} \frac{\sum_{k=1}^{2} p_{kj} I_{k}^{*}}{\sum_{k=1}^{2} p_{kj} N_{k}} + (\mu_{2} + \delta_{2})\right)} \left[(\mu_{2}(N_{2} - e_{2}I_{2}^{*}) + \delta_{2}(N_{2} - I_{2}^{*})) \left(\frac{(p_{21})^{2} \beta_{1}}{\sum_{k=1}^{2} p_{k1} N_{k}} + \frac{(p_{22})^{2} \beta_{2}}{\sum_{k=1}^{2} p_{k2} N_{k}}\right) \left(1 - \sum_{j=1}^{2} \beta_{j} p_{2j} \frac{\sum_{k=1}^{2} p_{kj} I_{k}^{*}}{\sum_{k=1}^{2} p_{kj} N_{k}}\right) - (\delta_{2} + e_{2}\mu_{2}) \sum_{j=1}^{2} \beta_{j} p_{2j} \frac{\sum_{k=1}^{2} p_{kj} I_{k}^{*}}{\sum_{k=1}^{2} p_{kj} N_{k}}\right] (6.15)$$

Since, $\mathcal{J}_2(x) \geq 0$ and $\mathcal{J}_3(x) \geq 0$, hence all off-diagonal entries of the Jacobian matrix are nonnegative and so, the function H(x) is monotone. Therefore by monoticity of a matrix H(x) implies that model (6.1) has a unique positive fixed point if and only if $\mathcal{R}_0 > 1$. This completes the first part of the proof for Theorem 6.6.2 and due to less traceability of our model we will utilizing numerical simulations to demonstrate the global stability of the endemic equilibrium (see Figure 6.1).

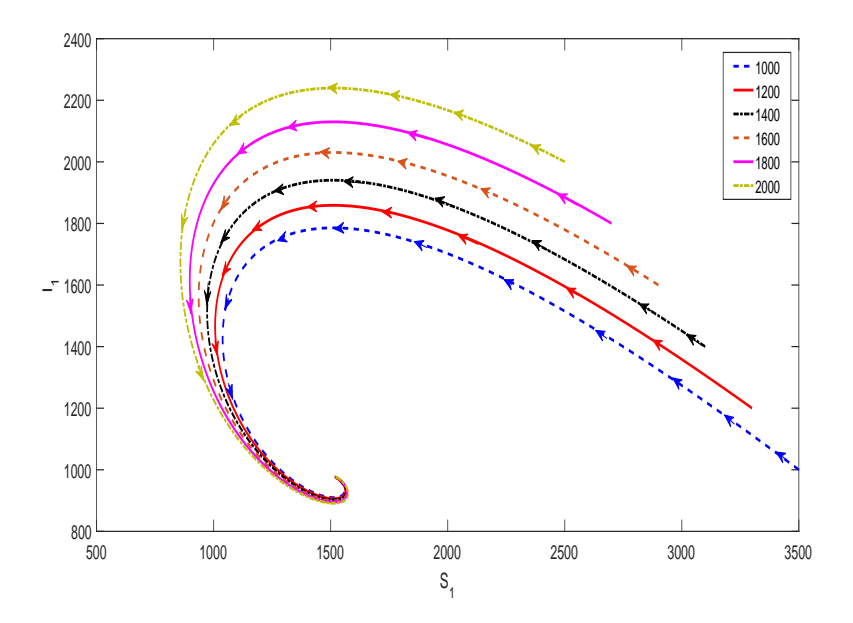


Figure 6.1: Phase portrait illustrating the global stability of \mathcal{E}^* for system (6.1) in the S_1 - I_1 plane with $\mathcal{R}_0 = 2.84$ (we set $\beta_1 = \beta_2 = 1.5$). Each curve in the plot corresponds to a different initial condition, and all these curves converge to the equilibrium \mathcal{E}^* (where $S_1 = S_2 \doteq 1500$, $I_1 = I_2 \doteq 1000$) over time

6.7 Optimal culling

Vaccination and culling of infected animals are the only feasible ways to control brucellosis transmission. Vaccinating animals prevents susceptibility to the disease and culling of infectious animals reduces the density of infected animals thereby reducing the contact between susceptible and infected animals. However, in many brucellosis endemic countries farmers cannot afford the cost of vaccines, and this leaves culling as the only disease intervention strategy. In this section, we wish to explore the impact of culling on controlling the spread of the disease. Thus, we will modify model (6.1) to include culling control $u_i(t)$, i = 1, 2. The controls, $u_i(t)$ are represented as functions of time and assigned reasonable upper and lower bounds. The modified model is given by

$$\begin{cases}
\frac{dS_{i}}{dt} = \mu_{i}(N_{i} - e_{i}I_{i}) - \sum_{j=1}^{2} \beta_{j}p_{ij}S_{i} \frac{\sum_{k=1}^{2} p_{kj}I_{k}}{\sum_{k=1}^{2} p_{kj}N_{k}} - \mu_{i}S_{i} + \delta_{i}R_{i}, \\
\frac{dI_{i}}{dt} = \mu_{i}e_{i}I_{i} + \sum_{j=1}^{2} \beta_{j}p_{ij}S_{i} \frac{\sum_{k=1}^{2} p_{kj}I_{k}}{\sum_{k=1}^{2} p_{kj}N_{k}} - (\mu_{i} + u_{i}(t) + \alpha_{i})I_{i}, \\
\frac{dR_{i}}{dt} = \alpha_{i}I_{i} - (\mu_{i} + \delta_{i})R_{i}.
\end{cases} (6.16)$$

The control set is defined as

$$\Theta = \{u_i \mid 0 \le u_i(t) \le U_i, \}, \quad i = 1, 2,$$

where U_i denotes the upper bound for the culling effort in patch i.

In what follows we introduce an objective functional J to formulate the optimization problem of interest, namely, that of identifying the most effective strategies over the admissible set of $(u_1(t), u_2(t))$. The overall objective is to minimize the numbers of infectious animals over a finite time interval [0, T] at minimal costs. The objective functional J is thus defined as

$$J(u_{1}, u_{2}) = J_{1}(u_{1}) + J_{2}(u_{2})$$

$$= \int_{0}^{T} \left[A_{1}I_{1} + B_{1}u_{1}I_{1} + \frac{C_{1}}{2}u_{1}^{2} \right] dt + \int_{0}^{T} \left[A_{2}I_{2} + B_{2}u_{2}I_{2} + \frac{C_{2}}{2}u_{2}^{2} \right] dt$$

$$= \int_{0}^{T} \left[A_{1}I_{1} + A_{2}I_{2} + B_{1}u_{1}I_{1} + B_{2}u_{2}I_{2} + \frac{C_{1}}{2}u_{1}^{2} + \frac{C_{2}}{2}u_{2}^{2} \right] dt, \quad (6.17)$$

where J_1 and J_2 represents objective functions for patch 1 and 2 respectively, A_i , B_i and C_i are positive balancing coefficients transferring the integrals into monetary quantity over a finite period of T years. Precisely, A_i represents the cost (due to the loss of animals) associated with the number of infected animals in patch i and B_i represent the cost associated with the number of infected animals culled in patch i. The objective functional in (6.17) also includes quadratic terms with coefficients C_i , to indicate potential non-linearities in the costs.

The existence and uniqueness of optimal control can be proven by applying a standard results in optimal control theory [61, 62]. The necessary conditions that optimal controls must satisfy are derived using Pontryagin's Maximum Principle [63]. Thus, system (6.16) is converted into an equivalent problem, namely the problem of minimizing the Hamiltonian H given by:

$$H(t) = \sum_{i=1}^{2} \left(A_i I_i + B_i u_i I_i + \frac{C_i}{2} u_i^2 + \lambda_{S_i} \frac{dS_i}{dt} + \lambda_{I_i} \frac{dI_i}{dt} + \lambda_{R_i} \frac{dR_i}{dt} \right),$$

where $\lambda_{g_i}(t)$, g = S, I, R, i = 1, 2, are the adjoint functions to be determined. Thus, given an optimal control pair (u_1^*, u_2^*) and corresponding states (S_i, I_i, R_i) , there exist adjoint functions [61] satisfying

$$\frac{d\lambda_{S_i}(t)}{dt} = -\frac{\partial H}{\partial S_i}, \quad \frac{d\lambda_{I_i}(t)}{dt} = -\frac{\partial H}{\partial I_i}, \quad \text{and} \quad \frac{d\lambda_{R_i}(t)}{dt} = -\frac{\partial H}{\partial R_i}. \tag{6.18}$$

From (6.18) we have

$$\begin{cases}
\frac{d\lambda_{S_{i}}}{dt} &= \mu_{i}\lambda_{S_{i}} + (\lambda_{S_{i}} - \lambda_{I_{i}}) \sum_{j=1}^{2} \beta_{j} p_{ij} \frac{\sum_{k=1}^{2} p_{kj} I_{k}}{\sum_{k=1}^{2} p_{kj} I_{k}}, & i = 1, 2, \\
\frac{d\lambda_{I_{1}}}{dt} &= (\lambda_{S_{1}} - \lambda_{I_{1}}) \left(\frac{\beta_{1} p_{11}^{2} S_{1}}{p_{11} N_{1} + p_{21} N_{2}} + \frac{\beta_{2} p_{12}^{2} S_{1}}{p_{12} N_{1} + p_{22} N_{2}} \right) \\
&+ (\lambda_{S_{2}} - \lambda_{I_{2}}) \left(\frac{\beta_{1} S_{2} p_{11} p_{21}}{p_{11} N_{1} + p_{21} N_{2}} + \frac{\beta_{2} S_{2} p_{12} p_{22}}{p_{12} N_{1} + p_{22} N_{2}} \right) - A_{1} - B_{1} u_{1} + \alpha_{1} (\lambda_{I_{1}} - \lambda_{R_{1}}) \\
&+ \mu_{1} e_{1} (\lambda_{S_{1}} - \lambda_{I_{1}}) + (\mu_{1} + u_{1}) \lambda_{I_{1}} \\
\frac{d\lambda_{I_{2}}}{dt} &= (\lambda_{S_{1}} - \lambda_{I_{1}}) \left(\frac{\beta_{1} S_{1} p_{11} p_{21}}{p_{11} N_{1} + p_{21} N_{2}} + \frac{\beta_{2} S_{1} p_{12} p_{22}}{p_{12} N_{1} + p_{22} N_{2}} \right) \\
&+ (\lambda_{S_{2}} - \lambda_{I_{2}}) \left(\frac{\beta_{1} p_{21}^{2} S_{2}}{p_{11} N_{1} + p_{21} N_{2}} + \frac{\beta_{2} p_{22}^{2} S_{2}}{p_{12} N_{1} + p_{22} N_{2}} \right) - A_{2} - B_{2} u_{2} + \alpha_{2} (\lambda_{I_{2}} - \lambda_{R_{2}}) \\
&+ \mu_{2} e_{2} (\lambda_{S_{2}} - \lambda_{I_{2}}) + (\mu_{2} + u_{2}) \lambda_{I_{2}} \\
\frac{d\lambda_{R_{i}}}{dt} &= \mu_{i} \lambda_{R_{i}} + \delta_{i} (\lambda_{R_{i}} - \lambda_{S_{i}}), \quad i = 1, 2,
\end{cases}$$
(6.19)

with transversality conditions $\lambda_{g_i}(T) = 0$. Furthermore, the optimal controls are characterized by the optimality conditions:

$$u_i^*(t) = \min\left\{U_i, \max\left(\frac{(\lambda_{I_i} - B_i)I_i}{C_i}, 0\right)\right\}, \quad i = 1, 2$$
(6.20)

In what follows we will utilize the forward-backward sweep method [61] together with parameter values in Table 6.1 and the residence-matrix defined in Table 6.2 to determine numerical solutions of our optimality system. Our main goal will be to explore the effects of optimal culling on the transmission and control of brucellosis under the following cases:

- (a) **Scenario 1**: No culling in high risk population (patch 1), that is, $u_1 = 0$.
- (b) **Scenario 2**: Low intensity culling in high risk population, $u_1 = 0.45$.

In all the above scenarios we assumed that culling intensity in low risk population is always above average and we fixed it at $u_2 = 0.8$. Scenario 1 is assumed to apply to farmers who rear livestock near game reserves. Prior studies highlighted that livestocks reared in proximity to game reserves mix with wildlife on almost daily basis [89], despite the fact that in many countries where brucellosis is endemic, intervention measures to control the spread of zoonotic infections among wildlife are not available. Scenario 2 represents heterogeneity on culling intensity. This scenario may exist in communal farming zones where one farmer say X may have resources (knowledge and financial capacity) to perform culling at the high intensity

while another farmer say Y does not have enough resources to perform culling at an intensity that does not exceed the average.

In all the simulation results presented in this section we used parameter and initial values from Table 6.1 as well as the residence matrix in Table 6.2. For simplicity, in our numerical simulation we set $A_1 = A_2 = 1$ so that the minimization of the infectious animal population has the same importance/weight in all the patches. Further, we set $B_1 = B_2 = 0.2$ and $C_1 = C_2 = 2 \times 10^{-5}$. The values of the weight constants B_i and C_i were determined through numerical simulations, precisely for these values the cost are low and the control efforts can be applied at maximum intensity in all scenarios suggested above.

For each strategy and coupling intensity described in Table 6.2, we find the total number of new infections given by the following formula

$$\Gamma = \Gamma_{1} + \Gamma_{2}
= \int_{0}^{T} \left[\mu_{1} e_{1} I_{1} + \sum_{j=1}^{2} \beta_{j} p_{1j} S_{1} \frac{\sum_{k=1}^{2} p_{kj} I_{k}}{\sum_{k=1}^{2} p_{kj} N_{k}} \right] dt
+ \int_{0}^{T} \left[\mu_{2} e_{2} I_{2} + \sum_{j=1}^{2} \beta_{j} p_{2j} S_{2} \frac{\sum_{k=1}^{2} p_{kj} I_{k}}{\sum_{k=1}^{2} p_{kj} N_{k}} \right] dt,$$
(6.21)

where Γ_i represent the total number of new infections for path i and the total cost associated with infected animals and the controls J, which is given by (6.17). In what follows we determine the effects of optimal culling under different coupling intensity and mobility patterns (see Table 6.2).

Table 6.3: The total number of newly infected animals over a ten-year period and the total cost J with respect to the control strategy under scenario 1.

	Γ_1	Γ_2	Γ	J_1	J_2	J	\mathcal{R}_0
1	7.12×10^{3}	950.321	8.06×10^3	0	162.15	162.15	3.03
2	5.81×10^{3}	3.95×10^3	9.76×10^{3}	0	499.38	499.38	2.31
3	6.835×10^{3}	1.665×10^3	8.5×10^{3}	0	239.95	239.95	2.80
4	6.13×10^{3}	2.50×10^3	8.63×10^{3}	0	331.68	331.68	2.36

In Table 6.3 we present the values of the total number of new infections and J for scenario 1. We can clearly observe that the highest total number of new

infections recorded in patch 1 over a ten-year period under all possible coupling cases is $\Gamma_1 = 7.12 \times 10^3$ and this occurs when the coupling intensity is weak and the mobility pattern is symmetric. Moreover, when the coupling intensity is weak and the mobility pattern is symmetric patch 2 records the lowest total number of new infections is $\Gamma_2 = 950.321$ under all possible coupling cases over the same period. However, this coupling case (weak and symmetric) is associated with the lowest total number of new infections $\Gamma = 8.06 \times 10^3$ as well as the total cost J = 162.15. We surmise that due to weak animal mobility the spread of the disease will be highly confined in independent patches, with more infections being observed in the risk patch (patch 1).

In Table 6.3 we can also observe that strong symmetric coupling gives the lowest total number of new infections for patch 1 only $\Gamma = 5.81 \times 10^3$, while patch 2 will record the highest total of new infections $\Gamma_2 = 3.95 \times 10^3$ and overall this will yield the highest total of new infections $\Gamma = 9.76 \times 10^3$ in the community. This clearly demonstrate that increased short-term dispersal of animals strongly influence the transmission and control of brucellosis.

Next, we compare the impact of presence and absence of time dependent culling on brucellosis transmission dynamics under scenario 1 (Figure 6.2-6.5) over a tenyear period. Figure 6.2-6.5 shows the number of infected animals per patch, with and without optimal culling under weak symmetric coupling, strong symmetric coupling, weak asymmetric coupling and strong asymmetric coupling, respectively. As we can observe, whenever the coupling is weak despite its skewness, then the optimal control policy will not have a significant impact in patch 1 compared to patch 2 where the number of infections decrease with time. However, whenever the coupling is strong the number of infected animals in both patches decrease with time but with more effect being noticed in patch 2 where there is disease control.

Figure 6.6 shows the optimal control profile for $u_2(t)$: (a) when the costs of culling are low and (b) when the costs of culling are high (we set $B_2 = C_2 = 2$), recall that due to the absence of control in patch 1, $u_1(t) = 0$. As is shown, when the costs of culling are either low or high, the control profile starts from the maximum initially and stays there for more than half of the entire period before it switches to its minimum. Precisely, when the costs of culling are low the control profile stays

at its maximum for a longer period of time compared to when the costs are high. This clearly demonstrates that the control is highly sensitive cost parameters, thus under low costs optimal culling can be implemented at maximum intensity for a long period of time.

Table 6.4: The total number of newly infected animals over a ten-year period and the total cost J with respect to the control strategy under scenario 2.

	Γ_1	Γ_2	Γ	J_1	J_2	J	\mathcal{R}_0
1	4.98×10^{3}	747.20	5.73×10^{3}	5.74×10^{3}	1.02×10^{3}	6.76×10^{3}	3.03
2	3.32×10^{3}	2.47×10^{3}	5.79×10^{3}	3.94×10^{3}	2.44×10^{3}	6.38×10^{3}	2.31
3	4.70×10^{3}	1.02×10^{3}	5.72×10^{3}	5.42×10^{3}	1.25×10^{3}	6.67×10^{3}	2.80
4	3.74×10^{3}	1.38×10^{3}	5.12×10^3	4.38×10^{3}	1.53×10^{3}	5.91×10^{3}	2.36

We further investigate the impact of low intensity optimal culling in the risk patch (patch 1), we set $u_1 = 0.45$ while u_2 remains fixed at 0.8. Results for this scenario are depicted in Table 6.4 and Figure 6.7-6.11. As we have observed earlier (Table 6.3) the highest total number of new infections occurs when the coupling intensity is weak and symmetric. We also observe that the presence of control in patch 1 leads to a reduction in the total number of new infections by 30.1%, 21.4% and 28.9% in patch 1 only, patch 2 only and overall (patch 1 and patch 2 combined), respectively. From Table 6.4 it is also evident that the lowest total number of new infections occurs when we have strong asymmetric coupling, $\Gamma = 5.12 \times 10^3$. As observed in Table 6.3, the highest total number of new infections in the community will occur under strong symmetric coupling, $\Gamma = 5.79 \times 10^3$.

Figure 6.7-6.10 demonstrates the impact of optimal culling under all possible coupling cases. As shown, in Figure 6.7-6.10 the total number of infected animals per patch decreases as a result of the optimal policy. Figure 6.11 shows the optimal control profiles for controls $u_1(t)$ and $u_2(t)$ with low cost parameters. As we can observe, both u_1 and u_2 starts from the maximum initially, and stays there for a long time before they switch to the minimum just before the final time horizon.

6.8 Discussion

We have provided a mathematical framework to investigate the role of short-term animal dispersal on transmission and control of brucellosis in a heterogeneous population. The proposed model comprises of two patches and animal dispersal has been modeled using a Lagrangian approach. Our study is applicable in communal lands where animal mobility is highly uncontrolled. Hence it is well known that a single herd of livestock in these communities can be exposed to a high variable number of contacts with others herds of livestock for a short time frame. This heterogeneity in animal contacts may contribute significantly to the transmission and control of brucellosis.

The basic reproduction number \mathcal{R}_0 of the proposed model was computed and analyzed. We observed that it is a function of several factors such as the transmission rates, natural mortality rate, proportions of vertical transmission and the proportion of time that animals of each patch spend in their patch and the other patch. Precisely, we found that \mathcal{R}_0 depends on the characteristics of both patches. However, in the absence of animal mobility we observed that each patch has its own reproduction number \mathcal{R}_{0i} i=1,2, which depends entirely on the characteristics of that patch. With the aid of model parameter values and initial population levels in [38], we demonstrated numerically that whenever there is no animal mobility $\mathcal{R}_{01} = 1.4$ and $\mathcal{R}_{02} = 0.04$, which implies that the disease dies out in low risk patch (patch 2) and persists in high risk patch (patch 1). However, with animal mobility incorporated we noted that \mathcal{R}_0 will always be greater than 2 demonstrating that animal mobility will increase the spread of the disease in the community. In particular, we observed that \mathcal{R}_0 will be highest when the coupling intensity is weak and the mobility pattern is symmetric, $\mathcal{R}_0 = 3.03$. Analytical methods were also used to demonstrate that whenever $\mathcal{R}_0 \leq 1$ then the brucellosis dies out in the community and when $\mathcal{R}_0 > 1$ a unique endemic equilibrium exists and the disease is uniformly persistent.

Meanwhile, we applied optimal control theory to the proposed model to identify optimal culling strategies that can lead to effective control of brucellosis in the community. Two controls representing culling of infectious animals in each patch were incorporated into the original model. Two possible scenario that characterize disease control in developing nations were evaluated. Scenario 1 entails no control (we set $u_1 = 0$) in high risk patch while control is above average (we set $u_2 = 0.8$) among the low risk population. We hypothesized that this scenario mirror livestock farming in areas that are in proximity to wildlife. Due to the unavailability of resources in most developing nations, it follows that control of brucellosis among wildlife is less prioritized. In scenario 2, we set $u_1 = 0.45$ and $u_2 = 0.8$. We also suggested that this scenario may represent two herds of livestock that belong to two different farmers who share grazing lands. One farmer may have some financial resources to maintain culling at an intensity above average while the other does not have enough financial capacity to do so.

Under scenario 1 we observed that the lowest and highest total number of new infections will be recorded in the community under weak symmetric coupling and strong symmetric coupling, respectively. Meanwhile we observed that by introducing a control in high risk patch, the total number of new infections decreases by 30.1%, 21.4% and 28.9% in patch 1 only, patch 2 only and overall (patch 1 and patch 2 combined), respectively. The numerical results provided evidence that, as expected, controlling the two patches gives the best reduction in brucellosis prevalence. Our result show that animal mobility plays an important role in shaping the long term dynamics of brucellosis, which subsequently impact the design of its optimal control strategies.

Several avenues for future research arise from this work. First, future research should asses the role of seasonal variations and short-term animal mobility on the persistence of brucellosis. Seasonal availability of water and pastures have a significant influence on pastoral farming, hence there is need to investigate its impact on the persistence of brucellosis. Second, although we were able to establish the uniqueness and uniform persistence result for the endemic equilibrium, we did not resolve the stability of this equilibrium point analytically and that remains an interesting topic for our future research.

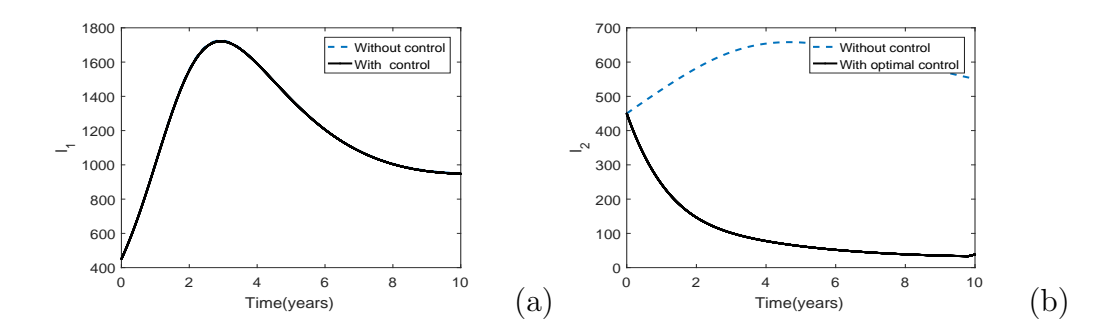


Figure 6.2: Simulation results of the proposed two patch brucellosis model for scenario 1 under weak symmetric coupling (a) the number of infected animals in patch 1 (b) the number of infected animals in patch 2. In all the figures the dotted blue and solid black curves represent the infected population, without and with control, respectively.

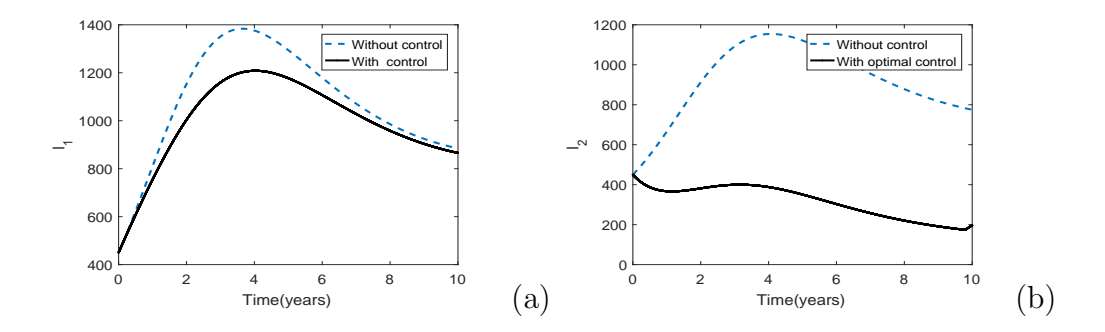


Figure 6.3: Simulation results of the proposed two patch brucellosis model for scenario 1 under strong symmetric coupling (a) the number of infected animals in patch 1 (b) the number of infected animals in patch 2. In all the figures the dotted blue and solid black curves represent the infected population, without and with control, respectively.

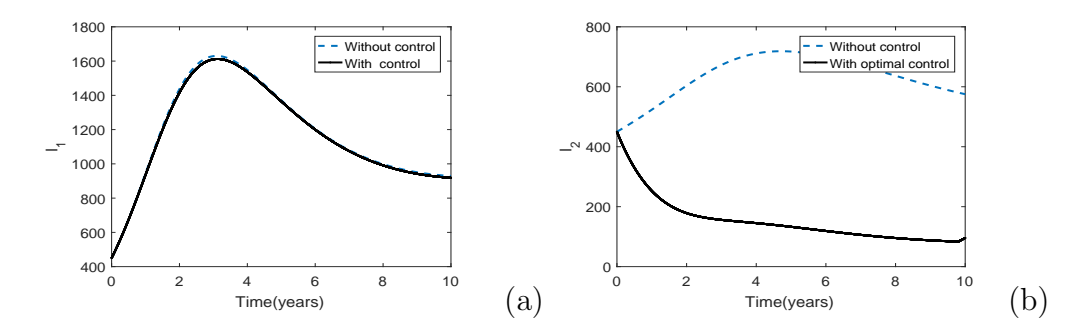


Figure 6.4: Numerical illustrations demonstrating the effects of optimal intervention strategies on controlling the long-term brucellosis dynamics for scenario 1 under weak asymmetric coupling (a) the number of infected animals in patch 1 (b) the number of infected animals in patch 2. In all the figures the dotted blue and solid black curves represent the infected population, without and with control, respectively.

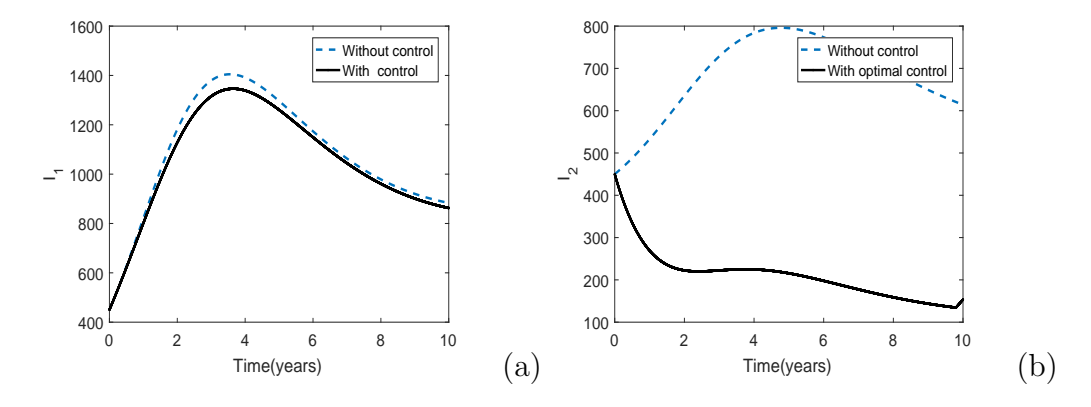


Figure 6.5: Numerical illustrations demonstrating the effects of optimal intervention strategies on controlling the long-term brucellosis dynamics for scenario 1 under strong asymmetric coupling (a) the number of infected animals in patch 1 (b) the number of infected animals in patch 2. In all the figures the dotted blue and solid black curves represent the infected population, without and with control, respectively.

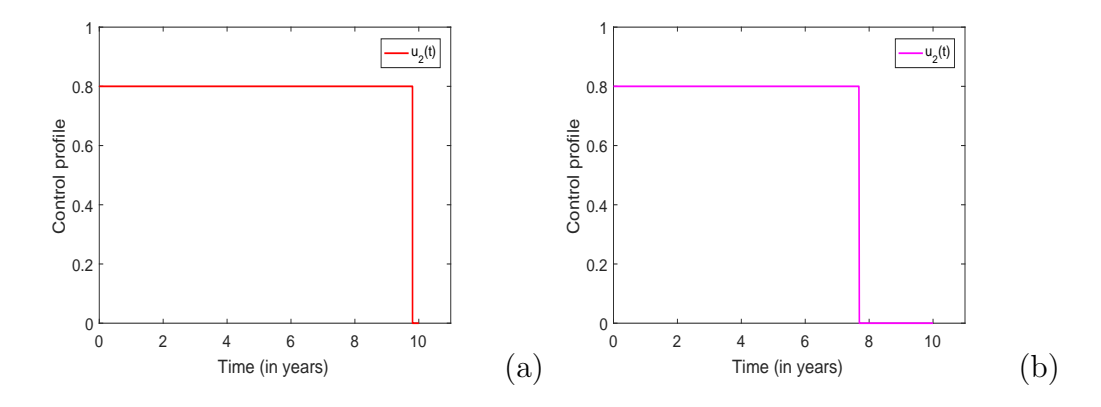


Figure 6.6: The control profile for scenario 1 (a) low costs (b) high cost of culling

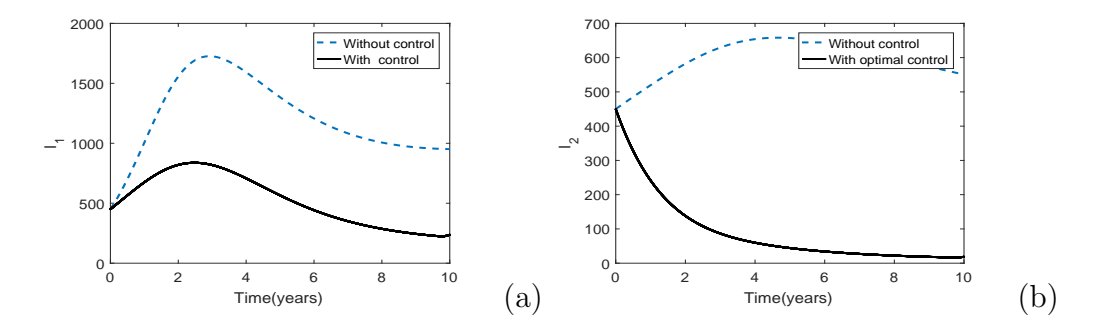


Figure 6.7: Simulation results of the proposed two patch brucellosis model for scenario 2 under weak symmetric coupling (a) the number of infected animals in patch 1 (b) the number of infected animals in patch 2. In all the figures the dotted blue and solid black curves represent the infected population, without and with control, respectively.

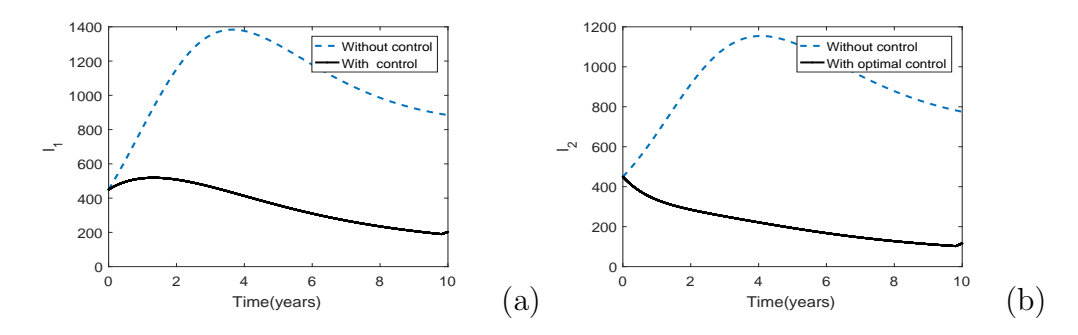


Figure 6.8: Simulation results of the proposed two patch brucellosis model for scenario 2 under strong symmetric coupling (a) the number of infected animals in patch 1 (b) the number of infected animals in patch 2. In all the figures the dotted blue and solid black curves represent the infected population, without and with control, respectively.

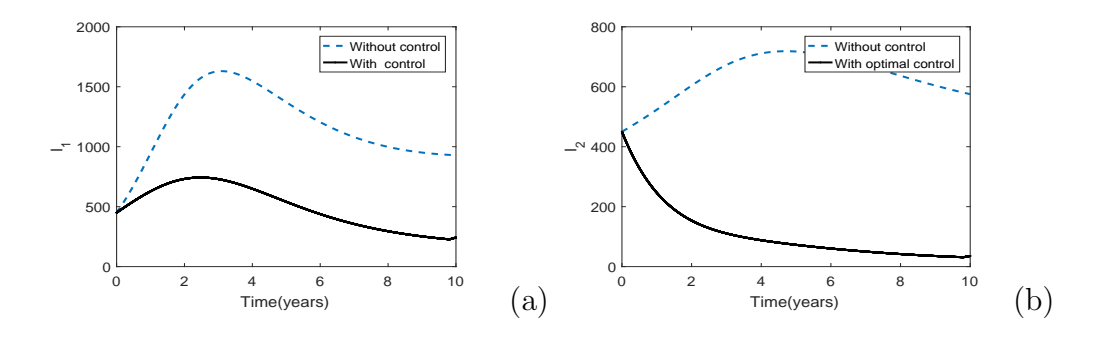


Figure 6.9: Numerical illustrations demonstrating the effects of optimal intervention strategies on controlling the long-term brucellosis dynamics for scenario 2 under weak asymmetric coupling (a) the number of infected animals in patch 1 (b) the number of infected animals in patch 2. In all the figures the dotted blue and solid black curves represent the infected population, without and with control, respectively.

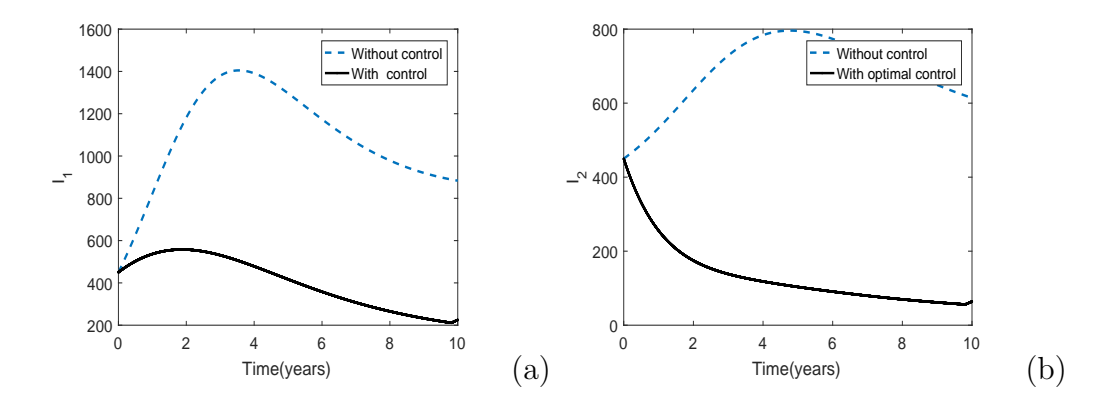


Figure 6.10: Numerical illustrations demonstrating the effects of optimal intervention strategies on controlling the long-term brucellosis dynamics for scenario 1 under strong asymmetric coupling (a) the number of infected animals in patch 1 (b) the number of infected animals in patch 2. In all the figures the dotted blue and solid black curves represent the infected population, without and with control, respectively.

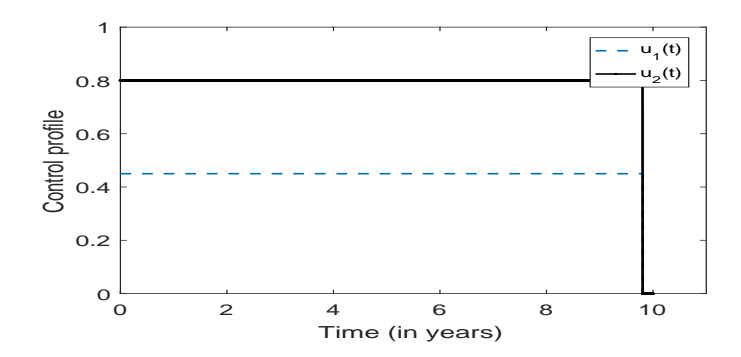


Figure 6.11: The control profile for scenario 2.

Chapter 7

Dynamics and stability analysis of a brucellosis model with two discrete delays

7.1 Introduction

Brucellosis is one of the neglected zoonotic diseases that remains a major public health problem world over, especially in Middle Eastern countries, southern Europe and North Africa, countries in South and Central Asia, sub-Saharan Africa, Mexico, the Caribbean, and countries in South and Central America [90], with an annual occurrence of more than 500 000 cases [43].

In animals, brucellosis is usually transmitted through direct contact between a susceptible and an infectious animal or indirectly, i.e. when a susceptible animal ingest contaminated forages or the excrement containing large quantities of bacteria, generally discharged by infected animals [39]. In humans, however, majority of the infections result from direct or indirect exposure to infected animals or consumption of raw animal products such as unpasteurized milk or cheese [91]. Since human-to-human transmission of the disease is extremely rare [64], the ultimate management of human brucellosis can be achieved through effective control of brucellosis in live-stock. Some researchers postulates that eradication of brucellosis in animals can be attained by combining vaccination with test-and-slaughter programs [90].

Mathematical models have proved to be essential guiding tools for epidemiologists, biologists as well as policy makers. Models can provide solutions to phenomena which are difficult to measure practically. Recently, a number of mathematical models have been proposed to study the spread and control of brucellosis (see, for example [5, 30, 31, 39, 66, 44, 92, 93, 94, 95, 33], and references therein). A limitation of these previous studies however, is the non-inclusion of the time taken before an infectious animal is detected and culled, despite the fact that in many countries where the disease is endemic lack of financial and human resources often results on delay in detection and culling of infectious animals. The size of this delay may play an important role on minimizing the spread of the disease in the community.

It is therefore essential to gain a better and more comprehensive understanding of the effects of time delay on brucellosis transmission and control. Prior studies have shown that epidemic models with time delay often exhibit periodic solutions and as a consequence understanding the nature of these periodic outbreaks plays a crucial role on designing policies that can successful control the disease. In fact, a recent analysis of brucellosis dataset in countries where the disease is endemic have shown that the disease incidences exhibit a strong periodic behavior with mortality and morbidity of the disease concentrated in a few months each year [27, 28]. Understanding the impact of such seasonal variations is crucial on managing the spread of the disease in the community.

Our main goal in this chapter is to explore the dynamics and stability analysis of a brucellosis model with two discrete delays. Hence we formulated a mathematical model, that incorporates two discrete delays. The first delay represents the incubation period while the second accounts for the time taken to detect and cull infectious animals. In addition, we subdivide the total animal population into classes of susceptible, vaccinated, infectious undetected and infectious detected animals. In certain situations immediate slaughter of detected animals may not be feasible and more often these animals are isolated from the rest. However, due to lack of financial and human resources, in addition to lack of knowledge and attitude of farmers, isolation of detected animals has not been a successful practice in most developing nations where animal infections are rampant. Thus in our modelling process we assume that a proportion of detected animals that are not immediately culled are

also responsible for disease transmission. Utilizing both analytical and numerical results we have demonstrated that the two delays can destabilize the system and lead to Hopf bifurcation.

The chapter is organised as follows. The model description is given in Section 7.2. Analytical and numerical results are given in Section 7.3 and 7.4, respectively. We end with Section 7.5 of conclusions.

7.2 Mathematical model

We subdivide the total animal population N(t) into compartments of: susceptible S(t), vaccinated V(t), undetected infectious animals $I_1(t)$ and infectious detected and unculled $I_2(t)$. Although, brucellosis can be transmitted indirectly (environmental transmission), prior studies [92, 30] suggest that indirect transmission plays a relatively small role on the spread of brucellosis, and as such we have ignored this aspect in our study. Brucellosis dynamics in this study are governed by the following autonomous system:

$$\begin{cases}
\frac{dS(t)}{dt} &= A - \beta[I_1(t) + (1-p)I_2(t)]S(t) - (\mu + \sigma)S(t) + \kappa V(t), \\
\frac{dV(t)}{dt} &= \sigma S(t) - \gamma \beta[I_1(t) + (1-p)I_2(t)]V(t) - (\mu + \kappa)V(t), \\
\frac{dI_1(t)}{dt} &= \beta[I_1(t-\tau_1) + (1-p)I_2(t-\tau_1)][S(t-\tau_1) + \gamma V(t-\tau_1)] \\
-(\alpha + \mu + d)I_1(t), \\
\frac{dI_2(t)}{dt} &= \alpha I_1(t-\tau_2) - (\mu + c + d)I_2(t),
\end{cases} (7.1)$$

where A is the recruitment rate through birth, μ is the natural death rate, β is the disease direct transmission rate, p is the fraction of detected animals that have been culled, σ is the vaccination rate, κ is the vaccination waning rate, τ_1 represents the latency delay, τ_2 is the delay in detection, γ is the modification factor, α is the rate at which animals are detected and quarantined, c is the culling rate of detected animals, d disease induced death.

7.3 Analytical results

7.3.1 Initial conditions

The appropriate space for system (7.1) is $X = \mathcal{C}([-\tau, 0], \mathbb{R}^4_+)$ the Banach space of continuous functions mapping the interval $[-\tau, 0]$ into \mathbb{R}^4_+ equipped with sub-norm where $\tau = \max\{\tau_1, \tau_2\}$. From the standard results of functional differential equations [96] it follows that, given any initial conditions $x_0 \in X$ there exists a unique solution $\phi(t, x_0) = (S(t, x_0), V(t, x_0), I_1(t, x_0), I_2(t, x_0))$ of system (7.1), which satisfies $\phi_0 = x_0$, the initial conditions are given by

$$S(\theta) = x_0^1(\theta), \quad V(\theta) = x_0^2(\theta), \quad I_1(\theta) = x_0^3(\theta), \quad I_2(\theta) = x_0^4(\theta), \quad \theta \in [-\tau, 0], \quad (7.2)$$

where $x_0 = (x_0^1, x_0^2, x_0^3, x_0^4) \in X$, with $x_0^i(\theta) \ge 0$, $(\theta \in [-\tau, 0], i = 1, 2, ..., 4)$ and $x_0^3(0), x_0^4(0) > 0$.

7.3.2 The basic reproduction Number

By direct calculation, we find that system (7.1) when $\tau_1 = \tau_2 = 0$, has a disease-free equilibrium \mathcal{E}^0 , given by $\mathcal{E}^0 = (S^0, V^0, 0, 0)$, with

$$S^0 = \frac{A(\mu + \kappa)}{\mu(\mu + \sigma + \kappa)}, \quad V^0 = \frac{A\sigma}{\mu(\mu + \sigma + \kappa)}, \quad \text{and} \quad S^0 + \gamma V^0 = \frac{A(\mu + \kappa + \gamma \sigma)}{\mu(\mu + \sigma + \kappa)}.$$

By utilizing the next generation matrix method [50], one can deduce that the basic reproduction number of model (7.1) is

$$\mathcal{R}_0 = \frac{\beta(S^0 + \gamma V^0)(\alpha(1-p) + k_2)}{k_1 k_2},$$

with $k_1 = (\mu + \alpha + d)$, and $k_2 = (\mu + c + d)$.

7.3.3 Stability of the disease-free equilibrium

In this section, we study the local and global stability of the disease-free equilibrium.

Theorem 7.3.1 The disease-free equilibrium \mathcal{E}^0 of model (7.1) is locally asymptotically stable when $\mathcal{R}_0 < 1$ and unstable when $\mathcal{R}_0 > 1$.

Proof 16 To study the local stability of the disease-free equilibrium \mathcal{E}^0 , we linearized system (7.1) about this point and obtained the characteristic equation, given by the following determinant:

$$\begin{vmatrix}
-(\mu+\sigma)-\lambda & \kappa & -\beta S^{0} & -\beta(1-p)S^{0} \\
\sigma & -(\mu+\kappa)-\lambda & -\gamma\beta V^{0} & -\gamma\beta(1-p)V^{0} \\
0 & 0 & (S^{0}+\gamma V^{0})\beta e^{-\lambda\tau_{1}}-k_{1}-\lambda & \beta(S^{0}+\gamma V^{0})(1-p)e^{-\lambda\tau_{1}} \\
0 & 0 & \alpha e^{-\lambda\tau_{2}} & -k_{2}-\lambda
\end{vmatrix} = 0,$$
(7.3)

where λ is the eigenvalue.

From (7.3) the characteristic equation is

$$\left\{ \lambda + \mu \right\} \left\{ (\lambda + \sigma + \kappa + \mu) \right\} \left\{ [\lambda + k_2] [\lambda + k_1 - \beta (S^0 + \gamma V^0) e^{-\lambda \tau_1}] - (1 - p) \alpha \beta (S^0 + \gamma V^0) e^{-\lambda (\tau_1 + \tau_2)} \right\} = 0.$$
(7.4)

Clearly, $-\mu$ and $-(\sigma+\kappa+\mu)$ are eigenvalues and the other two can be determined from the following equation

$$(\lambda + k_2)(\lambda + k_1 - \beta(S^0 + \gamma V^0)e^{-\lambda \tau_1}) - (1 - p)\alpha\beta(S^0 + \gamma V^0)e^{-\lambda(\tau_1 + \tau_2)} = 0. \quad (7.5)$$

Let

$$g(\lambda, \tau_1, \tau_2) = (\lambda + k_2)(\lambda + k_1 - \beta(S^0 + \gamma V^0)e^{-\lambda \tau_1}) - (1 - p)\alpha\beta(S^0 + \gamma V^0)e^{-\lambda(\tau_1 + \tau_2)}.$$
 (7.6)

Through direct calculation one can easily verify that $g(\lambda, \tau_1, \tau_2)$ is an analytic function and it follows that

$$\begin{cases} g(0, \tau_1, \tau_2) = k_1 k_2 (1 - \mathcal{R}_0), \\ g(\lambda, 0, 0) = (\lambda + k_2) (\lambda + k_1 - \beta (S^0 + \gamma V^0)) - (1 - p) \alpha \beta (S^0 + \gamma V^0). \end{cases}$$

Now we proceed to investigate the distribution of the solutions of (7.5) in the following cases.

(a) If $\mathcal{R}_0 < 1$, then $g(0, \tau_1, \tau_2) > 0$. Since the derivative $g'_{\lambda}(\lambda, \tau_1, \tau_2) > 0$ for $\lambda \geq 0$, $\tau_1 > 0$ and $\tau_2 > 0$, (7.5) has no zero root and positive real roots for all positive τ_1 and τ_2 . Now we assume that the solution of (7.5) does not have any purely imaginary roots $\lambda = i\omega$, ($\omega > 0$) for some $\tau_1 > 0$, $\tau_2 = 0$. Then by computation, ω must be positive real root of

$$\omega^4 + \left\{ k_1^2 + k_2^2 - \left[\beta (S^0 + \gamma V^0) \right]^2 \right\} \omega^2 + (k_1 k_2)^2$$

$$-\left[\beta(S^0 + \gamma V^0)\left[k_2 + \alpha(1-p)\right]\right]^2 = 0. \tag{7.7}$$

If $\mathcal{R}_0 < 1$ the equation (7.7) has no positive roots. Hence (7.5) does not have any purely imaginary roots. We can easily see that the roots of $g(\lambda, 0, 0) = 0$ all have negative real parts when $\mathcal{R}_0 < 1$. By the implicit function theorem and the continuity of $g(\lambda, \tau_1, \tau_2)$, we know that all roots of (7.5) have negative real parts for positive τ_1 and $\tau_2 = 0$ which implies that \mathcal{E}^0 is stable.

- (b) If R₀ = 1 then g(0, τ₁, τ₂) > 0. Since the derivative g'(λ, τ₁, τ₂) > 0 for λ ≥ 0 , τ₁ > 0 and τ₂ > 0, (7.5) has a simple zero and no positive root for all positive τ₁ and τ₂. By the same argument in case (a), we can obtain that all roots of (7.5) have negative real parts for positive τ₁ and τ₂ = 0 except a zero root. Thus ε⁰ is a degenerate equilibrium of codimension and is stable except in one direction.
- (c) If $\mathcal{R}_0 > 1$, then $g(0, \tau_1, \tau_2) < 0$. Since we have $\lim_{\lambda \to \infty} g(\lambda, \tau_1, \tau_2) = \infty$ and $g'(\lambda, \tau_1, \tau_2) > 0$ for $\lambda \geq 0$, $\tau_1 > 0$ and $\tau_2 > 0$, (7.5) has a unique positive real root for all positive τ_1 and $\tau_2 = 0$ and \mathcal{E}^0 is unstable.

Theorem 7.3.2 The disease-free equilibrium of model (7.1) is globally asymptotically stable when $\mathcal{R}_0 \leq 1$ and unstable when $\mathcal{R}_0 > 1$.

Proof 17 We denote by x_t the translation of the solution of the system (7.1), that is, $x_t = (S(t+\theta), V(t+\theta), I_1(t+\theta), I_2(t+\theta))$ where $\theta \in [-\tau, 0]$ and $\tau = \max\{\tau_1, \tau_2\}$. We consider the following Lyapunov functional

$$\mathcal{U}(x_t) = \frac{\beta \left[\alpha(1-p) + k_2\right]}{k_1 k_2} I_1(t) + \frac{\beta(1-p)}{k_2} I_2(t) + \frac{\beta \alpha(1-p)}{k_2} \int_{t-\tau_2}^t \left[I_1(\theta)\right] d\theta + \frac{\beta^2 \left[\alpha(1-p) + k_2\right]}{k_1 k_2} \int_{t-\tau_1}^t \left\{ \left[I_1(\theta) + (1-p)I_2(\theta)\right] \left[S(\theta) + \gamma V(\theta)\right] \right\} d\theta.$$

Taking the derivative of \mathcal{U} along the solutions of (7.1) gives

$$\frac{d\mathcal{U}(x_t)}{dt} = \frac{\beta \left[\alpha(1-p) + k_2\right]}{k_1 k_2} \beta \left[I_1(t-\tau_1) + (1-p)I_2(t-\tau_1)\right] \left[S(t-\tau_1) + \gamma V(t-\tau_1)\right] \\
+ \gamma V(t-\tau_1) \left[\frac{\beta \left[\alpha(1-p) + k_2\right]}{k_2} I_1(t) + \frac{\beta(1-p)}{k_2} \alpha I_1(t-\tau_2) - \beta(1-p)I_2(t)\right] \\
+ \frac{\beta \left[\alpha(1-p) + k_2\right]}{k_1 k_2} \beta \left[I_1(t) + (1-p)I_2(t)\right] \left[S(t) + \gamma V(t)\right]$$

$$-\frac{\beta \left[\alpha(1-p)+k_{2}\right]}{k_{1}k_{2}}\beta\left[I_{1}(t-\tau_{1})+(1-p)I_{2}(t-\tau_{1})\right]\left[S(t-\tau_{1})+\gamma V(t-\tau_{1})\right]$$

$$+\gamma V(t-\tau_{1})$$

$$+\frac{\beta(1-p)}{k_{2}}\alpha I_{1}(t)-\frac{\beta(1-p)}{k_{2}}\alpha I_{1}(t-\tau_{2})$$

$$=\frac{\beta \left[\alpha(1-p)+k_{2}\right]}{k_{1}k_{2}}\beta\left[S(t)+\gamma V(t)\right]\left[I_{1}(t)+(1-p)I_{2}(t)\right]$$

$$-\beta\left[I_{1}(t)+(1-p)I_{2}(t)\right]$$

$$\leq\beta\left[\frac{\beta \left[\alpha(1-p)+k_{2}\right]\left[S^{0}+\gamma V^{0}\right]}{k_{1}k_{2}}-1\right]\left[I_{1}(t)+(1-p)I_{2}(t)\right]$$

$$=\beta\left[\mathcal{R}_{0}-1\right]\left[I_{1}(t)+(1-p)I_{2}(t)\right]. \tag{7.8}$$

Therefore, $\dot{\mathcal{U}} < 0$ holds if $\mathcal{R}_0 < 1$. Furthermore, $\dot{\mathcal{U}} = 0$ if $\mathcal{R}_0 = 1$. Therefore, the largest invariant set of $\dot{\mathcal{U}}$ is a singleton $\{\mathcal{E}^0\}$ such that $S(t) = S^0$, $V(t) = V^0$, $I_1(t) = I_2(t) = 0$. It follows from the LaSalle's invariance principle [46] that the disease-free equilibrium of system (7.1) denoted by \mathcal{E}^0 is globally asymptotically stable whenever $\mathcal{R}_0 \leq 1$. This completes the proof of Theorem 7.3.2.

7.3.4 Disease persistence

System (7.1) is said to be uniformly persistent if there exists a constant $\eta_0 > 0$ such that any solution $(S(t), V(t), I_1(t), I_2(t))$ of (7.1) satisfies

$$\liminf_{t\to\infty} S(t) \geq \eta_0, \qquad \liminf_{t\to\infty} V(t) \geq \eta_0, \qquad \liminf_{t\to\infty} I_1(t) \geq \eta_0, \qquad \liminf_{t\to\infty} I_2(t) \geq \eta_0.$$

Now we give a result on the uniform persistence of system (7.1). To proceed we introduce the following notation and terminology. Denote by $P(t), t \geq 0$ the family of solution operators corresponding to (7.1). The ω -limit set $\omega(x)$ of x consists of $y \in X$ such that there exists a sequence $t_n \longrightarrow \infty$ as $n \longrightarrow \infty$ with $P(t_n)x \longrightarrow y$ as $n \longrightarrow \infty$.

Theorem 7.3.3 System (7.1) is uniformly persistent, if it satisfies $\mathcal{R}_0 > 1$.

Proof 18 Let

 $X^0 = \{x_0 \in X : x_0^3(0) > 0, x_0^4(0) > 0\}, \quad \partial X = X \setminus X^0 = \{x_0 \in X : x_0^3(0) = 0\}$ or $x_0^4(0) = 0\}$ which is relatively closed in X.

In what follows we demonstrate that X^0 is positively invariant for P(t). From the third and fourth equations of (7.1) we have

$$\frac{dI_1(t)}{dt} \ge -(\alpha + \mu + d)I_1(t), \quad \frac{dI_2(t)}{dt} \ge -(\mu + c + d)I_2(t). \tag{7.9}$$

Since $I_1(0, x_0) = x_0^3(0) > 0$, we have $I_2(0, x_0) = x_0^4(0) > 0$ it follows from (7.9) that

$$I_1(t, x_0) \ge x_0^3(0) \cdot e^{-(\alpha + \mu + d)t}, \quad I_2(t, x_0) \ge x_0^4(0) \cdot e^{-(\mu + c + d)t}, \quad \forall t \ge 0.$$

Thus X^0 is positively invariant for P(t).

We set

$$M_{\partial} = \{x_0 \in X : \phi(t)x_0 \text{ satisfies (7.1)} \text{ and } \phi(t)x_0 \in \partial X, \forall t \ge 0\}.$$

We claim that

$$M_{\partial} = \{ (S, V, 0, 0) \}. \tag{7.10}$$

Assuming $\phi(t) \in M_{\partial}$, $\forall t \geq 0$, it suffices to show that $I_1(t) = I_2(t) = 0$, $\forall t \geq 0$. If it is not true, then there exists $t_0 > 0$ such that either (a) $I_1(t_0) > 0$, $I_2(t_0) = 0$; or (b) $I_1(t_0) = 0$, $I_2(t_0) > 0$. For case (a), from the fourth equation of (7.1) we have

$$\left[\frac{dI_2}{dt}\right]_{t=t_0} = \alpha I_1(t_0 - \tau_2) > 0.$$

Hence there is an $\epsilon_0 > 0$ such that $I_2(t) > 0$, $\forall t \in (t_0, t_0 + \epsilon_0)$. On the other hand, from $I_1(t) > 0$ there exists ϵ_1 $(0 < \epsilon_1 < \epsilon_0)$ such that $I_1(t) > 0$, $\forall t \in (t_0, t_0 + \epsilon_1)$. Thus we have $I_1(t) > 0$, $I_2(t) > 0$, $\forall t \in (t_0, t_0 + \epsilon_1)$ which contradicts the assumption that $(S(t), V(t), I_1(t), I_2(t)) \in M_{\partial}$, $\forall t \geq 0$. Similarly, we can obtain a contradiction for case (b). This proves the claim (7.10).

Let $\mathcal{F} = \bigcap_{x \in F_b} \omega(x)$, where F_b is the global attractor of P(t) restricted to ∂X . We show that $\mathcal{F} = \{\mathcal{E}^0\}$. In fact, from $\mathcal{F} \subseteq M_\partial$ and the first and second equation of (7.1), we have $\lim_{t \to \infty} S(t) = S^0$ and $\lim_{t \to \infty} V(t) = V^0$. Thus, $\{\mathcal{E}^0\}$ is the isolated invariant set in X.

Next we show that $W^S(\mathcal{E}^0) \cap X_0 = \emptyset$. If this is not true, then there exists a solution $(S^t, V^t, I_1^t, I_2^t) \in X^0$ such that

$$\lim_{t \to \infty} S(t) = \frac{A(\mu + \kappa)}{\mu(\mu + \sigma + \kappa)}, \qquad \lim_{t \to \infty} V(t) = \frac{A\sigma}{\mu(\mu + \sigma + \kappa)}, \qquad \lim_{t \to \infty} I_1(t) = 0,$$
$$\lim_{t \to \infty} I_2(t) = 0,.$$

For any sufficiently small constant $\epsilon > 0$, there exists a positive constant $T_0 = T_0(\epsilon)$ such that $S(t) > S^0 - \epsilon > 0$, $V(t) > V^0 - \epsilon > 0$, $\forall t > T_0$. For the constant ϵ given above, it follows from the third and fourth equations of (7.1) that

$$\frac{dI_1(t)}{dt} \geq \beta [I_1(t-\tau_1) + (1-p)I_2(t-\tau_1)][(S^0 - \epsilon) + \gamma(V^0 - \epsilon)]
-(\alpha + \mu + d)I_1(t),$$

$$\frac{dI_2(t)}{dt} = \alpha I_1(t-\tau_2) - (\mu + c + d)I_2(t), \quad t \geq T_0 + \tau$$
(7.11)

If $I_1(t)$, $I_2(t) \longrightarrow \infty$, then by a standard comparison argument and the nonnegativity, the solution

 $(\tilde{I}_1(t), \tilde{I}_2(t))$ of the following monotone system

$$\frac{d\tilde{I}_{1}(t)}{dt} = \beta [\tilde{I}_{1}(t-\tau_{1}) + (1-p)\tilde{I}_{2}(t-\tau_{1})][(S^{0}-\epsilon) + \gamma(V^{0}-\epsilon)]
-(\alpha+\mu+d)\tilde{I}_{1}(t),$$

$$\frac{d\tilde{I}_{2}(t)}{dt} = \alpha \tilde{I}_{1}(t-\tau_{2}) - (\mu+c+d)\tilde{I}_{2}(t), \quad t \geq T_{0} + \tau$$
(7.12)

with initial condition $\tilde{I}_1(t) = I_1(t)$, $\tilde{I}_2(t) = I_2(t)$, $\forall t \in [T_0, T_0 + \tau]$ converges to (0,0) as well. Thus $\lim_{t\to\infty} \widehat{W}(t) = 0$, where $\widehat{W}(t) > 0$ is defined by

$$\widehat{W}(t) = \frac{\beta \left[\alpha(1-p) + k_2\right]}{k_1 k_2} \widetilde{I}_1(t) + \frac{\beta(1-p)}{k_2} \widetilde{I}_2(t) + \frac{\beta \alpha(1-p)}{k_2} \int_{t-\tau_2}^t \left[\widetilde{I}_1(\zeta)\right] d\zeta + \frac{\beta^2 \left[\alpha(1-p) + k_2\right] \left[(S^0 - \epsilon) + \gamma(V^0 - \epsilon)\right]}{k_1 k_2} \int_{t-\tau_1}^t \left[\widetilde{I}_1(\zeta) + (1-p)\widetilde{I}_2(\zeta)\right] d\zeta.$$

Differentiating $\widehat{W}(t)$ with respect to time t yields

$$\left[\frac{d\widehat{W}(t)}{dt}\right]_{(7.12)} = \left[\frac{\beta^2 \left[\alpha(1-p) + k_2\right] \left[\left(S^0 - \epsilon\right) + \gamma(V^0 - \epsilon)\right]}{k_1 k_2} - \beta\right] \cdot \left[\widetilde{I}_1(t) + (1-p)\widetilde{I}_2(t)\right].$$

Since $\mathcal{R}_0 > 1$, we have $\frac{\beta^2 \left[\alpha(1-p) + k_2\right] \left[\left(S^0 - \epsilon\right) + \gamma(V^0 - \epsilon)\right]}{k_1 k_2} - \beta > 0$ for a sufficiently small ϵ . Therefore $\widehat{W}(t)$ goes to either infinity or a positive number as $t \longrightarrow \infty$, which leads to a contradiction with $\lim_{t \longrightarrow \infty} \widehat{W}(t) = 0$. Thus we have $W^S(\mathcal{E}^0) \cap X_0 = \emptyset$. Define $m: X \to \mathbb{R}_+$ by $m(x_0) = \min\{x_0^3(0), x_0^4(0)\}$, $\forall x_0 \in X$. It is clear that $X^0 = m^{-1}(0, \infty)$ and $\partial X = m^{-1}(0)$. Thus by [97] theorem 3 we have $\lim_{t \longrightarrow \infty} (I_1(t), I_2(t)) \ge (\eta_1, \eta_1)$ for some constant $\eta_1 > 0$. Let $\eta_0 = \min\{\eta_1, \epsilon\}$

where ϵ is the constant such that $\liminf_{t\to\infty} S(t) \geq \epsilon > 0$, $\liminf_{t\to\infty} V(t) \geq \epsilon > 0$. We showed that $\liminf_{t\to\infty} S(t) \geq \eta_0$, $\liminf_{t\to\infty} V(t) \geq \eta_0$, $\liminf_{t\to\infty} I_1(t) \geq \eta_0$, $\liminf_{t\to\infty} I_2(t) \geq \eta_0$. This completes the proof of Theorem 7.3.3.

7.3.5 Existence of the endemic equilibrium

Theorem 7.3.4 If $\mathcal{R}_0 > 1$, model (7.1) admits a unique endemic equilibrium.

Proof 19 The endemic equilibrium $\mathcal{E}^* = (S^*, V^*, I_1^*, I_2^*)$ of model (7.1) is determine by equations

$$\begin{cases}
A - \beta[I_1(t) + (1-p)I_2(t)]S(t) - (\mu + \sigma)S(t) + \kappa V(t) &= 0, \\
\sigma S(t) - \gamma \beta[I_1(t) + (1-p)I_2(t)]V(t) - (\mu + \kappa)V(t) &= 0, \\
\beta[I_1(t) + (1-p)I_2(t)][S(t) + \gamma V(t)] - k_1 I_1(t) &= 0, \\
\alpha I_1(t) - k_2 I_2(t) &= 0.
\end{cases} (7.13)$$

From the last equation in (7.13) we have

$$I_2 = \frac{\alpha I_1}{k_2}.\tag{7.14}$$

The first two equations in (7.13) gives

$$\begin{cases}
S = \frac{A[\gamma\beta(1 + \frac{\alpha(1-p)}{k_2})I_1 + \mu + \kappa]}{[\beta(1 + \frac{\alpha(1-p)}{k_2})I_1 + \mu + \sigma][\gamma\beta(1 + \frac{\alpha(1-p)}{k_2})I_1 + \mu + \kappa] - \kappa\sigma}, \\
V = \frac{A\sigma}{[\beta(1 + \frac{\alpha(1-p)}{k_2})I_1 + \mu + \sigma][\gamma\beta(1 + \frac{\alpha(1-p)}{k_2})I_1 + \mu + \kappa] - \kappa\sigma}.
\end{cases} (7.15)$$

For $I_1 \neq 0$, substituting (7.14) into the third equation in (7.13) gives

$$S + \gamma V = \frac{k_1 k_2}{\beta [\alpha (1 - p) + k_2]}. (7.16)$$

Substituting (7.15) into (7.16) yields

$$F(I_1) = \frac{A[\gamma\beta(1 + \frac{\alpha(1-p)}{k_2})I_1 + \mu + \kappa + \gamma\sigma]}{[\beta(1 + \frac{\alpha(1-p)}{k_2})I_1 + \mu + \sigma][\gamma\beta(1 + \frac{\alpha(1-p)}{k_2})I_1 + \mu + \kappa] - \kappa\sigma} - \frac{k_1k_2}{\beta[\alpha(1-p) + k_2]}.$$
(7.17)

Direct calculations shows

$$F'(I_1) = -\frac{A\beta^2 \left[1 + \frac{\alpha(1-p)}{k_2}\right]^2 \left[\gamma^2 \beta I_1^2 \left[1 + \frac{\alpha(1-p)}{k_2}\right] + 2\gamma(\gamma\sigma + \mu + \kappa)I_1\right] + M}{\left[\left[\beta\left(1 + \frac{\alpha(1-p)}{k_2}\right)I_1 + \mu + \sigma\right]\left[\gamma\beta\left(1 + \frac{\alpha(1-p)}{k_2}\right)I_1 + \mu + \kappa\right] - \kappa\sigma\right]^2} < 0,$$
(7.18)

where

$$M = A\beta \left[1 + \frac{\alpha(1-p)}{k_2} \right] \left[\gamma \sigma(2\kappa + \mu) + \gamma^2 \sigma(\mu + \sigma) + (\mu + \kappa)^2 \right].$$

then the function $F(I_1)$ is monotonic decreasing for $I_1 > 0$, then we can define the function

 $F(0) = \frac{k_1 k_2}{\beta [\alpha (1-p) + k_2]} [\mathcal{R}_0 - 1].$

Therefore, by monotonicity of a function $F(I_1)$ there exists a unique endemic equilibrium $\mathcal{E}^* = (S^*, V^*, I_1^*, I_2^*)$

7.3.6 Stability of the endemic equilibrium

In this section, we will investigate the local and global stability of the endemic equilibrium point.

Theorem 7.3.5 The endemic equilibrium \mathcal{E}^* of the system (7.1) is locally asymptotically stable if $\mathcal{R}_0 > 1$ and conditions (7.21) are satisfied.

Proof 20 The characteristics equation of system (7.1) on the infected equilibrium \mathcal{E}^* is given by the following determinant

$$\begin{vmatrix}
-(\mu + \sigma) - \lambda & \kappa & -\beta S^* & -\beta (1 - p) S^* \\
\sigma & -(\mu + \kappa) - \lambda & -\gamma \beta V^* & -\gamma \beta (1 - p) V^* \\
r_{31} & r_{32} & r_{33} & r_{34} \\
0 & 0 & \alpha e^{-\lambda \tau_2} & -(\mu + c + d) - \lambda
\end{vmatrix} = 0, \quad (7.19)$$

with

$$r_{31} = \beta[I_1^* + (1-p)I_2^*]e^{-\lambda\tau_1}, \qquad r_{32} = \gamma\beta[I_1^* + (1-p)I_2^*]e^{-\lambda\tau_1},$$

$$r_{33} = (S^* + \gamma V^*)\beta e^{-\lambda\tau_1} - (\alpha + \mu + d) - \lambda, \qquad r_{34} = \beta(S^* + \gamma V^*)(1-p)e^{-\lambda\tau_1}.$$

After some algebraic manipulations one can show that the characteristic equation has the form

$$\lambda^4 + a_1 \lambda^3 + a_2 \lambda^2 + a_3 \lambda + a_4 = 0 \tag{7.20}$$

with

$$a_1 = 4\mu + \kappa + \alpha + \sigma + 2d + c + \beta(\gamma + 1)(I_1^* + (1-p)I_2^*) - (S^* + \gamma V^*)\beta e^{-\lambda \tau_1},$$

$$a_{2} = \beta^{2}(S^{*} + \gamma^{2}V^{*})(I_{1}^{*} + (1 - p)I_{2}^{*})e^{-\lambda\tau_{1}} + \mu(\mu + \kappa + \sigma) + \gamma\beta^{2}(I_{1}^{*} + (1 - p)I_{2}^{*})^{2}$$

$$+\beta(\gamma\mu + \gamma\sigma + \kappa + \mu)(I_{1}^{*} + (1 - p)I_{2}^{*}) - \alpha\beta(1 - p)(S^{*} + \gamma V^{*})e^{-\lambda(\tau_{1} + \tau_{2})}$$

$$+(\mu + \alpha + d - (S^{*} + \gamma V^{*})\beta e^{-\lambda\tau_{1}})(2\mu + \kappa + \sigma + \beta(\gamma + 1)(I_{1}^{*} + (1 - p)I_{2}^{*}))$$

$$+(\mu + c + d)(3\mu + \kappa + \sigma + \alpha + d + \beta(\gamma + 1)(I_{1}^{*} + (1 - p)I_{2}^{*})$$

$$-\beta(S^{*} + \gamma V^{*})e^{-\lambda\tau_{1}}),$$

$$\begin{split} a_3 &= \left[\beta(S^* + \gamma V^*)(\kappa + \gamma \sigma) + \beta^2 \gamma (S^* + \gamma V^*)(I_1^* + (1-p)I_2^*)\right] [I_1^* \\ &+ (1-p)I_2^*]\beta e^{-\lambda \tau_1} \\ &+ \left[\mu(S^* + \gamma^2 V^*)\right] [I_1^* + (1-p)I_2^*] \beta^2 e^{-\lambda \tau_1} + \mu \left[\mu + \kappa + \sigma\right] \left[\mu + \alpha + d\right. \\ &- (S^* + \gamma V^*)\beta e^{-\lambda \tau_1}\right] \\ &+ \gamma \beta^2 \left[I_1^* + (1-p)I_2^*\right]^2 \left[\mu + \alpha + d - (S^* + \gamma V^*)\beta e^{-\lambda \tau_1}\right] \\ &+ \mu \left[\mu + c + d\right] \left[\mu + \kappa + \sigma\right] \\ &+ \beta \left[\gamma \mu + \gamma \sigma + \mu + \kappa\right] \left[I_1^* + (1-p)I_2^*\right] \left[\mu + \alpha + d - (S^* + \gamma V^*)\beta e^{-\lambda \tau_1}\right] \\ &+ \gamma \beta^2 \left[\mu + c + d\right] \left[I_1^* + (1-p)I_2^*\right]^2 + \beta^2 \left[\mu + c + d\right] (S^* + \gamma^2 V^*) \\ &\cdot \left[I_1^* + (1-p)I_2^*\right] e^{-\lambda \tau_1} \\ &+ \beta \left[\mu + c + d\right] \left[\gamma \mu + \gamma \sigma + \kappa + \mu\right] \left[I_1^* + (1-p)I_2^*\right] + \alpha \beta^2 (1-p)(S^* + \gamma^2 V^*) \\ &\cdot \left[I_1^* + (1-p)I_2^*\right] e^{-\lambda (\tau_1 + \tau_2)} \\ &+ \left[\mu + c + d\right] \left[2\mu + \kappa + \sigma + \beta (\gamma + 1)(I_1^* + (1-p)I_2^*)\right] \left[\mu + \alpha + d\right. \\ &- \beta (S^* + \gamma V^*) e^{-\lambda \tau_1}\right] \\ &- \alpha \beta (1-p)(S^* + \gamma V^*) \left[2\mu + \kappa + \sigma + \beta (\gamma + 1)(I_1^* + (1-p)I_2^*)\right] e^{-\lambda (\tau_1 + \tau_2)}, \end{split}$$

$$a_{4} = \left[\mu + c + d\right] \left[\beta(S^{*} + \gamma V^{*})(\kappa + \gamma \sigma) + \gamma \beta^{2}(S^{*} + \gamma V^{*})(I_{1}^{*} + (1 - p)I_{2}^{*})\right]$$

$$\cdot \left[I_{1}^{*} + (1 - p)I_{2}^{*}\right] \beta e^{-\lambda \tau_{1}} + \left[\mu + c + d\right] \mu(S^{*} + \gamma^{2}V^{*}) \left[I_{1}^{*} + (1 - p)I_{2}^{*}\right] \beta^{2}e^{-\lambda \tau_{1}}$$

$$+ \mu \left[\mu + c + d\right] \left[\kappa + \mu + \sigma\right] \left[\mu + \alpha + d - (S^{*} + \gamma V^{*})\beta e^{-\lambda \tau_{1}}\right]$$

$$+ \gamma \beta^{2} \left[\mu + c + d\right] \left[I_{1}^{*} + (1 - p)I_{2}^{*}\right]^{2} \left[\mu + \alpha + d - (S^{*} + \gamma V^{*})\beta e^{-\lambda \tau_{1}}\right]$$

$$+ \beta \left[\mu + c + d\right] \left[\gamma \mu + \gamma \sigma + \kappa + \mu\right] \left[I_{1}^{*} + (1 - p)I_{2}^{*}\right] \left[\mu + \alpha + d\right]$$

$$- (S^{*} + \gamma V^{*})\beta e^{-\lambda \tau_{1}}$$

$$+ \alpha \gamma \beta^{2} (1 - p)(S^{*}\sigma + \kappa V^{*}) \left[I_{1}^{*} + (1 - p)I_{2}^{*}\right] e^{-\lambda(\tau_{1} + \tau_{2})}$$

$$+ \alpha (\gamma \beta)^{2} (1 - p)V^{*} \left[\mu + \sigma + \beta(I_{1}^{*} + (1 - p)I_{2}^{*})\right] \left[I_{1}^{*} + (1 - p)I_{2}^{*}\right] e^{-\lambda(\tau_{1} + \tau_{2})}$$

$$+\alpha\beta^{2}(1-p)S^{*}\left[\mu+\kappa+\gamma\beta(I_{1}^{*}+(1-p)I_{2}^{*})\right]\left[I_{1}^{*}+(1-p)I_{2}^{*}\right]e^{-\lambda(\tau_{1}+\tau_{2})}$$
$$-\alpha\beta(1-p)(S^{*}+\gamma V^{*})\left[\mu(\kappa+\mu+\sigma)+\beta(\gamma\mu+\gamma\sigma+\kappa+\mu)(I_{1}^{*}+(1-p)I_{2}^{*})\right]e^{-\lambda(\tau_{1}+\tau_{2})}$$
$$-\alpha\beta(1-p)(S^{*}+\gamma V^{*})\left[\gamma\beta^{2}(I_{1}^{*}+(1-p)I_{2}^{*})^{2}\right]e^{-\lambda(\tau_{1}+\tau_{2})}.$$

By the Routh-Hurwitz criterion, all roots of the characteristics equation (7.20) have negative real parts and the endemic equilibrium \mathcal{E}^* of system (7.1) is locally asymptotically stable if $\tau_1 = \tau_2 = 0$, if and only if: $a_i > 0$ (i = 1, 2, 3, 4), $M_1 = a_1 > 0$,

$$M_{2} = \begin{bmatrix} a_{1} & a_{3} \\ 1 & a_{2} \end{bmatrix} > 0, \qquad M_{3} = \begin{bmatrix} a_{1} & a_{3} & a_{5} \\ 1 & a_{2} & a_{4} \\ 0 & a_{1} & a_{3} \end{bmatrix} > 0,$$

$$and$$

$$M_{4} = \begin{bmatrix} a_{1} & a_{3} & 0 & 0 \\ 1 & a_{2} & a_{4} & 0 \\ 0 & a_{1} & a_{3} & 0 \\ 0 & 1 & a_{2} & a_{4} \end{bmatrix} > 0. \tag{7.21}$$

Now, we wish to explore if there is a possibility of having complex roots with positive real part for (a) $\tau_1 > 0$, $\tau_2 = 0$ and (b) $\tau_1 = 0$, $\tau_2 > 0$. We now proceed to explore the above cases as follows:

(a) If $\tau_1 > 0$, $\tau_2 = 0$, then the characteristics equation (7.20) becomes

$$\lambda^4 + a_{11}\lambda^3 + a_{21}\lambda^2 + a_{31}\lambda + a_{41} = e^{-\lambda\tau_1}(m_{11}\lambda^3 + m_{21}\lambda^2 + m_{31}\lambda + m_{41}), (7.22)$$

with

$$a_{11} = 4\mu + \kappa + \alpha + \sigma + 2d + c + \beta(\gamma + 1)(I_1^* + (1-p)I_2^*),$$

$$a_{21} = \mu(\mu + \kappa + \sigma) + \gamma \beta^{2} (I_{1}^{*} + (1 - p)I_{2}^{*})^{2}$$

$$+ \beta(\gamma \mu + \gamma \sigma + \kappa + \mu) (I_{1}^{*} + (1 - p)I_{2}^{*})$$

$$+ (\mu + \alpha + d)(2\mu + \kappa + \sigma + \beta(\gamma + 1)(I_{1}^{*} + (1 - p)I_{2}^{*}))$$

$$+ (\mu + c + d)(3\mu + \kappa + \sigma + \alpha + d + \beta(\gamma + 1)(I_{1}^{*} + (1 - p)I_{2}^{*})),$$

$$\begin{split} a_{31} &= \mu \left[\mu + \kappa + \sigma \right] \left[\mu + \alpha + d \right] + \gamma \beta^{2} \left[I_{1}^{*} + (1 - p) I_{2}^{*} \right]^{2} \left[\mu + \alpha + d \right] \\ &+ \mu \left[\mu + c + d \right] \left[\mu + \kappa + \sigma \right] + \beta \left[\gamma \mu + \gamma \sigma + \mu + \kappa \right] \left[I_{1}^{*} + (1 - p) I_{2}^{*} \right] \\ &\cdot \left[\mu + \alpha + d \right] \\ &+ \gamma \beta^{2} \left[\mu + c + d \right] \left[I_{1}^{*} + (1 - p) I_{2}^{*} \right]^{2} \\ &+ \beta \left[\mu + c + d \right] \left[\gamma \mu + \gamma \sigma + \kappa + \mu \right] \left[I_{1}^{*} + (1 - p) I_{2}^{*} \right] \\ &+ \left[\mu + c + d \right] \left[2\mu + \kappa + \sigma + \beta (\gamma + 1) (I_{1}^{*} + (1 - p) I_{2}^{*}) \right] \left[\mu + \alpha + d \right] , \\ a_{41} &= \mu \left[\mu + c + d \right] \left[\kappa + \mu + \sigma \right] \left[\mu + \alpha + d \right] \\ &+ \gamma \beta^{2} \left[\mu + c + d \right] \left[I_{1}^{*} + (1 - p) I_{2}^{*} \right]^{2} \left[\mu + \alpha + d \right] \\ &+ \beta \left[\mu + c + d \right] \left[\gamma \mu + \gamma \sigma + \kappa + \mu \right] \left[I_{1}^{*} + (1 - p) I_{2}^{*} \right] \left[\mu + \alpha + d \right] , \end{split}$$

$$m_{11} = (S^* + \gamma V^*)\beta,$$

$$m_{21} = -\beta^{2}(S^{*} + \gamma^{2}V^{*})(I_{1}^{*} + (1 - p)I_{2}^{*}) + \alpha\beta(1 - p)(S^{*} + \gamma V^{*})$$
$$+(S^{*} + \gamma V^{*})\beta(2\mu + \kappa + \sigma + \beta(\gamma + 1)(I_{1}^{*} + (1 - p)I_{2}^{*}))$$
$$+(\mu + c + d)\beta(S^{*} + \gamma V^{*}),$$

$$m_{31} = -\left[\beta(S^* + \gamma V^*)(\kappa + \gamma \sigma) + \beta^2 \gamma(S^* + \gamma V^*)(I_1^* + (1 - p)I_2^*)\right] \times \left[I_1^* + (1 - p)I_2^*\right]\beta$$

$$-\left[\mu(S^* + \gamma^2 V^*)\right] \left[I_1^* + (1 - p)I_2^*\right]\beta^2 + \mu\left[\mu + \kappa + \sigma\right] \left[(S^* + \gamma V^*)\beta\right]$$

$$+\gamma\beta^2 \left[I_1^* + (1 - p)I_2^*\right]^2 \left[(S^* + \gamma V^*)\right]$$

$$+\beta\left[\gamma\mu + \gamma\sigma + \mu + \kappa\right] \left[I_1^* + (1 - p)I_2^*\right] \left[(S^* + \gamma V^*)\beta\right]$$

$$-\beta^2 \left[\mu + c + d\right] \left(S^* + \gamma^2 V^*\right) \left[I_1^* + (1 - p)I_2^*\right]$$

$$-\alpha\beta^2 (1 - p)(S^* + \gamma^2 V^*) \left[I_1^* + (1 - p)I_2^*\right]$$

$$+\left[\mu + c + d\right] \left[2\mu + \kappa + \sigma + \beta(\gamma + 1)(I_1^* + (1 - p)I_2^*)\right] \left[\beta(S^* + \gamma V^*)\right]$$

$$+\alpha\beta(1 - p)(S^* + \gamma V^*) \left[2\mu + \kappa + \sigma + \beta(\gamma + 1)(I_1^* + (1 - p)I_2^*)\right],$$

$$m_{41} = -\left[\mu + c + c\right] \left[\beta(S^* + \gamma V^*)(\kappa + \gamma \sigma) + \gamma \beta^2 (S^* + \gamma V^*)(I_1^* + (1 - p)I_2^*)\right] \left[I_1^* + (1 - p)I_2^*\right] \beta$$

$$-\left[\mu + c + d\right] \mu(S^* + \gamma^2 V^*) \left[I_1^* + (1 - p)I_2^*\right] \beta^2$$

$$+\mu \left[\mu + c + d\right] \left[\kappa + \mu + \sigma\right] \left[(S^* + \gamma V^*)\beta\right]$$

$$+\gamma \beta^2 \left[\mu + c + d\right] \left[I_1^* + (1 - p)I_2^*\right]^2 \left[(S^* + \gamma V^*)\beta\right]$$

$$+\beta \left[\mu + c + d\right] \left[\gamma \mu + \gamma \sigma + \kappa + \mu\right] \left[I_1^* + (1 - p)I_2^*\right] \left[(S^* + \gamma V^*)\beta\right]$$

$$-\alpha\gamma\beta^{2}(1-p)(S^{*}\sigma+\kappa V^{*})[I_{1}^{*}+(1-p)I_{2}^{*}]$$

$$-\alpha(\gamma\beta)^{2}(1-p)V^{*}[\mu+\sigma+\beta(I_{1}^{*}+(1-p)I_{2}^{*})][I_{1}^{*}+(1-p)I_{2}^{*}]$$

$$-\alpha\beta^{2}(1-p)S^{*}[\mu+\kappa+\gamma\beta(I_{1}^{*}+(1-p)I_{2}^{*})][I_{1}^{*}+(1-p)I_{2}^{*}]$$

$$+\alpha\beta(1-p)(S^{*}+\gamma V^{*})[\mu(\kappa+\mu+\sigma)$$

$$+\beta(\gamma\mu+\gamma\sigma+\kappa+\mu)(I_{1}^{*}+(1-p)I_{2}^{*})]$$

$$+\alpha\beta(1-p)(S^{*}+\gamma V^{*})[\gamma\beta^{2}(I_{1}^{*}+(1-p)I_{2}^{*})^{2}].$$

Now we need to show that all roots of (7.22) have negative real parts for all $\tau_1 \in (0, \tau^*)$. To do so, we show that (7.22) does not have any purely imaginary roots for all $\tau_1 \in (0, \tau^*)$. We assume that $\lambda = i\omega$ with $\omega > 0$ is a root of (7.22). Then ω must satisfy the following system:

$$\begin{cases} \omega^4 - a_{21}\omega^2 + a_{41} &= (m_{41} - m_{21}\omega^2)\cos(\omega\tau_1) + (m_{31}\omega - m_{11}\omega^3)\sin(\omega\tau_1), \\ a_{31}\omega - a_{11}\omega^3 &= (m_{31}\omega - m_{11}\omega^3)\cos(\omega\tau_1) - (m_{41} - m_{21}\omega^2)\sin(\omega\tau_1). \end{cases}$$

$$(7.23)$$

Now, we square both sides of each equation above and add the resulting equations, thus ω , must be a positive root of

$$\omega^8 + b_1 \omega^6 + b_2 \omega^4 + b_3 \omega^2 + b_4 = 0, \tag{7.24}$$

where

$$\begin{cases}
b_1 = a_{11}^2 - 2a_{21} - m_{11}^2, \\
b_2 = a_{21}^2 + 2(a_{41} - a_{11}a_{31} + m_{11}m_{31}) - m_{21}^2, \\
b_3 = a_{31}^2 + 2(m_{21}m_{41} - a_{21}a_{41}) - m_{31}^2, \\
b_4 = a_{41}^2 - m_{41}^2.
\end{cases} (7.25)$$

Let $z = \omega^2$, then (7.24) becomes

$$F(z) = z^4 + b_1 z^3 + b_2 z^2 + b_3 z + b_4 = 0. (7.26)$$

One can observe that, if $b_i \geq 0$, (i = 1, 2, 3, 4), then (7.26) has no positive roots. Therefore (7.22) does not have any purely imaginary roots for all $\tau_1 \in (0, \tau^*)$ so that all roots of the characteristic equation (7.22) have negative real parts and the endemic equilibrium \mathcal{E}^* of (7.1) is stable for all $\tau_1 \in (0, \tau^*)$.

(b) If $\tau_2 > 0$, $\tau_1 = 0$ then the characteristics equation (7.20) becomes

$$\lambda^4 + \alpha_{11}\lambda^3 + \alpha_{21}\lambda^2 + \alpha_{31}\lambda + \alpha_{41} = e^{-\lambda\tau_2}(n_{11}\lambda^3 + n_{21}\lambda^2 + n_{31}\lambda + n_{41}) \quad (7.27)$$

$$\alpha_{11} = 4\mu + \kappa + \alpha + \sigma + 2d + c + \beta(\gamma + 1)(I_1^* + (1-p)I_2^*) - (S^* + \gamma V^*)\beta,$$

$$\alpha_{21} = \beta^{2}(S^{*} + \gamma^{2}V^{*})(I_{1}^{*} + (1 - p)I_{2}^{*}) + \mu(\mu + \kappa + \sigma)$$

$$+\gamma\beta^{2}(I_{1}^{*} + (1 - p)I_{2}^{*})^{2} + \beta(\gamma\mu + \gamma\sigma + \kappa + \mu)(I_{1}^{*} + (1 - p)I_{2}^{*})$$

$$+(\mu + \alpha + d - (S^{*} + \gamma V^{*})\beta)(2\mu + \kappa + \sigma + \beta(\gamma + 1)(I_{1}^{*} + (1 - p)I_{2}^{*}))$$

$$+(\mu + c + d)(3\mu + \kappa + \sigma + \alpha + d + \beta(\gamma + 1)(I_{1}^{*} + (1 - p)I_{2}^{*})$$

$$-\beta(S^{*} + \gamma V^{*})),$$

$$\alpha_{31} = \left[\beta(S^* + \gamma V^*)(\kappa + \gamma \sigma) + \beta^2 \gamma(S^* + \gamma V^*)(I_1^* + (1 - p)I_2) \right] [I_1^* + (1 - p)I_2^*] \beta + \left[\mu(S^* + \gamma^2 V^*) \right] [I_1^* + (1 - p)I_2^*] \beta^2$$

$$+ \mu \left[\mu + \kappa + \sigma \right] \left[\mu + \alpha + d - (S^* + \gamma V^*) \beta \right]$$

$$+ \gamma \beta^2 \left[I_1^* + (1 - p)I_2^* \right]^2 \left[\mu + \alpha + d - (S^* + \gamma V^*) \beta \right]$$

$$+ \mu \left[\mu + c + d \right] \left[\mu + \kappa + \sigma \right]$$

$$+ \beta \left[\gamma \mu + \gamma \sigma + \mu + \kappa \right] \left[I_1^* + (1 - p)I_2^* \right] \left[\mu + \alpha + d - (S^* + \gamma V^*) \beta \right]$$

$$+ \gamma \beta^2 \left[\mu + c + d \right] \left[I_1^* + (1 - p)I_2^* \right]^2$$

$$+ \beta^2 \left[\mu + c + d \right] \left[\gamma \mu + \gamma \sigma + \kappa + \mu \right] \left[I_1^* + (1 - p)I_2^* \right]$$

$$+ \beta \left[\mu + c + d \right] \left[\gamma \mu + \gamma \sigma + \kappa + \mu \right] \left[I_1^* + (1 - p)I_2^* \right]$$

$$+ \left[\mu + c + d \right] \left[2\mu + \kappa + \sigma + \beta(\gamma + 1)(I_1^* + (1 - p)I_2^*) \right]$$

$$\cdot \left[\mu + \alpha + d - \beta(S^* + \gamma V^*) \right].$$

$$\alpha_{41} = [\mu + c + c] \left[\beta (S^* + \gamma V^*)(\kappa + \gamma \sigma) + \gamma \beta^2 (S^* + \gamma V^*)(I_1^* + (1 - p)I_2^*) \right]$$

$$\cdot [I_1^* + (1 - p)I_2^*] \beta$$

$$+ [\mu + c + d] \mu (S^* + \gamma^2 V^*) \left[I_1^* + (1 - p)I_2^* \right] \beta^2$$

$$+ \mu \left[\mu + c + d \right] \left[\kappa + \mu + \sigma \right] \left[\mu + \alpha + d - (S^* + \gamma V^*) \beta \right]$$

$$+ \gamma \beta^2 \left[\mu + c + d \right] \left[I_1^* + (1 - p)I_2^* \right]^2 \left[\mu + \alpha + d - (S^* + \gamma V^*) \beta \right]$$

$$+ \beta \left[\mu + c + d \right] \left[\gamma \mu + \gamma \sigma + \kappa + \mu \right] \left[I_1^* + (1 - p)I_2^* \right] \left[\mu + \alpha + d - (S^* + \gamma V^*) \beta \right]$$

$$- (S^* + \gamma V^*) \beta \right],$$

$$n_{11} = 0, \quad n_{21} = \alpha \beta (1 - p)(S^* + \gamma V^*)$$

$$n_{31} = -\alpha \beta^2 (1-p)(S^* + \gamma^2 V^*) [I_1^* + (1-p)I_2^*]$$

$$\alpha\beta(1-p)(S^*+\gamma V^*)[2\mu+\kappa+\sigma+\beta(\gamma+1)(I_1^*+(1-p)I_2^*)],$$

$$n_{41} = -\alpha \gamma \beta^{2} (1-p) (S^{*}\sigma + \kappa V^{*}) [I_{1}^{*} + (1-p)I_{2}^{*}]$$

$$-\alpha (\gamma \beta)^{2} (1-p) V^{*} [\mu + \sigma + \beta (I_{1}^{*} + (1-p)I_{2}^{*})] [I_{1}^{*} + (1-p)I_{2}^{*}]$$

$$-\alpha \beta^{2} (1-p) S^{*} [\mu + \kappa + \gamma \beta (I_{1}^{*} + (1-p)I_{2}^{*})] [I_{1}^{*} + (1-p)I_{2}^{*}]$$

$$+\alpha \beta (1-p) (S^{*} + \gamma V^{*}) [\mu (\kappa + \mu + \sigma) + \beta (\gamma \mu + \gamma \sigma + \kappa + \mu)$$

$$.(I_{1}^{*} + (1-p)I_{2}^{*})]$$

$$+\alpha \beta (1-p) (S^{*} + \gamma V^{*}) [\gamma \beta^{2} (I_{1}^{*} + (1-p)I_{2}^{*})^{2}].$$

Using the same discussion as in the above case then (7.27) can be written as

$$h(z) = z^4 + c_1 z^3 + c_2 z^2 + c_3 z + c_4 = 0 (7.28)$$

with

$$\begin{cases}
c_1 = \alpha_{11}^2 - 2\alpha_{21}, \\
c_2 = \alpha_{21}^2 + 2(\alpha_{41} - \alpha_{11}\alpha_{31}) - n_{21}^2, \\
c_3 = \alpha_{31}^2 + 2(n_{21}n_{41} - \alpha_{21}\alpha_{41}) - n_{31}^2, \\
c_4 = \alpha_{41}^2 - n_{41}^2.
\end{cases} (7.29)$$

It follows that all roots of (7.27) have negative real parts for $\tau_2(0, \tau_2^*)$ when $c_j \geq 0$, j = 1, 2, 3, 4 and this implies that endemic equilibrium is locally asymptotically stable for $\tau_2 \in (0, \tau_2^*)$. This completes the proof.

We now explore the global stability of the endemic equilibrium.

Theorem 7.3.6 If $\mathcal{R}_0 > 1$, then \mathcal{E}^* is globally asymptotically stable.

Proof 21 Let us consider the Lyapunov function

$$\mathcal{W}(t) = \mathcal{W}_1(t) + \mathcal{W}_2(t) + \mathcal{W}_3. \tag{7.30}$$

Here,

$$\mathcal{W}_{1}(t) = \left\{ S(t) - S^{*} - S^{*} \ln \left(\frac{S(t)}{S^{*}} \right) \right\} + \left\{ V(t) - V^{*} - V^{*} \ln \left(\frac{V(t)}{V^{*}} \right) \right\}
+ \left\{ I_{1}(t) - I_{1}^{*} - I_{1}^{*} \ln \left(\frac{I_{1}(t)}{I_{1}^{*}} \right) \right\}
+ \frac{\beta(1 - p)(S^{*} + \gamma V^{*})I_{2}^{*}}{\alpha I_{1}^{*}} \left\{ I_{2}(t) - I_{2}^{*} - I_{2}^{*} \ln \left(\frac{I_{2}(t)}{I_{2}^{*}} \right) \right\},$$

$$\mathcal{W}_{2}(t) = \beta S^{*} I_{1}^{*} \int_{0}^{\tau_{1}} \left\{ \frac{I_{1}(t-\omega)S(t-\omega)}{S^{*}I_{1}^{*}} - 1 - \ln\left(\frac{I_{1}(t-\omega)S(t-\omega)}{S^{*}I_{1}^{*}}\right) \right\} d\omega \\
+ \beta \gamma V^{*} I_{1}^{*} \int_{0}^{\tau_{1}} \left\{ \frac{I_{1}(t-\omega)V(t-\omega)}{V^{*}I_{1}^{*}} - 1 - \ln\left(\frac{I_{1}(t-\omega)V(t-\omega)}{V^{*}I_{1}^{*}}\right) \right\} d\omega \\
+ \beta (1-p)S^{*}I_{2}^{*} \int_{0}^{\tau_{1}} \left\{ \frac{I_{2}(t-\omega)S(t-\omega)}{S^{*}I_{2}^{*}} - 1 - \ln\left(\frac{I_{2}(t-\omega)S(t-\omega)}{S^{*}I_{2}^{*}}\right) \right\} d\omega \\
+ \beta \gamma (1-p)V^{*}I_{2}^{*} \int_{0}^{\tau_{1}} \left\{ \frac{I_{2}(t-\omega)V(t-\omega)}{V^{*}I_{2}^{*}} - 1 - \ln\left(\frac{I_{2}(t-\omega)V(t-\omega)}{V^{*}I_{2}^{*}}\right) \right\} d\omega ,$$

$$\mathcal{W}_{3}(t) = \beta (1-p)(S^{*} + \gamma V^{*})I_{2}^{*} \int_{0}^{\tau_{2}} \left\{ \frac{I_{1}(t-\omega)}{I_{1}^{*}} - 1 - \ln\left(\frac{I_{1}(t-\omega)}{I_{1}^{*}}\right) \right\} d\omega . (7.31)$$

The derivatives of $W_1(t)$ are given by

$$\frac{dW_1(t)}{dt} = \left(1 - \frac{S^*}{S(t)}\right) \frac{dS}{dt} + \left(1 - \frac{V^*}{V(t)}\right) \frac{dV}{dt} + \left(1 - \frac{I_1^*}{I_1(t)}\right) \frac{dI_1}{dt} + \frac{\beta(1-p)(S^* + \gamma V^*)I_2^*}{\alpha I_1^*} \left(1 - \frac{I_2^*}{I_2(t)}\right) \frac{dI_2}{dt}.$$
(7.32)

Substituting the appropriate differentials from (7.1) we have

$$\frac{dW_{1}(t)}{dt} = \left\{ 1 - \frac{S^{*}}{S(t)} \right\} \left\{ A - \beta [I_{1}(t) + (1-p)I_{2}(t)]S(t) - (\mu + \sigma)S(t) + \kappa V(t) \right\}
+ \left\{ 1 - \frac{V^{*}}{V(t)} \right\} \left\{ \sigma S(t) - \gamma \beta [I_{1}(t) + (1-p)I_{2}(t)]V(t) - (\mu + \kappa)V(t) \right\}
+ \left\{ 1 - \frac{I_{1}^{*}}{I_{1}(t)} \right\} \left\{ \beta [I_{1}(t - \tau_{1}) + (1-p)I_{2}(t - \tau_{1})][S(t - \tau_{1}) \right\}
+ \gamma V(t - \tau_{1})] - k_{1}I_{1}(t) \right\}
+ \frac{\beta (1-p)(S^{*} + \gamma V^{*})I_{2}^{*}}{\alpha I_{1}^{*}} \left\{ 1 - \frac{I_{2}^{*}}{I_{2}(t)} \right\} \left\{ \alpha I_{1}(t - \tau_{2}) - k_{2}I_{2}(t) \right\}.$$
(7.33)

At endemic equilibrium, we have

$$\begin{cases}
A &= \beta[I_1^* + (1-p)I_2^*]S^* + (\mu+\sigma)S^* - \kappa V^*, \\
(\mu+\kappa)V^* &= \sigma S^* - \gamma \beta[I_1^* + (1-p)I_2^*]V^*, \\
k_1I_1^* &= \beta[I_1^* + (1-p)I_2^*][S^* + \gamma V^*], \\
k_2I_2^* &= \alpha I_1^*.
\end{cases} (7.34)$$

Using the above constants we have

$$\frac{d\mathcal{W}_{1}(t)}{dt} = \mu S^{*} \left(2 - \frac{S(t)}{S^{*}} - \frac{S^{*}}{S(t)} \right) + \kappa V^{*} \left(2 - \frac{S(t)}{S^{*}} \cdot \frac{V^{*}}{V(t)} - \frac{S^{*}}{S(t)} \cdot \frac{V(t)}{V^{*}} \right)$$

$$+\mu V^* \left(3 - \frac{S^*}{S(t)} - \frac{V(t)}{V^*} - \frac{S(t)}{S^*} \cdot \frac{V^*}{V(t)}\right)$$

$$+\beta I_1^* S^* \left(2 - \frac{S(t)}{S^*} \cdot \frac{I_1(t)}{I_1^*} - \frac{S^*}{S(t)}\right)$$

$$+\beta (1-p) S^* I_2^* \left(2 - \frac{S(t)}{S^*} \cdot \frac{I_2(t)}{I_2^*} - \frac{S^*}{S(t)} - \frac{I_1(t)}{I_1^*}\right)$$

$$+\beta \gamma V^* I_1^* \left(3 - \frac{S^*}{S(t)} - \frac{I_1(t)}{I_1^*} \cdot \frac{V(t)}{V^*} - \frac{S(t)}{S^*} \cdot \frac{V^*}{V(t)}\right)$$

$$+\beta \gamma (1-p) V^* I_2^* \left(3 - \frac{S^*}{S(t)} - \frac{S(t)}{S^*} \cdot \frac{V^*}{V(t)} - \frac{I_2(t)}{I_2^*} \cdot \frac{V(t)}{V^*} - \frac{I_1(t)}{I_1^*}\right)$$

$$+\beta I_1(t-\tau_1) S(t-\tau_1) \left(1 - \frac{I_1^*}{I_1(t)}\right)$$

$$+\beta (1-p) I_2(t-\tau_1) S(t-\tau_1) \left(1 - \frac{I_1^*}{I_1(t)}\right)$$

$$+\beta \gamma I_1(t-\tau_1) V(t-\tau_1) \left(1 - \frac{I_1^*}{I_1(t)}\right)$$

$$+\beta \gamma (1-p) I_2(t-\tau_1) V(t-\tau_1) \left(1 - \frac{I_1^*}{I_1(t)}\right)$$

$$+\beta \gamma (1-p) I_1(t-\tau_2) S^* \left(\frac{I_2^*}{I_1^*} - \frac{I_2^*}{I_2(t)} \cdot \frac{I_2^*}{I_1^*}\right)$$

$$+\beta \gamma (1-p) I_1(t-\tau_2) V^* \left(\frac{I_2^*}{I_1^*} - \frac{I_2^*}{I_2(t)} \cdot \frac{I_2^*}{I_1^*}\right) .$$

$$(7.35)$$

The derivatives of W_2 are given by

$$\begin{split} \frac{d\mathcal{W}_{2}(t)}{dt} &= \beta S^{*}I_{1}^{*}\frac{d}{dt}\int_{0}^{\tau_{1}}\Big\{\frac{I_{1}(t-\omega)S(t-\omega)}{S^{*}I_{1}^{*}} - 1 - \ln\Big(\frac{I_{1}(t-\omega)S(t-\omega)}{S^{*}I_{1}^{*}}\Big)\Big\}d\omega \\ &+ \beta \gamma V^{*}I_{1}^{*}\frac{d}{dt}\int_{0}^{\tau_{1}}\Big\{\frac{I_{1}(t-\omega)V(t-\omega)}{V^{*}I_{1}^{*}} - 1 \\ &- \ln\Big(\frac{I_{1}(t-\omega)V(t-\omega)}{V^{*}I_{1}^{*}}\Big)\Big\}d\omega \\ &+ \beta (1-p)S^{*}I_{2}^{*}\frac{d}{dt}\int_{0}^{\tau_{1}}\Big\{\frac{I_{2}(t-\omega)S(t-\omega)}{S^{*}I_{2}^{*}} - 1 \\ &- \ln\Big(\frac{I_{2}(t-\omega)S(t-\omega)}{S^{*}I_{2}^{*}}\Big)\Big\}d\omega \\ &+ \beta \gamma (1-p)V^{*}I_{2}^{*}\frac{d}{dt}\int_{0}^{\tau_{1}}\Big\{\frac{I_{2}(t-\omega)V(t-\omega)}{V^{*}I_{2}^{*}} - 1 \\ &- \ln\Big(\frac{I_{2}(t-\omega)V(t-\omega)}{V^{*}I_{2}^{*}}\Big)\Big\}d\omega \\ &= \beta S^{*}I_{1}^{*}\int_{0}^{\tau_{1}}\frac{d}{dt}\Big\{\frac{I_{1}(t-\omega)S(t-\omega)}{S^{*}I_{1}^{*}} - 1 - \ln\Big(\frac{I_{1}(t-\omega)S(t-\omega)}{S^{*}I_{1}^{*}}\Big)\Big\}d\omega \\ &+ \beta \gamma V^{*}I_{1}^{*}\int_{0}^{\tau_{1}}\frac{d}{dt}\Big\{\frac{I_{1}(t-\omega)V(t-\omega)}{V^{*}I_{1}^{*}} - 1 \\ &- \ln\Big(\frac{I_{1}(t-\omega)V(t-\omega)}{V^{*}I_{1}^{*}}\Big)\Big\}d\omega \end{split}$$

$$\begin{split} &+\beta(1-p)S^*I_2^*\int_0^{\tau_1}\frac{d}{dt}\Big\{\frac{I_2(t-\omega)S(t-\omega)}{S^*I_2^*}-1\\ &-\ln\Big(\frac{I_2(t-\omega)S(t-\omega)}{S^*I_2^*}\Big)\Big\}d\omega\\ &+\beta\gamma(1-p)V^*I_2^*\int_0^{\tau_1}\frac{d}{dt}\Big\{\frac{I_2(t-\omega)V(t-\omega)}{V^*I_2^*}-1\\ &-\ln\Big(\frac{I_2(t-\omega)V(t-\omega)}{V^*I_2^*}\Big)\Big\}d\omega,\\ &=-\beta S^*I_1^*\int_0^{\tau_1}\frac{d}{d\omega}\Big\{\frac{I_1(t-\omega)S(t-\omega)}{S^*I_1^*}-1-\ln\Big(\frac{I_1(t-\omega)S(t-\omega)}{S^*I_1^*}\Big)\Big\}d\omega\\ &-\beta\gamma V^*I_1^*\int_0^{\tau_1}\frac{d}{d\omega}\Big\{\frac{I_1(t-\omega)V(t-\omega)}{V^*I_1^*}-1\\ &-\ln\Big(\frac{I_1(t-\omega)V(t-\omega)}{V^*I_1^*}\Big)\Big\}d\omega\\ &-\beta(1-p)S^*I_2^*\int_0^{\tau_1}\frac{d}{d\omega}\Big\{\frac{I_2(t-\omega)S(t-\omega)}{S^*I_2^*}-1\\ &-\ln\Big(\frac{I_2(t-\omega)S(t-\omega)}{S^*I_2^*}\Big)\Big\}d\omega\\ &-\beta\gamma(1-p)V^*I_2^*\int_0^{\tau_1}\frac{d}{d\omega}\Big\{\frac{I_2(t-\omega)V(t-\omega)}{V^*I_2^*}-1\\ &-\ln\Big(\frac{I_2(t-\omega)V(t-\omega)}{V^*I_2^*}\Big)\Big\}d\omega\\ &=\beta S^*I_1^*\Big[\frac{I_1(t)S(t)}{S^*I_1^*}-\frac{I_1(t-\tau_1)S(t-\tau_1)}{S^*I_1^*}+\ln\Big(\frac{I_1(t-\tau_1)S(t-\tau_1)}{I_1(t)S(t)}\Big)\Big]\\ &+\beta\gamma V^*I_1^*\Big[\frac{I_1(t)V(t)}{S^*I_2^*}-\frac{I_1(t-\tau_1)V(t-\tau_1)}{V^*I_2^*}\\ &+\ln\Big(\frac{I_2(t-\tau_1)V(t-\tau_1)}{I_1(t)V(t)}\Big)\Big]\\ &+\beta(1-p)S^*I_2^*\Big[\frac{I_2(t)S(t)}{S^*I_2^*}-\frac{I_2(t-\tau_1)S(t-\tau_1)}{S^*I_2^*}\\ &+\ln\Big(\frac{I_2(t-\tau_1)S(t-\tau_1)}{I_2(t)V(t)}\Big)\Big]\\ &+\beta\gamma(1-p)V^*I_2^*\Big[\frac{I_2(t)V(t)}{S^*I_2^*}-\frac{I_2(t-\tau_1)V(t-\tau_1)}{V^*I_2^*}\\ &+\ln\Big(\frac{I_2(t-\tau_1)S(t-\tau_1)}{I_2(t)V(t)}\Big)\Big]\\ &=\beta I_1^*S^*.\frac{S(t)}{S^*}.\frac{I_1(t)}{I_1^*}+\beta\gamma I_1^*V^*.\frac{V(t)}{V^*}.\frac{I_1(t)}{I_1^*}\\ &-\beta I_1(t-\tau_1)S(t-\tau_1)-\beta\gamma I_1(t-\tau_1)V(t-\tau_1)\\ &-\beta(1-p)I_2(t-\tau_1)S(t-\tau_1)-\beta\gamma I_1(t-\tau_1)V(t-\tau_1)\\ &-\beta(1-p)I_2(t-\tau_1)S(t-\tau_1)\\ &-\beta(1-p)I_2(t-\tau_1)S(t-\tau_1)-\beta\gamma I_1(t-\tau_1)V(t-\tau_1)\\ &-\beta(1-p)I_2(t-\tau_1)S(t-\tau_1)\\ &-\beta(1-p)I_2(t$$

$$-\beta \gamma (1-p) I_{2}(t-\tau_{1}) V(t-\tau_{1}) + \beta S^{*} I_{1}^{*} \ln \left(\frac{I_{1}(t-\tau_{1}) S(t-\tau_{1})}{I_{1}(t) S(t)} \right)$$

$$+\beta \gamma V^{*} I_{1}^{*} \ln \left(\frac{I_{1}(t-\tau_{1}) V(t-\tau_{1})}{I_{1}(t) V(t)} \right)$$

$$+\beta (1-p) S^{*} I_{2}^{*} \ln \left(\frac{I_{2}(t-\tau_{1}) S(t-\tau_{1})}{I_{2}(t) S(t)} \right)$$

$$+\beta \gamma (1-p) V^{*} I_{2}^{*} \ln \left(\frac{I_{2}(t-\tau_{1}) V(t-\tau_{1})}{I_{2}(t) V(t)} \right).$$

$$(7.36)$$

The derivatives of $W_3(t)$ are given by

$$\frac{dW_{3}(t)}{dt} = \beta(1-p)(S^{*} + \gamma V^{*})I_{2}^{*}\frac{d}{dt}\int_{0}^{\tau_{2}} \left\{\frac{I_{1}(t-\omega)}{I_{1}^{*}} - 1 - \ln\left(\frac{I_{1}(t-\omega)}{I_{1}^{*}}\right)\right\}d\omega$$

$$= \beta(1-p)(S^{*} + \gamma V^{*})I_{2}^{*}\int_{0}^{\tau_{2}}\frac{d}{dt}\left\{\frac{I_{1}(t-\omega)}{I_{1}^{*}} - 1 - \ln\left(\frac{I_{1}(t-\omega)}{I_{1}^{*}}\right)\right\}d\omega$$

$$= -\beta(1-p)(S^{*} + \gamma V^{*})I_{2}^{*}\int_{0}^{\tau_{2}}\frac{d}{d\omega}\left\{\frac{I_{1}(t-\omega)}{I_{1}^{*}} - 1 - \ln\left(\frac{I_{1}(t-\omega)}{I_{1}^{*}}\right)\right\}d\omega$$

$$= \beta(1-p)(S^{*} + \gamma V^{*})I_{2}^{*}\left\{\frac{I_{1}(t)}{I_{1}^{*}} - \frac{I_{1}(t-\tau_{2})}{I_{1}^{*}} + \ln\left(\frac{I_{1}(t-\tau_{2})}{I_{1}(t)}\right)\right\}$$

$$= \beta(1-p)S^{*}I_{2}^{*}.\frac{I_{1}(t)}{I_{1}^{*}} + \beta\gamma(1-p)V^{*}I_{2}^{*}.\frac{I_{1}(t)}{I_{1}^{*}} - \beta(1-p)S^{*}I_{2}^{*}I_{1}(t-\tau_{2}).\frac{1}{I_{1}^{*}}$$

$$- \beta\gamma(1-p)V^{*}I_{2}^{*}I_{1}(t-\tau_{2}).\frac{1}{I_{1}^{*}} + \beta(1-p)S^{*}I_{2}^{*}\ln\left(\frac{I_{1}(t-\tau_{2})}{I_{1}(t)}\right)$$

$$+ \beta\gamma(1-p)V^{*}I_{2}^{*}\ln\left(\frac{I_{1}(t-\tau_{2})}{I_{1}(t)}\right).$$
(7.37)

Combining the derivatives of $W_j(t)$, for j = 1, 2, 3, we have

$$\frac{d\mathcal{W}(t)}{dt} = \mu S^* \left\{ 2 - \frac{S(t)}{S^*} - \frac{S^*}{S(t)} \right\} + \kappa V^* \left\{ 2 - \frac{S(t)V^*}{S^*V(t)} - \frac{S^*V(t)}{S(t)V^*} \right\}$$

$$+ \mu V^* \left\{ 3 - \frac{S^*}{S(t)} - \frac{V(t)}{V^*} - \frac{S(t)V^*}{S^*V(t)} \right\}$$

$$+ \beta I_1^* S^* \left\{ 2 - \frac{S^*}{S(t)} - \frac{S(t - \tau_1)I_1(t - \tau_1)}{S^*I_1(t)} + \ln \left(\frac{I_1(t - \tau_1)S(t - \tau_1)}{I_1(t)S(t)} \right) \right\}$$

$$+ \beta (1 - p) S^* I_2^* \left\{ 2 - \frac{S^*}{S(t)} - \frac{S(t - \tau_1)I_2(t - \tau_1)I_1^*}{S^*I_2^*I_1(t)} - \frac{I_1(t - \tau_2)I_2^*}{I_1^*I_2(t)} \right\}$$

$$+ \ln \left(\frac{I_2(t - \tau_1)S(t - \tau_1)I_1(t - \tau_2)}{I_2(t)S(t)I_1(t)} \right) \right\}$$

$$+ \beta \gamma V^* I_1^* \left\{ 3 - \frac{S^*}{S(t)} - \frac{S(t)V^*}{S^*V} - \frac{V(t - \tau_1)I_1(t - \tau_1)}{V^*I_1(t)} \right\}$$

$$+ \ln \left(\frac{I_1(t - \tau_1)V(t - \tau_1)}{I_1(t)V(t)} \right) \right\}$$

$$+\beta\gamma(1-p)V^*I_2^*\left\{3-\frac{S^*}{S(t)}-\frac{S(t)V^*}{S^*V(t)}-\frac{V(t-\tau_1)I_1^*I_2(t-\tau_1)}{V^*I_1(t)I_2^*}\right.\\ \left.-\frac{I_1(t-\tau_2)I_2^*}{I_1^*I_2(t)}+\ln\left(\frac{I_2(t-\tau_1)V(t-\tau_1)I_1(t-\tau_2)}{I_2(t)V(t)I_1(t)}\right)\right\}.$$

Note that

$$2 \le \frac{S(t)}{S^*} + \frac{S^*}{S(t)}, \quad 2 \le \frac{S(t)V^*}{S^*V(t)} + \frac{S^*V(t)}{S(t)V^*}, \quad 3 \le \frac{S^*}{S(t)} + \frac{V(t)}{V^*} + \frac{S(t)V^*}{S^*V(t)} \quad (7.38)$$

for all S(t) > 0 and V(t) > 0, because the arithmetic mean is greater than or equal to the geometric mean. Further, note that $G(t) = 1 - g(t) + \ln g(t)$ is always nonpositive for any function g(t) > 0, and g(t) = 0 if and only if g(t) = 1. Hence, it follows that $W(t) \leq 0$ and consequently, $\dot{W}(t) \leq 0$. Moreover, the largest invariant set of $\dot{W}(t) = 0$ is a singleton where $S(t) \equiv S^*$, $V(t) \equiv V^*$, $I_1(t) \equiv I_1^*$, and $I_2(t) \equiv I_2^*$. Using the LaSalle's invariance principle [46], we conclude that the endemic equilibrium point \mathcal{E}^* is globally asymptotically stable if $\mathcal{R}_0 > 1$.

7.3.7 Hopf bifurcation analysis

In this section we determine criteria for Hopf bifurcation to occur using the time delay τ_1 and τ_2 as the bifurcation parameters to find the interval in which the infected equilibria is stable and unstable out of the same margins. Now to consider Hopf bifurcation we consider the cases (a) $\tau_1 = \tau_{10} > 0$, $\tau_2 = 0$ and (b) $\tau_2 = \tau_{20} > 0$ and $\tau_1 = 0$. Our analysis is as follows:

(a) When $\tau_1 = \tau_{10} > 0$ and $\tau_2 = 0$ we need to show that $\frac{dRe\lambda(\tau_{10})}{d\tau_1} > 0$ differentiating (7.22) with respect to τ_1 we get

$$\begin{cases} (4\lambda^3 + 3a_{11}\lambda^2 + 2a_{21}\lambda + a_{31})\frac{d\lambda}{d\tau_1} \\ = \left[-\tau_1 e^{-\lambda\tau_1} (m_{11}\lambda^3 + m_{21}\lambda^2 + m_{31}\lambda + m_{41}) + e^{-\lambda\tau_1} (3m_{11}\lambda^2 + 2m_{21}\lambda + m_{31}) \right] \frac{d\lambda}{d\tau_1} - \lambda e^{\lambda\tau_1} (m_{11}\lambda^3 + m_{21}\lambda^2 + m_{31}\lambda + m_{41}). \end{cases}$$

This gives

$$\left(\frac{d\lambda}{d\tau_{1}}\right)^{-1} = \frac{4\lambda^{3} + 3a_{11}\lambda^{2} + 2a_{21}\lambda + a_{31}}{-\lambda e^{-\lambda\tau_{1}}(m_{11}\lambda^{3} + m_{21}\lambda^{2} + m_{31}\lambda + m_{41})} + \frac{3m_{11}\lambda^{2} + 2m_{21}\lambda + m_{31}}{\lambda(m_{11}\lambda^{3} + m_{21}\lambda^{2} + m_{31}\lambda + m_{41})} - \frac{\tau_{1}}{\lambda}$$

$$= \frac{3\lambda^{4} + 2a_{11}\lambda^{3} + a_{21}\lambda^{2} - a_{41}}{-\lambda^{2}(\lambda^{4} + a_{11}\lambda^{3} + a_{21}\lambda^{2} + a_{31}\lambda + a_{41})} + \frac{2m_{11}\lambda^{3} + m_{21}\lambda^{2} - m_{41}}{\lambda^{2}(m_{11}\lambda^{3} + m_{21}\lambda^{2} + m_{31}\lambda + m_{41})} - \frac{\tau_{1}}{\lambda}.$$

Thus,

$$\operatorname{sign}\left[\frac{d(Re\lambda)}{d\tau_1}\right]_{\lambda=i\omega_0} = \operatorname{sign}\left[Re\left(\frac{d\lambda}{d\tau_1}\right)^{-1}\right]_{\lambda=i\omega_0}$$

$$= \operatorname{sign} \left[Re \left[\frac{3\lambda^4 + 2a_{11}\lambda^3 + a_{21}\lambda^2 - a_{41}}{-\lambda^2(\lambda^4 + a_{11}\lambda^3 + a_{21}\lambda^2 + a_{31}\lambda + a_{41})} \right]_{\lambda = i\omega_0} \right]$$

$$+ \operatorname{sign} \left[Re \left[\frac{2m_{11}\lambda^3 + m_{21}\lambda^2 - m_{41}}{\lambda^2(m_{11}\lambda^3 + m_{21}\lambda^2 + m_{31}\lambda + m_{41})} \right]_{\lambda = i\omega_0} \right]$$

$$= \operatorname{sign} \left[Re \left[\frac{3\omega_0^4 - 2a_{11}\omega_0^3i - a_{21}\omega_0^2 - a_{41}}{\omega_0^2(\omega_0^4 - a_{11}\omega_0^3i - a_{21}\omega_0^2 + a_{31}\omega_0i + a_{41})} \right] \right]$$

$$+ \operatorname{sign} \left[Re \left[\frac{-2m_{11}\omega_0^3i - m_{21}\omega_0^2 - m_{41}}{-\omega_0^2(-m_{11}\omega_0^3i - m_{21}\omega_0^2i + m_{31}\omega_0i + m_{41})} \right] \right]$$

$$= \operatorname{sign} \left[\frac{3\omega_0^8 + 2(a_{11}^2 - 2a_{21})\omega_0^6}{\omega_0^2[(\omega_0^4 - a_{21}\omega_0^2 + a_{41})^2 + (a_{31}\omega_0 - a_{11}\omega_0^3)^2]} \right]$$

$$+ \operatorname{sign} \left[\frac{(a_{21}^2 + 2(a_{41} - a_{11}a_{31}))\omega_0^4 - a_{41}^2}{\omega_0^2[(\omega_0^4 - a_{21}\omega_0^2 + a_{41})^2 + (a_{31}\omega_0 - a_{11}\omega_0^3)^2]} \right]$$

$$+ \operatorname{sign} \left[\frac{m_{41}^2 - 2m_{11}^2\omega_0^6 - (m_{21}^2 - 2m_{11}m_{11})\omega_0^4}{\omega_0^2[(m_{41} - m_{21}\omega_0^2)^2 + (m_{31}\omega_0 - m_{11}\omega_0^3)^2]} \right]$$

$$= \operatorname{sign} \left[\frac{3\omega_0^8 + 2(a_{11}^2 - m_{11}^2 - 2a_{21})\omega_0^6}{\omega_0^2 [(\omega_0^4 - a_{21}\omega_0^2 + a_{41})^2 + (a_{31}\omega_0 - a_{11}\omega_0^3)^2]} \right]$$

$$+ \operatorname{sign} \left[\frac{(a_{21}^2 - m_{21}^2 + 2(a_{41} + m_{11}m_{31} - a_{11}a_{31}))\omega_0^4 - a_{41}^2 + m_{41}^2}{\omega_0^2 [(\omega_0^4 - a_{21}\omega_0^2 + a_{41})^2 + (a_{31}\omega_0 - a_{11}\omega_0^3)^2]} \right]$$

$$= \operatorname{sign} \left[\frac{4\omega_0^6 + 3(a_{11}^2 - m_{11}^2 - 2a_{21})\omega_0^4}{[(\omega_0^4 - a_{21}\omega_0^2 + a_{41})^2 + (a_{31}\omega_0 - a_{11}\omega_0^3)^2]} \right]$$

+sign
$$\left[\frac{2(a_{21}^2 - m_{21}^2 + 2(a_{41} + m_{11}m_{31} - a_{11}a_{31}))\omega_0^2 + k_0}{[(\omega_0^4 - a_{21}\omega_0^2 + a_{41})^2 + (a_{31}\omega_0 - a_{11}\omega_0^3)^2]}\right].$$

with

$$k_0 = a_{31}^2 - m_{31}^2 + 2(m_{21}m_{41} - a_{21}a_{41}).$$

Lemma 7.1

Suppose that x_i , i = 1, 2, 3, 4, are the roots of equation $g(x) = x^4 + \vartheta_1 x^3 + \vartheta_2 x^2 + \vartheta_3 x + \vartheta_4 = 0$ ($\vartheta_3 < 0$) and x_4 is the largest positive root, then

$$\left\{\frac{dg(x)}{dx}\right\}_{x=x_4} > 0.$$

In our case considering $F(z) = z^4 + b_1 z^3 + b_2 z^2 + b_3 z + b_4 = 0$ defined in (7.26), and assuming $b_3 < 0$ and ω_0^2 as the largest positive root we have

$$\frac{dRe\lambda}{d\tau_1} = \frac{\frac{dF(z)}{dz}}{\left[(\omega_0^4 - a_{21}\omega_0^2 + a_{41})^2 + (a_{31}\omega_0 - a_{11}\omega_0^3)^2\right]} > 0.$$

The above analysis can be summarized into the following theorem:

Theorem 7.3.7 Suppose that (a) $\mathcal{R}_0 > 1$. If either (b) $b_4 < 0$ or (c) $b_4 \ge 0$ and $b_3 < 0$ is satisfied, and ω_0 is the largest positive simple root of (7.26) then the infected equilibrium \mathcal{E}^* of model (7.1) is locally asymptotically stable when $\tau_1 < \tau_{10}$ and unstable when $\tau_1 > \tau_{10}$ where

$$\tau_{10} = \frac{1}{\omega_0} \arccos \left[\frac{(m_{41} - m_{21}\omega_0^2)(\omega_0^4 - a_{21}\omega_0^2 + a_{41})}{(m_{41} - m_{21}\omega_0^2)^2 + (m_{31}\omega_0 - m_{11}\omega_0^3)^2} + \frac{(m_{31}\omega_0 - m_{11}\omega_0^3)(a_{31}\omega_0 - a_{11}\omega_0^3)}{(m_{41} - m_{21}\omega_0^2)^2 + (m_{31}\omega_0 - m_{11}\omega_0^3)^2} \right],$$

$$(7.39)$$

when $\tau_1 = \tau_{10}$, a Hopf bifurcation occurs, that is a family of periodic solutions bifurcates from \mathcal{E}^* as τ_1 passes through the critical value τ_{10} .

(b) When $\tau_2 = \tau_{20} > 0$ and $\tau_1 = 0$ we also need to show that $\frac{dRe\lambda(\tau_{20})}{d\tau_2} > 0$ differentiating (7.27) with respect to τ_2 we get

$$\begin{cases} (4\lambda^3 + 3\alpha_{11}\lambda^2 + 2\alpha_{21}\lambda + \alpha_{31})\frac{d\lambda}{d\tau_2} \\ = \left[-\tau_2 e^{-\lambda\tau_2} (n_{21}\lambda^2 + n_{31}\lambda + n_{41}) + e^{-\lambda\tau_2} (2n_{21}\lambda + n_{31}) \right] \frac{d\lambda}{d\tau_2} \\ -\lambda e^{\lambda\tau_2} (n_{31}\lambda + n_{41}). \end{cases}$$

This gives

$$\left(\frac{d\lambda}{d\tau_2}\right)^{-1} = \frac{4\lambda^3 + 3\alpha_{11}\lambda^2 + 2\alpha_{21}\lambda + \alpha_{31}}{-\lambda e^{-\lambda\tau_2}(n_{21}\lambda^2 + n_{31}\lambda + n_{41})} + \frac{2n_{21}\lambda + n_{31}}{\lambda(n_{21}\lambda^2 + n_{31}\lambda + n_{41})} - \frac{\tau_2}{\lambda}$$

$$= \frac{3\lambda^4 + 2\alpha_{11}\lambda^3 + \alpha_{21}\lambda^2 - \alpha_{41}}{-\lambda^2(\lambda^4 + \alpha_{11}\lambda^3 + \alpha_{21}\lambda^2 + \alpha_{31}\lambda + \alpha_{41})} + \frac{n_{21}\lambda^2 - n_{41}}{\lambda^2(n_{21}\lambda^2 + n_{31}\lambda + n_{41})} - \frac{\tau_2}{\lambda}.$$

Thus,

$$= \operatorname{sign} \left[\frac{3\omega_0^8 + 2(\alpha_{11}^2 - 2\alpha_{21})\omega_0^6}{\omega_0^2 [(\omega_0^4 - \alpha_{21}\omega_0^2 + \alpha_{41})^2 + (\alpha_{31}\omega_0 - \alpha_{11}\omega_0^3)^2]} \right]$$

$$+ \operatorname{sign} \left[\frac{(\alpha_{21}^2 - n_{21}^2 + 2(\alpha_{41} - \alpha_{11}\alpha_{31}))\omega_0^4}{\omega_0^2 [(\omega_0^4 - \alpha_{21}\omega_0^2 + \alpha_{41})^2 + (\alpha_{31}\omega_0 - \alpha_{11}\omega_0^3)^2]} \right]$$

$$+ \operatorname{sign} \left[\frac{-\alpha_{41}^2 + n_{41}^2}{\omega_0^2 [(\omega_0^4 - \alpha_{21}\omega_0^2 + \alpha_{41})^2 + (\alpha_{31}\omega_0 - \alpha_{11}\omega_0^3)^2]} \right]$$

$$= \operatorname{sign} \left[\frac{4\omega_0^6 + 3(\alpha_{11}^2 - 2\alpha_{21})\omega_0^4}{[(\omega_0^4 - \alpha_{21}\omega_0^2 + \alpha_{41})^2 + (\alpha_{31}\omega_0 - \alpha_{11}\omega_0^3)^2]} \right]$$

$$+ \operatorname{sign} \left[\frac{2(\alpha_{21}^2 - n_{21}^2 + 2(\alpha_{41} - \alpha_{11}\alpha_{31}))\omega_0^2}{[(\omega_0^4 - \alpha_{21}\omega_0^2 + \alpha_{41})^2 + (\alpha_{31}\omega_0 - \alpha_{11}\omega_0^3)^2]} \right]$$

$$+ \operatorname{sign} \left[\frac{\alpha_{31}^2 - n_{31}^2 + 2(n_{21}n_{41} - \alpha_{21}\alpha_{41})}{[(\omega_0^4 - \alpha_{21}\omega_0^2 + \alpha_{41})^2 + (\alpha_{31}\omega_0 - \alpha_{11}\omega_0^3)^2]} \right].$$

Lemma 7.2 Suppose that x_i , i = 1, 2, 3, 4, are the roots of equation $g(x) = x^4 + \varphi_1 x^3 + \varphi_2 x^2 + \varphi_3 x + \varphi_4 = 0$ ($\varphi_3 < 0$) and x_4 is the largest positive root, then

$$\left\{ \frac{dg(x)}{dx} \right\}_{x=x_4} > 0.$$

In our case considering $h(z) = z^4 + c_1 z^3 + c_2 z^2 + c_3 z + c_4 = 0$ defined in (7.28), and assuming $c_3 < 0$ and ω_0^2 as the largest positive root we have

$$\frac{dRe\lambda}{d\tau_2} = \frac{\frac{dh(z)}{dz}}{\left[(\omega_0^4 - \alpha_{21}\omega_0^2 + \alpha_{41})^2 + (\alpha_{31}\omega_0 - \alpha_{11}\omega_0^3)^2\right]} > 0.$$

The above analysis can be summarized into the following theorem:

Theorem 7.3.8 Suppose that (a) $\mathcal{R}_0 > 1$. If either (b) $c_4 < 0$ or (c) $c_4 \ge 0$ and $c_3 < 0$ is satisfied, and ω_0 is the largest positive simple root of (7.28) then the infected equilibrium \mathcal{E}^* of model (7.1) is locally asymptotically stable when $\tau_2 < \tau_{20}$ and unstable when $\tau_2 > \tau_{20}$ where

$$\tau_{20} = \frac{1}{\omega_0} \arccos \left[\frac{(n_{41} - n_{21}\omega_0^2)(\omega_0^4 - \alpha_{21}\omega_0^2 + \alpha_{41})}{(n_{41} - n_{21}\omega_0^2)^2 + n_{31}^2\omega_0^2} \right]$$

$$+\frac{n_{31}\omega_0(\alpha_{31}\omega_0 - \alpha_{11}\omega_0^3)}{(n_{41} - n_{21}\omega_0^2)^2 + n_{31}^2\omega_0^2}\Big],\tag{7.40}$$

when $\tau_2 = \tau_{20}$, a Hopf bifurcation occurs, that is a family of periodic solutions bifurcates from \mathcal{E}^* as τ_2 passes through the critical value τ_{20} .

From the analysis above, we can deduce that Hopf bifurcations may arise if conditions in Theorem 7.3.7 and 7.3.8 are satisfied. Thus, the introduction of time delay in system (7.1) can destabilize the system.

7.4 Numerical results

In order to explore the behavior of system (7.1) and illustrate the stability of the equilibria solutions, we numerically solve system (7.1) using MATLAB and parameter values adopted from Table 7.1.

Table 7.1: Model parameters and variables and their baseline values

Symbol Definition		Value	Unit	Source
\overline{d}	Elimination rate due to brucellosis,	0.15	$year^{-1}$	[30]
p	Fraction of infectious animals culled upon detection	on 0.5	-	[98]
β	Direct transmission rate	3.844×10^{-1}	6 animal ⁻¹ year	$^{1}[92]$
κ	Vaccination waning rate	0.4	$year^{-1}$	[30]
μ	Natural elimination rate	0.25	$year^{-1}$	[92]
γ	Modification factor	0.18	-	[30]
A	Recruitment rate	76434	animals $year^{-1}$	[92]
σ	Vaccination rate	0.316	$year^{-1}$	[30]
α	Detection rate	Varied	$year^{-1}$	-
c	Culling rate	0.15	$year^{-1}$	[30]

In Fig. 7.1 we illustrate the effects of varying the delay ($\tau_1 = \tau_2$) on the dynamics of system (7.1). Figure 7.1(a) and (b) demonstrate that the system approaches the stable disease-free or endemic equilibrium for $\mathcal{R}_0 < 1$ and $\mathcal{R}_0 > 1$, respectively. One should note that according to Theorem 7.3.2 and 7.3.6, the stability of the model steady states does not depend on the value of the time delays, but rather on the basic reproduction number \mathcal{R}_0 , only. In addition, we observe that the range of values for the two time delays does not lead to periodic solutions but an increase in

both delays translate to an increase in the infectious population, both detected and undetected.

Fig. 7.2 depicts the numbers of infectious undetected and infectious detected animals over time with varying delays. The results clearly show that the incubation related delay (τ_1) has more influence on shaping the dynamics of brucellosis compared to the culling related delay (τ_2). More precisely, the incubation period delay significantly increases the infectious population (both detected and undetected) for 0 < t < 20 and there after its impact will be the same as that of detection (τ_2).

In Fig. 7.3 we illustrate the stability of the disease-free equilibrium \mathcal{E}^0 with $\tau_1 = 30$ and $\tau_2 = 5$ (note that $\mathcal{R}_0 = 0.686281$). As we can observe, for certain parameter values and initial population levels, system (7.1) exhibits some periodic oscillation. Precisely, we note that the infected population $(I_1(t))$ and $I_2(t)$ oscillates with a reduced amplitude from the start till when t is approximately 400, thereafter the oscillations dies off the solutions converges to the disease-free equilibrium. These simulation results demonstrate the occurrence of periodic solutions through Hopf bifurcation for delay values $\tau_1 = 30$ and $\tau_2 = 5$. In contrast, we can observe that there are no periodic oscillations for the uninfected populations S(t) and V(t).

In Fig. 7.4, we demonstrate the dynamic for model system (7.1) with respect to the stability of infection-free equilibrium for different pair of delay values (τ_1, τ_2) and from the simulation results we can conclude that both delays do not have a huge influence on the stability of disease-free equilibrium.

In Fig. 7.5 we observe that for certain parameter values and initial population levels, system (7.1) may admit periodic oscillations when $\mathcal{R}_0 > 1$. As we can observes, when $\mathcal{R}_0 = 3.77333$ both the solutions of the infected and uninfected populations exhibits periodic oscillation for a certain period, before stability at endemic point is attained.

In Fig. 7.6, we illustrate the dynamics for model system (7.1) with respect to the stability of endemic equilibrium for several pair of delay values (τ_1, τ_2) . The results confirm that the incubation related delay τ_1 has more influence on shaping the dynamic of brucellosis compared to the culling related delay τ_2 .

To explore influence of model parameters on the reproduction number \mathcal{R}_0 , we perform a local sensitivity analysis of the basic reproduction number following the

approach in [99]. The local sensitivity analysis will be useful on identifying parameters with greatest influence to change \mathcal{R}_0 . To this end, denoting by Φ the generic parameter of system (7.1), we evaluate the *normalised sensitivity index*

$$S_{\Phi} = \frac{\Phi}{\mathcal{R}_0} \frac{\partial \mathcal{R}_0}{\partial \Phi},\tag{7.41}$$

which indicates how sensitive \mathcal{R}_0 is to a change of parameter Φ . Model parameters with positive index increase the value of \mathcal{R}_0 whenever they are increased while those with a negative index decrease the value of \mathcal{R}_0 whenever they are increased. We consider the parameter values in Table 1, and we set $\alpha = 0.015$ in order to evaluate the normalized sensitivity index and the results are depicted in Figure 7.7. Here, we observe that parameters A, β , κ , γ , have a positive correlation with \mathcal{R}_0 , such that increasing these parameters will increase \mathcal{R}_0 . However, it is the increase of A and β that has the greatest influence to change \mathcal{R}_0 . Precisely, increasing either A or β by 50% will increase \mathcal{R}_0 by 50%. We also note, that increasing parameters c, μ , σ , d, p, and α , will lower the reproduction number.

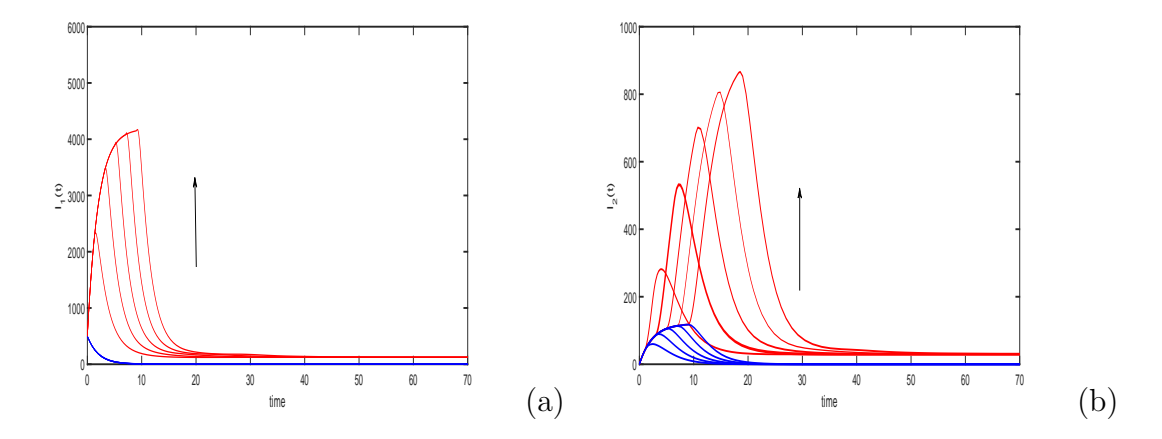


Figure 7.1: Stability of the infected and free-infected equilibrium of model system (7.1) showing plots of $I_1(t)$ and $I_2(t)$ with varying delay ($\tau_1 = \tau_2$). The direction of the arrow depict an increase in delay with a step size of 2.0 starting from 2.0 to 10. The blue patterns in both (a) and (b) highlights brucellosis dynamics when $\mathcal{R}_0 < 1$ while the red pattern are for $\mathcal{R}_0 > 1$. Initial population levels were assumed as follows S(0) = 1000 animals, V(0) = 500 animals, $I_1(0) = 500$ animals and $I_2(0) = 0$ animals.

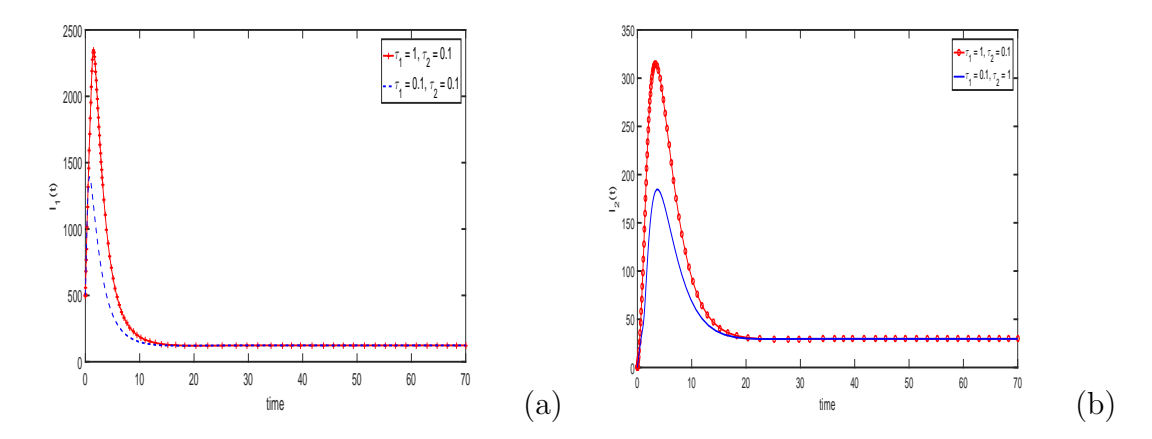


Figure 7.2: Numerical solutions of model system (7.1) illustrating the effects of different time delay on brucellosis infection level in the community. Initial population levels were assumed as follows S(0) = 1000 animals, V(0) = 500 animals, $I_1(0) = 500$ animals and $I_2(0) = 0$ animals.

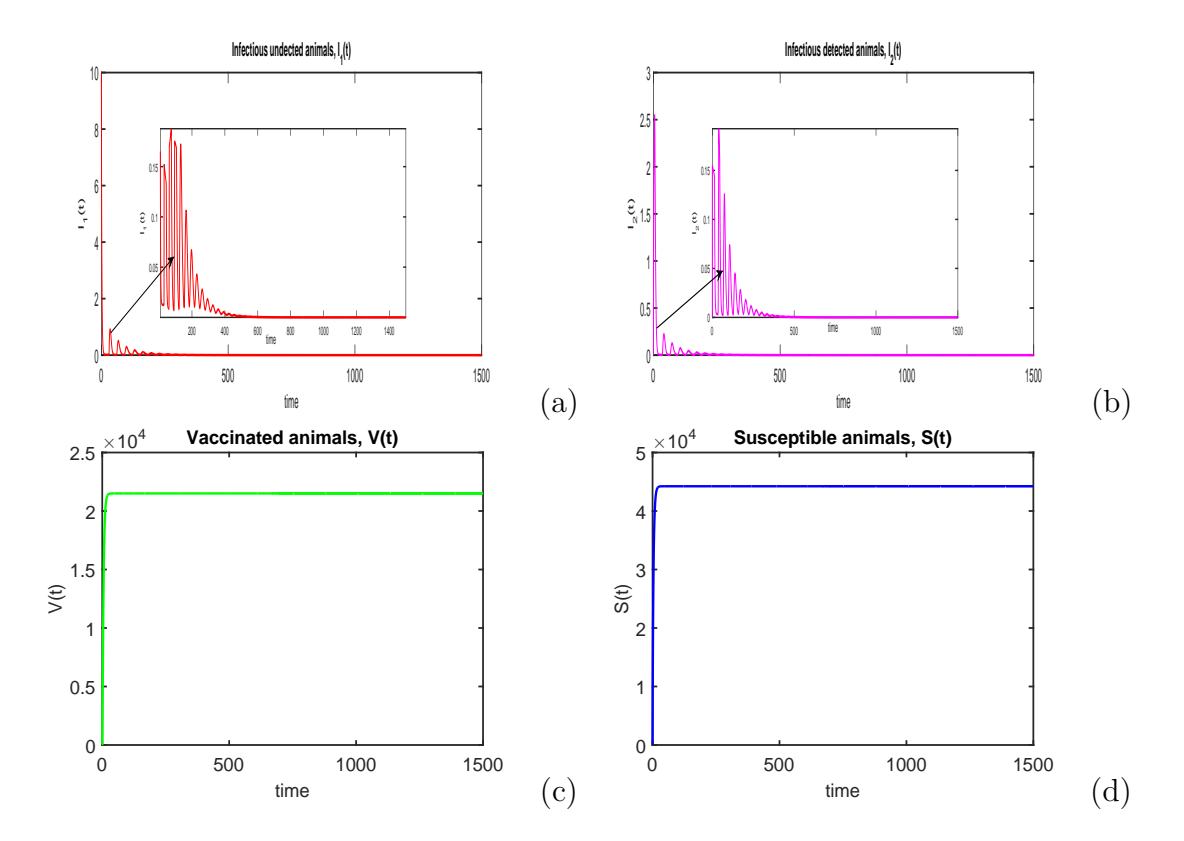


Figure 7.3: Numerical solutions demonstrating the stability of \mathcal{E}^0 equilibrium of model system (7.1) with $\mathcal{R}_0 = 0.686281$. We set $\tau_1 = 30$, $\tau_2 = 5$, $\beta = 6.844 \times 10^{-6}$ animal⁻¹ year⁻¹, $\gamma = 0.2$, $\alpha = 0.15$ year⁻¹, A = 16434 animals year⁻¹ and the remainder retained the baseline values in Table 7.1. Further, we set the initial conditions as follows S(0) = 100 animals, V(0) = 0 animals, $I_1(0) = 10$ animals and $I_2(0) = 0$ animals

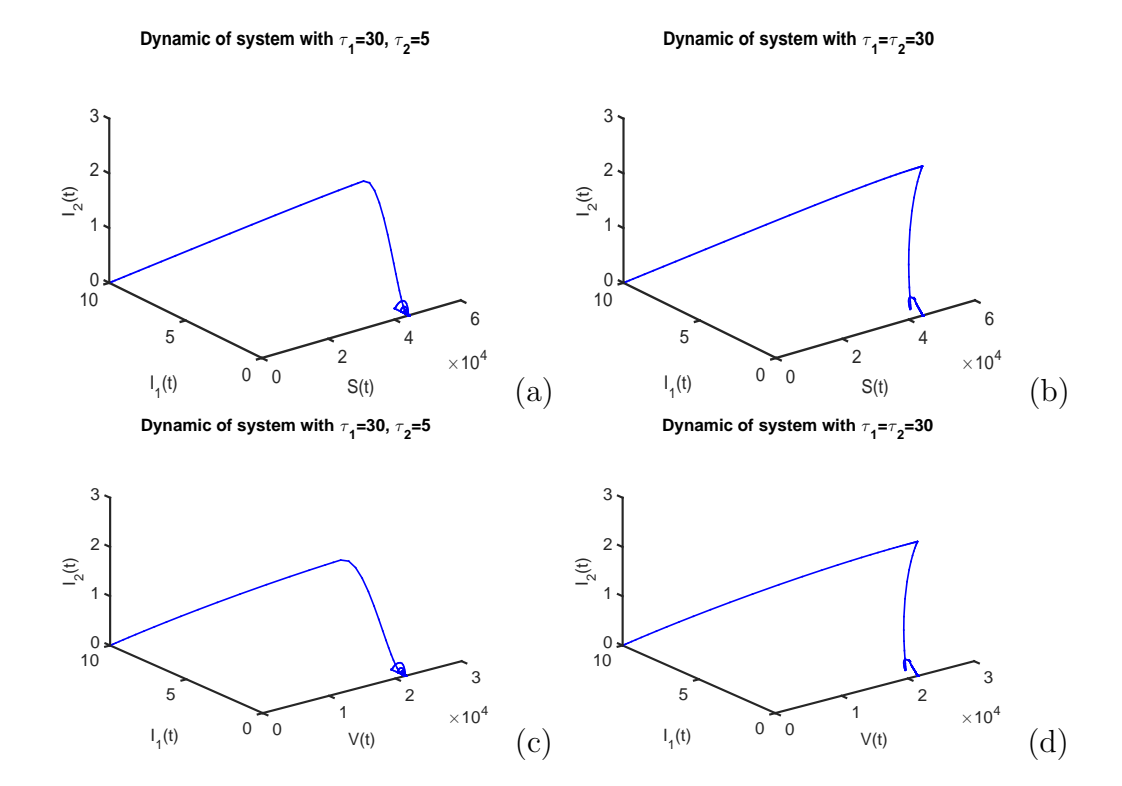


Figure 7.4: Dynamics of model system (7.1) for different values of (τ_1, τ_2) , which illustrate the stability of infection-free equilibrium \mathcal{E}^0 at $\mathcal{R}_0 = 0.686281$. We set $\beta = 6.844 \times 10^{-6} \text{ animal}^{-1} \text{ year}^{-1}$, $\gamma = 0.2$, $\alpha = 0.15 \text{ year}^{-1}$, A = 16434 animals year⁻¹ and the remainder retained the baseline values in Table 7.1. Further, we set the initial conditions as follows S(0) = 100 animals, V(0) = 0 animals, $I_1(0) = 10 \text{ animals}$ and $I_2(0) = 0 \text{ animals}$

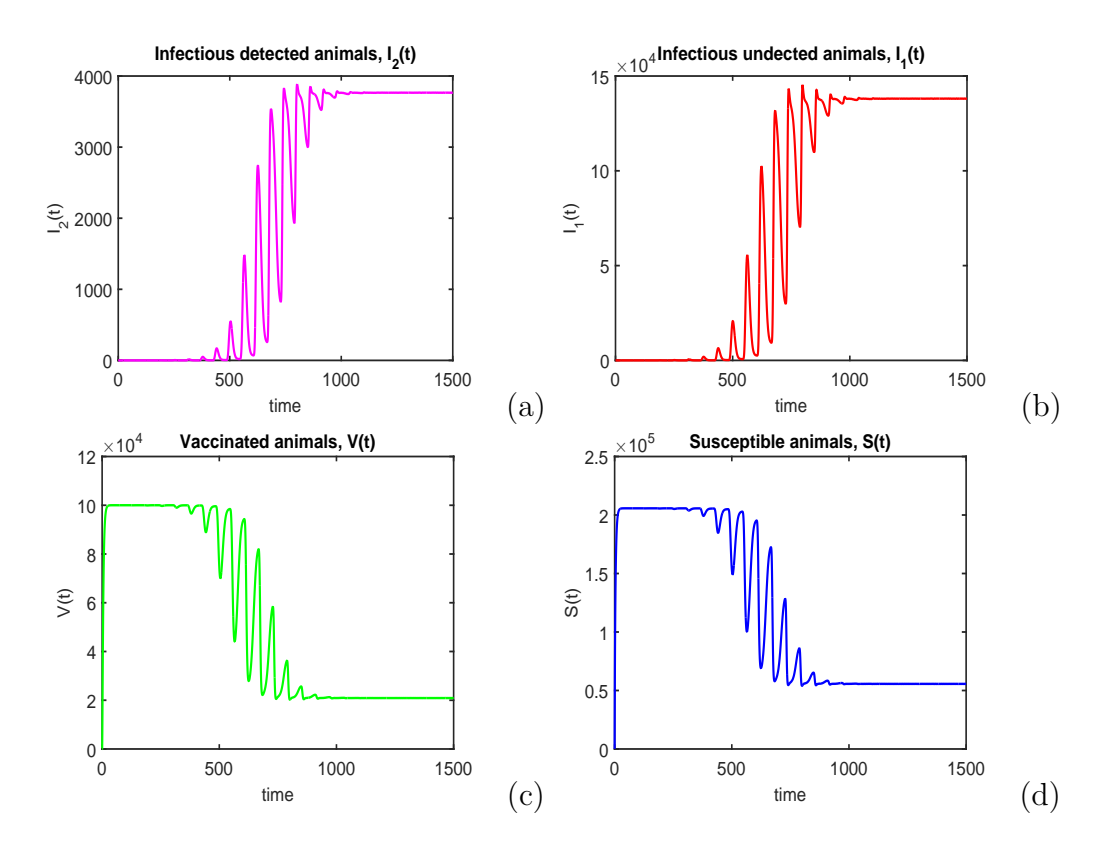


Figure 7.5: Stability of \mathcal{E}^* equilibrium of model system (7.1) with $\mathcal{R}_0 = 3.77333$. The time delay τ_1 was fixed to be 60 and τ_2 was fixed to be 1. We set the model parameters and variables as follows: $\beta = 6.844 \times 10^{-6} \text{ animal}^{-1} \text{year}^{-1}$, $\gamma = 0.2$, $\alpha = 0.015 \text{ year}^{-1}$, S(0) = 100 animals, V(0) = 0 animals, $I_1(0) = 10 \text{ animals}$, $I_2(0) = 0 \text{ animals}$ while the other parameter values are as in Table 7.1.

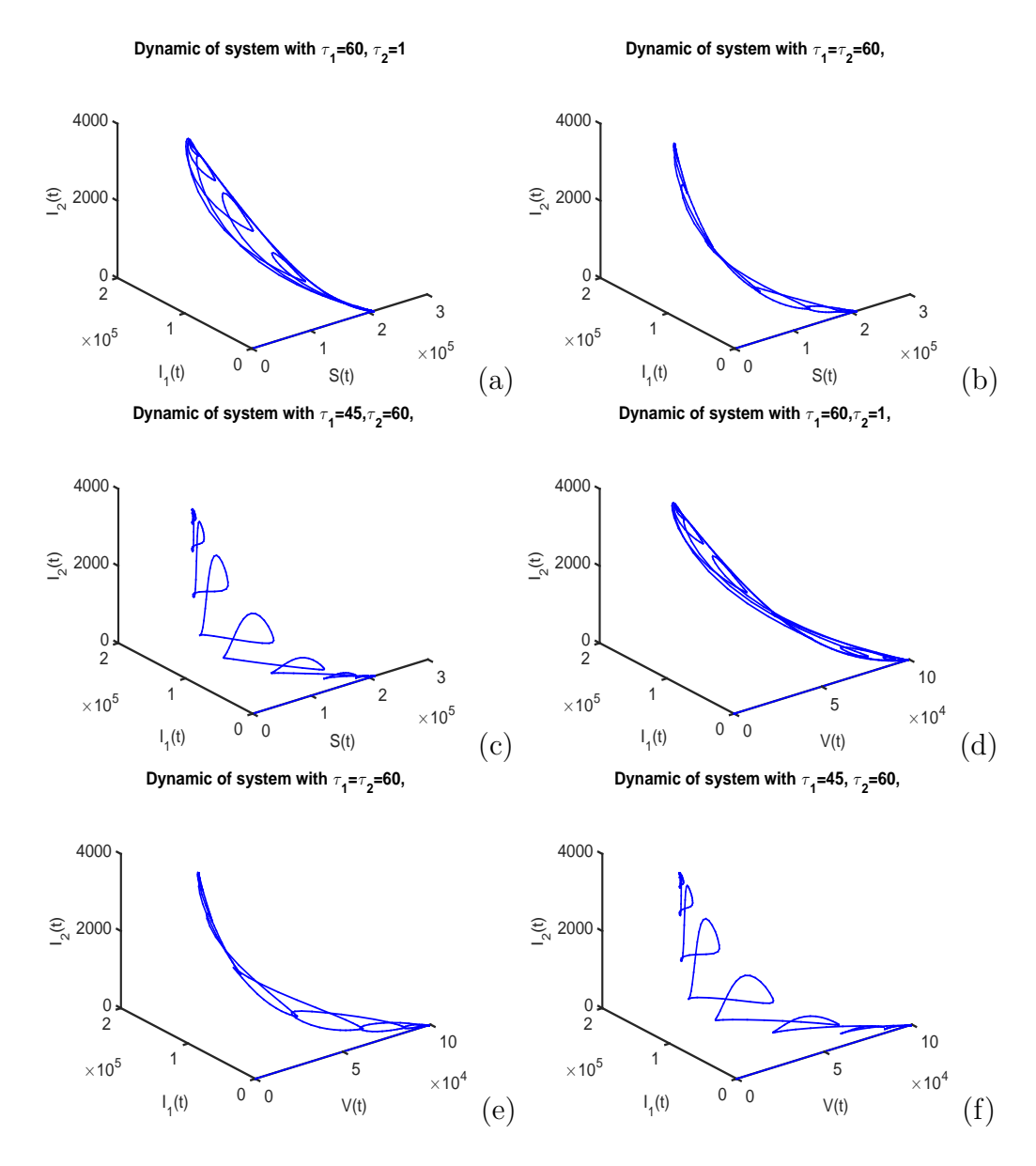


Figure 7.6: Numerical results of model system (7.1) for different values of (τ_1, τ_2) , which demonstrate the stability of infected equilibrium \mathcal{E}^* at $\mathcal{R}_0 = 3.77333$. We set the model parameters and variables as follows: $\beta = 6.844 \times 10^{-6} \text{ animal}^{-1} \text{year}^{-1}$, $\gamma = 0.2$, $\alpha = 0.015 \text{ year}^{-1}$, S(0) = 100 animals, V(0) = 0 animals, $I_1(0) = 10 \text{ animals}$, $I_2(0) = 0 \text{ animals}$ while the other parameter values are as in Table 7.1.

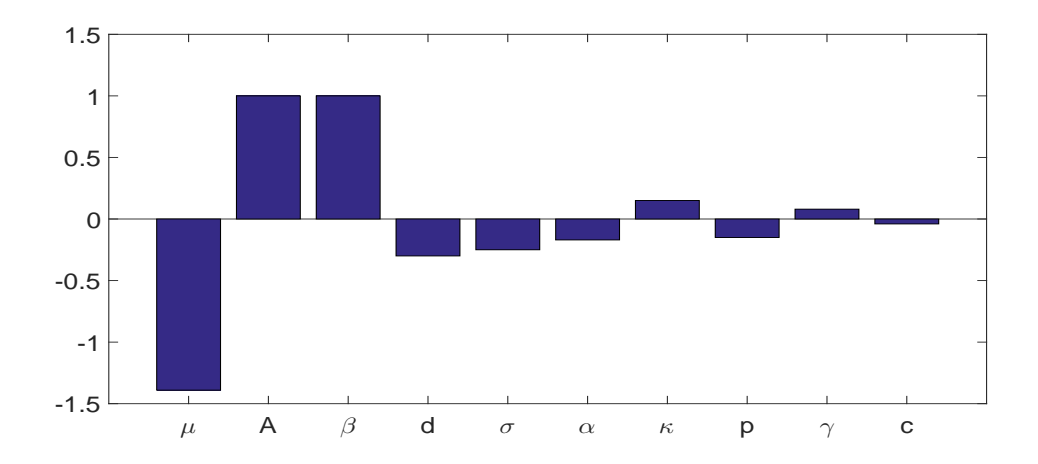


Figure 7.7: Sensitivity index for \mathcal{R}_0 with respect to model parameters that define it.

7.5 Conclusion

Zoonotic brucellosis remains a major public health problem in many developing nations. This is mainly attributed to several challenges associated with effective disease control in these nations. The challenges for effective control of brucellosis in developing nations range from inadequate veterinary personnel and vaccines as well the failure by farmers to adhere to some of the aforementioned brucellosis control and eradication program activities. Furthermore, these challenges often lead to delay in detection and culling of infectious animals. In this chapter, we developed and analysed a mathematical model for brucellosis infection that incorporates two discrete delays. The first delay accounts for the latent period and the second delay represents the time taken to detect infectious animals. We computed the basic reproduction number and demonstrated that it is an important threshold quantity for stability of equilibria. By constructing suitable Lyapunov functionals, it has been shown that the model has a globally asymptotically stable infection-free equilibrium whenever the reproduction is less than unity. Further, it has been demonstrated that whenever the model reproduction number is greater than unity then the model has a unique endemic equilibrium point which is globally asymptotically stable. Numerical simulations are carried out to illustrate the main results.

Although culling of symptomatic animals is a relatively easy strategy to imple-

ment, it is worth noting that some studies suggests that culling of both infected and susceptible animal may be more effective [72, 100]. The rationale being that by decreasing the host density, the number of contacts per unit time between animals is low thereby reducing disease transmission. In [100] it was demonstrated that culling of both susceptible and symptomatic animals only can be effective whenever the number of infected host is above a certain critical level [100]. We expect to improve this study in our future work by developing brucellosis model(s) with time delay that will enable us to compare aforementioned aspects.

Chapter 8

Conclusion and future work

In this dissertation we developed, analysed and simulated five mathematical models for brucellosis infection. On the first objective, we developed a non-autonomous brucellosis model in order to explore the effects seasonality and control strategies on brucellosis transmission. Optimal vaccination and environmental decontamination has been performed with the goal to minimize the numbers of the exposed and infectious animals and the associated costs. The results demonstrated that the optimal control can greatly reduce the numbers of the exposed and infectious animals and keep these populations at low levels, a significantly better outcome compared to that with regular control. It has been observed that the optimal control strategies strongly depend on the cost parameters. Further, results throughout the chapter highlight the difference between the autonomous and periodic models.

On the second objective, a modeling framework that aims to investigate effects of vertical transmission, chronic brucellosis and culling on the transmission dynamics of brucellosis, is studied. The dynamics of the disease were explored for both periodic and non-periodic environments. Further, the impact of time dependent culling control on the spread and control of brucellosis for in both environments was investigated. The results demonstrated that the percentage of symptomatic animals that become carriers/chronic has a strong influence on the impact of culling control to minimize the spread of brucellosis in the community.

On the third objective, we proposed a two-patch model with the aim to study the effects of animal movement and seasonality on brucellosis transmission. We started our analysis on model with fixed coefficients where detailed results were obtained, showing the rich dynamics of brucellosis transmission due to the spatial variation. We extended our model to a time-periodic environment that represents seasonal oscillation. The study demonstrates that the incorporation of spatial and temporal variations leads to rich and complex dynamics that are distinct from those observed from prior models based on homogeneous environments. Our results also indicate that the prevention and intervention strategies need to take into account the spatial and temporal heterogeneities in order to effectively control brucellosis while optimize the use of available resources.

On the fourth objective, we developed a brucellosis model with a view to explore the role of short-term animal dispersal on transmission and control of brucellosis in a heterogeneous population. The proposed model comprised of two patches and animal dispersal was modeled using a Lagrangian approach. Our study is applicable in communal lands/ public farms where animal mobility is highly uncontrolled. Prior studies have shown that in public farms a single herd of livestock can be exposed to a high variable number of contacts with other herds of livestock for a short time frame. This heterogeneity in animal contacts may contribute significantly to the transmission and control of brucellosis. Optimal culling of infectious animals in each patch has been utilized for effective control of brucellosis in the community. Our results show that short-term animal movements plays an integral role in the transmission and control of brucellosis.

On the final objective, we studied the dynamics and stability of a brucellosis model with two discrete delays. The first delay accounts for the latent period and the second delay represents the time taken to detect infectious animals. The results suggest that the two delays can destabilize the system and periodic solutions can arise through Hopf bifurcation.

Our work has managed to provide significant improvement to the existing knowledge regarding the transmission dynamics of bucellosis in animal populations. Our study can be improved by considering the following aspects:

- The aid of realistic data is a crucial step in the modeling process. Our challenge is that, the scarcity of brucellosis data at present limits our ability to calibrate some important results in our models.
- Further understanding of the spatial dynamics of brucellosis would be en-

hanced if reaction-diffusion modeling is carried out, but our current study on the spatial modeling of brucellosis is based on the patch structure.

- Culling of both infected and susceptible animals as disease control strategy
 was not considered in the models developed in this thesis. Culling both infected and susceptible decreases the host density which will reduce the disease
 transmission.
- The effects of short-term animal mobility in a periodic environment mainly due to pastoral can also be investigated.
- Although both autonomous and non-autonomous models were used, stochastic
 epidemic models were never used to investigate the transmission and control
 of brucellosis in this dissertation. In future we hope to utilize these models
 to understand the transmission and control of the brucellosis in both periodic
 and non-periodic environments.

Appendix: Publications arising from this thesis

- 1). Paride O. Lolika, Steady Mushayabasa, Claver P. Bhunu, Chairat Modnak, Jin Wang., (2017). Modeling and analyzing the effects of seasonality on brucellosis infection. Chaos, Solitons & Fractals., 104:338–349.
- 2). Paride O. Lolika, Chairat Modnak, Steady Mushayabasa., (2018). On the dynamics of brucellosis infection in bison population with vertical transmission and culling., Mathematical Biosciences, 305, 42-54.
- 3). Chayu Yang, **Paride O. Lolika**, Steady Mushayabasa, Jin Wang., (2017). Modeling the spatiotemporal variations in brucellosis transmission. Nonlinear Analysis: Real World Applications: vol. 38, 49–67.
- 4). Paride O. Lolika and Steady Mushayabasa. On the role of short-term animal movements on the persistence of brucellosis, Mathematics 2018, 6, 154; doi:10.3390/math6090154.
- 5). **Paride O. Lolika** and Steady Mushayabasa, Dynamics and Stability Analysis of a Brucellosis Model with Two Discrete Delays, Discrete Dynamics in Nature and Society, vol. 2018, Article ID 6456107, 20 pages, 2018. https://doi.org/10.1155/2018/6456107.

Bibliography

- [1] M.J. Corbel, Brucellosis: An overview, Emerg. Infect. Dis., 3 (1997): 213-221.
- [2] G. Pappas, N. Akritidis, M. Bosikovski, and E. Tasianos, Brucellosis, N. Engl. J. Med., 352 (2005): 2325-2336.
- [3] M.J. Mangen, J. Otte, D. Pfeiffer, and P. Chilonda, Bovine brucellosis in Sub-Sahara Africa: Estimation of sero-prevalence and impact on meat and milk offtake potential, Livestock Policy Discussion Paper N. 8, Food and Agriculture Organization of the United Nations (FAO) Livestock Information and Policy Branch, Rome, 2002.
- [4] M.L. Boschiroli, V. Foulogone, and D. O'Callaghan, Brucellosis: A worldwide zoonosis, *Curr. Opin. Microbiol.*, 4 (2001): 58-64.
- [5] M.T. Li, G.Q. Sun, Y.F. Wu, J. Zhang, Z. Jin. Transmission dynamics of a multi-group brucellosis model with mixed cross infection in public farm. Appl. Math. Comput. 2014, 237, 582-594.
- [6] E.J. Richey and C. Dix Harrel, Brucella Abortus (Brucellosis) in Beef Cattle, University of Florida, IFAS Extension, VM 100 (1997): 1-6.
- [7] C.M. Carpenter, W.T. Hubbert . Brucellosis in: Disease transmitted from animal to man, sixth (Eds.) T G Hull, Charles C. Thomas, Ilinois, USA. 1963; 126-169.
- [8] M.M.H. Sewel and D.W. Brocklesby (Eds.), *Handbook on Animal Diseases in the Tropics*, 4th Ed., Bailliere Tindall: London, 1990.

- [9] B. Abbas, H. Agab. A Review of camel brucellosis. Prev vet Med 2002; 55(1):47-56.
- [10] J. Godfroid, K. Nielsen, C. Saegerman. Diagnosis of Brucellosis in Livestock and Wildlife. Croat Med J 2010; 51(4):296-305.
- [11] V. Dobrean, A. Opris, and S. Daraban, An epidemiological and surveillance overview of brucellosis in Romania, *Vet. Mic.*, 90 (2002): 157-163.
- [12] H. Kraus, A. Weber, B. Enders, H.G. Schierfer, W. Slenczka, H. Zahner. Zoonotic disease, infection diseases transmitted from animals to human, second ed 1996:400 pp.
- [13] J. Parnas, W. Kruger, E. Toppich. Die Brucellosis des Menschen (Human Brucellosis), VEB VErlag Volk und Gesundhei, Berlin Eds 1966;566 pp.
- [14] M.M. Madkour, *Madkour's Brucellosis*, Springer Verlag: Heidelberg, Berlin, 2001.
- [15] M. Corbel. Brucellosis in humans and animals. World Health Organization in collaboration with the Food and Agriculture Organization of the United Nations and the World Organization for Animal Health 2006.
- [16] E. Schelling, S. Daoud, D.M. Daugla, P. Diallo, M. Tanner, J. Zinssatag .Morbidity and nutrition patterns of three nomadic pastoralist communities of Chad Acta trop 2005;95:16-25.
- [17] M-Tao Li, Sun Gui-Quan, Zhnag Yi Wei, Jin Z. Model-based evaluation of strategies to control brucellosis in China. International Journal of Environmental Research and Public Health. 2017, 14, 295; doi:10.3390/ijerph1430295
- [18] C. Diguimbaye, E. Schelling, S. Daoud, J. Nicolet, P. Boerlin, M. Tanner, J. Zinsstag. Brucellosis and Q-fever seroprevalences of nomadic pastoralists and their livestock in Chad Prev Vet Med 2003;61:279-93.
- [19] A.M. Bonfiglioli and C. Watson, (1992)-Pastoralists at a crossroad: survival and development issues in African pastoralism. Unite Nations International Chil-

- dren's Emergency Fund (UNICEF)/UN Sudano-Sahelian office (UNSO) Project for Nomadic Pastoralists in Africa (NOPA), New York.
- [20] FAO 2001, Pastoralism in the new millennium. FAO Animal Production and Health Paper NO.150. Annexe III: Worldwide Tables of pastoral Peoples.FAO, Rome. Available at: www.fao.org/docrep/005/Y2647E/y2647e17.htm Poo(accessed on 5 April 2013).
- [21] S. Bokaie, L. Sharifi, H. Alizadeh. Epidemiological survey of brucellosis in human and animals in Birjand, East of Iran. J Anim Vet Advan 2008;7:460-63.
- [22] D.J. Daley, J. Gani. Epidemic Modeling: An Introduction. NY: Cambridge University Press 2005.
- [23] H.W. Hethcote. "The mathematics of infectious diseases." Society for Industrial and Applied Mathematics 2000; 42:599-653.
- [24] D. Bernoulli, S. Blower. "An attempt at a new analysis of the mortality caused by smallpox and of the advantages of inoculation to prevent it." Reviews in Medical Virology 2004;14:275-88.
- [25] F. Brauer, C. Castillo-Chvez. Mathematical Models in Population Biology and Epidemiology. NY: Springer 2001.
- [26] World Health Organization, *Brucellosis in Humans and Animals*, WHO Press, 2006.
- [27] K. Aune, J.C. Rhyan, R. Russell, T.J. Roffe, and B. Corso, Environmental persistence of *Brucella* abortus in the Greater Yellowstone area, *Journal of Wildlife Management*, 76 (2012): 253-261.
- [28] W. Beauvais, I. Musallam, and J. Guitian, Vaccination control programs for multiple livestock host species: An age-stratified, seasonal transmission model for brucellosis control in endemic settings, *Parasites & Vectors*, 9 (2016): 55.
- [29] M. Kretzschmar, J. Wallinga, M. Gail, K. Krickeberg, J. Samet, A.Tsiatis, W. Wong. Mathematical Models in Infectious Disease Epidemiology. Springer 2010.

- [30] Q. Hou, X. Sun, J. Zhang, Y. Liu, Y. Wang, and Z. Jin, Modeling the transmission dynamics of sheep brucellosis in Inner Mongolia autonomous region, China, *Mathematical Biosciences*, 242 (2013): 51-58.
- [31] P. O. Lolika, S. Mushayabasa, C.P. Bhunu, C. Modnak, J. Wang, Modeling and analyzing the effects of seasonality on brucellosis infection, Chaos, Solitons & Fractals, 104 (2017) 338–349.
- [32] M. Li, G. Sun, J. Zhang, Z. Jin, X. Sun, Y. Wang, B. Huang, Y. Zheng. Transmission dynamics and control for a brucellosis model in Hinggan League of Inner Mongolia, China. Math. Biosci. Eng. 2014, 11, 1115-1137.
- [33] M.T. Li, Z. Jin, G.Q. Sun, et al. Modeling direct and indirect disease transmission using multi-group model. J Math Anal Appl; 446(2):1292-309 (2017).
- [34] P. Lou, L. Wang, X. Zhang, J. Xu, K. Wang. Modelling Seasonal Brucellosis Epidemics in Bayingolin Mongol Autonomous Prefecture of Xinjiang, China, 2010-2014. BioMed Res. Int. 2016, 2016, 5103718.
- [35] D.O. Montiel, M. Bruce, K. Frankena, H. Udo, A. van der Zijpp, J. Rushton. Financial analysis of brucellosis control for small-scale goat farming in the Bajo region, Mexico. Prev. Vet. Med. 2015, 118, 247-259.
- [36] L. Yang, Z.W. Bi, Z.Q. Kou, X.J. Li, M. Zhang, M. Wang, L.Y. Zhang, Z.T. Zhao. Time-series analysis on human brucellosis during 20042013 in Shandong province, China. Zoonoses Public Health 2015, 62, 228-235.
- [37] J. Zinsstag, F. Roth, D. Orkhon, G. Chimed-Ochir, M. Nansalmaa, J. Kolar, P. Vounatsou. A model of animal-human brucellosis transmission in Mongolia. Prev. Vet. Med. 2005, 69, 77-95.
- [38] E. Abatih, L. Ron, N. Speybroeck, B. Williams, D. Berkvens, Mathematical analysis of the transmission dynamics of brucellosis among bison, Math. Meth. Appl. Sci, 38 3818-3832 (2015).
- [39] J. Zhang, G-Q. Sun , X-D. Sun, Q. Hou , M. Li, et al. Prediction and control of brucellosis transmission of dairy cattle in Zhejiang Province, China. PloS ONE 9(11): e108592, 2014.

- [40] G.G. Jorge, N. Raul, Analysis of a model of bovine brucellosis using singular perturbations, J. Math. Biol. 33 (1994) 211-223.
- [41] B. Alnseba, B. Chahrazed, M. Pierre, A model for ovine brucellosis incorporating direct and indirect transmission, J. Biol. Dyn. 4 (2010) 2-11.
- [42] F. C. Mufinda, F. Boinas, C. Nunes, Prevalence and factors associated with human brucellosis in livestock professionals, Revista de Sade Pblica,51 (2017):57. doi:10.1590/S1518-8787.2017051006051.
- [43] E. Shevtsova, A. Shevtsov, K. Mukanov, M. Filipenko, D. Kamalova, I. Sytnik, et al., Epidemiology of brucellosis and genetic diversity of *brucella* abortus in Kazakhstan, PLoS ONE 11(12) (2016), e0167496.
- [44] V. Racloz, E. Schelling, N. Chitnis, F. Roth, J. Zinsstag. Persistence of brucellosis in pastoral systems. Rev Sci Tech., 32(1):61-70 (2013).
- [45] J.P. LaSalle. Stability of nonautonomous systems. Nonlinear Anal Theory Methods Appl,1976;1(1):83-91.
- [46] J.P. LaSalle, *The stability of dynamical systems*, CBMS-NSF Regional Conference Series in Applied Mathematics 25, SIAM: Philadelphia, 1976.
- [47] A. Fall, A. Iggdr, G. Sallet, and J. Tewa, Epidemiological models and lyapunov exponents, Math.Model.Nat.Phenom., 2 (2007), pp. 6283.
- [48] W.A. Coppel, stability and Asymptotic Behavior of Differential Equations, Health, Boston, 1965.
- [49] J.S. Muldowaney. Compound matrices and ordinary differential equations, Rocky Mountam J Math 1990; 20:857-72.
- [50] P. van den Driessche and J. Watmough, Reproduction number and subthreshold endemic equilibria for compartment models of disease transmission, *Mathematical Biosciences*, 180 (2002): 29-48.
- [51] M.N. Seleem, S.M. Boyle, Sriranganathan N. Brucellosis: A re-emerging zoonosis. Veterinary Microbiology, 140:392-398, 2010.

- [52] A. Bingl, N. Ycemen, O. Meo. Medically treated intraspinal "Brucella granuloma. Surgical Neurology, 52:570-576, 1999.
- [53] L. Liu, X. Zhao, Y. Zhou, A tuberculosis model with seasonality. Bull Math Biol 72 (2010) 931-952.
- [54] V. Lakshmikantham, S.Leela, A.A. Martynyuk, Stability Analysis of nonlinear Systems, Marcel Dekker. Inc., New York, Basel, 1989.
- [55] W. Wang and X.-Q. Zhao, Threshold dynamics for compartment epidemic models in periodic environments, *Journal of Dynamics and Differential Equations*, 20 (2008): 699-717.
- [56] D. Posny and J. Wang, Computing basic reproductive numbers for epidemiological models in nonhomogeneous environments, Applied Mathematics and Computation, 242 (2014): 473-490.
- [57] F. Zhang and X.Q. Zhao. A periodic epidemic model in a patchy environment. Journal of Mathematical Analysis and Applications, 325: 496-516, 2007.
- [58] X.-Q. Zhao, Dynamical Systems in Population Biology, Springer: New York, 2003.
- [59] X.Q. Zhao. Uniform persistence in processes with application to nonautonomous competitive models. Journal of Mathematical Analysis and Applications 258: 87-101, 2001.
- [60] D.L. Lukes, Differential Equations: Classical to Controlled, Mathematics in Science and Engineering, Academic Press, New York, NY, USA, 1982.
- [61] S. Lenhart, J. T. Workman, Optimal Control Applied to Biological Models, Chapman and Hall, 2007.
- [62] W.H. Fleming, R.W. Rishel. Deterministic and stochastic optimal control, Springer-verag, New York, 1975.
- [63] L.S. Pontryagin, V.T. Boltyanskii, R.V. Gamkrelidze, E.F. Mishchenko, The mathematical theory of optimal processes. New Jersey: Wiley; 1962.

- [64] J. Godfroid, Brucellosis in wildlife. Rev. sci. ettch. Off. int. Epiz, 21(2):277-286 (2002).
- [65] M. R. Hasanjani Roush, S. Ebrahimpour S, Human brucellosis: An overview, Caspian J Intern Med, 6(1) (2015) 46-47.
- [66] C. Yang, P. O. Lolika, S. Mushayabasa, J. Wang J, Modeling the spatiotemporal variations in brucellosis transmission. Nonlinear Analysis: Real World Applications 38 (2017), 49-67.
- [67] P. O. Lolika, S. Mushayabasa. Dynamics and stability analysis of a brucellosis model with two discrete delays. Discrete Dynamics in Nature and Society, vol. 2018, Article ID 6456107, 20 pages, 2018.
- [68] E. Kazak, H. Akaln, E. Ylmaz, et al. Brucellosis: a retrospective evaluation of 164 cases, Singapore Med J, 57(11) (2016) 624-629.
- [69] I. D. Aitken, Diseases of Sheep. 4th edition. Blackwell Publishing Ltd, Oxford, UK. Pp. (2007) 137–142.
- [70] K. A. Alexander, J.K. Blackburn, M.E. Vandewalle, R. Pesapane, E. K. Baipoledi, et al., Buffalo, bush meat, and the Zoonotic threat of brucellosis in Botswana. PLoS ONE 7(3) (2012): e32842. doi:10.1371/journal.pone.0032842.
- [71] M. Minas, A. Minas, K. Gourgulianis, A. Stournara, Epidemiological and clinical aspects of human brucellosis in Central Greece, Jpn J Infect Dis 60 (2007) 362-366.
- [72] L. Bolzoni, V. Tessoni, M. Groppi, G. A. De Leo, React or wait: which optimal culling strategy to control infectious diseases in wildlife, J. Math. Biol. 69 (2014) 1001-1025.
- [73] M. Zamri-Saad, M. I. Kamarudin, Control of animal brucellosis: The Malaysian experience. Asian Pac J Trop Med, 9(12) (2016) 1136-1140.
- [74] M.Y. Li and J.S. Muldowney, A geometric approach to global-stability problems, SIAM J. Math. Anal., 27 (1996): 1070-1083.

- [75] H.L. Smith and P. Waltman, *The Theory of the Chemostat*, Cambridge University Press: Cambridge, 1995.
- [76] H. Joshi, S., Lenhart, S. Hota, S., F. Agusto, F. (2015). Optimal control of an SIR model with changing behavior through an education campaign. Electronic Journal of Differential Equations, (2015), 50, 1-14.
- [77] A. J. Krener, The High Order Maximum Principle and its Application to Singular Exteremals, SIAM Journal on Control and Optimization, 15 (1997), 256-293.
- [78] Z. Shuai, J.A.P. Heesterbeek, and P. van den Driessche, Extending the type reproduction number to infectious disease control targeting contact between types, J. Math. Biol, 67 (2013), 1067-1082.
- [79] H.I. Freedman, S. Ruan, and M. Tang, Uniform persistence and flows near a closed positively invariant set, *J. Dyn. Differ. Equat.*, 6 (1994): 583-600.
- [80] M.Y. Li, J.R. Graef, L.Wang, and J. Karsai, Global dynamics of a SEIR model with varying total population size, *Math. Biosci.*, 160 (1999): 191-213.
- [81] H.R. Thieme, Convergence results and a Poincare-Bendixon trichotomy for asymptotically autonomous differential equations, J. Math. Biol. 30 (1992) 755763.
- [82] H.R. Thieme, Persistence under relaxed point-dissipativity (with application to an endemic model), SIAM J. Math. Biosci.166 (1993) 407435
- [83] R. Peng and X.-Q. Zhao, A nonlocal and periodic reaction-diffusion-advection model of a single phytoplankton species, *Journal of Mathematical Biology*, 72 (2016): 755-791.
- [84] R. Peng and X.-Q. Zhao, A reaction-diffusion SIS epidemic model in a time-periodic environment, *Nonlinearity*, 25 (2012): 1451-1471.
- [85] X. Yu and X.-Q. Zhao, A nonlocal spatial model for Lyme disease, *Journal of Differential Equations*, 261 (2016): 340-372.
- [86] A. Dobson, M. Meagher. The population dynamics of Brucellosis in the Yellowstone National Park. Ecology 1996; 77:1026-1036.

- [87] P.O. Lolika, C. Modnak, S. Mushayabasa. On the dynamics of brucellosis infection in bison population with vertical transmission and culling Mathematical Biosciences, doi.org/10.1016/j.mbs.2018.08.009.
- [88] H.W. Hethcote, and H.R. Thieme, (1985). Stability of the endemic equilibrium in epidemic models with subpopulations. Mathematical Biosciences, 75, 205227.
- [89] N.V. Meunier, P. Sebulime, R.G. White & R. Kock, 2017, Wildlife-livestock interactions and risk areas for cross-species spread of bovine tuberculosis, Onderstepoort Journal of Veterinary Research 84(1), a1221. https://doi.org/10.4102/ojvr.v84i1.1221.
- [90] E.M. Potter, (2013) Brucellosis: A chapter in Foodborne infections and intoxication, 4th Edition, Morris J. G and Potter E. M (eds), Elsevier Inc.
- [91] A.J. Al-Tawfiqa, A. AbuKhamsinb. A 24-year study of the epidemiology of human brucellosis in a health-care system in Eastern Saudi Arabia. Journal of Infection and Public Health, 2, 81-85, (2009).
- [92] Q. Hou and X. Sun. Modeling sheep brucellosis transmission with a multi-stage model in Changling County of Jilin Province, China. J. Appl. Math. Comput. vol. 51, pp 227-244 (2016).
- [93] P. Lou, L. Wang, X. Zhang, J. Xu, K. Wang. Modelling Seasonal Brucellosis Epidemics in Bayingolin Mongol Autonomous Prefecture of Xinjiang, China, 2010-2014. BioMed Research International Volume 2016 (2016), Article ID 5103718, 17 pages http://dx.doi.org/10.1155/2016/5103718
- [94] J. Tumwiine, G. Robert. A mathematical model for treatment of bovine brucellosis in cattle population. Journal of Mathematical Modelling, 5(2), 137-152, (2017).
- [95] J. Zhang, Z. Jin, Li Li, X.D. Sun. Cost assessment of control measure for brucellosis in Jilin province, China. Chaos, Solitons and Fractals, 104, 798-805 (2018).
- [96] J.K. Hale, S.M. Verduyn Lunel. Introduction to Functional Differential Equations. Springer-Verlag, 1993.

- [97] H. Smith, X. Zhao. Robust persistence for semi-dynamical systems, Nonlinear Anal. 46, 6169-6179, (2001).
- [98] L. Zhou, M. Fan, Q. Hou, Z. Jin, X. Sun. Transmission dynamics and optimal control of brucellosis in Inner Mongolia of China. Mathematical Biosciences and Engineering, Vol 15(2), pp. 543-567 (2018).
- [99] L. Arriola. Sensitivity analysis for quantifying uncertainty in mathematical models, Mathematical and Statistical Estimation Approaches in Epidemiology, G. Chowell, J.M. Hyman, L.M.A. Bettencourt, and C. Castillo-Chavez, eds., Springer, New York, 2009, pp. 195-248.
- [100] W. Zhou, Y. Xiao, & R.A. Cheke. (2016). A threshold policy to interrupt transmission of West Nile Virus to birds. Applied Mathematical Modelling, 40(19), 8794-8809.